VOLUME 10
NUMBER 1—2
1975

Acta biochimica et biophysica

ACADEMIAE SCIENTIARUM HUNGARICAE

AKADÉMIAI KIADÓ, BUDAPEST

ABBPAP 10 (1—2) 1—145 (1975)

Acta Biochimica et Biophysica

Academiae Scientiarum Hungaricae

Szerkeszti:

STRAUB F. BRUNÓ és ERNST JENŐ

Technikai szerkesztők:

SAJGÓ MIHÁLY és NIEDETZKY ANTAL

Szerkesztőség postai címe: 1502 Budapest, Pf. 7 (biokémia)
7643 Pécs, Pf. 99 (biofizika)

Az *Acta Biochimica et Biophysica* a Magyar Tudományos Akadémia idegen nyelvű folyóirata, amely angol nyelven (esetleg német, francia vagy orosz nyelven is) eredeti tanulmányokat közöl a biokémia és a biofizika — fehérjék (struktúra és szintézis), enzimek, nukleinsavak, szabályozó és transzport-folyamatok, bioenergetika, izom-összehúzódás, radiobiológia, biokibernetika, funkcionális és ultrastruktúra stb. — tárgyköréből.

A folyóirat negyedévenként jelenik meg, a négy füzet évente egy kb. 400 oldalas kötetet alkot. Kiadja az Akadémiai Kiadó.

Megrendelhető az Akadémiai Kiadónál (1363 Bp. Pf. 24.), a külföld részére pedig a Kultúra Könyv és Hírlap Külkereskedelmi Vállalatnál (1389 Budapest 62, P.O.B. 149).

The *Acta Biochimica et Biophysica*, a periodical of the Hungarian Academy of Sciences, publishes original papers, in English, on biochemistry and biophysics. Its main topics are: proteins (structure and synthesis), enzymes, nucleic acids, regulatory and transport processes, bioenergetics, excitation, muscular contraction, radiobiology, biocybernetics, functional structure and ultrastructure.

The Acta Biochimica et Biophysica is a quarterly, the four issues make up a volume of some 400 pages per annum. Manuscripts and correspondence with the editors and publishers should be sent to

Akadémiai Kiadó, Budapest 24, P.O.B. 502.

The subscription rate is $32.00 per volume. Orders may be placed with *Kultúra* Trading Co. for Books and Newspapers (1389 Budapest 62, P.O.B. 149) or with its representatives abroad, listed on p. 3 of the cover.

Acta Biochimica et Biophysica — журнал Академии Наук Венгрии, публикующий на английском языке (возможно и на немецком, французском и русском языках) оригинальные статьи по проблемам биохимии и биофизики — белков (структура и синтез), энзимов, нуклеиновых кислот, процессов регуляции и транспорта, биоэнергетики, мышечного сокращения, радиобиологии, биокибернетики, функциональной структуры и ультраструктуры и т. д.

Журнал выходит ежеквартально, выпуски каждого года составляют том объемом около 400 страниц. Журнал выпускает Издательство Академии Наук Венгрии.

Рукописи и корреспонденцию просим направлять по следующему адресу:

Akadémiai Kiadó, Budapest 24, P.O.B. 502.

Подписная цена — $ 32.00 за том. Заказы принимает:

Предприятие по внешней торговле книгами и газетами «Kultúra» (1389 Budapest 62, P.O.B. 149) или его заграничные агентства.

Acta Biochimica et Biophysica

Academiae Scientiarum Hungaricae

Volume 10

Akadémiai Kiadó, Budapest

1976

Contents

Subject Index

Author Index

Acta Biochim. et Biophys. Acad. Sci. Hung. Vol. 10 (1–2), pp. 1–5 (1975)

Charge-transfer Absorption Spectrum of the Complex of NAD and D-Glyceraldehyde-3-phosphate Dehydrogenase Modified with N-ethylmaleimide

(Short Communication)

MARIA VAS, L. BOROSS

Department of Enzymology, Institute of Biochemistry,
Hungarian Academy of Sciences, Budapest, Hungary

(Received November 11, 1974)

The near ultraviolet absorption spectrum of the complex of D-glyceraldehyde-3-phosphate dehydrogenase* and NAD was described first by Racker and Krimsky (1952), therefore it is often referred to as "Racker band". In early studies it was established that the free (unmodified) state of the reactive thiol group Cys-149 (Harris, Perham, 1968) in the active site of the enzyme is a basic requirement for the development of this absorption band (Racker, Krimsky, 1952; Velick, 1953). The hypothesis, however, that the essential thiol group plays an important role in the binding of the coenzyme proved to be erroneous: NAD can be bound to the enzyme in which Cys-149 is carboxymethylated (Friedrich, 1965) or mercaptidated with p-mercuribenzoate (Vas, Boross, 1970), but in these cases the Racker band does not develop.

In our earlier investigations we have found that the near ultraviolet absorption of the enzyme–coenzyme complex does not disappear, only changes upon modifying the Cys-149 SH group with silver ion (Boross, 1965) or cupric ion (Boross, Cseke, 1971). The alkylation of Cys-149 with bromoacetone, iodoacetic ethylester (Boross et al., 1966) or iodoacetamide (Friedrich, 1967) also results in a blue shift of the Racker band and in an increase of the molar absorption coefficient.

In the present experiments we found that modification of the essential SH group of pig muscle GAPD with NEM also affected the light absorption of the enzyme–coenzyme complex. As shown in Fig. 1. A, the broad absorption maximum of the native GAPD-NAD complex around 355 nm disappears and a shoulder develops at shorter wavelengths when Cys-149 reacts with NEM in all four subunits of the enzyme. The modification of this SH group in the apoenzyme does

* *Abbreviations:* GAPD, D-glyceraldehyde-3-phosphate dehydrogenase or D-glyceraldehyde-3-phosphate: NAD^+ oxidoreductase (phosphorylating) (EC 1. 2. 1.12.); NEM, N-ethylmaleimide; $(NEM)_4$-GAPD, GAPD-apoenzyme modified on residues Cys-149 with NEM; $(NEM)_4$-GAPD-$(NAD)_4$, GAPD-holoenzyme modified on residues Cys-149 with NEM.

not change the absorption spectrum. The binding of NAD to this NEM-modified GAPD ($(NEM)_4$-GAPD) results in a difference-absorption maximum around 310 nm (Fig. 1. B), i.e. the Racker band is shifted to the shorter wavelengths as compared to the original spectrum.

The absorption of the modified enzyme–coenzyme complex depends on the pH (Fig. 2). The inflexion point of the S-shaped pH-dependence curve is at pH 7.6 in 0.1 M phosphate buffer. (The phosphate ion is a substrate of the enzyme, i.e. the enzyme has a specific phosphate binding-site in the active centre.) Like in the native GAPD-NAD complex, the pH dependence of light absorption seems to be influenced by the anions of the solution; in Tris-HCl buffer the curve is shifted towards the acidic range. However, the inflexion points (apparent pK-values) of the pH-dependence curves in both phosphate and chloride-containing solutions are at higher pH-s than in the case of the unmodified GAPD-NAD complex (Cseke, Boross, 1970; Boross et al., 1969).

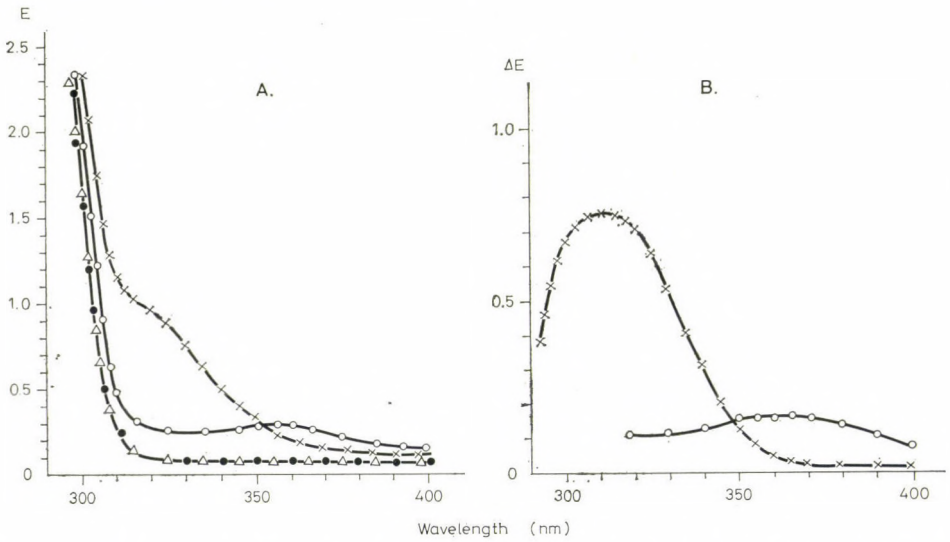

Fig. 1. Absorption spectrum (A) and difference spectrum (B) of GAPD-NAD complex after alkylation of Cys-149 with N-ethylmaleimide. 1.5×10^{-4} M NAD-free GAPD was reacted with 6.0×10^{-4} M NEM (i.e. 4 moles/mole tetramer) in 0.1 M phosphate buffer, pH 8.5, at 20°C. The completion of the reaction of residues Cys-149 was tested by measuring the disappearance of NEM absorption at 310 nm, by enzyme activity measurements, and by determining the remaining SH content. The spectra (A) were recorded at 5×10^{-5} M enzyme concentration in 0.1 M phosphate buffer, pH 8.5, at 20°C in the case of $(NEM)_4$-GAPD (● — ●), unmodified NAD-free GAPD (△ — △), $(NEM)_4$-GAPD incubated about 15 minutes with 2.0×10^{-4} M NAD (× — ×) and unmodified GAPD in the presence of 2.0×10^{-4} M NAD (○ — ○). The difference spectra (B) were calculated from these data for the NEM-treated (× — ×) and unmodified enzyme (○ — ○). The molar absorption differences at 310 and 365 nm are 4400 $M^{-1}\,cm^{-1}$ and 800 $M^{-1}\,cm^{-1}$, respectively calculated for the subunit molecular weight

The maximum extinction values at 310 nm in the alkaline region above pH 8.5 are the same in phosphate and Tris-HCl buffers. The molar extinction of the $(NEM)_4$-GAPD-$(NAD)_4$ complex in this pH region is about 6.3×10^3 per subunit, and the molar extinction difference for the complex formation (i.e. the change of absorption due to the binding of one NAD to the $(NEM)_4$-GAPD) is about 4.4×10^3. This value is about five times as high as the corresponding extinction difference of the native GAPD-NAD complex at 365 nm.

In contrast to the native enzyme–coenzyme complex the absorption of the $(NEM)_4$-GAPD-$(NAD)_4$ complex does not change inmediately as the pH of the solution is altered: if the pH of the solution is increased from 6.5 to 7.5 or to 8.5, the maximum extinction is reached after about 1 and 3 minutes, respectively. This indicates that the pH dependence of the modified complex is not a simple function of the dissociation of an ionizing (acidic) group, since protonation and deprotonation are fast processes. Therefore it seems very probable that the pH dependences in Fig. 2 reflect small conformational changes of the enzyme–coenzyme complex, and the conformation is optimal for the light absorption only in the alkaline range.

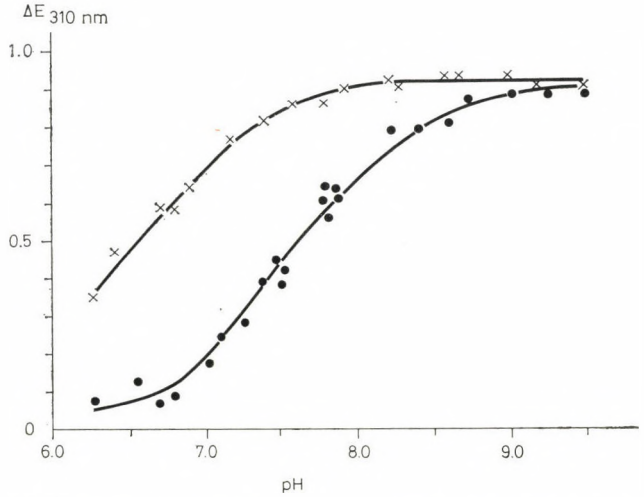

Fig. 2. pH dependence of the absorption difference at 310 nm of the charge-transfer complex between NAD and GAPD alkylated on Cys-149 with NEM. 5.0×10^{-5} M $(NEM)_4$-enzyme solutions were incubated with 2.0×10^{-4} M NAD for about 15 minutes at different pH values indicated on the abscissa in 0.1 M phosphate or Tris-HCl buffer, I = 0.05, at 20°C. Light absorption was measured at 310 nm and the absorption differences were calculated by subtracting the absorption of NAD and NAD-free enzyme (the latter two were independent of pH). The absorption differences were plotted against pH in phosphate (●—●) and Tris-HCl (×—×) buffers

The Racker band of native enzyme–coenzyme complex is due to a charge-transfer interaction, in which the enzyme is the electron donor and the pyridinium ring of the coenzyme is the electron acceptor. The nature of the electron–donor group has been studied by several authors. Some data indicated a tryptophan NAD interaction (Cilento, Tedeschi, 1964). Our earlier results suggested that the Cys-149 thiol group in an activated form could serve as electron donor (Cseke, Boross, 1967; Cseke, Boross, 1970; Boross et al., 1969; Boross, Cseke, 1971). Recent X-ray data (Buehner et al., 1973; Buehner et al., 1974) and the experimental results of Polgár (1975) on the ion-pair formation of Cys-149 thiol group with another side chain (presumably a histidine residue) support the electron-donor property of this mercaptide ionlike sulfur.

In the NEM-modified GAPD the Cys-149 residue is alkylated, therefore the charge-transfer absorption spectrum of the modified enzyme–coenzyme complex could be explained in two ways:

i) the nonbonding electron pairs of the alkylated Cys-149 sulfur atom serve as electron donor, and the charge-transfer excitation requires higher energy, i.e. the wavelength of the exciting photon must be shorter;

ii) another side chain of NEM-GAPD is located in the neighbourhood of bound NAD and serves as electron donor, and the absorption maximum of this charge-transfer spectrum lies at the shorter wavelengths.

The experimental results are insufficient to decide which alternative is true. We found that the Cys-153 residue of $(NEM)_4$-GAPD could not substitute the Cys-149 in the charge-transfer interaction, as the modification of Cys-153 with NEM did not abolish the modified Racker band at 310 nm, only decreased it to about one third (cf. Vas, 1975). In the case of the carboxamidomethylated GAPD-NAD complex the electron-donor role of an imidazole group was suggested (Friderich, 1967). This hypothesis may also be extended to the NEM-modified enzyme.

The change of enzyme–coenzyme charge-transfer spectrum that occurs on alkylation of Cys-149 with NEM, as well as the earlier results on the modification of GAPD-NAD with various reagents (Boross et al., 1966; Friedrich, 1967), lead to the conclusion that the covalent attachment of an alkyl group of structure $-\mathrm{CH}(-\mathrm{C}(=\mathrm{O})-\mathrm{R})-$ to Cys-149 is indispensable for the appearance of a "modified Racker band" in the 300–330 nm wavelength range. The neutral group R can be an alkyl group (e.g. $-CH_3$ as in the case of bromoacetone), an alkoxy group (e.g. $-O-C_2H_5$ when ethyl-iodoacetate is used), an $-NH_2$ (in the case of carboxamidomethylated enzyme) or an acyl-NH group (in NEM-modified GAPD).

The authors wish to express their thanks to Prof. F. B. Straub for helpful discussions and to Mrs M. Szentirmai and to Mrs M. Czéllai for their skilful technical assistance.

References

Boross, L. (1965) Biochim. Biophys. Acta *96* 52
Boross, L. (1969) Acta Biochim. Biophys. Acad. Sci. Hung *4* 57
Boross, L., Cseke, E. (1971) First European Biophysics Congress, Baden, Broda, E., Locker, A.. Springer–Lederer, H. eds., Verlag der Wiener Medizinischen Akademie Vol. VI. p. 123
Boross, L., Cseke, E., Vas, M. (1969) Acta Biochim. Biophys. Acad. Sci. Hung. *4* 301
Boross, L., Cseke, E., Friedrich, P. (1966) 3rd FEBS Meeting Abstract No. 261
Buehner, M., Ford, G. C., Moras, D., Olsen, K. W., Rossman, M. G. (1973) Proc. Natl. Acad. Sci. U.S.A. *70* 3052
Buehner, M., Ford, G. C., Moras, D., Olsen, K. W., Rossman, M. G. (1974) J. Mol. Biol. *82* 563
Cilento, G., Tedeschi, P. (1961) J. Biol. Chem. *236* 907
Cseke, E., Boross, L. (1967) Acta Biochim. Biophys. Acad. Sci. Hung. *2* 39
Cseke, E., Boross, L. (1970) Acta Biochim. Biophys. Acad. Sci. Hung. *5* 385
Friedrich, P. (1965) Biochim. Biophys. Acta *99* 371
Friedrich, P. (1967) Ph. D. Thesis
Harris, J. I., Perham, R. N. (1968) Nature *219* 1025
Polgár, L. (1975) Eur. J. Biochem. *51* 63
Racker, E., Krimsky, J. (1952) J. Biol. Chem. *198* 731
Shifrin, S. (1964) Biochim. Biophys. Acta *81* 205
Vas, M., Boross, L. (1970) Acta Biochim. Biophys. Acad. Sci. Hung. *5* 215
Vas, M. (1975) Biochim. Biophys. Acta, submitted for publication
Velick, S. F. (1953) J. Biol. Chem. *203* 563

Acta Biochim. et Biophys. Acad. Sci. Hung. Vol. 10 (1—2), pp. 7—16 (1975)

Cross-Linking and Coupling of Rabbit Muscle Aldolase and Glyceraldehyde-3-phosphate Dehydrogenase by Glutaraldehyde

J. HAJDU, MAGDA SOLTI, P. FRIEDRICH

Enzymology Department, Institute of Biochemistry,
Hungarian Academy of Sciences, Budapest, Hungary

(Received October 15, 1974)

The mode of cross-linking of rabbit-muscle aldolase and glyceraldehyde-3-phosphate dehydrogenase by glutaraldehyde was studied. The about 5 Å long reagent can partly cross-link subunits within the tetramers, whereas it is readily able to make intermolecular cross-links producing polymeric enzyme species. Of the two enzymes, glyceraldehyde-3-phosphate dehydrogenase has a greater tendency to polymerize in the presence of glutaraldehyde. In the case of aldolase, the inter- and intramolecular cross-links between subunits can be distinguished by SDS gel-electrophoresis. The copolymerization pattern of the two enzymes indicates that, though the formation of mixed polyenzymes can be detected by affinity chromatography on human erythrocyte ghosts, under the conditions tested these proteins do not form heterologous enzyme complexes that could be trapped by glutaraldehyde.

Introduction

Bifunctional reagents offer a unique chemical means to detect functional groups that are sterically close to each other in macromolecules. The two functional groups may reside in one and the same macromolecule or may belong to different macromolecules clustered in a multicomponent aggregate. Accordingly, bifunctional reagents have been applied with success in structure and function studies of single proteins (Quiocho, Richards, 1964) and supramolecular aggregates (Herz, Kaplan, 1972; Subramanian, 1973; Ellar et al., 1971).

In the present work a bifunctional reagent, glutaraldehyde, was used to cross-link and couple two genuinely "soluble" enzymes, aldolase and glyceraldehyde-3-phosphate dehydrogenase* from rabbit muscle. The aim of these investigations was twofold. First, to study the mode and extent of intra- and intermolecular cross-linking of the individual enzymes. Secondly, in view of the possible supramolecular organization of glycolytic enzymes (Clarke, Masters, 1973; Földi et al., 1973), to examine whether any heterologous complexes that can be trapped by glutaraldehyde are formed between these enzymes.

* *Abbreviations:* GAPD, Glyceraldehyde-3-phosphate dehydrogenase; SDS, sodium dodecyl sulfate.

Materials and methods

Aldolase (Fructose-1,6-bisphosphate: D glyceraldehyde-3-phosphate lyase, EC 4.1.2.13) (Taylor et al., 1948) and *GAPD* (D-glyceraldehyde-3-phosphate: NAD oxidoreductase [phosphorylating] EC 1.2.1.12) (Elődi, Szörényi, 1956) were prepared from rabbit muscle and recrystallized three times. Enzyme solutions were freed from ammonium sulfate by gel-filtration on a Sephadex G-50 column equilibrated with 50 mM potassium phosphate buffer, 2 mM EDTA, pH 7.5. Protein concentration was determined on the basis of extinction coefficients $A_{280}^{0.1\%} = 0.74$ (Biszku et al., 1964) for aldolase and $A_{280}^{0.1\%} = 1.0$ (Fox, Dandliker, 1956) for GAPD.

Aldolase activity was assayed by the method of Jagannathan et al. (1956). The specific activity of the enzyme, as defined earlier (Friedrich et al., 1971), was 47, which corresponds to 50 katal $\times$ mole^{-1}, calculated with a molecular weight of 158 000 (Kawahara, Tanford, 1966; Závodszky, Biszku, 1967) for aldolase.

GAPD activity was determined by Warburg's optical test in the following reaction mixture: 5 mM NAD, 5 mM D-glyceraldehyde-3-phosphate, 5 mM Na_2HAsO_4, 0.3 mM EDTA, 50 mM Tris-HCl, pH 7.5, and about 1.5 μg/ml (10^{-5} mM) GAPD. The specific activity of the enzyme was 380 katal $\times$ mole^{-1}, calculated with a molecular weight of 145 000 for GAPD (Elődi, 1958; Harrington, Karr, 1965).

Glutaraldehyde (commercial 25% aqueous solution, Merck or Reanal) was purified by vacuum distillation (Gillet, Gull, 1972); b. p. 77–79°C at 15 mmHg. The purity of the product was checked by the infrared spectrum. As the distillate contained only traces of water, glutaraldehyde stock solutions (2.5 M) were made up by weight. The purified product did not contain materials absorbing around 235 nm (Anderson, 1967; Richards, Knowles, 1968; Gillet, Gull, 1972). The reagent was kept at −20°C; under such conditions there was no change in the ultraviolet spectrum even after one year of storage. The concentration of glutaraldehyde solutions was checked by the method of Hajdu and Friedrich (1975).

Cross-linking of enzymes with glutaraldehyde was carried out at 0°C in 50 mM potassium phosphate buffer, 2 mM EDTA, pH 7.5. The initial concentration of glutaraldehyde varied from 1 to 5 mM. For protein concentration and incubation times see the legends.

Termination of the glutaraldehyde–protein reaction. The methods used so far for the termination of glutaraldehyde cross-linking of proteins, i.e. addition of bisulfite or Tris (Habeeb, Hiramoto, 1968; Kahan, Kaltschmidt, 1972), are of limited applicability because of their undesirable side-reactions or slowness. We introduced a new procedure for this purpose: unreacted glutaraldehyde was removed by trapping with hydrazine. This reagent has the advantages that it is generally not harmful to proteins, has no side reactions and reacts with glutaraldehyde very rapidly (cf. Hajdu, Friedrich, 1975).

As reagent 0.5 M $N_2H_5HSO_4$ solution, adjusted to pH 7.5, was used. To arrest cross-linking, a three-fold molar excess of hydrazine, relative to the initial

glutaraldehyde concentration, was added. As shown in Fig. 1 for aldolase, the activity decrease which accompanied cross-linking (cf. Fig. 2) stopped after the addition of hydrazine and remained constant for several hours. Similarly, the degree of polymerization, as tested by gel-chromatography (cf. below) did not further increase after hydrazine addition. Moreover, hydrazine did not alter the aggregational state produced by glutaraldehyde, as demonstrated by the identical gel-chromatographic patterns obtained immediately and 24 hours after the addition of hydrazine. Similar results were obtained for GAPD. At very high glutaraldehyde concentrations care must be taken to cope with acidification that occurs during the reaction.

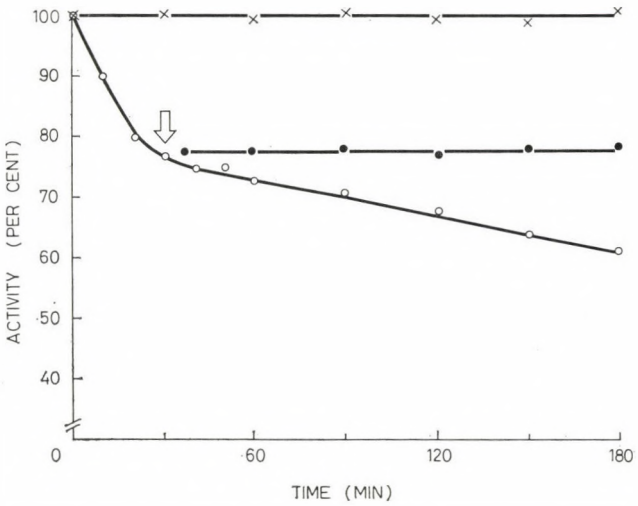

Fig. 1. Termination of aldolase–glutaraldehyde reaction with hydrazine. Aldolase (3.2×10^{-5} M) was incubated in 50 mM potassium phosphate — 2 mM EDTA buffer, pH 7.5, at 0°C with 15 mM $N_2H_5HSO_4$ (×) or 5 mM glutaraldehyde (○). To an aliquot of the latter sample 15 mM $N_2H_5HSO_4$ was added at 30 min (●)

Dimethylsuberimidate was prepared from suberonitrile according to Davies and Stark (1970). Cross-linking was carried out in 0.2 M Triethanolamine.HCl buffer, pH 8.5, with 2 mg/ml dimethylsuberimidate and 3 mg/ml GAPD at room temperature for 3 hours.

Gel-chromatography on Sephadex G-200. The products of cross-linking reactions were separated according to molecular weight on a 2.5×80 cm Sephadex G-200 column equilibrated with 50 mM potassium phosphate buffer containing 2 mM EDTA and 5 mM 2-mercaptoethanol, pH. 7.5, at 4°C. Samples of 2–5 ml containing 10–25 mg of protein were applied to the column. The column was calibrated with Blue Dextran, aldolase, GAPD and myoglobin (mol. weights:

2 000 000, 158 000, 145 000 and 17 500, respectively). Flow rate was 12 ml per hour.

Polyacrylamide gel-electrophoresis in the presence of SDS was carried out by the method of Fairbanks et al. (1971). Molecular weights were determined according to Weber and Osborn (1969). Gel-densitometry was carried out with a Kipp and Zonen Densitometer type DD2.

Human erythrocyte ghosts were prepared as described by Solti and Friedrich (1975). Human blood was washed three times in 0.9% NaCl–20 mM sodium phosphate buffer, pH 7.2. Cells were hemolyzed in 10 mM sodium phosphate buffer, pH 7.4. To one volume of packed red cells 14 volumes of hemolyzing buffer were added at 0°C. Ghosts were collected and then washed three times in 7 mM sodium phosphate buffer, pH 7.4, by centrifuging at 20 000 × g in a Janetzki K-24 centrifuge for 40 minutes at 0°C. The final ghost preparation was slightly pink and contained 8 to 10 mg dry weight per ml. About 10% of the total amount of GAPD present in the hemolysate remained associated to the ghosts.

Spectrophotometric measurements were performed in an Opton PMQ-II spectrophotometer at 25 ± 0.2°C.

Results and discussion

Effect of glutaraldehyde on the activity of aldolase and GAPD

Fig. 2 shows the progress curve of inactivation when aldolase, GAPD and an equimolar mixture of the two enzymes were treated with glutaraldehyde. It is seen that the activity losses of aldolase and GAPD, when treated separately, follow different kinetics; the aldolase curve is biphasic. In the mixture of the two enzymes the inactivation of GAPD is slightly accelerated, whereas that of aldolase is markedly slowed down. Throughout the 2-hour period examined all samples remained clear. However, on prolonged incubation, or at higher protein or glutaraldehyde concentration, precipitate formation occurred.

Gel-chromatography of glutaraldehyde-treated enzymes

To analyze the mode of cross-linking by the bifunctional reagent, the glutaraldehyde reaction was arrested by hydrazine after 60 minutes of incubation (cf. Fig. 2). The mixtures were fractionated on Sephadex G-200 columns. On the basis of molecular weight, the first peak in the elution profiles (Fig. 3) corresponds to species composed of more than two tetrameric enzyme molecules. This will be referred to as "oligotetramer" fraction. The shoulder on this peak contains enzyme dimers ("ditetramer" fraction), and the second peak comprises enzyme molecules that remained single during glutaraldehyde treatment ("monotetramer" fraction). The total enzyme activities and specific activities of these fractions are listed in Table 1.

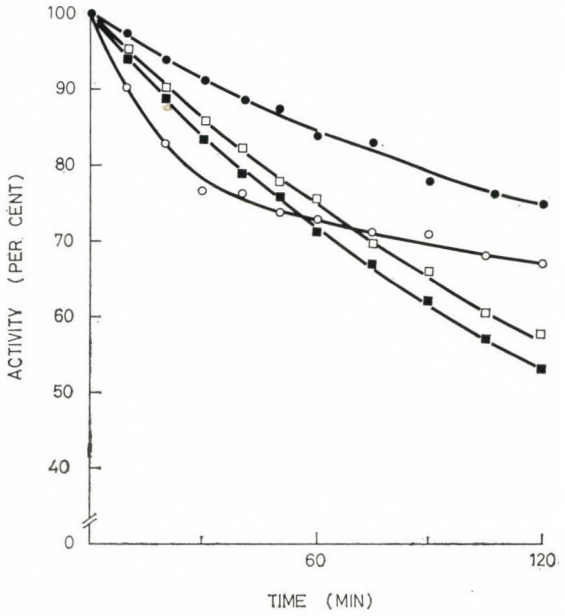

Fig. 2. Effect of glutaraldehyde on the activity of aldolase and GAPD. Aldolase, 3.2×10^{-5} M (5 mg/ml) (○); GAPD, 3.2×10^{-5} M (□); and a mixture of aldolase (●) and GAPD (■) (1.6×10^{-5} M each) was reacted with 5 mM glutaraldehyde in 50 mM potassium phosphate buffer — 2 mM EDTA, pH 7.5, at 0°C. The activity of untreated enzymes was taken as 100%

Table 1

Enzyme activities of cross-linked fractions separated by Sephadex G-200 gel chromatography

Reaction conditions cf. Figs 2 and 3

Enzyme(s) treated with glutaraldehyde	Activity*, per cent		Specific activity**, per cent		
	Monotetramer	Oligo- and ditetramers	Monotetramer	Ditetramer	Oligotetramer
Aldolase	54	46	98	75	56
GAPD	35	65	97	69	57
Aldolase + GAPD	59	41	—	—	—
	32	68	—	—	—

* Total enzyme units applied to the column were taken as 100%
** The specific activities of the native enzymes were taken as 100%

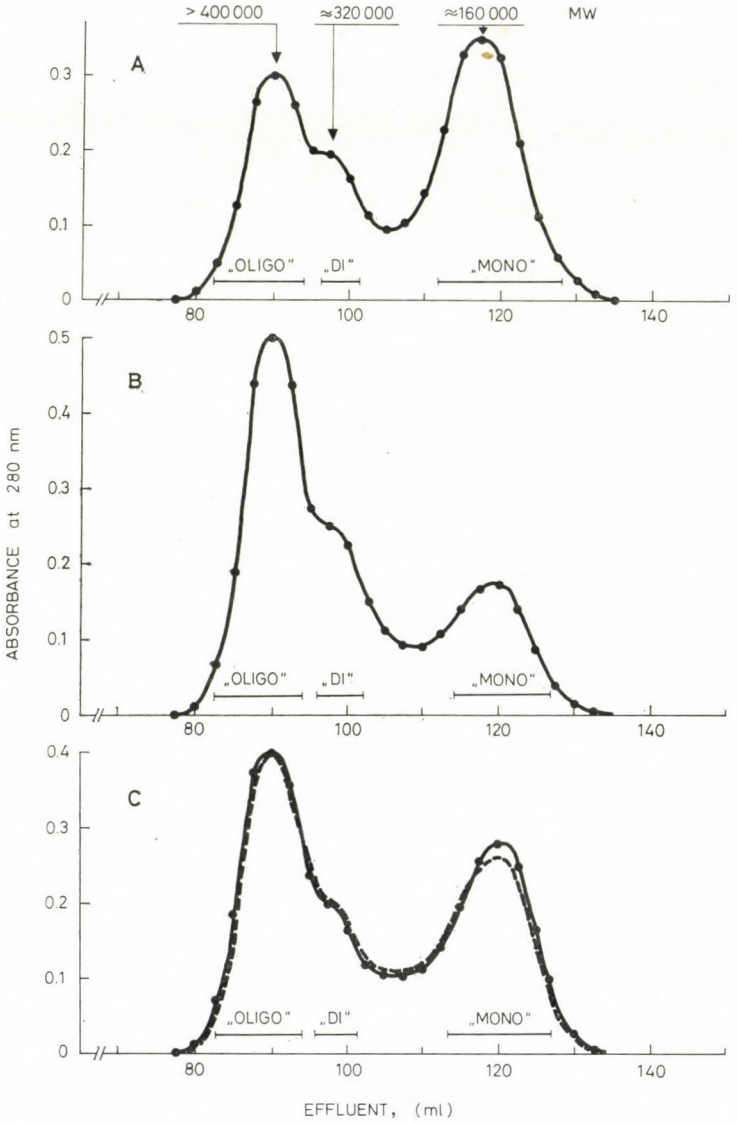

Fig. 3. Gel-chromatography of enzymes cross-linked with glutaraldehyde. The mixtures given in Fig. 2 were incubated for 60 minutes, then polymerization was stopped with hydrazine and an aliquot was gel-chromatographed on a Sephadex G-200 column. In each run 10 mg of protein was applied to the column. A, aldolase; B, GAPD; C, aldolase + GAPD. The dotted line in C is the calculated average of A and B

It is seen from the data that GAPD has a markedly enhanced tendency to polymerize in the presence of glutaraldehyde, as compared to aldolase. Furthermore, the copolymerization pattern of the two enzymes can be accounted for by the superposition of the two separate patterns. It appears that aldolase and GAPD do not interfere with each other's polymerization, although in the initial phase GAPD markedly protects aldolase from inactivation by glutaraldehyde.

SDS gel-electrophoresis of cross-linked enzymes

The "oligotetramer" and "monotetramer" fractions obtained by gel-chromatography were subjected to SDS polyacrylamide gel-electrophoresis to study the structure of cross-linked products (Fig. 4). On the densitometric tracing of electrophoretograms of both aldolase and GAPD monotetramer fractions there are two bands: the faster ones correspond to the subunit molecular weight of aldolase and GAPD (39 000 and 37 000, respectively), whereas the slower ones have molecular weights (76 000 and 74 000 for aldolase and GAPD, respectively) expected for subunit dimers. The finding that the single-subunit band is much stronger than the subunit-dimer band suggests that glutaraldehyde is hardly able to cross-link subunits within the tetramers. This is probably due to the shortness of glutaraldehyde, since dimethylsuberimidate, another bifunctional reagent about twice as long as glutaraldehyde, can readily form intramolecular intersubunit cross-links with these enzymes (cf. Fig. 4 D for GAPD and also Davies, Stark [1970]).

On the electrophoretic pattern of aldolase "oligotetramer" fraction, in addition to the above single-subunit band, a split dimer band was found (molecular weights 79 000 and 76 000). Bands corresponding to subunit trimer and tetramer are scarcely discernible. The splitting of dimer band is probably due to the circumstance that the inter- and intramolecular cross-links between subunits occur at different points of the polypeptide chains, which affects SDS binding and results in a difference of apparent molecular weights.* The "oligotetramer" fraction of GAPD, in keeping with the marked propensity of this enzyme for polymerization, reveals strong subunit trimer and tetramer bands, and even higher polymers can be seen.

The "oligotetramer" fraction of the aldolase + GAPD copolymerization mixture gave an electrophoretic pattern which, as in the case of gel chromatography, can largely be accounted for by the superposition of individual patterns. It should be noted, however, that the resolving power of the system in the 73 000 to

* Davies and Stark (1970) also observed a slight increase of the apparent molecular weight of proteins treated with bifunctional reagents. Such phenomena caution against the use of molecular-weight-standard series in SDS gel-electrophoresis produced by the aid of bifunctional reagents (e.g. Payne, 1973).

79 000 dalton range, where a mixed subunit-dimer would appear, is rather poor, therefore, some minor band can be overlooked. At any rate, there is definitely no major new band attributable to GAPD-aldolase hetero cross-links.

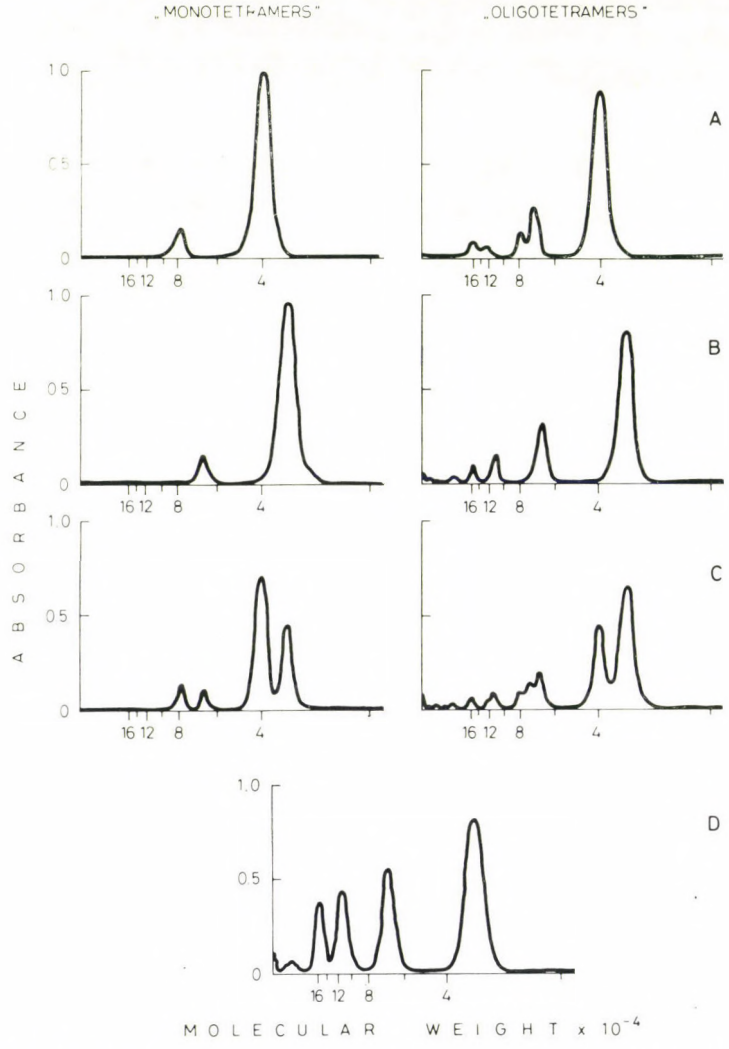

Fig. 4. Densitometric tracing of SDS-gel-electrophoretic patterns of cross-linked products obtained by gel-chromatography. (A), aldolase; (B), GAPD and (C), aldolase + GAPD fractions. (D), GAPD cross-linked with dimethylsuberimidate. About 20 μg of protein was applied to each gel

Detection of heteropolymers by specific binding to erythrocyte ghosts

In the foregoing we excluded the occurrence of preferential coupling of aldolase to GAPD, relative to homopolymerization, by glutaraldehyde under the conditions applied. However, we also had to ascertain whether heteropolymers were formed at all, as the complete lack of hetero-species might also reflect the existence of enzyme–enzyme complexes (in the wrong position for glutaraldehyde coupling). Alternatively, the failure of one enzyme to react with the other may also be due to some peculiar distribution of charge and surface geometry of the two proteins.

In the attempt to detect heteropolymers we made use of our observation that erythrocyte ghosts bind rabbit-muscle GAPD preferentially to rabbit-muscle aldolase; in an equimolar mixture GAPD completely prevents the binding of aldolase (Solti, Friedrich, 1975). Thus the erythrocyte ghost could be used as an affinity adsorbent for GAPD. Table 2 shows that this phenomenon also holds for glutaraldehyde-treated enzymes. There was little aldolase activity associated

Table 2

Binding of polymerized enzymes to erythrocyte ghosts

Enzymes were polymerized as described in Fig. 2. To attain the same degree of polymerization (about 70%), GAPD, aldolase and (GAPD + aldolase) samples were polymerized for 60, 180 and 90 minutes, respectively. Cross-linking was stopped with hydrazine and the mixtures were gel-filtered on a Sephadex G-50 column equilibrated with 7 mM sodium phosphate buffer, pH 7.4. Ghosts were prepared as described in Methods. Binding was performed in suspensions containing 3 mg dry weight/ml ghost and 1 mg/ml of each enzyme at 0°C for 12 hours. Unbound enzymes were removed by washing the ghost pellet three times in 7 mM sodium phosphate buffer, pH 7.4. Enzyme activities of the membrane pellet and washing supernatants were measured. The total enzyme units added to ghosts were taken as 100%

Polymerized enzyme(s) added to ghosts	Activity measured	Enzyme activity recovered, per cent		
		on membrane	in supernatant	total
Poly-GAPD	GAPD	40	15	55
Poly-Aldolase	Aldolase	7	65	72
Poly-GAPD + Poly-Aldolase	GAPD	48	20	68
	Aldolase	0.8	80	81
Poly-{GAPD + Aldolase}	GAPD	33	21	54
	Aldolase	10	64	74

to the membrane if ghosts were incubated with a mixture of separately polymerized enzymes. However, the membrane acquired appreciable aldolase activity, if ghosts were incubated with the copolymerization mixture. Since the membrane-associated aldolase molecules are most probably bound *via* GAPD molecules, this result indicates the presence of GAPD–aldolase mixed polymers.

It is difficult to draw quantitative conclusions concerning the amount of mixed polymers, because of the inevitable loss of enzyme activity that occurs on binding to the membrane (Solti, Friedrich, 1975).

The picture that emerges from these experiments suggests that the polymerization of GAPD and aldolase caused by glutaraldehyde is a random process, under the conditions applied, i.e. there is no indication of its being influenced by any heterologous enzyme complex formation. On the other hand, the altered time course of activity loss in the mixture of aldolase and GAPD might be the consequence of enzyme–enzyme interactions.

References

Anderson, P. J. (1967) J. Histochem. Cytochem. *15* 652–661
Biszku, E., Boross, L., Szabolcsi, G. (1964) Acta Physiol. Acad. Sci. Hung. *25* 161–167
Clarke, F. M., Masters, C. J. (1973) Biochim. Biophys. Acta *327* 223–226
Davies, G. E., Stark, G. R. (1970) Proc. Nat. Acad. Sci. U.S. *66* 651–656
Ellar, D. J., Munoz, E., Salton, M. R. J. (1971) Biochim. Biophys. Acta *225* 140–150
Elődi, P. (1958) Acta Physiol. Acad. Sci. Hung. *13* 199–206
Elődi, P., Szörényi, E. (1956) Acta Physiol. Acad. Sci. Hung. *9* 339–350
Fairbanks, G., Steck, T. L., Wallach, D. F. H. (1971) Biochemistry *10* 2606–2617
Fox, J. B., Dandliker, W. B. (1956) J. Biol. Chem. *221* 1005–1017
Földi, J., Szabolcsi, G., Friedrich, P. (1973) Acta Biochim. Biophys. Acad. Sci. Hung. *8* 263–265
Friedrich, P., Arányi, P., Nagy, I. (1971) Acta Biochim. Biophys. Acad. Sci. Hung. *7* 11–19
Gillet, R., Gull, K. (1972) Histochemie *30* 162–168
Habeeb, A. F. S. A., Hiramoto, R. (1968) Arch. Biochem. Biophys. *126* 16–26
Hajdu, J., Friedrich, P. (1975) Anal. Biochem. (in the press)
Harrington, W. F., Karr, G. M. (1965) J. Mol. Biol. *13* 885–893
Herz, F., Kaplan, E. (1972) Proc. Soc. Exp. Biol. Med. *140* 720–723
Jagannathan, V., Sing, K., Damodoran, M. (1956) Biochem. J. *63* 94–105
Kahan, L., Kaltschmidt, E. (1972) Biochemistry *11* 2691–2698
Kawahara, K., Tanford, C. (1966) Biochemistry *5* 1579–1584
Payne, J. W. (1973) Biochem. J. *135* 867–873
Quiocho, F. A., Richards, F. M. (1964) Proc. Nat. Acad. Sci. U.S. *52* 833–839
Richards, F. M., Knowles, J. R. (1968) J. Mol. Biol. *37* 231–233
Solti, M., Friedrich, P. (1975) in preparation
Subramanian, A. R. (1972) Biochemistry *11* 2710–2714
Taylor, J. F., Green, A. A., Cori, G. T. (1948) J. Biol. Chem. *173* 591–604
Weber, K., Osborn, M. (1969) J. Biol. Chem. *244* 4406–4412
Závodszky, P., Biszku, E. (1967) Acta Biochim. Biophys. Acad. Sci. Hung. *3* 109–112

Acta Biochim. et Biophys. Acad. Sci. Hung. Vol. 10 (1—2), pp. 17—24 (1975)

Quinaldate as an Inhibitor of Mitochondrial Oxidation at the Substrate Dehydrogenase Level

T. KŐNIG

2nd Institute of Biochemistry, Semmelweis University Medical School, Budapest, Hungary

(Received October 15, 1974)

Quinaldate (quinoline-2-carboxylate) inhibits the oxidation of substrates of rat-liver and kidney mitochondria. The concentration of quinaldate required to cause a 50-per-cent inhibition of ADP-activated oxygen uptake slightly differs with various substrates in the same type of mitochondria, and differs with the same substrate in the case of the two types of mitochondria and lies within the mM order of magnitude. In higher concentrations, quinaldate also inhibits the resting respiration (i.e. without ADP). The endogenous respiration of liver mitochondria is also inhibited. The inhibition of oxygen uptake of uncoupled or repeatedly frozen and thawed mitochondria shows the same sensitivity to quinaldate as that of untreated mitochondria in the presence of ADP. TMPD + ascorbate oxidation is not inhibited at all. NADH oxidation (in sonicated mitochondria) is only slightly inhibited even by high concentrations of quinaldate. The inhibition by quinaldate is reversible and of mixed type with respect to 3-hydroxybutyrate as substrate in liver mitochondria, with a K_I of about 0.1 mM. It can be concluded that quinaldate inhibits mitochondrial oxidation at the level of substrate dehydrogenases.

Introduction

Quinaldate (quinoline-2-carboxylate) is one of the physiological end-products of tryptophan catabolism in mammals and is excreted in the urine (Takahashi et al., 1956; Brown, Price, 1956). According to Hanson et al. (1969), quinaldate in appropriate concentration inhibits gluconeogenesis from lactate in intact rat and isolated perfused rat liver by inhibiting the oxidative decarboxylation of pyruvate in liver mitochondria. On the other hand, they claim that quinaldate does not inhibit kidney mitochondrial metabolism *in vitro*. Using quinaldate as an inhibitor of pyruvate metabolism in liver mitochondria, we observed that it inhibited also the oxidation of other mitochondrial substrates and a similar effect could be demonstrated with rat-kidney mitochondria, too. Therefore, it seemed interesting to investigate the mechanism of action of this compound more closely. In this paper it will be shown that quinaldate inhibits mitochondrial oxidation at the level of dehydrogenases. Part of the present work has been published in abstract form (Kőnig, 1972).

Abbreviations: EGTA, ethylenglycol bis-(aminoethyl)-tetraacetic acid; TMPD, N,N,N',N'-tetramethyl-p-phenylenediamine; PCP, pentachlorophenol; RLM, rat-liver mitochondria; RKM, rat-kidney mitochondria.

Materials and methods

Rat-liver and kidney mitochondria were prepared essentially according to Schneider (1948) in a medium containing 250 mM sucrose, 1 mM EDTA (or EGTA) and 4 mM Tris-HCl buffer, pH 7.2, with a teflon-glass homogenizer driven by hand and washed twice in the same medium.

Oxygen uptake was measured with a Clark-type oxygen electrode at 37°C in 3 ml volume in a medium containing 80 mM KCl, 1.0 mM EDTA, 5 mM phosphate-K-Tris, pH 7.2, 20 mM Tris-HCl buffer, pH 7.2. Substrates were added in the form of either Na or Tris salt. Quinaldic acid was used as its Tris salt. The pH of all solutions was 7.2. Other experimental details are given in the legend of figures and tables. The protein content of mitochondrial preparations was determined according to Lowry et al. (1951).

Results

Fig. 1 demonstrates some characteristics of quinaldate action on mitochondrial respiration: a prompt inhibition of ADP-activated ("state 3") 3-hydroxybutyrate oxidation of liver mitochondria (curve a); an inhibition of endogenous respiration of liver mithocondria (curve b); an inhibition of pyruvate + malate

Table 1

Approximate concentrations of quinaldate that cause 50-per-cent inhibition of oxygen uptake in mitochondria in "state 3"

The standard reaction medium contained 2.5 mM ADP, 3.2 mg mitochondrial protein in the case of liver and 2.7 mg in the case of kidney

Substrate(s)	Quinaldate, mM	
	liver	kidney
10 mM pyruvate + 3.33 mM malate	1	2
3 mM 2-oxoglutarate (+ 8.5 mM malonate)	1	4
3.33 mM 3-hydroxybutyrate	1	2*
3 mM glutamate + 3.33 mM malate	2	2
5 mM succinate (+ 2 μM rotenone)	5	8
2 mM isocitrate (+ 3.33 mM malate + 0.3 mM arsenite)	6	4
60 μM palmitoylcarnitine		
+ 3.33 mM malate	< 1	
+ 6.5 mM malonate	< 1	
+ 6.5 mM malonate and 3.33 mM malate	< 1	

* + 3.33 mM malate

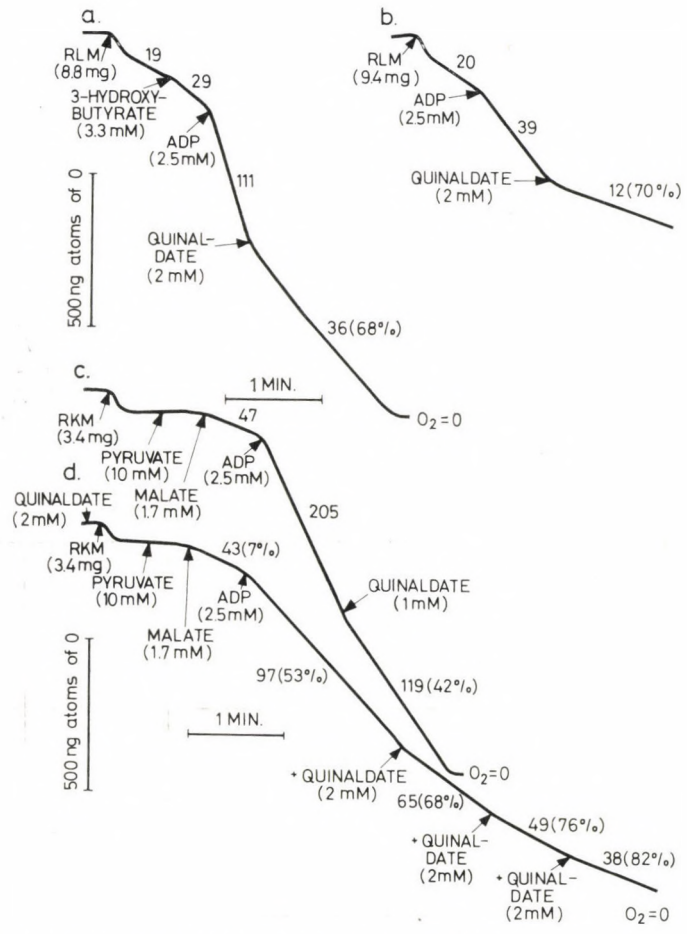

Fig. 1. Characteristics of inhibition of mitochondrial oxidation by quinaldate. Standard reaction medium. Other additions are given at the corresponding figures. The numbers show the oxygen uptake in ng. atoms/mg protein × min, those in brackets give the percentage of inhibition

respiration of kidney mitochondria (curve c, d) which shows saturation kinetics (curve d); in higher concentration an inhibition of the resting ("state 4") respiration, too (curve d). These observations indicate that quinaldate does not uncouple oxidative phosphorylation, it does not act by inhibiting the translocation of substrates through the inner membrane of mitochondria.

Table 1 shows the approximate concentration of quinaldate that causes 50-per-cent inhibition of ADP-activated oxygen uptake of mitochondria in the presence of different substrates. It can be seen that the oxidation of all tested mitochondrial substrates is inhibited, the sensitivities of the oxidation of different

substrates to quinaldate are slightly different and not the same in liver and kidney mitochondria.

In order to locate the action of quinaldate, its effect was studied with uncoupled and repeatedly frozen and thawed mitochondria. As it can be seen in Table 2, both liver and kidney mitochondria show the same sensitivity to quinaldate compared with their appropriate controls after either uncoupling or

Table 2

Effect of quinaldate on native, uncoupled and frozen-thawed mitochondria

The standard reaction medium contained in experiment 1: 10 mM pyruvate, 1.7 mM malate, 4.8 mg rat-kidney mitochondria, and where indicated, 2.5 mM ADP or 17 μM PCP. In experiment 2: 10 mM pyruvate, 1.7 mM malate, 2.5 mM ADP, 3.8 mg rat-kidney mitochondria. In experiment 3: 3.3 mM 3-hydroxybutyrate, 2.5 mM ADP and 9.3 mg rat-liver mitochondria. The reactions were started by the addition of substrates.

No. of experiment	Additions	Oxygen uptake ng atoms/min/mg	Inhibition, per cent
1	Pyruvate + malate oxidation		
	+ ADP	223	–
	+ ADP + 2 mM quinaldate	100	55
	+ PCP	223	–
	+ PCP + 2 mM quinaldate	107	52
2	Pyruvate + malate oxidation		
	Native mitochondria		
	Control	305	–
	+ 2 mM quinaldate	145	52
	10 times frozen-thawed mitochondria		
	Control	243	–
	+ 2 mM quinaldate	126	48
3	3-hydroxybutyrate oxidation		
	Native mitochondria		
	Control	109	–
	+ 0.8 mM quinaldate	51	53
	5 times frozen-thawed mitochondria		
	Control	79	–
	+ 0.8 mM quinaldate	37	53

repeated freezing and thawing. Thus, quinaldate does not act by altering the penetration of substrates across the mitochondrial inner membrane and its effect is independent of the energy state of mitochondria.

Fig. 2 shows an experiment in which the effect of quinaldate on the oxygen uptake of kidney mitochondria was studied by adding different substrates successively to the incubation mixture. As it can be seen, in the presence of a given

concentration of quinaldate, the inhibition of oxygen uptake gradually decreases upon the successive addition of isocitrate and succinate to the system containing already pyruvate and malate. From this experiment two important conclusions can be drawn, namely, that quinaldate – at this concentration at least – acts neither on a common component of the respiratory chain, nor on oxidative phosphorylation.

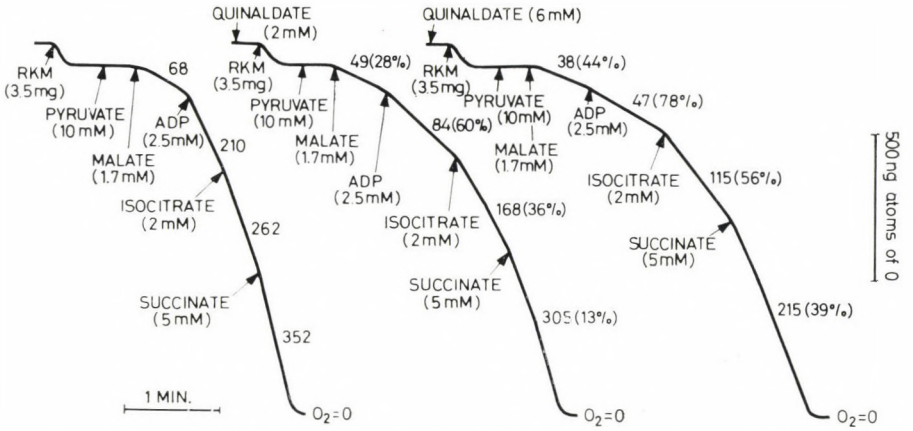

Fig. 2. Site of action of quinaldate. Standard reaction medium. Other details as in Fig. 1

Table 3

Effect of quinaldate on NADH and TMPD + ascorbate oxidation

In the case of NADH oxidation the standard reaction medium contained 2.14 mg sonicated rat-kidney mitochondrial protein. Sonication was performed in 0.03 M K-phosphate (pH 7.0) in an MSE sonicator with 20 kc, 60 W for 4×15 sec with 30 sec breaks. The reaction was started by the addition of 3.33 mM NADH. In the case of TMPD + ascorbate oxidation the standard reaction medium contained 2.5 mM ADP and 1.38 mg rat-kidney mitochondrial protein. The reaction was started by the subsequent addition of 0.3 mM TMPD and 3 mM ascorbate

	Oxygen uptake ng. atoms/ min/mg	Inhibition, per cent
NADH oxidation		
Control	602	–
+ 10 mM quinaldate	575	4
+ 20 mM quinaldate	531	12
+ 30 mM quinaldate	478	21
TMPD + ascorbate oxidation		
Control	628	–
+ 30 mM quinaldate	628	0

Table 4

Reversibility of inhibition by quinaldate

A suspension of rat-kidney mitochondria was preincubated in the standard reaction medium with 12 mM quinaldate at 0°C for 5 min. A portion was used directly for activity measurements. The greater part of mitochondrial suspension was diluted 02fold with the medium used for isolation of mitochondria and washed by centrifugation. This washing procedure was repeated and mitochondria suspended in the isolation medium. Control suspension was preincubated with H_2O and treated exactly in the same way. Protein was determined in all mitochondrial suspensions used for activity measurements. Oxygen uptake was measured in the standard reaction medium which contained 2.5 mM ADP and 10 mM pyruvate + 3.33 mM malate as substrates.

	Quinaldate in the medium, mM	Oxygen uptake, ng. atoms/ min/mg	Inhibition, per cent
Control	—	213	—
	2	115	46
	12	62	71
Preincubated with 12 mM quinaldate	2	115	46
	12	66	69
Control 2× washed	—	244	—
	2	114	53
Preincubated with 12 mM quinaldate 2× washed	—	230	—
	2	114	50

These conclusions were supported by direct evidences from experiments in which the effect of quinaldate on the oxidation of TMPD + ascorbate and NADH (in sonicated mitochondria) was studied. The data of Table 3 clearly demonstrate that the oxidation of cytochrome c is not inhibited at all even by 30 mM quinaldate. The finding that NADH oxidation is inhibited noticeably by only very high concentrations of quinaldate indicates at the same time that the inhibitory effect of quinaldate on mitochondrial oxygen uptake is exerted at the level of substrate dehydrogenases.

To elucidate the mechanism of action of quinaldate, some characteristics of its inhibitory effect were studied. As Table 4 shows, the inhibition by quinaldate of pyruvate + malate oxidation in kidney mitochondria is completely reversible. Inhibition was not enhanced by pre-incubation at high quinaldate concentration, it decreased upon dilution, and could be completely reversed if quinaldate was removed by washing the mitochondria.

Since the inhibitory effect of quinaldate can not be influenced by cysteamine or mercaptoethanol, it does not act on SH groups.

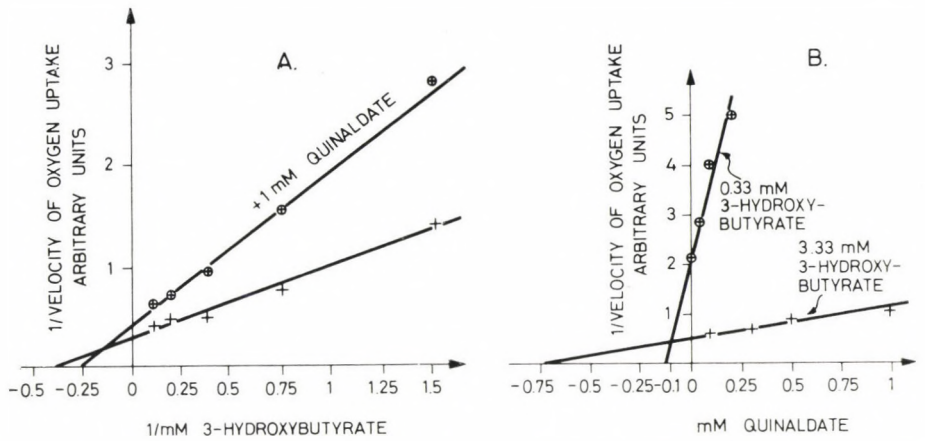

Fig. 3. Type of inhibition of 3-hydroxybutyrate oxidation by quinaldate. Standard reaction medium, 2.5 mM ADP and 9 mg rat-liver mitochondrial protein. Endogenous respiration was subtracted from the values of oxygen uptake measured in the presence of substrate. A: Lineweaver—Burk plot. B: Dixon plot

Kinetic analysis shows (Fig. 3) that the inhibition of 3-hydroxybutyrate oxidation by quinaldate with liver mitochondria is of mixed type, and quinaldate has a K_i of about 0.1 mM.

Discussion

From the experiments presented it can be concluded that quinaldate in the concentrations used does not act on the translocation of substrates across the mitochondrial inner membrane, it does not uncouple or inhibit oxidative phosphorylation and does not inhibit the respiratory chain. Therefore, our finding that the oxidation of all mitochondrial substrates tested is inhibited by quinaldate can be explained on the basis of an inhibitory effect by quinaldate on mitochondrial substrate dehydrogenases. The fact that isolated dehydrogenases of extra- and intramitochondrial origin are also inhibited by quinaldate (Kőnig et al., in prep.) corroborates the validity of this explanation.

With the exception of dehydrogenations, the other mitochondrial functions tested are apparently not influenced at all by quinaldate according to our experiments. These observations suggest that the inhibitory effect of quinaldate on dehydrogenases shows some specificity. From the facts that quinaldate inhibits a great variety of dehydrogenases having substrates of very different chemical structure, and inhibition is kinetically mixed type, it seems improbable that quinaldate interacts with the substrate binding site of dehydrogenases. Since NAD- and FAD-linked dehydrogenases are both inhibited by quinaldate, it is also unlikely

that quinaldate interacts with the coenzyme-binding site. Therefore, quinaldate is most probably bound to that part of the active centre of dehydrogenases which is involved in the catalytic process itself and may be identical or very similar in all dehydrogenases. Another paper deals with the specificity and kinetic analysis of the inhibition by quinaldate of isolated dehydrogenases.

Thanks are due to Mrs E. Pocskay for her excellent technical assistance.

References

Brown, R. R., Price, J. M. (1956) J. Biol. Chem. *219* 985
Hanson, R. L., Ray, P. D., Walter, P., Lardy, H. A. (1969) J. Biol. Chem. *244* 4351
Kőnig, T. (1972) Abstr. Commun. Meet. Fed. Eur. Biochem. Soc. 8. Abstr. No. 652
Kőnig, T., Kocsis, B., Pocskay, E., in preparation
Lowry, O. H., Rosebrough, N. J., Farr, A. L., Randall, R. J. (1951) J. Biol. Chem. *193* 265
Schneider, W. C. (1948) J. Biol. Chem. *176* 259
Takahashi, H., Kaihara, M., Price, J. M. (1956) J. Biol. Chem. *223* 705

Acta Biochim. et Biophys. Acad. Sci. Hung. Vol. 10 (1–2), pp. 25–30 (1975)

On the Mechanism of Activation of CaATPase by a Single Univalent Cation

ILMA SZÁSZ

Department of Cell Metabolism, National Institute of Haematology and Blood Transfusion, Budapest, Hungary

(Received August 28, 1974)

It has been demonstrated with ox-brain microsome membranes that the mechanism of CaATPase activation by a single univalent cation is different in case of Na^+—ont he one hand—and K^+ and its congeners—on the other. Whereas Na^+ increases the amount of ^{32}P protein (phosphorylated intermediate), K^+ causes only an insignificant increase or decrease compared to the Ca^{2+}-containing sample. Our findings support the assumption that the altered activity of the Na—K—ATPase (modified by the presence of Ca^{2+}) is responsible for the univalent cation activation of the CaATPase.

Introduction

Ca^{2+}-dependent ATPase (ATP-phosphohydrolase, EC 3.6.1.3) activity was demonstrated in cell membranes (Dunham, Glynn, 1961; Wins, Schoffeniels, 1966; Cha et al., 1971a) and studied in detail in red blood-cell ghosts. Cha et al. (1971b) briefly reported the existence of a phosphorylated intermediate of the CaATPase in RBC membrane fragments. Recently Knauf et al. (1974) even separated the phosphoproteins associated with CaATPase and Na–K–ATPase in human red cell ghosts. The mechanism of the maintenance of electroneutrality during Ca-pump activity is unknown so far: no simultaneous movement of other ions could be clearly demonstrated. Although CaATPase was found to be activated by a single univalent cation (K^+, Na^+, Rb^+, NH_4^+) in RBC membranes (Schatzmann, Rossi, 1971; Bond, Green, 1971), Schatzmann and Rossi (1971) deny the counter-ion role of univalent cations in the Ca- pump; they raised the possibility that Na–K–ATPase modified by the presence of Ca^{2+} was responsible for the phenomenon. In order to learn more about the function of the single univalent cation-activated CaATPase in cell membranes, we intended to study the mechanism of this activation. To this end the behaviour of the so-called "phosphorylated intermediate" of the enzyme was investigated parallel with its activation by a single univalent cation.

Abbreviations: CDTA, (1,2-cyclohexylene-dinitrilo)-tetraacetate; EGTA, ethylene-glycol-bis-(β-aminoethylether)-N,N'-tetraacetate; RBC, red blood cell.

Materials and methods

RBC membranes and ox-brain microsomes were used in the experiments. RBC membranes were prepared essentially by the method of Davis and Vincenzi (1971) (in a 20 mosmol NaCl medium containing 1 mM EDTA buffered to pH 7.4 with Tris). Ox-brain microsomes were prepared in sucrose medium according to Tanaka and Strickland (1965). Optimal Ca^{2+} activation was found to be at 0.1mM with RBC membranes, and 0.05 mM with microsomes. Above these concentrations Ca^{2+} caused an inhibition of the ouabain-insensitive ATPase activity. Incubation media were as follows: 3 mM Tris-ATP, 3 mM Mg^{2+}, 40 mM imidazole-Cl, pH 7.5, 0.1 mM ouabain. For RBC membranes Ca^{2+} concentration was 0.1 mM, protein content: 0.3 mg/ml, for ox-brain microsomes Ca^{2+} concentration was 0.05 mM, protein content 0.075 mg/ml. Incubation temperature was 37°C, incubation time with RBC membranes 90 minutes, with microsomes 30 minutes. After deproteinization, P_i was determined in the supernatant according to Fiske and SubbaRow (1925).

For isotope experiments ^{32}P-ATP (specific activity: 20 μCi/μmole ATP) was prepared according to Glynn and Chappel (1964). Incubation media were as follows. For RBC membranes: 0.2 mM ^{32}P-Tris-ATP, 1 mM Mg^{2+}, 10 mM imidazole-Cl (pH 7.5), 1 mg/ml protein. (Incubation temperature: 20°C.) For ox-brain microsomes: 0.1 mM ^{32}P-Tris-ATP, 0.1 mM Mg^{2+}, 10 mM imidazole-Cl (pH 7.5), 2 mg/ml protein. (Incubation temperature 0°C.) Final volume was 2 ml in both cases. Incubation time varied between 1 and 120 sec. ATPase activity was determined by measuring the liberated $^{32}P_i$ in a liquid sample counting GM tube after the extraction of P_i according to the Berenblum–Chain method as modified by Martin and Doty (1949). Simultaneously, the amount of ^{32}P protein was determined according to the technique of Post et al. (1965) elaborated for the determination of the phosphorylated intermediate of the Na pump.

Results

In non-isotopic experiments 50 mM univalent cations activated the Ca-ATPase to the following extents: in case of ox-brain microsomes: Na^+ (42%) > > $Rb^+ \sim NH_4^+$ (35–36%) > K^+ (33%) > Li^+ (25%), in case of RBC membranes: Na^+ (38%) > Rb^+ > NH_4^+ (25–28%) > K^+ (20%) > Li^+ (10%). Half-maximum activation was in good agreement with the results of Bond and Green (1971). The highest effectivity of Na^+ was most probably due to the smaller competition between Ca^{2+} and Na^+ under the chosen conditions.

In isotopic experiments with RBC membranes at room temperature measurable enzyme activity could be obtained only at relatively high substrate and at even higher Mg^{2+} concentrations. ATPase activity under these circumstances could be enhanced by Ca^{2+}. On the other hand, if ox-brain microsomes were

incubated at room temperature, a 40–50% or even higher breakdown of ATP was observed and even trace amounts of Ca^{2+} caused an inhibition of the ATPase activity in good agreement with the findings of Rodnight et al. (1966). Incubating the ox-brain microsomes at 0°C, however, and reducing thereby ATP hydrolysis to 10–20%, the essentials of the non-isotopic experiments could be reproduced in tracer experiments as well. Ca^{2+} up to 1 mM concentration activated significantly the MgATPase activity and K^+ and Na^+ caused a further activation of about 29–33%. Na^+ and K^+ effects were not additive and the activation proved to be ouabain-insensitive.

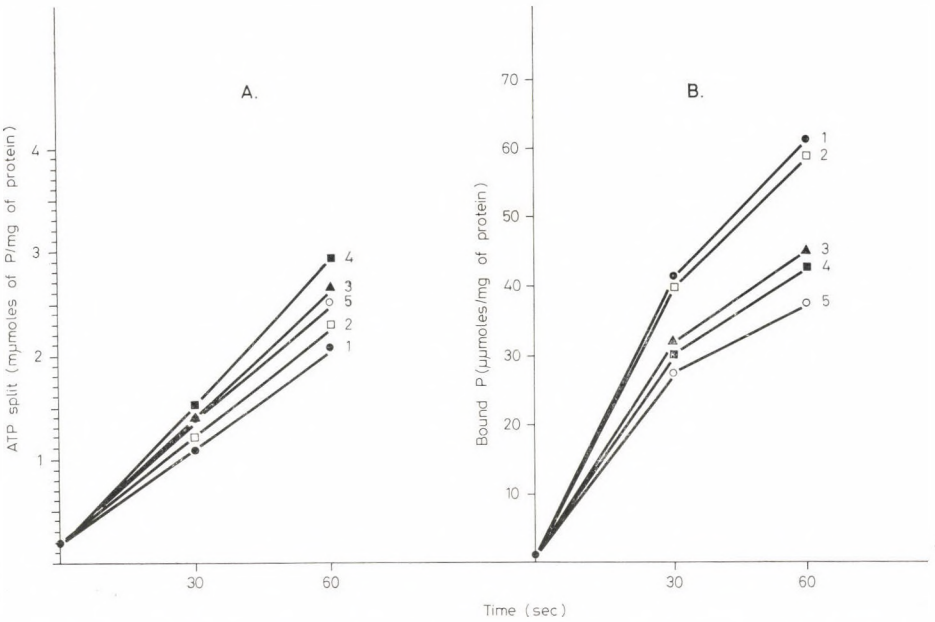

Fig. 1 Effect of Ca^{2+} on the ATPase activity (A) and P-protein formation (B) of ox-brain microsomes. 1: 4 mM Tris EGTA, 2: 1 μM Ca^{2+}, 3: 0.05 mM Ca^{2+}, 4: 0.5 mM Ca^{2+}, 5: 5 mM Ca^{2+}

With ox-brain microsomes the amount of ^{32}P protein was found to be progressively lower on increasing Ca^{2+} concentration from traces to 5 mM (Fig. 1). Due to the high affinity of RBC membranes to P_i and the consequent aspecific adsorption of $^{32}P_i$ (Blake et al. 1967), the same pattern could be found with RBC membranes only if the TCA-washing solutions (from the second washing on) also contained 100 mM inorganic phosphate (instead of 5 mM). Due to the phosphate adsorption the RBC-membrane preparations tested were not ideal for studying the behaviour of ^{32}P protein. However, the results with RBC membranes under the above conditions, are so similar to those obtained with ox-brain micro-

somes that it seems probable that we deal with the same enzyme in both membrane preparations.

In Ca^{2+}-free medium the amount of ^{32}P protein increases significantly in the presence of Na^+ and decreases in the presence of K^+ and its congeners. These changes are attributed to the reactivation of the phosphorylation and dephosphorylation steps of the Na–K–ATPase, respectively (Post et al., 1969). We have

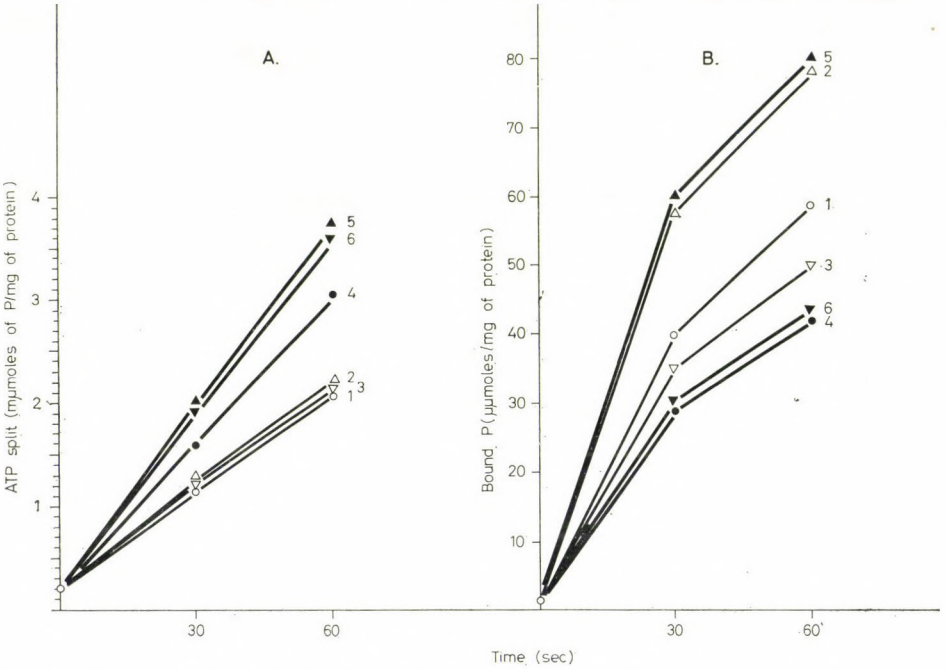

Fig. 2 Effect of Na^+ or K^+ on the ATPase activity (A) and P-protein (B) formation of ox brain microsomes in the presence and absence of Ca^{2+}. 1: 4 mM Tris-EGTA, 2: 4 mM Tris-EGTA + 80 mM Na^+, 3: 4 mM Tris-EGTA + 80 mM K^+, 4: 0.5 mM Ca^{2+}, 5: 0.5 mM Ca^{2+} + 80 mM Na^+, 6: 0.5 mM Ca^{2+} + 80 mM K^+

found that in the presence of 0.5 mM Ca^{2+} which inhibits significantly the Na–K–transport ATPase, 80 mM Na^+ increases the amount of the ^{32}P protein, whereas 80 mM K^+ induces only insignificant changes (slight increase or decrease compared to the Ca^{2+}-containing samples) while increasing ATPase activity (Fig. 2). Similar results were obtained with the congeners of K^+ (Rb^+, NH_4^+, Li_+) as well. Essentially the same ATPase activities were measured in the presence of 0.25 mM ouabain with an insignificant further increase in P_i liberation in addition to the activity obtained in the presence of Ca^{2+} + Na^+ or Ca^{2+} + K^+. The amount of phosphoprotein was slightly reduced by ouabain in systems containing Ca^{2+} + + Na^+, whereas slightly increased in those containing Ca^{2+} + K^+ (Fig. 3). This agrees with the finding of Rodnight et al. (1966) in case if they applied an ionic

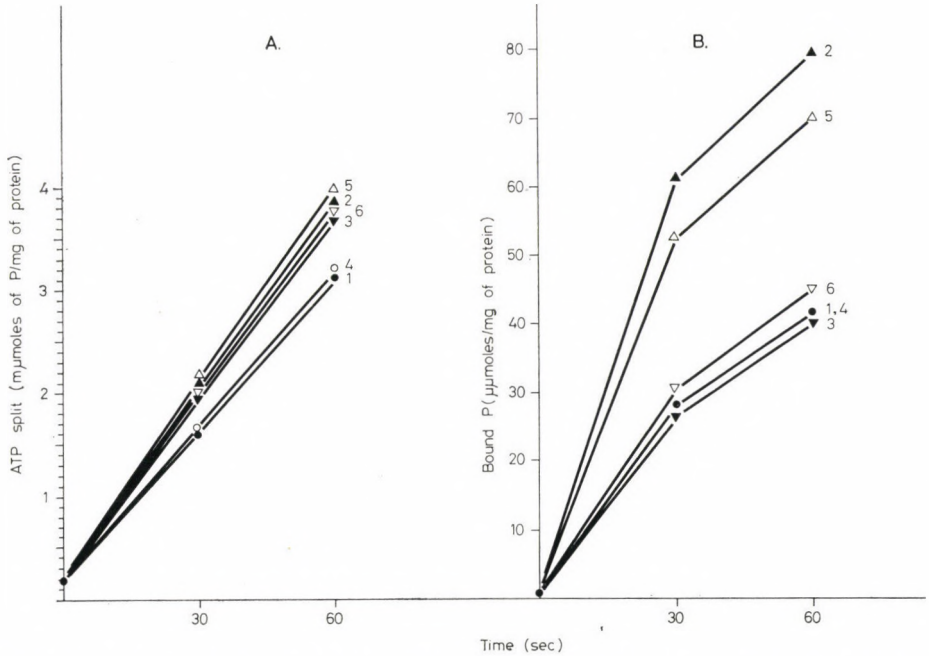

Fig. 3. Effect of ouabain on the ATPase activity (A) and P-protein formation (B) of ox-brain microsomes in the presence of $Ca^{2+} \pm Na^+$ or K^+. 1: 0.5 mM Ca^{2+}, 2: 0.5 mM Ca^{2+} + 80 mM Na^+, 3: 0.5 mM Ca^{2+} + 80 mM K^+, 4: 0.5 mM Ca^{2+} + 0.25 mM ouabain, 5: 0.5 mM Ca^{2+} + 80 mM Na^+ + 0.25 mM ouabain, 6: 0.5 mM Ca^{2+} + 80 mM K^+ + 0.25 mM ouabain

medium similar to ours (but without Ca^{2+}), which resulted in submaximal ATPase activity, but maximal ^{32}P-protein formation in brain microsomes.

With 4 mM EGTA (in the absence of univalent cations (the formation of the ^{32}P-protein could not be blocked. 1–4 mM EDTA or CDTA, however, prevented its formation, which indicates that Mg^{2+} is essential for phosphorylation. The lower amounts of ^{32}P protein in the presence of Ca^{2+} might suggest the activation of dephosphorylation by Ca^{2+}. With CDTA + excess Ca^{2+} or Ca^{2+} + K^+, however, we could not obtain such an appreciable decrease in the amount of preformed phosphorylated protein, which occurs in Na–K–transport ATPase activity on the addition of K^+.

Discussion

According to the above results, the phosphoprotein formed in the presence of Ca^{2+} + Na^+ or K^+ shows striking similarities and well-defined differences compared to the behaviour of the phosphoprotein of the K–Na–ATPase. Knauf

et al. (1974) have found that the amount of the separated Ca + Mg-phosphoprotein was slightly decreased if Na^+ or $Na^+ + K^+$ was added to the erythrocyte ghosts. Simultaneously, the amount of the phosphoprotein attributed to the Na–K–ATPase increased. The enhancement was similar in the two ionic media. This finding suggests that 1. it is the K–Na–ATPase that is affected (activated) by univalent cations in the presence of Ca^{2+}, 2. Na^+ promotes phosphorylation in the presence of Ca^{2+}, whereas K^+, at least if added together with Na^+, does not facilitate dephosphorylation. The mentioned authors did not focus their attention on the effect of K^+ itself in $Ca^{2+} + Mg^{2+}$-containing medium. Our results suggest that in the presence of Ca^{2+}, K^+ and its congeners do not cause significant decrease in the amount of the phosphoprotein, not even in the absence of Na^+.

Schatzmann and Rossi (1971) suggested the following mechanism for the operation of K–Na–ATPase altered by Ca^{2+}: 1. Ca^{2+} might replace Na^+ or K^+; 2. one alkali cation activates both the phosphorylation and the hydrolysis steps; 3. Ca^{2+} uncouples the enzyme and turns it into simple Na^+-activated and K^+-activated ATPase. Our observation on the behaviour of phosphoprotein parallel with the single univalent cation activation of CaATPase also indicates that it is the K–Na–ATPase that is involved in the phenomenon. Furthermore, it reveals that a distinction should be made between activation elicited by Na^+ or K^+ and its congeners. If Na^+ is added, an increased phosphorylation and a K^+-independent dephosphorylation could be assumed (Ca^{2+} might act at the dephosphorylation step, cf. Schatzmann and Rossi's hypothesis 2. above) which results in an amount of phosphoprotein not significantly different from that formed in the $Ca^{2+} + Mg^{2+}$ medium without alkali metal cations.

Part of this work was done at the Department of Physiology, University of Leicester. Thanks are due to Prof. R. Whittam for all his kind help and valuable advice.

References

Blake, A., Leader, D. P., Whittam, R. (1967) J. Physiol. *193* 467
Bond, G. H., Green, J. W. (1971) Biochim. Biophys. Acta *241* 393
Cha, Y. N., Shin, B. C., Lee, K. S. (1971a) J. Gen. Physiol. *57* 202
Cha, Y. N., Shin, B. C., Lee, K. S. (1971b) Fed. Proc. *30* 199
Davis, W., Vincenzi, F. F. (1971) Life Sciences *10* 401
Dunham, E. T., Glynn, I. M. (1961) J. Physiol. *156* 274
Fiske, C. R., SubbaRow, Y. (1925) J. Biol. Chem. *66* 375
Glynn, I. M., Chappel, J. B. (1964) Biochem. J. *90* 147
Knauf, P. A., Proverbio, F., Hoffman, J. F. (1974) J. Gen. Physiol. *63* 324
Martin, J. B., Doty, D. M. (1949) Anal. Chem. *21* 965
Post, R. I., Sen, A. K., Rosenthal, A. S. (1965) J. Biol. Chem. *240* 1437
Post., R. L., Kume, S., Tobin, T., Orcutt, B., Sen, A. K. (1969) J. Gen. Physiol. *54* 30
Rodnight, R., Hems, D. A., Lavin, B. L. (1966 Biochem. J. *101* 502
Schatzmann, H. J., Rossi, G. L. (1971) Biochim. Biophys. Acta *241* 379
Tanaka, R., Strickland, K. P. (1965) Arch. Biochem. Biophys. *111* 583
Wins, P., Schoffeniels, E. (1966) Biochim. Biophys. Acta *120* 341

Acta Biochim. et Biophys. Acad. Sci. Hung. Vol. 10 (1–2), pp. 31–36 (1975)

A "Cytotoxic" Factor Released from Unactivated Human Lymphocytes

MARIA T. SZABÓ, F. ANTONI

1st Institute of Biochemistry, Semmelweis University School of Medicine, Budapest, Hungary

(Received August 22, 1974)

A protein mixture named LTx, was released from human tonsillar lymphocytes, when incubated at 37°C in either "individual" or "mixed" cultures. LTx caused a decrease in the incorporation of ^{14}C-labelled amino acids of the target lymphocytes, while the release of ^{51}Cr from labelled target cells increased. Target cells were found to bind the "toxic" protein.

Introduction

Lymphoid cells can be activated *in vitro* either specifically (with antigens) or non-specifically (with mitogens, e.g. PHA.) In both cases various types of soluble molecules are released, and it is generally assumed that these substances play the role of effector mediators in cellular immunity.

One of these mediators termed lymphotoxin (Granger, Kolb, 1969) or cytotoxin (Peter et al., 1973) is a protein and has been identified as a cytotoxic factor on the basis of its ability to kill target cells, as reflected by the decreased number of cells, decreased rate of amino-acid incorporation into cellular protein and release of ^{51}Cr or ^{14}C-labelled proteins of prelabelled cells. The aim of our present investigation was to answer the question, whether tonsillar lymphocytes, incubated *in vitro* without any activation or in mixed cultures, produce proteins exerting a toxic effect on tonsillar lymphocytes used as target cells.

Materials and methods

All experiments were carried out with lymphocytes isolated from tonsils (removed surgically) of children of 3–10 years (Piffkó et al., 1970). Cells or cell mixtures from 3–5 pooled tonsils were incubated ($1-2\times10^7$ cells/ml) under sterile conditions at 37°C for different periods of time in 100-ml sealed flasks in TC-199 or MEM solution (Eagle's minimal essential medium). The incubation volume was 10 ml. Cells were removed by centrifuging (2500 rpm for 10 minutes)

* *Abbreviation:* PHA, phytohemagglutinin.

at the end of incubation and the effect of the supernatant was investigated on target cells.

^{51}Cr release from ^{51}Cr-labelled target cells was estimated in the presence of the cell-free supernatant. ^{51}Cr activity was measured in a well-type gamma-counter.

To study the effect of the "toxic" supernatant on the amino-acid incorporation of target cells after a 30 min pulse label, the cell-free supernatant was dialysed, freeze-dried (LTx) and dissolved in Hanks' solution. Cells were washed twice with Hanks' solution, proteins were precipitated, washed TCA and finally dissolved in alkali for the determination of protein content by Lowry's method and incorporation with the aid of liquid scintillation spectrometry.

Lymphocytes isolated freshly from pooled tonsils were used as target cells. They were suspended in MEM, TC-199 or Hanks' solution ($5 \times 10^6 - 10^7$ cells/ml).

Results were calculated from the data of 3 parallel batches. The figures represent the results of single experiments.

^{14}C-1-valine(U) 125 mCi mMole and $Na_2{}^{51}CrO_4$ 45 Ci/g: V.V.R. Prague. MEM, TC-199 and Hanks' solutions were supplemented with 0.2 μg/ml glutamine, 100 μg/ml penicillin, 100 μg/ml streptomycin. All solutions were produced at the National Health Service Center (OKI) Budapest.

Results

1. The supernatant obtained after 72 hours of incubation of "mixed" cells enhanced the release of ^{51}Cr from ^{51}Cr-prelabelled target cells as compared to their spontaneous release of ^{51}Cr (Fig. 1).

2. After 72 hours of incubation of "mixed" cells – LTx – prepared from the supernatant, had an inhibitory effect on the ^{14}C-valine incorporation of the target cells, the inhibition was dependent on the amount of LTx protein and became evident within 3 hours. If the time of LTx production was shortened from 72 to 3 hours, the inhibitory effect on amino-acid incorporation remained unaltered. These results allowed us to assume that the formation of LTx was not a consequence of interrelations prevailing in "mixed cells". This suggestion was supported by experiments in which LTx prepared after the incubation of "individual" cells was also effective. The effect of LTx released from "individual" cells after a 4-hour incubation is demonstrated in Fig. 2. Based on these results it could be presumed that the release of LTx from individual or mixed cells was not a consequence of cell destruction, – which seems negligible in the course of the short (4 hours) incubation period.

3. ^{14}C-labelled LTx was prepared from the supernatant of mixed cultures after a 72-hour incubation period. Target cells were incubated at 4 or 37 °C in Hanks' solution for 0–3 hours in the presence of labelled LTx protein. Cells were washed "thoroughly" and their labelling was determined. A considerable part of

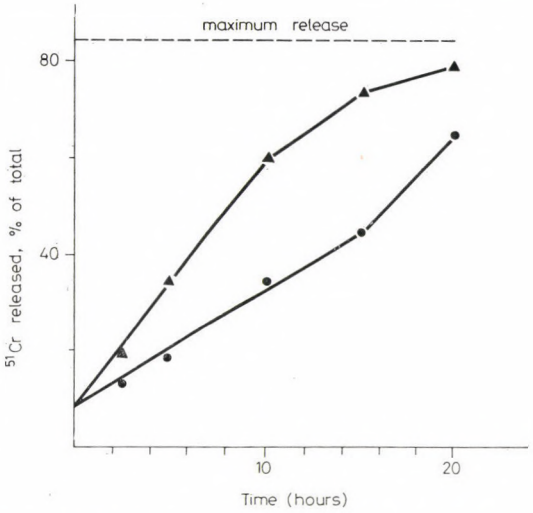

Fig. 1. ^{51}Cr release in the presence of LTx. ^{51}Cr-labelled lymphocytes (5×10^6 cells/ml) were incubated in TC-199 medium at 37°C under sterile conditions in the presence: (▲—▲—▲) and absence (●—●—●) of LTx. LTx is the threefold diluted supernatant of "mixed culture" lymphocytes, 1.5×10^7 cells/ml incubated in TC-199 medium at 37° for 72 hours

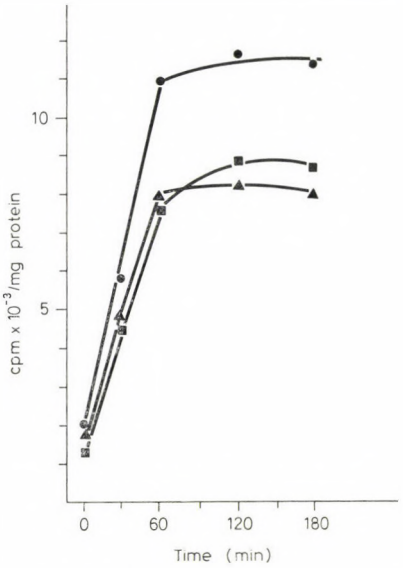

Fig. 2. ^{14}C-valine incorporation into the proteins of target cells in the presence of LTx prepared from "individual" and "mixed culture" cells. 10^7 cells/ml were incubated at 37°C in Hanks' solution. At times indicated, a 30-min pulse label was applied with ^{14}C-valine (μCi/ml). Control: ●—●; LTx: ▲—▲ (330 μg/ml) was prepared from "individual" lymphocytes after a 4- hour incubation period in MEM. LTx: ■—■ (340 μg/ml) was prepared from "mixed culture" lymphocytes after a 4-hour incubation period in Hanks' solution

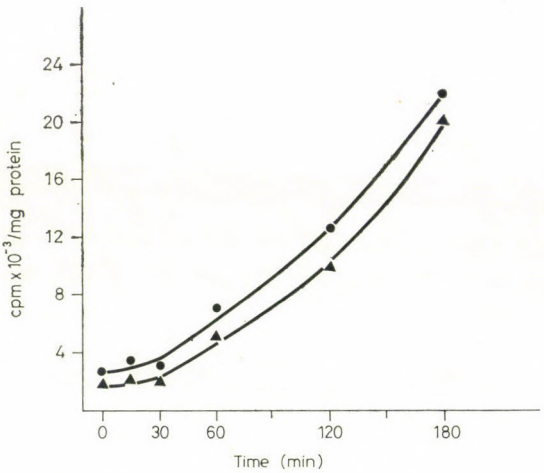

Fig. 3. Uptake of ^{14}C-labelled LTx by target cells at 37° and 4°C. 2.8×10^7 cells were incubated in 1 ml MEM in the presence of 300 μg/ml ^{14}C-labelled LTx. ^{14}C-labelled LTx was prepared from the supernatant of "mixed" cells (10^7 cells/ml) incubated for 72 hours in the presence of ^{14}C-valine (0.3 μCi/ml). Uptake of ^{14}C-LTx at 37°C: ●—●—● and at 4°C: ▲—▲—▲

the ^{14}C-labelled protein was bound by target cells even at low temperature (Fig. 3). The binding of human lymphotoxin to the surface of target cells was assumed by Hessinger et al. (1973) based on similar experiments.

4. The relation between amino-acid incorporation into proteins of target cells and the uptake of amino acid by the same cells was investigated in the following way. Target cells incubated in the presence or absence of unlabelled LTx were pulse-labelled for 30 minutes with ^{14}C-valine. The cells were then washed twice with equal volume of Hanks' solution containing 500 μg/ml valine and precipitated with TCA. The radioactivity of the TCA supernatant was determined, which gave the amount of labelled amino acid that entered the cells without being incorporated into proteins. In addition to the inhibition of amino-acid incorporation into proteins, a simultaneous inhibition of amino-acid uptake could be demonstrated (Fig. 4).

5. Irrespective of its origin ("mixed" or "individual" cultures), if a solution of LTx–protein mixture was heated for 5 minutes (pH 7.2) in a boiling water bath, the centrifuged supernatant did not interfere with the amino-acid incorporation of the target cells.

Discussion

Our investigations point to the fact that in experiments *in vitro* a protein mixture is released both from unactivated and "mixed" lymphocytes isolated from human tonsils which has a toxic effect on target cells also isolated from tonsils,

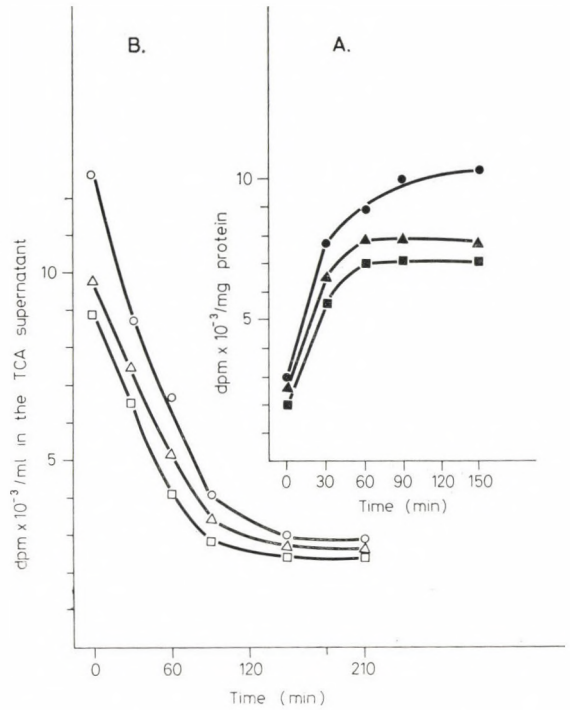

Fig. 4. ^{14}C-valine incorporation into cellular proteins and ^{14}C-valine uptake in the presence of LTx. LTx was prepared from the supernatant of "mixed" cells incubated for 72 hours in MEM. Target cells (10^7 cells/ml) were incubated in Hanks' medium. At the indicated times they received a 30-min pulse label with ^{14}C-valine (1 μCi/ml). A: incorporation into proteins (closed circles). B: amino-acid uptake (open circles). Control: ●—○; LTx (260 μg/ml): ▲—△; LTx (580 μg/ml): ■—□

i.e. it inhibits the incorporation of labelled amino acid and enhanced the release of ^{51}Cr from labelled cells.

Based on our results, we may suggest that the ability to form and to release the "toxic" protein is an endogenous feature of lymphocytes and probably of all lymphoid cells. This assumption is supported by Thistlethwaite (1964) according to whom "normal animals possess lymphoid cells which, when cultured *in vitro*, are capable of lysing syngenic as well as histo-incompatible target cell".

We also assume that the release of the "toxic" protein is due to interchanges *in vitro* between different cell types present in an individual tonsil. Our investigations concerning the ^{51}Cr-binding capacity of tonsillar lymphocytes are in agreement with this concept (Szabó et al., 1974).

According to our investigations, a protein mixture is released from tonsillar lymphocytes in the course of incubation *in vitro*. One component of the mixture

is bound by allogenic tonsillar cells (as target cells) and the amino-acid uptake of these is presumably altered as a consequence of this interaction. Thus it is possible, although we did not investigate any syngenic target cells, that some definite proteins which are in close connection with lymphoid cells *in vivo* and are readily released *in vitro*, may have a regulatory role in cell metabolism. A similar biological role was ascribed to "lymphokines" by Morley, who claimed that lymphotoxin also belongs to this category including all cellular mediators (Morley et al., 1973).

Our results do not prove, but at the same time do not preclude, the possible connection between lymphotoxin and the protein mixture which is released *in vitro* both from "individual" and "mixed" lymphocytes and is toxic for target lymphocytes. Based on its deleterious effect on target cells, this connection is very likely.

The authors are indebted to Dr Imola Varga for valuable help in carrying out the experiments, and to Miss Judit Szabó for skilled technical assistance.

References

Granger, G. A., Kolb, W. P. (1968) J. Immunol. *101* 111
Hessinger, D. A., Daynes, R. A., Granger, G. A. (1973) Proc. Nat. Acad. Sci. *70* 3082
Morley, J., Wolstencroft, R. A., Dumonde, D. C. in Handbook of Experimental Immunology (ed. by D. M. Weir) Blackwell, Oxford, 1973. Vol, II. Chapter 28
Peter, J. B., Stratton, J. A., Stemple, K. E., Yu, D., Cardin, C. (1973) J. Immunol. *111* 770
Piffkó, P., Köteles, G. J., Antoni, F. (1970) Pract. otorhinolaryng. *32* 305
Szabó, M. T., Hrabák, A., Antoni, F. (1974) J. Nuclear Med. *15* 750
Thislethwaite, J. R. (1974) Fed. Proc. 33 Abstracts 599, 3158

Acta Biochim. et Biophys. Acad. Sci. Hung. Vol. 10 (1—2), pp. 37—49 (1975)

Steroid Spectrum in Human Urine as Revealed by Gas Chromatography I. Qualitative Analysis of C_{19}—$C_{21}O_{2-3}$ Steroids

L. KECSKÉS, ZSUZSANNA JURICSKAY

Central Laboratory, University Medical School, Pécs, Hungary

(Received June 24, 1974; in revised form, September 4, 1974)

C_{19}—$C_{21}O_2$ steroids of urine can be analyzed under isothermal conditions by gas chromatography after a pretreatment consisting of mild acid hydrolysis, simultaneous extraction with toluene (or, in the case of $C_{21}O_3$ steroids, enzymatic hydrolysis followed by ether extraction), a short purification step and the formation of derivative. Separation of acetyl derivatives could be achieved by three columns: 3% SE-30, 1.3% NGS and 3% QF-1. These were needed because the separation of 3α-hydroxy-5α-androstan-17-one from 3α-hydroxy-5β-androstan-17-one and that of 3α,20α-dihydroxy-5β-pregnane from 3α,20α-dihydroxy-5α-pregnane could be accomplished only in the NGS fluid phase and QF-1 stationary phase, respectively.

At the same time, this method gives information on the secretion of anabolic androgenic steroids and on the secretion and metabolism of progesterone and 17-hydroxy-progesterone in the human body.

The application of a retention-index system specified for the steroid skeleton and substituents offers the possibility to correlate retention times to molecular structure, which facilitates the identification of problematic metabolites.

Steroid spectra as shown by gas chromatography seem to be a promising tool in the early diagnosis of pregnancy on the basis of the increase in the excretion of 3α,20α-dihydroxy-5β-pregnane.

Abbreviations: A, 3α-hydroxy-5α-androstan-17-one (androsterone), aPd, 5α-pregnanediol group; DHA, 3β-hydroxy-5-androstene-17-one (dehydroepiandrosterone); E, 3α-hydroxy-5β-androstan-17-one (etiocholanolone); Gas Chrom Q, silanized siliceous earth washed with acid; "I", retention index; FID, flame ionization detector; m, arithmetical mean; NGS, neopentylglycol-succinate polyester, liquid phase; 11-OA, 3α-hydroxy-5α-androstan-11,17-dione (11-oxo-androsterone); 11-OHA, 3α,11β-dihydroxy-5α-androstan-17-one (11-hydroxy androsterone); 11-OE, 3α-hydroxy-5β-androstan-11,17-dione (11-oxo-etiocholanolone); Pd, 5β-pregnanediol group; P-20-one, 3α-hydroxy-5β-pregnane-20-one; PT, 3α,17α,20α-trihydroxy-5β-pregnane (pregnanetriol); QF-1, fluoroalkylmethyl-polysiloxan, fluid phase; R, the extent of "resolution" of two neighbouring peaks; RRT, retention time relative to 5α-cholestane; "standard deviation" SE-30, methyl-substituted poly siloxan, fluid phase; S.N., "steroid number"; TMSi trimethylsilyl derivative; T, 17β-hydroxy androst-4-ene-3-one.

Introduction

Methods combining radioactive isotope labelling with protein binding or with immune reactions made the analysis of steroid hormones possible also from the human serum. In spite of this, the importance of the analysis of steroids in the urine has not decreased, as the above methods are applicable only to biologically active steroids and do not give a full account of steroid metabolism.

Gas chromatography has been employed in steroid analysis for more than 10 years. In the field of clinical endocrinology, however, the method is far from being fully exploited. Most of the papers published deal with the determination of a special steroid or steroid group, often after a long purification process. Only few authors (Hoek, van Kampen, 1968; Horning, 1968; Horning, Horning, 1970) have applied a method, multicomponent analysis, which give a comprehensive view of urinary steroid spectrum.

The great advantage of gas chromatography appears in such type of analyses, as a chromatogram differing from the normal is an indicator of steroid metabolism disorder well before the quantitative analysis (e.g., a large pregnanetriol peak points to the disturbance of steroid hydroxylation in the adrenal gland), which makes the diagnosis of endocrine diseases easier. With this possibility in view, a simple method for the analysis of urinary steroids has been developed which can be accomplished without programmed heating. In order to maintain isothermal conditions and to minimize purification necessary before gas chromatographic analysis, the overall steroid spectrum had to be divided into three parts – I: $C_{19}C_{21}O_{2-3}$; II: $C_{21}O_{4-5}$ and III: phenol steroids. In the present paper the analysis of the metabolites of group I., i.e. androgenic anabolic steroids, progesterone and 17-hydroxy-progesterone will be described.

Materials and methods

Extraction and derivative formation

One tenth of the urine collected during 24 hours was used for the experiments. C_{19} and $C_{21}O_2$ steroids were obtained from the urine by mild acid hydrolysis and simultaneous extraction by toluene (Scheme 1). Pregnanetriol, a representative of $C_{21}O_3$ steroids, was enzymatically hydrolysed and extracted with ether (Scheme 2). From a portion of the neutral steroid extract TMSi and from another portion acetyl derivatives were prepared, as derivatives are better separated than native steroids. Furthermore, in the case of two or three functional groups only the derivatives give a quantitatively evaluable chromatogram. An extract corresponding to about 1/1000 part of the daily urine was injected into the column.

Scheme 1

Determination of steroids of the urine by gas chromatography after acid hydrolysis

1/10 of daily urine

1. pH adjusted to 1.0 + addition of 1/2 volume of toluene. Refluxing for 20 min.
2. Addition of 1/10 volume of 60% sulphuric acid followed by refluxing for 20 min.
3. Separation of the organic phase, repeated extraction with 2×1/2 volume of toluene
4. Extraction of the combined toluene phases with 2×1/5 volume of 2 N NaOH
5. Washing of the organic phase with distilled water twice, dried over Na_2SO_4, evaporation

Neutral steroid extract

TM-Silylation

1. Addition of 0.5 ml of hexamethyldisilazane and 3 drops of trimethylchlorosilane to 1/2 part of the extract. Incubated at room temperature for one hour
2. Evaporation under CO_2
3. Dissolved in 100 μl of benzene

Gas chromatography

on 1.3% NGS
FID, column temp.: 210°C
Glass column 6 feet×2 mm i.d.
Carrier gas: N_2

Acetylation

1. Addition of 0.1 ml of pyridine and 0.5 ml of acetic anhydride to 1/2 part of the extract. Incubation in a water bath at 65°C for 30 min.
2. Evaporation under CO_2
3. Dissolved in 100 μl of ethanol

Gas chromatography

1. Separation of A + E, 11-OA, 11-OHA, P-20-on, Pd complex on 3% SE-30. Column temp.: 230°C
2. Separation of A and E with 1.3% NGS
   Column temp.: 210°C
3. Separation of 5α-pregnanediol and 5β-pregnanediol on 3% QF-1
   Column temp.: 210°C, FID
   Glass column 6 feet×2 mm i.d.
   Carrier gas: N_2

Apparatus

Analyses were performed on a Packard 7300 gas chromatograph, at column temperatures of 210°C or 230°C. The carrier gas was nitrogen of high purity. The components were detected by FID. Three kinds of liquid phases were applied: Gas Chrom Q (80–100 mesh, Carlo Erba, Milano) moistened with 3% SE-30 (Merck, Darmstadt), 3% QF-1 (Carlo Erba, Milano) or with 1.3% NGS (Applied Science), in a glass column 6 feet in height with an inner diameter of 2 mm.

Scheme 2

Determination of steroids in the urine by gas chromatography after enzymatic hydrolysis

1/10 of daily urine

1. Heating up to boiling
2. pH adjusted to 5.2 with acetic acid–sodium acetate buffer; addition of 1000 U/ml of Glucuronidase – Aryl sulphatase ("Calbiochem"). Incubated at 37°C for 24 hours
3. Extraction with $3 \times 1/2$ vol. of ether
4. Extraction of the combined ether phases with $2 \times 1/2$ vol. of 2 N NaOH
5. Washing of the organic phase with water twice, dried over Na_2SO_4, evaporation

Acetylation (or TM-silylation) and gas chromatography

Results

The first chromatogram (Fig. 1) shows the TMSi steroids of an extract of female urine from the early period of the secretion phase, after acid hydrolysis on an NGS column. In this case PT is absent from the spectrum as being a molecule – it was broken down during hydrolysis owing to its sensitivity to heat and acids. Compounds A, E, DHA, 11-OA, 11-OE and Pd gave separate peaks on the chromatogram; peak A, however, may contain 3β,20β-dihydroxy-5α-pregnane as well and its resolution (R) from Pd is only 0.71.

A disadvantage of the application of acetyl derivatives is that $C_{19}O_2$ steroids cannot be separated from each other on a QF-1 column. On the other hand, its advantage lies in the fact that, unlike TMSi derivatives, isomers of 5β-pregnanediol are well-separated from both the 5α-pregnanediol group and $C_{19}O_2$ steroids (Fig. 2).

Acetyl steroids can be only partially separated even on an SE-30 column (Fig. 3); DHA, however, is separated from A and E, the latters appearing as one common peak. Isomers of 5β-pregnanediol are incompletely separated from 3α, 20α-dihydroxy-5α-pregnane.

Resolution of the individual steroids of the crude extract obtained by the extraction procedures applied by us cannot be achieved on a packed column, in a single run and with the liquid phases and derivatives described in the literature (Van den Heuvel et al., 1960; Chamberlain et al., 1964). In the case of incomplete separation, the chromatogram obtained is not more than an empirical curve; it was in that sense how Hoek and Van Kampen (1968) used gas-chromatographic steroid spectra for clinical diagnosis. According to our experience, the exact quantitation of steroid excretion can be achieved also from a crude extract if the analysis is performed in two or three runs. There are two alternative ways for this; a) working with two kinds of derivatives (TMSi and acetyl) and b) working with a single type of derivatives (acetyl) on two or three columns.

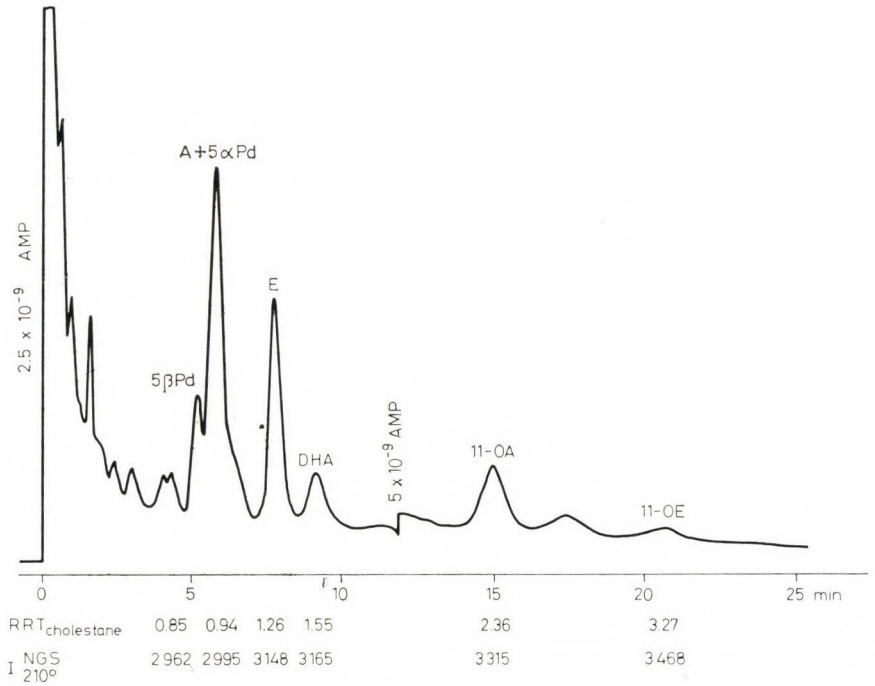

Fig. 1. Gas–liquid chromatogram after acid hydrolysis and silylation of the steroids of an extract of female urine collected in the early secretion phase. Conditions: 1.3% NGS column, inlet temp. 230°, column temp. 210°. Detection: FID

An advantage of acetyl derivatives is their stability; preparations can be stored for a long time without decomposition, which is not the case for TMSi steroids. With this point in view, our further investigations were focused on acetyl derivatives. When the acetyl extract is chromatographed on a 3% SE-30 column, all the important C_{19} steroids can be determined with the exception of A and E, and complex value is obtained for Pd (Fig. 3). It must be noted, however, that under physiological conditions 3α, 20α-dihydroxy-5β-pregnane constitutes the main bulk of Pd, whereas the amount of the other isomers is negligible, except for 3α, 20α-dihydroxy-5α-pregnane. The 5β and 5α pregnanediol group can be separated on a QF-1 column in a second run. Separation of A from E necessitates a third analysis on an NGS column (Fig. 4).

The identification of steroids is usually based on the retention times relative to cholestane. Though this may be a reliable method in one laboratory, it is far from being satisfactory for general use. It was in order to eliminate this ambiguity that Kováts (1958) suggested the use of retention index (I).

In Tables 1 and 2 the retention indices and retentions relative to cholestane of 25 steroids used as references are listed. From the retention index values, the

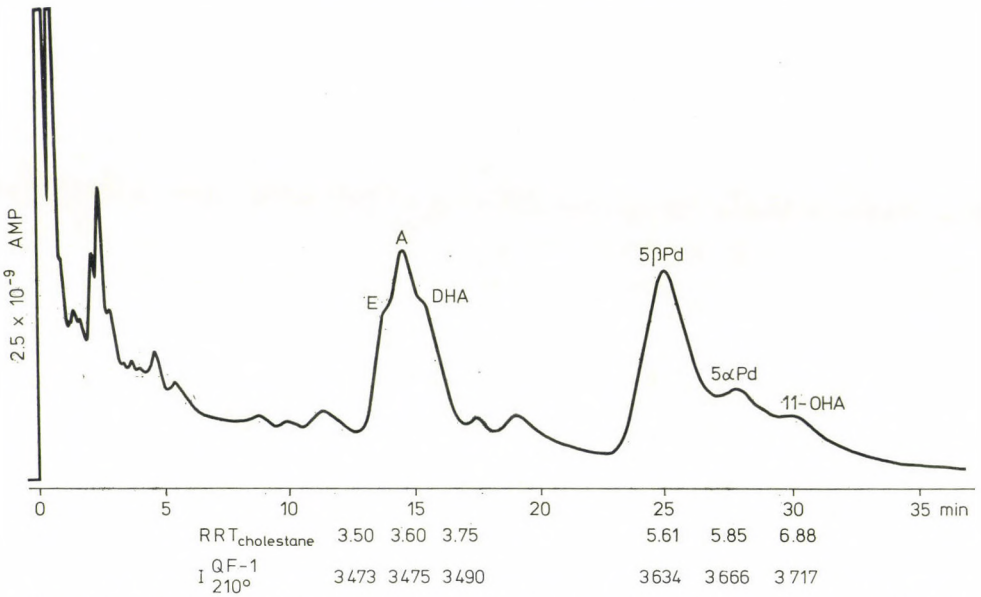

Fig. 2. Gas–liquid chromatogram after acid hydrolysis and acetylation of the steroids of an extract of female urine collected in the secretion phase. Conditions: 3% QF-1 column, inlet temp. 230°, column temp. 210°. Detection: FID

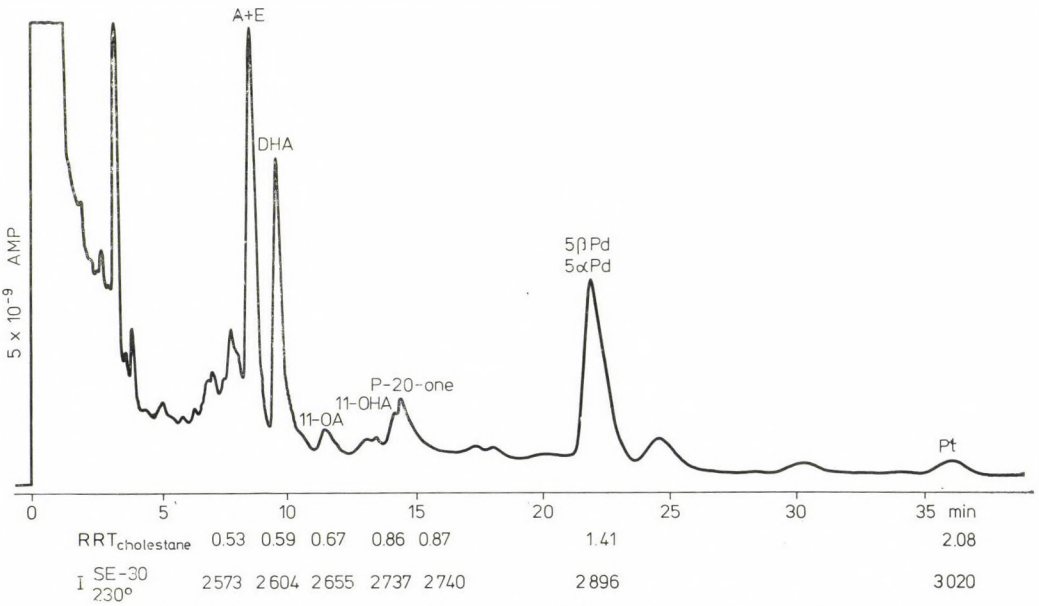

Fig. 3. Gas–liquid chromatogram after enzymatic hydrolysis and acetylation of the steroids of an extract of female urine collected in the secretion phase. Conditions: 3% SE-30 column, inlet temp. 250°, column temp. 230°. Detection: FID

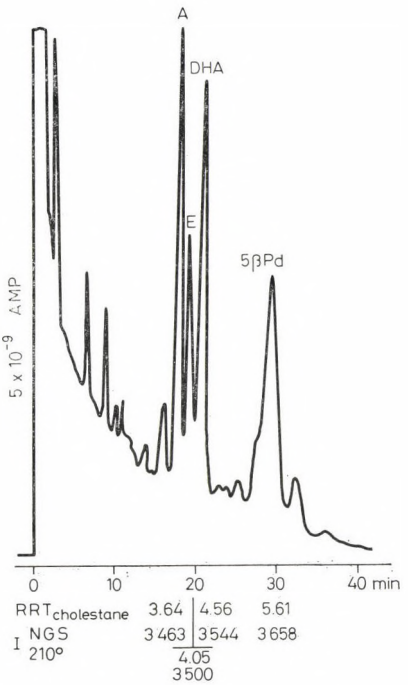

Fig. 4. Gas–liquid chromatogram after acid hydrolysis and acetylation of the steroids of an extract of female urine collected in the secretion phase. Conditions: 1.3% NGS column, inlet temp. 230°, column temp. 210°. Detection: FID

retention index of the steroid skeleton and of the individual functional groups was calculated.

The retention indices of the functional groups were calculated in the following way: from the retention index of a reference steroid containing the functional group in question, that of a steroid of a similar structure but not containing that group was subtracted, e.g. I of 5α-androstan was subtracted from I of 5α-androstan-17-one and thus the retention effect of the 17-keto group was obtained in terms of index units. The results of these calculations are listed in Table 3, which shows the retention indices of the functional groups in each of the three liquid phases used in our experiments. On the basis of Table 3, the retention time of a steroid of an assumed structure can be determined on the chromatogram with the help of a normal paraffin series, or, conversely, the chemical structure of a component giving an unknown peak can be roughly predicted.

The reproducibility of the retention index values was tested on the acetyl derivatives of three steroids (DHA, 3β-hydroxy-5α-androstan-17-one and 3β, 20β-dihydroxy-5α-pregnane acetates). On a 3% QF-1 column, reproducibilities were 3490 ± 9.42, 3524 ± 7.13 and 3680 ± 8.5 index units, respectively, on the basis

Table 1

Retention indices of reference steroids

4-ene and 5-ene unsaturated steroids, the retention index of the 5-α steroid skeleton was used

Chemical name	Basic compound			TM silyl	Acetyl		
	NGS I 210°	QF-1 I 210°	SE-30 I 230°	NGS I 210°	NGS I 210°	QF-1 I 210°	SE-30 I 230°
5α-androstan	2257	2191	2016	—	—	—	—
5β-androstan	2269	2175	2013	—	—	—	—
5α-pregnane	2482	2403	2225	—	—	—	—
5β-pregnane	2442	2367	2196	—	—	—	—
5α-androstan-17-one	2839	2820	2283	—	—	—	—
3α-hydroxy-5α-androstan-17-one	3548	3275	2485	2995	3463	3475	2572
3β-hydroxy-5α-androstan-17-one	3574	3316	2491	3145	3548	3524	2617
3β-hydroxy-5-androstene-17-one	3602	3283	2480	3165	3544	3490	2604
3α-hydroxy-5α-androstan-11,17-dione	—	3536	2568	3315	3792	3756	2655
3α,11β-dihydroxy-5α-androstan-17-one	—	3556	2631	3637	4043	3717	2737
5α-androstan-3,17-dione	3605	3597	2506	—	—	—	—
4-androstene-3,17-dione	3779	3758	2575	—	—	—	—
17α-hydroxy-4-androstene-3-one	3785	3546	2597	3257	3747	3737	2698
17β-hydroxy-4-androstene-3-one	3813	3572	2597	3341	3767	3760	2704
17α-ethynyl-17β-hydroxy-4-androstene-3-one	3940	3552	2664	—	—	—	—
17α-methyl-17β-hydroxy-4-androstene-3-one	3804	3575	2637	—	—	—	—
17α-methyl-17β-hydroxy-4-estrene-3-one	3737	3509	2593	—	—	—	—
3α,20α-dihydroxy-5α-pregnane	3725	3320	2665	2852	3673	3656	2884
3β,20β-dihydroxy-5α-pregnane	3706	3271	2661	3009	3715	3680	2911
3α,20β-dihydroxy-5β-pregnane	3670	3232	2620	2961	3615	3609	2867
3β,20α-dihydroxy-5β-pregnane	3694	3234	2634	2885	3645	3650	2867
3β-hydroxy-5-pregnene-20-one	—	3403	2654	3308	—	3610	2767
3α,17α,20α-trihydroxy-5β-pregnane	—	3533	—	3288	—	3898	3020
3α,17α,21α-trihydroxy-5β-pregnane-11-20-dione	—	—	—	3910	—	—	—
5α-cholestane	3016	2995	2781	—	—	—	—

of standard deviation and 0.47%, 0.40% and 0.46% respectively on the basis of the variational coefficient $\left(\frac{s \times 100}{m}\right)$; on a 3% SE-30 column reproducibilities were 2604 ± 5.1, 2617 ± 4.3 and 2911 ± 7.3 index units and 0.40%, 0.32% and 0.50%, respectively.

Quantitative analysis was performed with internal standardization (relative calibration). Considering the multicomponent nature of the system to be analyzed and the different number of functional groups, several details ought to be discussed

Table 2

Retentions of reference steroids relative to 5α-cholestane

Chemical name	Basic compound			TM silyl	Acetyl		
	NGS 210°	QF-1 210°	SE-30 230°	NGS 210°	NGS 210°	QF-1 210°	SE-30 230°
5α-androstan	0.11	0.12	0.10	—	—	—	—
5β-androstan	0.12	0.11	0.09	—	—	—	—
5α-pregnane	0.22	0.21	0.18	—	—	—	—
5β-pregnane	0.20	0.19	0.16	—	—	—	—
5α-androstan-17-one	0.59	0.63	0.21	—	—	—	—
3α-hydroxy-5α-androstan-17-one	4.50	2.11	0.40	0.94	3.64	3.60	0.54
3β-hydroxy-5α-androstan-17-one	4.65	2.36	0.42	1.46	4.61	4.11	0.60
3β-hydroxy-5-androstene-17-one	5.36	2.16	0.39	1.55	4.56	3.75	0.59
3α-hydroxy-5α-androstan-11,17-dione	—	4.24	0.51	2.36	9.54	7.65	0.67
3α,11β-dihydroxy-5α-androstan-17-one	—	4.48	0.62	5.78	19.50	6.88	0.87
5α-androstan-3,17-dione	5.42	4.96	0.42	—	—	—	—
4-androstene-3,17-dione	8.90	7.66	0.52	—	—	—	—
17α-hydroxy-4-androstene-3-one	9.08	4.36	0.59	2.03	8.22	7.26	0.76
17β-hydroxy-4-androstene-3-one	9.88	4.68	0.59	2.57	8.70	7.74	0.85
17α-ethynyl-17β-hydroxy-4-androstene-3-one	14.46	4.43	0.75	—	—	—	—
17α-methyl-17β-hydroxy-4-androstene-3-one	9.14	4.71	0.63	—	—	—	—
17α-methyl-17β-hydroxy-4-estrene-3-one	7.95	3.95	0.56	—	—	—	—
3α,20α-dihydroxy-5α-pregnane	7.74	2.38	0.69	0.69	6.63	5.85	1.36
3β,20β-dihydroxy-5α-pregnane	7.34	2.09	0.68	0.97	7.51	6.24	1.48
3α,20β-dihydroxy-5β-pregnane	6.60	1.88	0.60	0.79	6.37	5.17	1.29
3β,20α-dihydroxy-5β-pregnane	7.07	1.89	0.63	0.65	6.12	5.75	1.29
3β-hydroxy-5-pregnene-20-one	—	2.97	0.66	2.34	—	5.35	0.96
3α,17α,20α-trihydroxy-5β-pregnane	—	4.21	—	2.22	—	11.03	2.08
3α,17α,21α-trihydroxy-5β-pregnane-11,20-dione	—	—	—	13.28	—	—	—
5α-cholestane	1.00	1.00	1.00	—	—	—	—

here; however, as this would go beyond the scope of the present paper, they will be dealt with in another communication. Nevertheless, one chromatogram is presented in Fig. 5. In this case the considerable increase in the excretion of one steroid results in a very characteristic chromatogram, which is of a diagnostical value even without quantitative evaluation. Fig. 5 shows that in the urine extract, analyzed in the form of TMSi derivatives on an NGS column, the amount of Pd is enormously increased, the corresponding peak well exceeds peak A (cf. Fig. 1). The analyzed urine was collected in early pregnancy; the biological test (Galli–Mainini reaction) performed just after the absence of menstruation was still negative when the increased amount of Pd in urine already indicated pregnancy. One week after the analysis the biological test proved to be positive as well.

Table 3

Retention-index values of the steroid skeleton and the substituents

Nucleus and substituens	NGS I 210°	QF-1 I 210°	SE-30 I 230°	Nucleus and substituens	NGS I 210°	QF-1 I 210°	SE-30 I 230°
C_{19} nucleus 5αH	2257	2191	2016	17α-hydroxy sec	588	417	289
5βH	2269	2175	2013	17β-hydroxy sec	616	443	289
C_{21} nucleus 5αH	2482	2403	2225	17α-hydroxy tert	—	264	139
5βH	2443	2367	2196	17α-silyl sec	60	—	—
C_{27} nucleus 5αH	3051	2995	2781	17β-silyl sec	144	—	—
C_{19} nor	−67	−85	−44	17α-silyl tert	326	—	—
4-ene + 3-one	940	938	292	17α-acetyl sec	550	608	390
5-ene + 3β-hydroxy	763	463	197	17β-acetyl sec	570	631	396
5-ene + 3β-silyl	326	—	—				
5-ene + 3β-acetyl	705	670	321	20α-hydroxy	534	399	226
				20β-hydroxy	489	357	228
3α-hydroxy (5αH)	709	455	202				
3β-hydroxy (5αH)	735	496	208	20α-silyl	222	—	—
3α-hydroxy (5βH)	738	508	196	20β-silyl	221	—	—
3β-hydroxy (5βH)	717	468	200				
				20α-acetyl	566	598	365
3α-silyl (5αH)	156	—	—	20β-acetyl	523	573	352
3β-silyl (5αH)	306	—	—				
3α-silyl (5βH)	297	—	—	21-silyl	108	—	—
3β-silyl (5βH)	220	—	—				
				3-one (5α)	766	777	223
3α-acetyl (5αH)	625	655	294	3-one (5β)	745	784	220
3β-acetyl (5αH)	710	704	334	11-one	320	281	80
3α-acetyl (5βH)	649	669	319	17-one	582	629	267
3β-acetyl (5βH)	636	685	306	20-one	512	537	221
				17α-methyl + 17β-hydroxy	607	380	329
11β-hydroxy	642	242	165	17α-methyl + 17β-silyl	253	—	—
				17α-ethynyl + 17β-hydroxy	743	423	356

Discussion

In the case of TMSi derivatives, the separation on an NGS column of the $C_{19}O_2$ part of the steroid spectrum is rendered difficult by the presence of $C_{21}O_2$ steroids in the extract. The separation of the main component of the latter, i.e. 3α, 20α-dihydroxy-5β-pregnane (RRT_{ch}: 0.85) from androsterone (RRT_{ch}: 0.94) is not completely satisfactory.

In the separation of another isomer, 3β, 20β-dihydroxy-5α-pregnane (RRI_{ch}: 0.97) is also taken into account, we find that this component cannot be separated

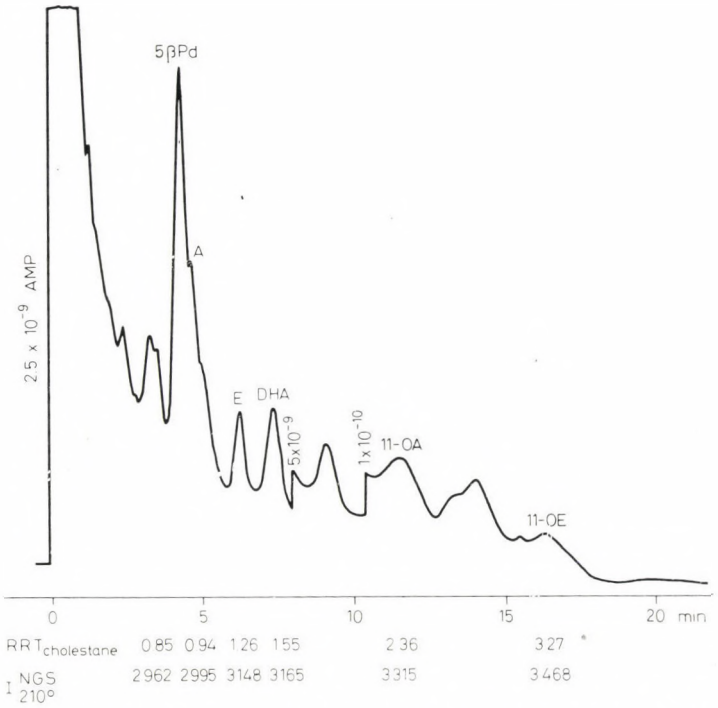

Fig. 5. Gas–liquid chromatogram of the silylated steroids of an extract of urine collected in early pregnancy. Conditions as in Fig. 1

from peak A. The use of TMSi derivatives is rendered even more unfavorable by their limited storability.

With acetyl derivatives there is no interference between $C_{19}O_2$ steroids and the pregnanediol group, a point that drew our attention to acetyl steroids. Though the acetyl derivatives of A and E are not separated on an SE-30 column, sometimes the knowledge of their sum is sufficient, as these two steroids have about the same diagnostic significance in human endocrinology. However, the good separation of DHA is most remarkable, as DHA plays an important role in the diagnosis of adrenal tumours. The separation of A from E, if necessary, can be achieved on an NGS column. However, the use of an NGS column alone is not recommended for the exclusive analysis of acetyl steroids because of the long time requirement. Another difficult task in the analysis of steroid spectra is the separation of pregnanediol isomers. If this is also needed, a QF-1 column must be employed as well. It is well-known that results from different laboratories are not consistent as regards both elution order of pregnanediol isomers and their retention times relative to cholestane. The elution order of the four pregnanediol iso-

mers analyzed by us and that of 3α, 20α-dihydroxy-5β-pregnane isolated from the urine are most consistent with the results of Van der Molen et al. (1968).

From the steroid component of the human metabolic profile, Horning and Horning (1970) succeeded in resolving the whole neutral steroid spectrum in one chromatographic run. In order to attain this, however, the enzymatic hydrolysis of the urine, temperature programming and the formation of double derivatives (TMSi ether plus metoxim) are needed, in addition to a greater number of plates which requires a column length of 12 feet. These conditions are not available everywhere. The same goes for capillary columns, too (Vőlmin, 1970). We assume that the method recommended here could promote the wider application of gas chromatography in endocrinology because of its modest technical requirements in the analysis of the overall steroid spectrum. The $C_{19}-C_{21}O_3$ part of the steroid spectrum furnishes valuable information on the secretion and metabolism of progesterone and 17-hydroxy-progesterone and of the androgen-anabolic hormones of the adrenal glands and the gonads.

We extensively employed the retention-index system in the field of steroid chromatography, which we consider all the more reasonable as its use in other fields of gas chromatography is more and more widespread. This effort of ours agrees with that of several authors (Ballie et al., 1971; Takács et al., 1973), who also characterize the chromatographic motilities of steroids by retention indices. The specification of retention indices to the steroid skeleton and to the functional groups was accomplished on the basis of the "steroid number" concept of Van den Heuvel and Horning (1962).

This concept is based on the observation that the logarithm of the retention times of steroids can be expressed as the sum of the "contributions" of the carbons skeleton and the functional groups. To determine the "steroid number" of a steroid is to compare its RRT relative to cholestane to that of androstane and cholestane under the same conditions. These two references correspond to S.N. 19 and 27, respectively. The S.N. of the steroid in question can be read from the straight line determined by these two pairs of values in a co-ordinate system representing the logarithm of RRT values versus S.N. The effect of a functional group is to increase S.N. as compared to the carbon skeleton, and the increment is characteristic of the functional group.

In the knowledge of retention effect of the functional groups, retention time and molecular structure can be correlated, which facilitates the identification of an unknown metabolite.

We consider that the application of the retention-index system offers several advantages as compared to the system of steroid numbers. On the one hand, in the former case, reference points are supplied by the normal alcane series, thus no special references are needed (androstane, cholestane and, in polar phases, various cholesteryl-esters); furthermore, the identification of steroids becomes linked to the generally used retention-index system of Kováts.

According to our experiments, steroid spectra supplied by gas chromatography seem to be valuable in the early diagnosis of pregnancy too, as – under

the conditions of physiological pregnancy – already a few days after the first absence of menstruation the excretion of Pd is increased to 6–7 mg/day or even higher, whereas it is only 3–5 mg/day during the secretion phase of the menstruation cycle.

The authors are indebted to Professor W. Klyne and Dr D. N. Kirk (Steroid Reference Collection, London), to the Organon Pharmaceutical Factory OSS (representative in Hungary: MgPh Edina Neuber), to Dr Attila Szentirmai (Pharmaceutical Research Institute, Budapest) and to Dr Petr Bocek (Institute of Instrumental Analytical Chemistry, Czechoslovak Academy of Sciences, Brno), who greatly helped us by making reference steroids available for us.

The devoted and versatile technical assistance of Mrs Melinda Temesi is gratefully acknowledged.

References

Ballie, T. A., Brooks, C. J. W., Middleditch, B. S. (1971) in Advances in Chromatography. Zlatkis, A. (editor) p. 147.

Chamberlain, J., Knights, B. A. Thomas, G. H. (1964) J. Endocr. *28* 235

Hoek, W., van Kampen, E. J. (1968) Clinica Chim. Acta *19* 371

Horning, E. C. (1968) in Gas Phase Chromatography of Steroids. Eik-Nes, K. B., Horning. E. C. (editors) Springer-Verlag, Berlin, Heidelberg, New York, p. 55.

Horning, E. C., Horning, M. G. (1970) in Advances in Chromatography. Zlatkis, A. (editor) Chromathography Symposium Department of Chemistry, University of Houston, Houston p. 226.

Kováts, E. (1958) Helvetica Chim. Acta *41* 1915

Takács, J. M., Kocsi, E., Garamvölgyi, E., Eckhardt, E., Lombosi, T., Nyiredi, Sz., Borbély, I., Krasznai, Gy. (1973) J. of Chromatography *81* 1

VandenHeuvel, W. J., Sweeley, C. C., Horning, E. C. (1960) J. Am. Chem. Soc. *82* 3481

VandenHeuvel, W. J., Greech, B. G., Horning, E. C. (1962) Anal. Biochem. *4* 191

VandenHeuvel, W. J., Horning, E. C. (1962) Biochem. Biophys. Acta *64* 416

VandenHeuvel, W. J., Horning, E. C. (1967) in The Gas Liquid Chromagraphy of Steroids. Grant, J. K. (editor) University Press, Cambridge, p. 39.

Van der Molen, H. J., Rommerts, F. F. G., Groen, D. (1968) in Gas Phase Chromatography of Steroids. Eik-Nes, K. B., Horning, E. C. (editors) Springer-Verlag, Berlin, Heidelberg, New York, p. 193.

Vőlmin, J. A. (1970) Chromatographia *3* 233

Acta Biochim. et Biophys. Acad. Sci. Hung. Vol. 10 (1—2), pp. 51—56 (1975)

Study of Alternative Substrates in the Catalytic Reaction of N-acetyl-transferase

I. ALKONYI, E. PÁLFI, D. SZABÓ

Institute of Biochemistry, University Medical School, Pécs, Hungary

(Received March 28, 1974)

In the enzymatic acetylation of para-nitroaniline the esters of para-amino-benzoic acid act as inhibitors since they serve as alternative acceptor substrates. The extent of inhibition is increased by increasing the number of carbon atoms of the alcohol moiety of the esters. The apparent K_m value of esters as acceptor substrates decreases by almost one order of magnitude from 1.1×10^{-4} to 2.5×10^{-5} M within the methylester–butylester series. It has been shown by kinetic analyses that the esters are non-competitive inhibitors in respect of the acetyl donor, whereas they are competitive inhibitors in respect of the acetyl acceptor, in the acetylation reaction of paranitroaniline.

Introduction

It has been shown by Jenne and Boyer (1962) and by Weber and Cohen (1967) that the acetylation reaction catalyzed by acetyl-coenzyme A: arylamine N-acetyl-transferase (EC 2.3.1.5) follows the so-called ping-pong mechanism. This type of kinetics is thoroughly discussed in its generalized form by Cleland (1963).

It has long been known among others from the work of Chou and Lipmann (1952) and Sekeris and Herrlich (1964), that this enzyme has a very broad specificity, especially in respect of the acceptor substrate. This fact and the important role of the enzyme in arylamine metabolism as suggested by Booth (1966) warrant the study of the principle of alternative substrates in the case of N-acetyl-transferase. From among the papers that treat the theory of alternative substrates those of Rudolph and Fromm (1970) and Ricard et al. (1972) might be mentioned.

In our experiments first the inhibition of acetylation of PNA* with acetyl-CoA was studied when various PABA esters were used as alternative acceptor substrates. Out of the five PABA esters tested by us, Riddle and Jencks (1971) only mentioned norcain, the ethylester of PABA. In the paper cited the kinetic constants of norcain in the acetylation reaction by para-nitrophenyl acetate are given. In the present work we examined PABA esters as substrates and alternative substrates in a system which contained acetyl-CoA as acetyl donor.

* *Abbreviations:* PNA, para-nitro-aniline; PABA, para-amino-benzoic acid

Materials and methods

The PABA esters used in the experiments were of "pure" grade (Fluka). Of similar grade were Ellman's reagent (Fluka) and acetyl-CoA (Serva). PNA and all other chemicals were purchased from Reanal (Hungary).

The enzyme was prepared from the acetone dry powder of pigeon liver, by acetone fractionation and purification on aluminium hydroxide gel according to the method of Tabor et al. (1953). The protein concentration of the preparation was 6 mg/ml as determined by the method of Ditterbrandt (1948).

In the monitoring of acetylation reactions, if PNA was used as acceptor substrate, the consumption of PNA was followed spectrophotometrically at 405 nm under conditions corresponding to the method of acetyl-CoA determination of Decker (1962). In the spectrophotometric measurements a Hitachi 124 type recording spectrophotometer was used. In calculating initial velocities, the progress curves were extrapolated to zero time. The condition of linearity was always met in the first 80 sec of the reactions, and mostly for time periods several times this value.

In the experiments where PABA esters were applied as sole acceptor substrates for the determination of the initial velocity of the acetylation reaction, on the basis of formation of free CoA, Ellman's (1959) reagent was used. The photometry was based on the absorption of the 5-thio-2-nitrobenzoate anion, which has an absorption maximum at 412 nm.

Results and discussion

In the study of PABA esters, as alternative acceptor substrates of the N-acetyl-transferase enzyme, first we examined the inhibitory effect of these esters varying the number of carbon atoms of the alcohol that esterifies PABA. (The basic reaction was the enzymatic acetylation of PNA with acetyl-CoA.) To this end, under otherwise identical conditions, a PABA ester as alternative acceptor was included in the reaction mixture in addition to the acceptor PNA. We examined which PABA ester had the strongest inhibitory effect on the acetylation of PNA. The results are shown in Table 1.

It is seen from the data that the inhibitory effect increases with the increasing carbon atom number of the esterifying alcohol. The butylester of PABA is acetylated at the highest rate, thus the acetylation of PNA is most pronouncedly inhibited in the presence of this ester. (It is known that the analgetic effect of these local anaesthetics also increases with increasing chain length of the esterifying alcohol.) Our data are in accord with those of Jacobsen (1961), according to which the decrease of electron-withdrawing effect, or the increase of electron-donor property, of the substituent in *para*-position on the aromatic amine increases the rate of acetylation. On the same grounds we interpret our results, according

Table 1

Inhibition of acetylation of PNA by PABA esters

PABA esters were dissolved in 50% alcohol. To the reaction mixtures not containing PABA esters the same amount of 50% alcohol was added. The composition of reaction mixtures was as follows: 6.7×10^{-2} M phosphate buffer, pH 6.8; 3.3×10^{-3} M EDTA Na_2H_2; 3.3×10^{-3} M 2-mercaptoethanol; 3.3×10^{-3} M KOH. PABA esters were of concentration 2.14×10^{-5} M; PNA 6.6×10^{-5} M; acetyl-CoA: 3.3×10^{-5} M. The acetylation reaction was started by the addition of 0.1 ml enzyme solution. The final volume of reaction mixtures was 3 ml; alcohol concentration 5%

Alternative acceptor substrate	Initial velocity of acetylation nmoles of p-nitro-acetanilide per min	Inhibition,* per cent
—	4.40	—
PABA methylester	2.54	42.3
PABA ethylester	2.17	50.7
PABA propylester	1.69	61.6
PABA i-propylester	1.69	61.6
PABA butylester	1.40	68.2

* In percentage of the initial velocity of the uninhibited reaction

to which the alternative acceptor character of Novokain (4-aminobenzoic acid-/β-diethylamino-ethyl ester) and Bukarban (N-sulphanylyl-N'-butylcarbamide) can only be detected if these compounds are present in a tenfold and hundredfold molar excess, respectively, relative to the 10^{-5} M concentration of PABA esters.

In the following, PABA esters were also tested as sole acceptor substrates, in order to determine their kinetic constants. The great similarity of the absorption spectra of PABA esters and their acetylated derivatives constituted an analytical problem, owing to which they could not be determined spectrophotometrically in the presence of each other. The method of Bratton and Marshall (1939) was also unsuitable, because it cannot be used for continuous kinetic measurements. On the other hand, this method could be successfully applied in the demonstration of the substrate nature of PABA esters. The use of Ellman's (1959) reagent solved the problem of kinetic measurements. With the aid of this compound the amount of free CoA formed in unit time, and indirectly the amount of acetylated PABA ester could be determined with satisfactory accuracy. The apparent K_m values of the PABA esters are shown in Table 2. (The concentration of the other substrate, acetyl-CoA, was very high, almost ensuring substrate saturation.)

It is apparent from the comparison of Tables 1 and 2 that within the methylester–butylester series the K_m value decreases in the direction in which the inhibi-

Table 2

The apparent K_m values of PABA esters

The composition of reaction mixtures: 2×10^{-2} M potassium phosphate buffer, pH 7.63; 6.6×10^{-3} M EDTA Na_2H_2; 1.33×10^{-4} M Ellman's reagent; 2×10^{-4} acetyl-CoA, PABA ester varied from 1×10^{-5} to 2×10^{-3} M. The acetylation reaction was started by the addition of 0.05 ml enzyme solution, the final volume of reaction mixtures was 1.5 ml, alcohol concentration 5%. The photometric reference did not contain Ellman's reagent. The absorbancy change of reaction mixtures not containing acceptor substrate was taken into account

PABA esters	Apparent K_m value
PABA methylester	1.1×10^{-4} M
PABA propylester	4.0×10^{-5} M
PABA butylester	2.5×10^{-5} M

tion by the alternative substrate increases. This finding is in complete accord with what was to be expected.

For the kinetic analysis of inhibition by PABA esters, norcain, the ethylester of PABA, was used as model compound. We examined whether the general principle of Rudolph and Fromm (1970) concerning alternative substrates holds in our case, and what is its actual form. According to this readily conceivable principle in a system of A, A', B the A' is a competitive antagonist of A (B is constant) and a non-competitive antagonist of B (A is constant) or alternatively, in a system of A, B, B' the B' is a non-competitive antagonist of A (B is constant) and a competitive antagonist of B (A is constant). Here A = the donor molecule, A' = the alternative donor molecule, B = the acceptor molecule, B' = the alternative acceptor molecule.

In the case of the presence of alternative substrates, the concept of enzyme inhibition is narrower than the general concept of the inhibition of enzyme reactions, it is obvious that also the concepts of competitive and non-competitive inhibitions, originally solely applied to enzyme inhibitions, may have modified meanings. The above principle, which was originally extended by the authors to cover also isotope competition, has only been corroborated by Purich and Fromm (1972) in respect of alternative substrates.

The experimental results in connection with the above principle are demonstrated in parts I and II of Fig. 1. It appears from Fig. 1, I that the inhibitory effect of norcain, present as alternative acceptor substrate beside PNA, cannot be completely warded off even at high acetyl-donor (acetyl-CoA) concentrations, i.e. in the A, B, A' system B' is a non-competitive antagonist of A (B is constant). Further, it is seen in Fig. 1, II that the inhibitory effect of norcain, present as alternative acceptor substrate beside PNA, can be completely prevented by increasing the concentration of acceptor PNA, consequently in the A, B, B' system

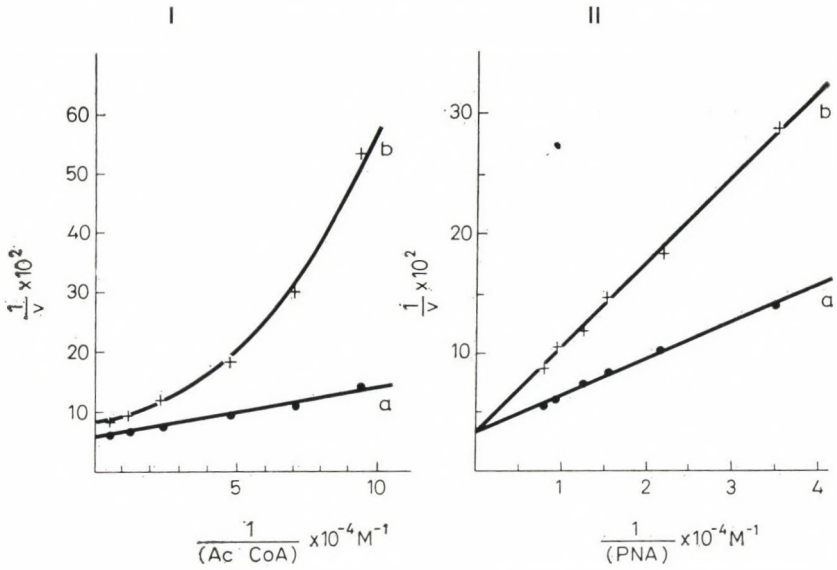

Fig. 1. The prevention of the acetylation of PNA with an excess of acetyl-CoA and PNA as plotted according to Lineweaver and Burk. v = nanomoles of para-nitro-acetanilide formed in 3 ml reaction mixture in one minute. PNA concentration was 6.6×10^{-5} M in all samples of curves I/a and I/b. Norcain was included in the mixture at a concentration of 2×10^{-5} M only in the samples of curve I/b. Acetyl-CoA concentration was 10^{-4} M in all samples of curves II/a and II/b. Norcain was included in the mixture at a concentration of 2.7×10^{-5} M only in the samples of curve II/b. The composition of reaction mixtures was otherwise the same as given in Table 1

B' is a competitive antagonist of B (A is constant). Thus, our data obtained in the ping-pong Bi-Bi reaction of N-acetyl-transferase strongly support the above-mentioned principle of Rudolph and Fromm (1970). It should be noted that several examples have been provided, although not thoroughly discussed, in the literature for the competitive inhibition of alternative substrates even in the case of the ping-pong Bi-Bi reaction of N-acetyl-transferase. For instance, Riddle and Jencks (1971) mention that the enzymatic acetylation of aniline with para-nitro-phenyl acetate is competitively inhibited in respect of the alternative substrates in the ping-pong Bi-Bi mechanism of the N-acetyl-transferase reaction but similar experiments have not yet been reported in the system used by us.

References

Booth, J. (1966) Biochem. J. *100* 745
Bratton, A. C., Marshall, E. K. (1939) J. Biol. Chem. *128* 545
Chou, T. C., Lipmann, F. (1952) J. Biol. Chem. *196* 89
Cleland, W. W. (1963) Biochim. Biophys. Acta *67* 104

Decker, K. (1962) in Methoden der enzymatischen Analyse H. U. Bergmeyer (editor) Verlag Chemie, Weinheim, p. 419
Ditterbrandt, M. (1948) Amer. J. Clin. Path. *18* 439
Ellman, G. L. (1959) Arch. Biochem. Biophys. *82* 70
Jacobson, K. B. (1961) J. Biol. Chem. *236* 343
Jenne, J. W., Boyer, P. D. (1962) Biochim. Biophys. Acta *65* 121
Purich, D. L., Fromm, H. J. (1972) Arch. Biochem. Biophys. *149* 307
Ricard, J., Noat, G., Got, C., Bore, M. (1972) Europ. J. Biochem. *31* 14
Riddle, B., Jencks, W. P. (1971) J. Biol. Chem. *246* 3250
Rudolph, F. B., Fromm, H. J. (1970) Biochemistry *9* 4660
Sekeris, C. E., Herrlich, P. (1964) Hoppe-Seyl. Z. *336* 130
Tabor, H., Mehler, A. H., Stadtman, E. R. (1953) J. Biol. Chem. *204* 127
Weber, W. W., Cohen, S. N. (1967) Mol. Pharmacology *3* 266

Acta Biochim. et Biophys. Acad. Sci. Hung. Vol. 10 (1—2), pp. 57—61 (1975)

Alkali Cation Effects on Mitochondrial Citrate Uptake

S. GYÖRGYI,* E. J. HARRIS

Department of Biophysics, University College London, England

(Received April 25, 1974 and in revised form July 5, 1974)

The effect of alkali cations on the rate of citrate uptake of rat-liver mitochondria and on the citrate adsorption has been studied. In each set of results, as in a series of comparative respiratory studies, Cs^+ is more stimulatory than the other ions. This effect might be the consequence of different electrostatic interactions between the membrane and ions in solution in the case of different cations.

Introduction

The respiratory rates of mitochondria stimulated by ADP or uncoupler are higher in alkali chloride media than in sucrose media of the same tonicity (Harris, Manger, 1968; Cereijo-Santalo, 1968). It has also been observed (Meisner, 1971; Meisner et al., 1972) that the rates of dicarboxylate and phosphate entry are enhanced by the addition of multiply-charged cations, though insignificant differences, or none at all, were observed between members of the alkali cations. Such effects suggest that one factor controlling the rate of substrate entry, and hence the maximum respiratory rate, is the charge on the membrane as affected by adsorption of cations. It is reasonable that adsorbed positive charges should lessen the energy requirement for the anion to enter the membrane from the aqueous phase. Amongst the singly-charged cations it might be the polarizability rather than the ability to penetrate the membrane that is important in this respect. We have chosen to study the effect of the alkali cations on the rate of citrate uptake and on what is presumed to be its adsorption on the membrane. In each set of results, as in a series of comparative respiratory studies, the largest cation of the series (when unhydrated), Cs^+, is more stimulatory than the other members. This contrasts with results of induced cation permeabilities in membranes exposed to the ionophores valinomycin, dinactin or gramicidin B which are in the series $Rb^+ > K^+ > Cs^+ > Na^+$ (Harris, 1968; Pressman, 1965).

* Present address: Institute of Biophysics, Semmelweis Medical University, Budapest, Hungary.

Materials and methods

Rat-liver mitochondria were prepared as described before (Harris et al., 1973). The final suspension was made at 50–70 mg protein/ml in 0.25 M sucrose. Protein was measured by a biuret method (Layne, 1957). Citrate uptakes were measured at 5°, 10° and 14°C, using suspensions containing 4 mg protein/ml in a medium with 100 mM HEPES brought to pH 7.0 with Tris base, 2 mM malate, 10 μM fluorocitrate, 0.2 mM EGTA, a trace amount of ^{3}H-inulin and when stated, the cation added as chloride to 20 mM. Citrate kinetics were observed by using the inhibitor-stop method (Fonyó, 1968; Palmieri et al, 1971). Mitochondria were incubated in 1 ml medium for 1 min, then the ^{14}C-labelled citrate was added to a final concentration of 0.1 mM. Uptake was stopped by adding 0.05 ml of 0.3 M benzene tricarboxylate (Tris salt) which inhibits citrate movement (Robinson et al., 1970). A stream of oxygen was passed through the suspension to provide mixing. After the inhibitor had been added, the mixture was rapidly centrifuged in a Coleman Microfuge. The supernatant was removed and 0.1 ml of 1.5 M perchloric acid was added to the tube to extract soluble constituents from the pellet. After stirring and recentrifuging, part of the extract was taken for radioactivity measurement in a liquid scintillation mixture. Controls were made in which the inhibitor was added before citrate. The ^{3}H-inulin measurements were used to correct for variations in the amount of medium carried by the pellet. The adsorbed citrate was measured by taking samples from incubation mixtures to which nigericin (to equilibrate the internal K^+ against external H^+) and the ionophore A. 23187 (to discharge mitochondrial Mg^{2+} and Ca^{2+}) (Reed, Lardy, 1972) had been added in presence of rotenone to inhibit respiration.

Results

Citrate uptake. The ratio between the mitochondrial citrate content, corrected for the citrate carried by the medium as deduced from the inulin measurements, and the applied citrate concentration increased with time for about 8 min at 14°. The rate was highest in presence of Cs^+, the order of the effects of the cations being $Cs^+ > Rb^+ > K^+ \geq Na^+ = Li^+$.

In order better to establish the significance of the difference between Cs^+, Rb^+ and K^+, sets of uptake measurements were made with these respective ions at 14°, 10° and 5°. The time course of the accumulation at the two higher temperatures is shown in Fig. 1. Straight lines were fitted to the points by the least squares method and the slopes with their standard errors are listed in Table 1. There is no significant difference between the effects of cations when tested at 5°, but the ^{14}C-citrate uptake is significantly higher in the presence of Cs^+ at 10° and 14°C and with Rb^+ at 10°C, than that of K^+ ($p < 0.01$).

Adsorption of citrate. The association of citrate with the mitochondria was measured in presence of rotenone, nigericin, the ionophore A. 23187, and EDTA

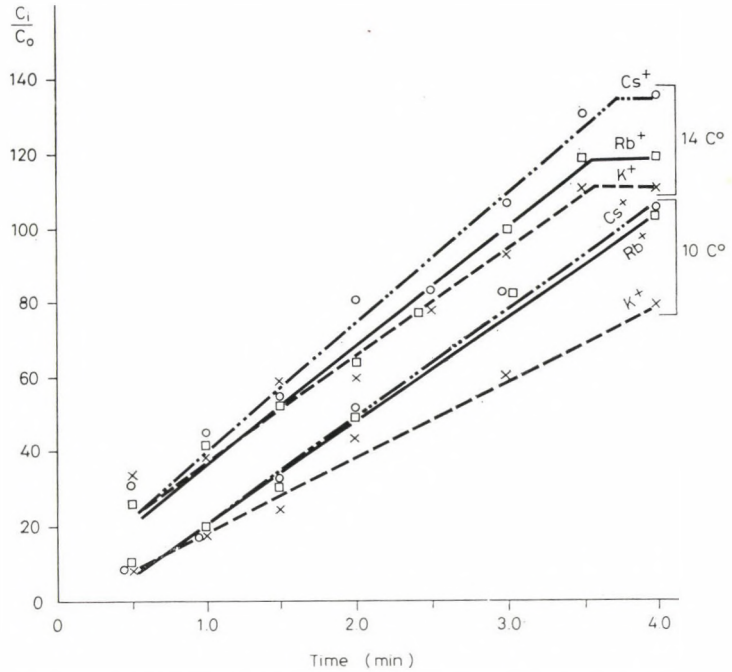

Fig. 1. Time courses of citrate uptake at 14 and 10°C in media containing different alkali chlorides. All media contained Tris HEPES buffer at 100 mM (pH 7.0), citrate 0.1 mM, malate 2 mM, fluorocitrate 10 μM, EGTA 0.2 mM and alternatively 20 mM CsCl (○), RbCl (□) or KCl (×). c_i: citrate concentration in medium (mM). Linearity of the values measured has been supposed, which is represented by the straight lines fitted to the points. However, there is no proof for linearity under 0.5 min, therefore the lines cannot be extrapolated to zero

(0.1 mM). The results in Table 2 show that the order of effect of the cations is $Cs^+ > Li^+ > Na^+ >$ None $> K^+ > Rb^+$ and especially the effect of Cs^+ is significant as compared to the control. The negative effects of K^+ and Rb^+ indicate that factors other than the unhydrated radii might take part in the regulation of citrate adsorption.

Discussion

The enhancement of the rate of entry of citrate and of the rate of oxidation of isocitrate in media supplemented with Cs^+ salt presumably reflects a lower energy requirement for the tricarboxylate to pass from the medium into the membrane when Cs^+ is adsorbed. Evidence has been given for a greater adsorption of citrate when Cs^+ is present. McLaughlin et al. (1970) have stressed the strong dependence of the electrostatic interaction between the membrane and ions

Table 1

Effects of different alkali cations at 20 mM concentration on the rate of citrate uptake measured in the first 5 min at different temperatures

Medium as in Methods with additions of alkali chloride to 20 mM. The three sets of results at different temperatures come from different mitochondrial preparations

Temperature (°C)	Cation	Citrate accumulation factor: concentration in mitochondria (nmoles/mg protein) divided by concentration in medium (mM) (min^{-1})	
			± S.E.
14	K^+	29.0	1.0
	Rb^+	32.4	1.1
	Cs^+	35.6	1.1
10	K^+	20.0	0.7
	Rb^+	26.6	0.8
	Cs^+	26.3	0.8
5	K^+	20.1	0.6
	Rb^+	21.1	0.7
	Cs^+	20.3	0.7

Table 2

Effect of alkali cations on the quantity of citrate associated with mitochondria under conditions where uptake is unlikely (Nigericin, Ca/Mg ionophore A. 23187 and rotenone present)

Mitochondria suspended at 3 mg protein/ml in 100 mM Tris-HEPES, pH 7.0, 0.3 μg nigericin, 15 μg rotenone and 0.07 μg A. 23187 per mg protein, [^{14}C]-citrate 0.23 mM, EDTA 0.15 mM and a trace of ^{3}H-inulin

Cation added to 20 mM	Net citrate corrected for quantity in inulin space n mole/mg protein
None	0.098
Li^+	0.145
Na^+	0.120
K^+	0.065
Rb^+	0.048
Cs^+	0.260

in solution on membrane charge. Of the alkali ions Cs^+ is the most polarizable; Böttcher (1943) has given them in 10^{-24} cm^3 as: Cs^+: 2.42, Rb^+: 1.50, K^+: 0.97, Na^+: 0.22 and Li^+: 0.02.

It is, of course, clear that cations with multiple charge (e.g. Ca^{2+}, Y^{3+}) will fulfil the postulated role of linking agent much more effectively than would any of the alkali cations, as noted by Meisner (1971; Meisner et al., 1972).

References

Böttcher, C. J. (1943) Rec. trav. Chim. Pays Bas *62* 325 quoted by A. J. Dekker in Solid State Physics, Macmillan, London 1958, p. 136

Cereijo-Santalo, R. (1968) Can. J. Biochem. *46* 55

Fonyó, A. (1968) Biochem. Biophys. Res. Comm. *32* 624

Harris, E. J., Manger, J. R. (1968) Biochem. J. *109* 239

Harris, E. J. (1968) in Membrane Models and Formation of Biological Membranes, L. Bolis and B. A. Pethica (editors), North Holland Press, Amsterdam, p. 247

Harris, E. J., Bangham, J. A., Wimhurst, J. M. (1973) Archs. Biochem. Biophys. *158* 236

Layne, E. (1957) Meth. Enzymology *3* 45

McLaughlin, S., Szabó, G., Eisenman, G., Ciani, S. (1970) Proc. Natl. Acad. Sci. U.S. *67* 1268

Meisner, H. (1971) Biochemistry *10* 3485

Meisner, H., Palmieri, F., Quagliariello, E. (1972) Biochemistry *11* 949

Palmieri, F., Prezioso, G., Quagliariello, E., Klingenberg, M. (1971) Europ. J. Biochem. *22* 66

Pressman, B. C. (1965) Proc. Natl. Acad. Sci. U.S. *53* 1076

Reed, R. W., Lardy, H. A. (1972) J. Biol. Chem. *247* 6970

Robinson, R. H., Williams, G. R., Halperin, M. L., Leznoff, C. C. (1970) Europ. J. Biochem. *15* 263

Acta Biochim. et Biophys. Acad. Sci. Hung. Vol. 10 (1—2), pp. 63—70 (1975)

Water Structure in Striated Muscle by Spin Labelling Technique

J. BELÁGYI

Central Laboratory, Medical University, Pécs, Hungary

(Received April 22, 1974)

The electron paramagnetic resonance (epr) spectra of a nitroxide-type free radical (4-hydroxy-2,2,6,6-tetramethyl-piperidinooxyl, *tempol*) equilibrated in muscle water were measured. The results were analyzed in terms of the correlation time or microviscosity. The correlation time of spin probe was only four–five times higher in muscle water than in physiological solutions. The mobility gradually decreased with decreasing relative water content, a restricted mobility having been observed at low relative water content ($i = 0.3$) only. The experimental results can be interpreted without assuming the major part of water phase in striated muscle to be icelike or semicrystalline.

Introduction

In the past decades several experiments were performed on biological systems in order to obtain information on the structure of water and its role in biological systems (Ernst, 1926; 1963). The knowledge of water structure is essential for understanding the different biological functions at submolecular level.

Frank and Evans (1945) introduced the term "frozen" or "icelike" solvent to interpret the strictly ordered association of solvent molecules around the dissolved solute molecules. The same expression have been used by Szent-Györgyi (1957) and Klotz (1958) referring to biological systems. It has been concluded that the water-surrounding proteins in solution or living striated muscle has an icelike structure. On the other hand, Ernst (1963) has pointed out that the relative vapour pressure decrease of cell water measured by differential manometer method (Ernst et al., 1950) in muscle tissue increased by drying the muscle step by step. The results reflected the continuous change of water structure in muscle tissue during dehydration. Furthermore, Pócsik (1967, 1969) has demonstrated the density of water to be higher than the density in bulk water, depending on the own water content of the striated muscle. This means that the increasing density of water is indicative of a gradually increasing boundedness of muscle water. This conclusion cannot be reconciled with the widely discussed and criticized iceberg hypothesis.

The present study is an attempt to add some data to the water structure during gradual dehydration in striated muscle. The spin probe epr method was

applied which had been successfully used by Sukhorukov et al. (1967) in the case of water-DNA and -RNA interaction. The spin-labelling or spin-probe technique proved to be a useful tool in investigating the structural changes in proteins or systems of biological interest (McConnell, McFarland, 1970; Hamilton, McConnell, 1968).

The previous methods on muscle did not permit the dynamic properties of water to be investigated in biological system, except the nuclear magnetic resonance (nmr) studies, which led to controversial conclusions. Many authors have described that the cellular water exists as an organized structure, and that a small fraction of it has a greater degree of hindered motional freedom (Hazlewood et al., 1969; Cope, 1969; Walter, Hope, 1971; Outhred, George, 1973). On the other hand, Finch et al. (1971) reported in the recent years that the mobility of the major fraction of water in muscle was like that of ordinary water. No evidence was found by Hansen (1971) for the existence of non-exchanging fractions of water with differing molecular mobilities. At last, Blinc et al. (1973) stated that the fraction of bound water in tobacco-mosaic-virus solution was much less than 1 per cent.

Materials and methods

The experiments were performed on fibre bundles of frog *(Rana esculenta)* sartorius muscle weighing about 60–90 mg. The fibre bundles were slightly stretched (about 10 per cent over the resting length and stored at 4°C for 16 hours in normal Ringer solution (115.5 mM NaCl, 2.0 mM KCl, 1.8 mM $CaCl_2$ and 2.4 mM $NaHCO_3$ in 1000 ml bidistilled water) which contained the tempol spin probe in concentrations of $10^{-4}-5\cdot10^{-4}$ M. We suppose that the incubation time chosen for the experiments ensured the equilibrium distribution of spin probe in the different water phases of muscle preparations. The height of the low-field component of the nitroxide probe was not changed by varying the time of incubation. It should be noted that the results and conclusions are limited by the fact that there could exist one or more such fractions of the cell water which are inaccessible to the spin probe applied in the experiments. Furthermore, small changes in muscle tissue during incubation cannot be excluded either. The fibre bundles were mounted on a special teflon device before epr measurement and, bound by threads on both ends, could be stretched to the desired length.

The epr spectra were taken at about 9500 MHz using a Zeiss ER 9 spectrometer at room temperature (22°C in the microwave cavity). The long axis of the fibre bundles was perpendicular to the applied magnetic field. The mass of the muscle preparations was measured with an accuracy of 0.1 mg, and the relative water content (i) of them was determined by the usual way:

$$i = \frac{m_i - m}{m},$$

where m_i is the mass of the muscle-fibre bundle in the ith state during dehydration and m is the mass of the dried tissue. The water was removed by drying the fibre bundles in a desiccator at room temperature (23°C). The mass of the dried muscle was taken after desiccation at 107 ± 3°C for 18 hours. The dehydration procedure does not preclude changes in the muscle-protein system which can appear as an inaccuracy in the determination of the epr spectrum parameters. The rotational correlation time characteristic of the tumbling rate of the spin probe was calculated by the equation given by Sukhorukov et al. (1967)

$$\tau_c = 8.4 \cdot 10^{-10} \Delta H_{+1} \left(\sqrt{I_{+1}/I_{-1}} - 1 \right) s$$

where I_{+1} and I_{-1} mean the intensities of the low- and high-field lines, and ΔH_{+1} is the peak-to-peak separation of the low-field line.

According to the experimental experiences, the epr spectrum of both weakly and strongly immobilized spin label can be observed at low water content, therefore, the spectrum parameters $\Delta H^{(+1)}$ and $2A_{zz}$ were determined as well. $\Delta H^{(+1)}$ is defined as the separation between the low-field line and central line of the spectrum of strongly immobilized spin label. The field calibration is based on the 13 G coupling constant of peroxyl-amine disulphonate.

Results

The epr spectra of the spin probe during dehydration of the muscle preparations are shown in Fig. 1 at different relative water contents (see the i values in the figure). As seen, the epr spectrum of the strongly immobilized spin probe can only be observed in the range of $i < 0.4$.

The rotational correlation time of the spin probe in non-dehydrated muscle-tissue preparations was $0.9 \cdot 10^{-10}$ s on the average. However, when the spin probe was dissolved in physiological Ringer solution, a rotational correlation time of $\tau_c = 0.2 \cdot 10^{-10}$ s was measured. If we assume that the classical Stokes low relation can be applied in the case of the water space of muscle tissue, the microviscosity of the muscle fluid is about 4 – 5 times higher than that of the physiological solution. Since studies on the muscle structure revealed the water phase of the striated muscle to be heterogeneous, a more correct quantitative study could only be done on single muscle fibres. At least three water phases can be distinguished in which the water can exist in states of different motional freedom. Ernst (1963) has emphasized the heterogeneous structure of cell water in striated muscle but, as first approximation, the water phase is considered as a homogeneous entirety of the muscle in the present paper.

The absence of strongly immobilized type signal at high relative water content has led us to suggest that the water space of striated muscle does not contain such major fractions, in which the water would be in the so-called icelike or

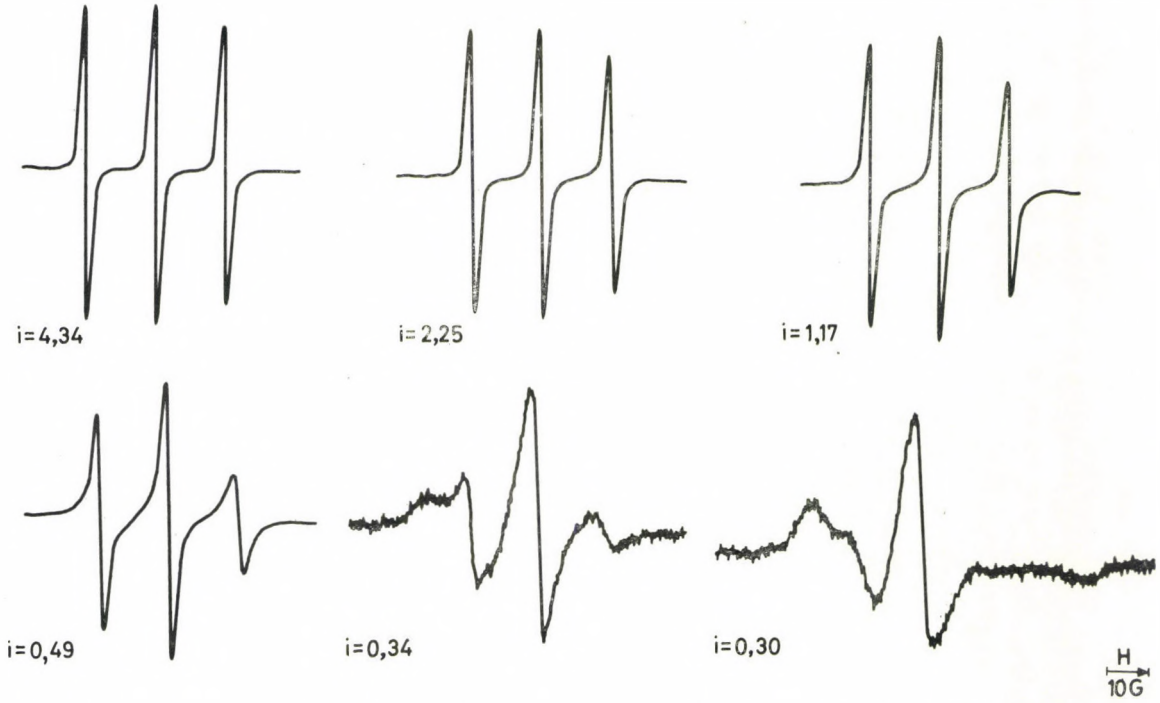

Fig. 1. Epr spectra of spin-labelled fibre bundles of frog sartorius depending on the relative water content. The *i* values indicate the actual relative water content during gradual dehydration. The magnetic field increases from left to right and, except gain, the same machine setting was applied in all cases

highly ordered structure, and that the amount of minor fractions with restricted motional freedom does not exceed 10 per cent of the whole water phase.

The dependence of spin-label-correlation time on relative water content is shown in Fig. 2. The curve fitted by calculator can be separated into two phases. At first, the correlation time gradually rises up to the five–sixfold of the original

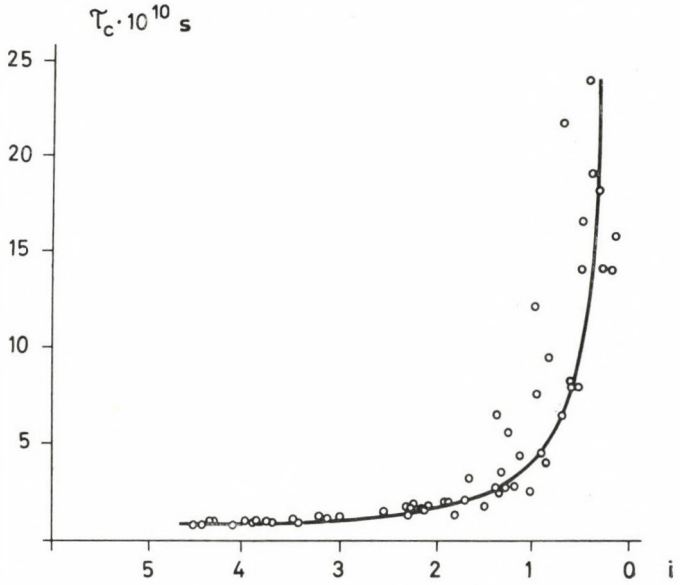

Fig. 2. Correlation time of spin probe plotted against relative water content (*i*). The solid line was fitted by calculator

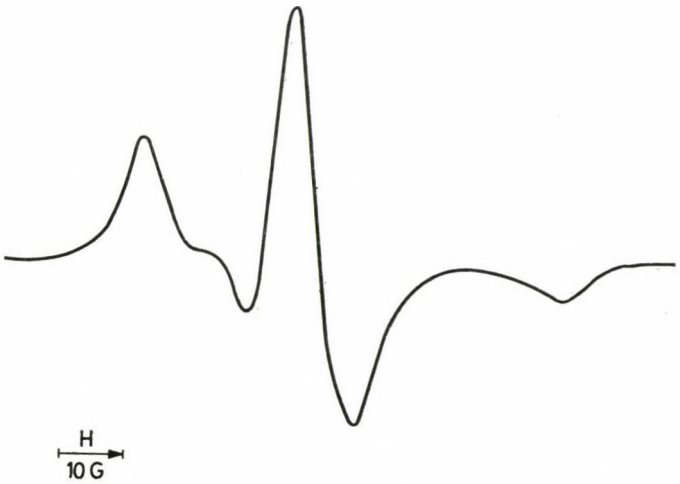

Fig. 3. Epr spectrum of dried muscle spin labelled with tempol in physiological state

value in the range of $i > 0.6$. However, a rapid increase can be observed at lower relative water content ($i < 0.6$) and at about $i = 0.3$, only the spectrum characteristic of the immobilized spin label can be recorded in most cases. The powderlike spectrum of dried muscle is shown in Fig. 3. The maximum component of the hyperfine coupling tensor is $2A_{zz} = 67$ G measured between the two outermost hyperfine extrema.

In the range of $i > 1.0$, the value of the isotropic hyperfine coupling constant (a_{iso}) coincides with the value measured in physiological solution, a_{iso} being equal to 16.8 G. By decreasing the relative water content to $1.0 < i < 0.4$, we could record only a slight change of the isotropic coupling constant within the limits of the experimental error. As the water concentration decreased to a relative water content of $i < 0.4$, a rapid change of a_{iso} could be observed, but also the spectrum of the strongly immobilized label appeared simultaneously.

In most cases, we could not exactly calculate the $2A_{zz}$ component because of the low concentration of the strongly immobilized label. Therefore, the $\Delta H^{(+1}$ parameter was measured which helps to interpret the strongly immobilized spin-label spectrum. According to the experiments, the $\Delta H^{(+1)}$ parameter increases with decreasing relative water content. At powderlike pattern spectrum, $\Delta H^{(+1)}$ has a final value of 27.6 G.

In Fig. 4, the reciprocal correlation time (frequency) is plotted against the relative water content. It gives a straight line fitted by the least square method with a Hewlett—Packard 9810 A calculator. The equation of the regression line is

$$\nu_c = -0.036 + 0.282\, i$$

where ν_c is measured in 10^{10} s^{-1} units.

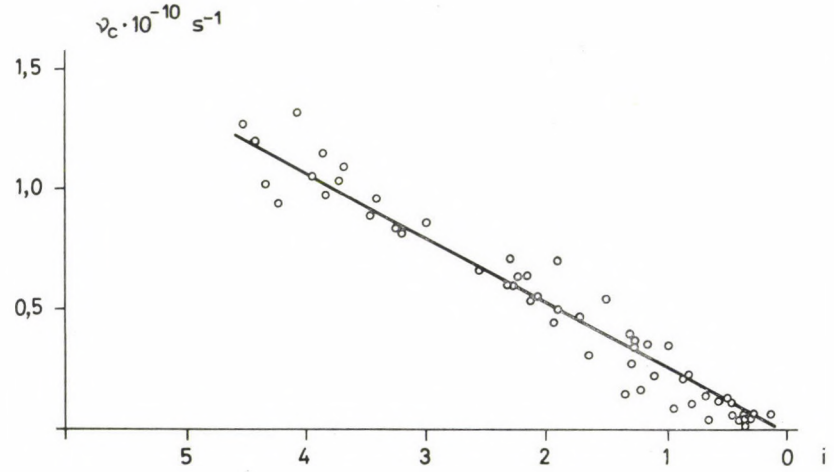

Fig. 4. The reciprocal correlation time of tempol spin probe plotted against the relative water content. The solid line was fitted by calculator

Discussion

The use of spin probes in biological systems enables the dynamic behaviour of fluid phases to be described, taking into account the parameters of the nitroxide type epr spectra. In our suggestion the tempol spin probe is equally distributed in the extracellular and intracellular water phases of the muscle. The spin probe has a high mobility measured by the rotational correlation time and on the basis of the three sharp-line epr spectrum if the water concentration in the muscle is physiological or the water content is near the physiological state. With decreasing relative water content, the rotational correlation time increased in hyperbolic relation to the relative water content. At about $i = 0.3$, the correlation time of the weakly immobilized spin probe could not be calculated; with further dehydration a solid component appeared which is characteristic of the strongly immobilized spin label.

Considering the line shape and correlation time of the spin probe in physiological state of the muscle, we conclude that the major fraction of water cannot exist in structural form characteristic of "crystalline" or highly ordered state. The nitroxide-free radical has lost only a little motional freedom in cell water when compared with physiological Ringer solution. This conclusion does not entirely agree with the experimental experiences derived from nmr data by Cope (1969), Hazlewood et al. (1969) and Belton et al. (1973), and it does not reconcile with the data reported by Finch et al. (1971).

The epr spectrum parameters reflect changes during gradual dehydration which are attributed to a dependence of the structural state of the cell water on the relative water content. A similar relation was found by Pócsik (1969), plotting the density of muscle water against the relative water content in the range of $i > 1$ at room temperature. The epr spectra exhibit rapid changes at about $i = 0.3$, i.e. the amount of water which represents 300 mg water per 1 g dried muscle may indicate some other phase of the muscle water. According to the terminology used in one part of the literature, this minor fraction is called "bound" water. The $\Delta H^{(+1)}$ parameter shows slight increase with further dehydration, indicating that the minor fraction has also a dynamic character. This result is in agreement with the conception of Ernst (1963) concerning the increasing boundedness of muscle water.

The author thanks Mrs J. Brucker for her technical assistance.

Note added on proof: After submission of the manuscript I learnt from a paper of Sachs and Latorre (1974) published in Biophysical Journal, April 1974, that in similar epr experiments, the water space of muscle could be approximated with a two-compartment fast-exchange model.

References

Belton, P. G., Jackson, R. R., Packer, K. J. (1972) Biochim. Biophys. Acta *286* 16
Blinc, R., Pirs, J., Easwaran, K., Ehrenberg, L. (1973) Biophys. J. *13* 622
Cope, F. W. (1969) Biophys. J. *9* 303
Ernst, E. (1926) Arch. Ges. Physiol. *213* 131
Ernst, E. (1963) Biophysics of the Striated Muscle, Akadémiai Kiadó, Budapest, pp. 109—121
Ernst, E., Tigyi, J., Zahorcsek, A. (1950) Acta Physiol. Acad. Sci. Hung. *1* 5
Finch, E. D., Harmon, J. F., Muller, B. H. (1971) Arch. Biochem. Biophys. *147* 299
Frank, H. S., Evans, M. W. (1945) J. Chem. Phys. *13* 507
Hamilton, C. L., McConnell, H. M. (1968) Spin Labels in Structural Chemistry and Molecular Biology, Ed. by A. Rick and M. Davidson, W. H. Freeman and Co. San Francisco p. 115
Hansen, J. R. (1971) Biochim. Biophys. Acta *230* 482
Hazlewood, C. F., Nichols, B. L., Chamberlain, N. F. (1969) Nature *222* 747
Klotz, I. M. (1958) Science *128* 815
McConnell, H. M., McFarland, B. G. (1970) Quart. Rev. Biophys. *3* 91
Outhred, R. K., George, E P. (1973) Biophys. J. *13* 97
Pócsik, S. (1967) Acta Bioehim. Biophys. Acad. Sci. Hung. *2* 149
Pócsik, S. (1969) Acta Biochim. Biophys. Acad. Sci. Hung. *4* 395
Sachs, F., Latorre, R. (1974) Biophys. J. *14* 316
Sukhorukov, B. I., Wasserman, A. M., Kozlova, L. A., Buchachenko, A. L. (1967) Dokl. Akad. Nauk SSSR *177* 454
Szent-Györgyi, A. (1957) Bioenergetics, Academic Press, New York
Walter, I. A., Hope, A. B. (1971) in Progress in Biophysics, Ed. by I. A. V. Buttler, D. Noble Pergamon Press, Oxford, p. 3

Acta Biochim. et Biophys. Acad. Sci. Hung. Vol. 10 (1–2), pp. 71–78 (1975)

Electronic Processes in Generation of Nerve Excitation

T. LAKATOS

Biophysical Institute, Medical University, Pécs, Hungary

(Received April 1, 1974)

In a frog sciatic nerve stained by very dilute solution of eosin (0.1 μmol/l — to 100 μmol/l) and illuminated with a rather intensive light (10,000–100,000 lux), a single electric stimulus elicited not a single response, but a train of spikes. Latency time and reversibility of the effect, threshold concentration, threshold illumination, frequency and full length of train of spikes were investigated in detail. The results of the experiments are in agreement with the theory according to which the generation of action potentials involves electronic processes.

Introduction

Photodynamic stimulation of nerves and muscles (cf. Lakatos, Kollár-Mórocz, 1969) supported the assumption that biological excitatory processes involve electronic phenomena and the scene of these is the excitable tissue which can act like a semiconductor (Ernst, 1955–56, 1956, 1963). As it was reported previously (Lakatos, 1969), frog sciatic nerve produced action potentials when stained with eosin and illuminated by visible light. However, the action potentials appeared at random, and it was almost impossible to record the phenomenon, i.e. spontaneous single nerve impulses or short burst of action potentials, which consisted of four to six spikes. Other experiments performed on sensitized loligo stellar nerve and nerve corde of shellfishes demonstrated the ability of illumination to evoke long-lasting firing of spikes (Lakatos, 1969). The present paper reports a phenomenon which is easily reproducible and suitable to carry out detailed investigations on photodynamic action in myelinated frog nerve.

The phenomenon was at first found on a myelinated nerve of the electric fish *Torpedo marmorata*;[1] later on, the effect was reproduced on frog sciatic nerve and systematic investigations were preformed on this subject.

Materials and methods

Sciatic nerves of the frog *Rana esculenta* were excised and checked electrophysiologically by measuring their stimulus threshold. The transistorized stimulator provided square wave pulses 0.1 ms in duration, the amplitude was adjust-

[1] Experiments with this fish were performed during a study in the Marine Biological Station of Kotor, Yugoslavia; Director: prof. Lyubisha Rakić.

able by an accuracy of 0.01 V. The excised nerve was soaked in a Ringer solution containing eosin as a sensitizer. FLUKA GA eosin-Y (2, 4, 5, 7-tetrabromin disodium fluorescein) was dissolved in Ringer solution in concentrations from 10^{-4} to 10^{-8} g/ml. Soaking time ranged from 10 minutes to 20 hours: the more dilute solution was used to stain the nerve, the longer soaking time was needed. Illumination was provided by a tungsten filament bulb. The focused light beam passed through a layer of $CuSO_4$ solution in order to eliminate heat rays. Illumination intensity was set on 10,000 – 100,000 lux. A moist chamber was used to avoid desiccation of the nerve. Temperature in the chamber was kept by a constant cooling at 10 ± 2°C. This range of temperature is much more advantageous for photodynamic effect than room temperature (20 to 25°C) is (Mathews, 1964; Rosenblum, 1960). Four platinum-wire electrodes were mounted in a plexiglass box which contained some Ringer solution to provide saturated vapour. The box was covered by brass plate which kept the inside of chamber dark and served as an electric shielding at the same time. A glass window made possible the illumination.

Action potential were recorded by taking single shots of the screen of the cathode-ray oscilloscope, the sensitivity of which was 50 μV/cm. Experiments were performed as follows.

The excised and stained nerve was placed on the electrodes and kept under observation in darkness to find out if it produced action potentials spontaneously. Its response to a single electric stimulus was also checked. Stimulus threshold was measured both in darkness and during illumination. The illuminated nerve was then stimulated by one impulse higher than the threshold and the response recorded.

Results

As mentioned above, a few preliminary experiments were performed on nerve trunks of the electric fish *Torpedo marmorata*. This has four pairs of nerve bundles, which mostly innervate the electric organ. Fig. 1 shows that this preparation (stained and illuminated in the usual way) produced a frequent response if stimulated but by one single pulse. Duration of the train of spikes was generally 1.5 s at least but never exceeded 2.0 s. Five peaks were found within an interval of 10 ms, that means, the immediate response was followed by some 1000 other spikes.

Systematic study of the phenomenon was performed on sciatic nerves of the frog *Rana esculenta*. A typical experiment is shown in Fig. 2. Action potential produced by a stained nerve was quite normal, without any change in its duration and shape. This is in good accordance with Lochmann's data (Lochmann, 1966) who found eosin to have no dark effect even in a concentration as high as 10^{-4} g per ml. When the illuminated nerve was stimulated by a pulse just above threshold the response was a single spike (Fig. 2 b). A slightly stronger stimulus elicited

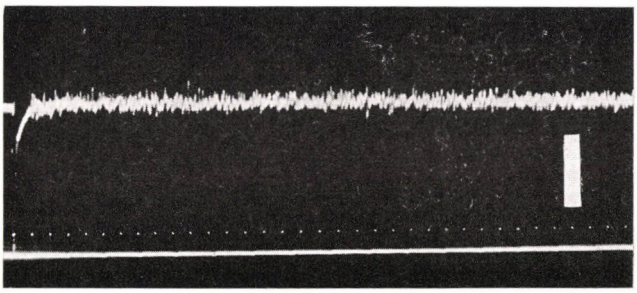

Fig. 1. Photodynamic response of a nerve of the fish *Torpedo marmorata*. Stimulus: 0.6 V; time mark: 10 ms; vertical bar: 200 μV

a train of spikes; further increase of stimulating pulse did not change the general pattern of the response (Fig. 2 c and d). This phenomenon was found in 224 out of 440 experiments. Usually, action potentials did not follow each other at such regular intervals; many times the nerves produced a response of the type shown in Fig. 3. In other cases a part of the burst was regularly periodical.

Latency time. A few minutes passed after the light had been switched on until the periodical response occurred. An evaluation of the data of 187 experiments disclosed that the eosin concentration influenced the latency time (Fig. 4 plot *A*), which latter depended on the light intensity but at relatively low and high illuminations. Plot *B* in Fig. 4 shows this relationship on the basis of evaluation of 409 data obtained with 368 nerves.

Threshold illumination. The phenomenon was studied in a range of illumination from 10,000 to 100,000 lux. The less the light intensity, the lower was the percentage of experiments in which the expected response appeared, and there was always a limit below which the effect never took place. The actual value of this threshold illumination depended on the concentration of eosin, as shown in Fig. 5.

Threshold concentration. When the solution of eosin was as concentrated as 10^{-3} g/ml or higher, the nerve died in a few minutes upon the effect of illumination of an intensity of 100 to 200 lux. If the concentration was 10^{-4} g/ml or less, it did not seem to cause any harm to the nerve. The relationship plotted in Fig. 5 holds in an inverse way, too, i.e. threshold concentration depended on the intensity of the illumination applied. However, an eosin concentration of 10^{-7} g per ml appeared to be an absolute threshold. Nerves stained with a solution of a concentration lower than this did not display the expected response, no matter how intense a light was used for illumination.

Reversibility of the effect. After the light had been switched off, the frequent response gradually faded out (Fig. 6 a) or disappeared completely (Fig. 6 b), but reappeared if the nerve was illuminated again. Forty-five out of 74 repeated experiments were successful in this respect.

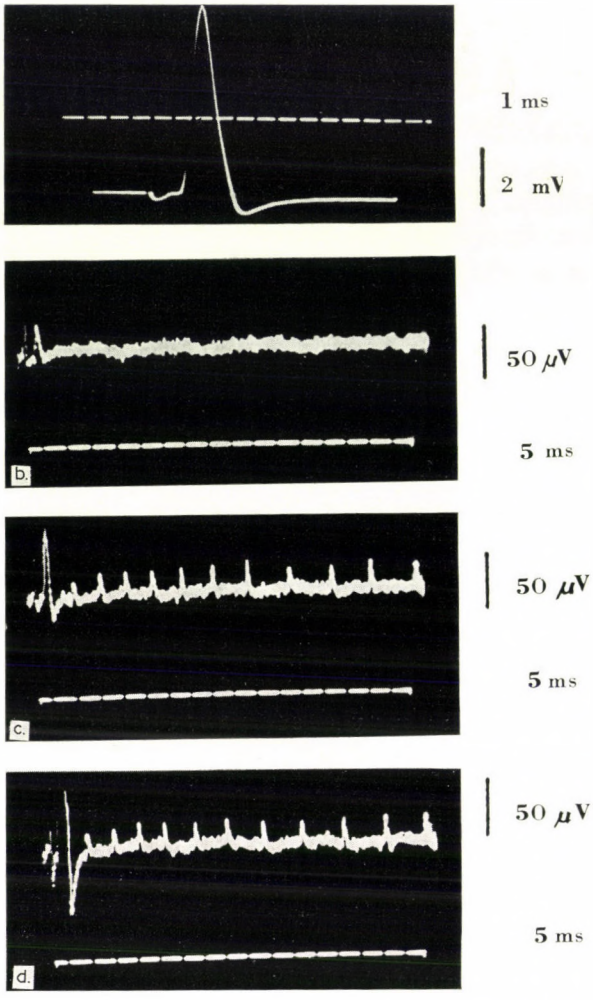

Fig. 2. Photodynamic response of sciatic nerve of the frog *Rana esculenta*. Concentration of eosin: 10^{-4} g/ml. a) Response of the stained nerve in darkness. Stimulus (0.4 V) was much over the threshold (0.2 V). Normal, nondistorted spike. b) Illuminated. Stimulus: 0.22 V, threshold: 0.20 V. c) Illuminated. Stimulus: 0.23 V, threshold: 0.20 V. d) Illuminated. Stimulus: 0.27 V, threshold: 0.20 V

The time necessary for disappearance of the effect after switching off the light varied within a relatively wide range. Sometimes the frequent response disappeared in 8 or 10 minutes, in some other cases it did not disappear, but was limited to a short one consisting of a few spikes only (e.g. Fig. 6 a). This state was reached by the 8th ± 1.5 minute on the average.

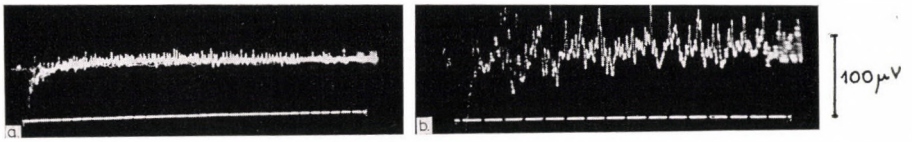

Fig. 3. Stained and illuminated frog nerve. Partly and non-regular response. Time mark: 5 ms

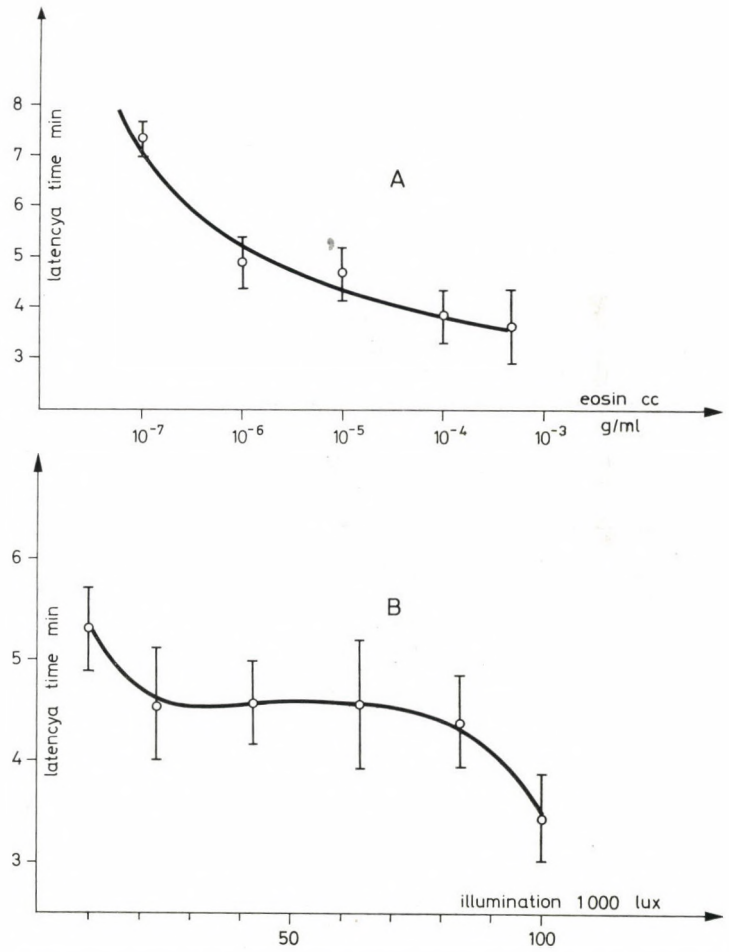

Fig. 4. A) Latency time plotted against eosin concentration. Vertical bars indicate errors of the means. B) Latency time plotted against illumination intensity. Bars indicate errors of the means

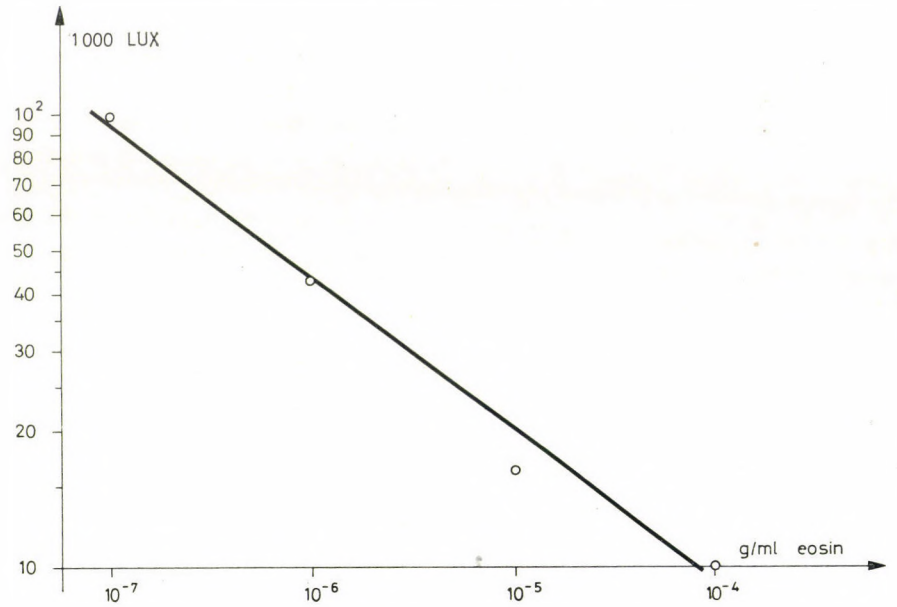

Fig. 5. Threshold illumination plotted against eosin concentration. Logarithmic representation

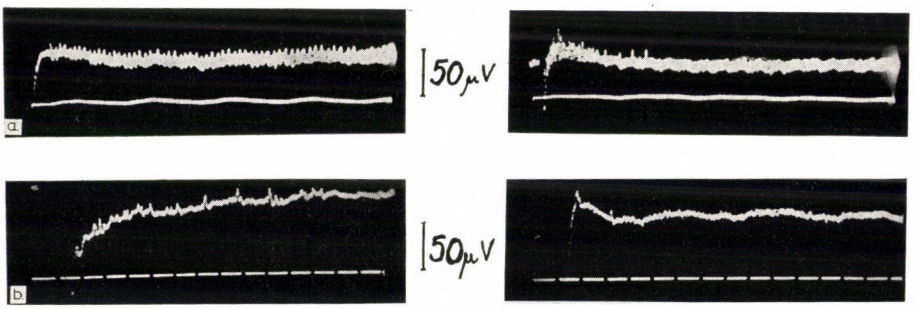

Fig. 6. a) Response of a stained nerve during illumination and in darkness 3.5 min after the light had been switched off. Total length of trace: 360 ms. b) Response of a stained nerve during illumination and in darkness 6 min after the light had been switched off. Time mark: 5 ms

Duration of the train of spikes. A number of experiments were performed in such a way as to enable the total length of the response to be recorded. The mean length was 39 ms obtained by averaging the durations of 25 trains of spikes. Standard error of mean was ± 4 ms. The length of a burst did not seem to depend on any of the concerned parameters, i.e. illumination, concentration of eosin, intensity of stimuli.

Time interval between two successive spikes in a train varied from 3 ms to 6 ms and, as demonstrated in Fig. 2, it increased near the end of a series.

Stimulus threshold against electric square wave pulses was measured before and after the nerves had been stained both in darkness and during illumination. In a short series of experiment involving 48 nerves both stimulating voltage and current were measured simultaneously. We checked by Student' test if it was any significant change of threshold upon the effect of illumination. Threshold given in Volts did not show any change within the accuracy of measurement (0.01 V): unstained and stained nerves had an average threshold of 0.16 V both in darkness and during illumination. Threshold measured in μAs were as follows: unstained nerves, 15.2 μA both in darkness and under illumination; stained nerves, 14.9 μA in darkness and 14.7 μA under illumination. The small change was not statistically significant by far ($t = 0.302$, $n = 24$). Stimulus threshold was usually checked with routine experiments, too. No change was found in stained nerves (average threshold of 180 nerves was 0.18 V both in darkness and during illumination).

Discussion

There is no doubt that the electronic structure of a dye molecule is capable of transforming photon energy of light into a stored electron-excitation energy on a triplet level (Lyovshin, 1951; Pringsheim, Vavilov, 1926) which has a lifetime as long as a few minutes. This energy could be transported into the protein molecules of the biologically excitable tissue of a nerve.

According to its general appearance the response looks like an oscillation of relaxation type. The energy of oscillation itself is stored in the excitable tissue; a continuous transport of an excess energy takes place from the excited electrons of dye molecules into the biological energy stores. When a stimulus overturns the steady state of the system an excitatory process occurs and consumes the stored energy. The depleted stores are refilled both by the usual biological restoring processes and the energy transported from the excited triplet states of the eosin molecules. This double energy supply keeps oscillating the unbalanced excitatory system of axons. In a short time the excess energy flow slows down, therefore, the time period between two consequent spikes becomes longer (Fig. 2); then, the spiking stops because of exhaustion of excess energy supply. This sort of increase of periods in serial spiking is a known physiological experience with naturally stimulated receptors (e.g. Hartline, 1934). The stimulus sets up a burst of spikes and the spiking slows down before it would stop completely. Similar phenomenon occurs also in a nerve (e.g. in a motor nerve of the cat, Bronk and Ferguson, 1935). Spontaneous firing can be elicited in a frog sciatic nerve by soaking it in Ca-free isotonic solution (Brink et al., 1946; Bíró et al., 1970). In Brink's experiments the time period corresponding to the base frequency was 3.2 ms at room temperature; this period varied between 3 and 6 ms in our experiments.

It was slightly longer than that found by Brink because the temperature in our experiments was about 10°C.

Photodynamic firing and other serial spikings are entirely different phenomena. Spontaneous activity is interpreted as a result of a depolarization which decreases the stimulus threshold; all these changes result in periodical spiking (c.f. Ridge and Walker, 1953); the required decrease of stimulus threshold ought to be 20 mV or more. We measured the threshold with an accuracy of 10 mV and did not find any decrease. On this basis we can assume that the combined action of eosin and light does not cause any change in the stimulus threshold; it is the electron excitation energy generated by light which serves as a stimulus.

The rate of energy supply from triplet states influenced the total length of bursts which varied within wide ranges. When a stimulus was followed by the next one, very soon the second response was shorter than the first one, and a serial stimulation (10 stimuli) cut the response short. After a resting period the nerve could produce the burst of spikes again for as long as in the first case, even though the light had been switched off. That means the energy stores are depleted by the excitation from the stimulated area, the illumination fills up the triplet states again, but this takes some time. When there is no more illumination the stored energy can migrate along the nerve and refills a part of the triplet states. This process could be repeated for a while, then the nerve fails to produce serial spiking (Fig. 6) because of final depletion of the triplet state store.

As a result of our experiments we can conclude that the energy stored in excited states of electrons plays a very important role in generating excitatory processes in an axon according to the electronic theory of biological excitation (Ernst, 1955–56) and, perhaps, we can figure out the initial electronic events in excitatory processes.

References

Biró, G., Gábor, K., Örkényi, J. (1970) Acta Biochim. Biophys. Acad. Sci. Hung. *5* 99
Brink, F., Bronk, D. W., Larrabbe, M. G. (1946) Ann. New York. Acad. Sci. *47* 457
Bronk, D. W., Ferguson, L. K. (1935) Amer. J. Physiol. *110* 700
Ernst, E. (1955–56) Wiss. Z. Humboldt Univ. Berlin, Math. Naturwiss. Reihe *5* 167
Ernst, E. (1956) Biofizika *1* 297
Ernst, E. (1963) Biophysics of the Striated Muscle. Akadémiai Kiadó, Budapest
Hartline, H. K. (1934) J. Cell. Comp. Physiol. *5* 229
Lakatos, T. (1969) Acta Biochim. Biophys. Acad. Sci. Hung. *4* 429
Lakatos, T., Kollár-Mórocz, A. (1969) Acta Biochim. Biophys. Acad. Sci. Hung. *4* 99
Lochmann, E. R. (1966) Studia Biophysica *1* 249
Lyovshin, V. L. (1951) Fotoluminescencia Zhidkih i Tverdih Veshtshestv, Moscow, 1951 (Photoluminescence of Fluids and Solids)
Mathews, M. M. (1964) Photochemistry and Photobiology *3* 75
Pringsheim, P., Vavilov, S. I. (1926) Z. f. Phys. *37* 705
Ridge, R. M. A. P., Walker, A. J. (1963) Problems in Biology (Ed.: Kerkut, G. A.) Boston *195*
Rosenblum, W. I. (1960) J. Cell. Comp. Physiol. *55* 73

Acta Biochim. et Biophys. Acad. Sci. Hung. Vol. 10 (1—2), pp. 79—82 (1975)

Extended Hückel Calculations on the Conformational Structure of Glucose-1-Phosphate

R. GÁSPÁR, jr.

Biophysical Institute, Medical University, Debrecen, Hungary

(Received May 10, 1974)

Extended Hückel-type rotational potential energy functions are presented for the glucose-1-phosphate molecular anion. Preferred conformations and rotational energy barriers are predicted. It is concluded that the phosphate-containing part of the molecule is very flexible and the $-CH_2OH$ group rotates freely.

Introduction

Conformational analysis of glucose-1-phosphate molecular anion (G-1-P) requires the minimization of its total molecular energy with respect to the torsional angles in the molecule, denoted by Θ_1, Θ_2, Θ_3 (see Fig. 1). In our earlier work we have calculated the electronic structure of the G-1-P molecule and of some other biologically important phosphates with the aid of the extended Hückel theory (Gáspár, 1971; Gáspár, 1972a; Gáspár, 1972b). Recently, quantum-chemical calculations have been made on different energy-rich phosphates and adenosine phosphates in the framework of the extended Hückel and the CNDO methods, respectively (Boyd, Lipscomb, 1969; Alving, Laki, 1972). Moreover, extended Hückel studies on the conformation of 5'-adenosine monophosphate and of D-ribose (C_3,-exo)-phosphate unit have been performed (Vasilescu et al., 1972a; Vasilescu et al., 1972b).

Calculation of the G-1-P molecule could be of interest and of importance for the understanding of the stereochemical behaviour of the molecule under various enzymatic and non-enzymatic processes. The conformational properties of the glucose-1-phosphate are predicted for the first time in the present paper by quantumchemical calculations.

Experimental

The extended Hückel method used here has been described in detail elsewhere (Gáspár, 1972a). The total Hückel electronic energy is computed to be the sum of the orbital energies of the electrons over the filled orbitals of the molecule,

$$\varepsilon = 2 \sum E_i$$

The total molecular energy can be written as:

$$E = 2\sum E_i + \sum_{n,n'} E_{n,n'} - \sum_{e,e'} E_{e,e'}$$

where the second and the third terms are the nuclear–nuclear and electron–electron repulsion energies, respectively. In the extended Hückel framework the approximation of the off-diagonal matrix elements H_{ij} is simulating the contribution of the nuclear repulsions to the total molecular energy (Kier, 1967). So the simple sum of the one electron energies behaves similarly to the true molecular energy. This fact enables the extended Hückel method to predict the equilibrium conformations of the molecules correctly with an overestimation of the barrier heights. The atomic co-ordinates were calculated for each conformation by a modified version of the QCPE 94 program on a CDC 3300 computer.

Results and discussion

The calculations on the G-1-P molecular anion were made on a series of conformations involving the rotation of the Θ_2 and Θ_3 torsional angles through 360 degrees and of the Θ_1 torsional angle through 120 degrees because of the threefold symmetry of the phosphate group. The torsional angle Θ_1 of the bonded atoms C_1–O_8–P_9–O_{10}, i.e. the angle between the planes formed by the atoms C_1–O_8–P_9 and O_8–P_9–O_{10}. Θ_1 is considered positive for a right-handed rotation; when looking along the bond P_9–O_8 the far bond O_8–C_1 rotates clock-wise with respect to the near bond P_9–O_{10}. Θ_2 and Θ_3 torsional angles were considered similarly, Θ_2 for the C_2–C_1–O_8–P_9 atoms and Θ_3 for the O_{16}–C_6–C_5–O_7 atoms. Bond lengths and bond angles were assumed to be fixed as described previously, and the possible re-orientations of the hydroxyl groups were neglected (Gáspár, 1972a).

The potential energy curves in Fig. 2 have been calculated by varying each torsional angle in turn keeping others at suitably chosen values. The potential energy curve for Θ_1 shows minima at about 0°, and also at 120° and 240°. Because of the threefold symmetry of the phosphate group these conformations are identical. The calculated barrier to rotation of the phosphate group about the O_8–P_9 bond is 1.21 eV.

The potential energy curve for Θ_2 shows minima at about 20°, 90°, 210° and 320°. The shape of the curve is quite steep around the minima at 20°, 90° and 320°; however, the region of the energy minimum at 210° (denoted by the full line) is broader and very deep. The humps in the Θ_2 curve between 60° and 150° may be smoothed out by the relaxation of the other groups of the molecule, e.g. hydroxyl groups, lone pairs etc. The barrier to rotation about the C_1–O_8 bond is 22.69 eV.

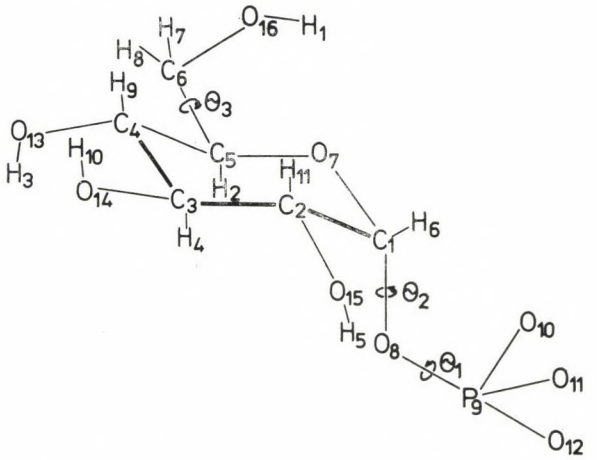

Fig. 1. G-1-P molecular anion. Notations for the conformational angles

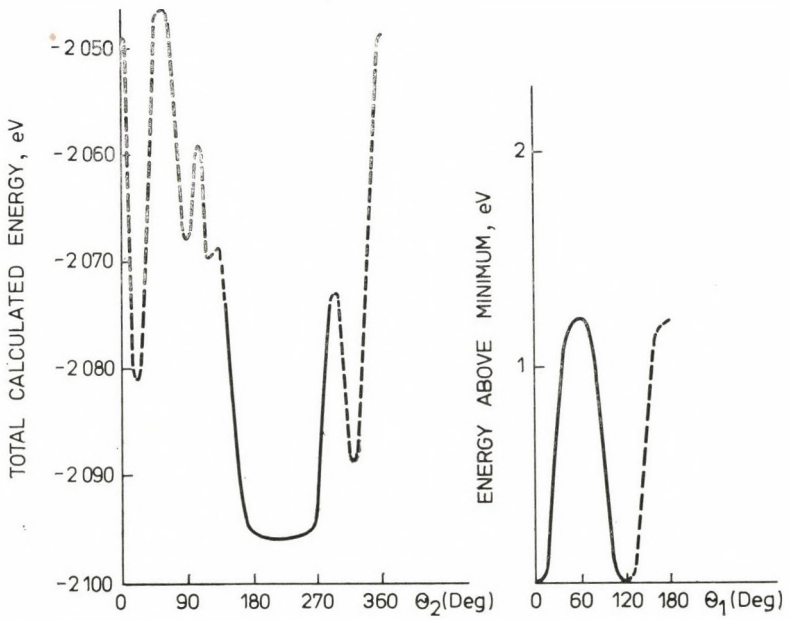

Fig. 2. Potential energy curves as a function of the torsional angles Θ_1, Θ_2. The values of the angles not varied are chosen so as to correspond to those in the most stable configuration, namely $\Theta_1 = 0°$, $\Theta_2 = 210°$. Since the phosphate group shows a threefold symmetry, the potential energy curve belonging to the change of Θ_1 has been calculated only in the $0-120°$ region (denoted by the full line)

In the case of the Θ_3 rotational angle the calculated potential energy curve shows an average fluctuation under 0.05 eV and so the force is practically independent of the rotational angle. Internal rotation around the C_5–C_6 bond may thus be considered to be "free".

The calculations for G-1-P molecule indicate a great conformational flexibility at the $COPO_3$ part of the molecule around the CO, respectively, OP axes, and the ground-state conformation of the molecule is energetically only slightly preferred. The conformational angles describing the ground-state conformations of the molecule are $\Theta_1 = 0°$, 120°, 240°; $\Theta_2 \approx 210°$ and $\Theta_3 = 0° - 360°$.

References

Alving, R. E., Laki, K. (1972) J. Theor. Biol. *34* 199
Boyd, D. B., Lipscomb, W. N. (1969) J. Theor. Biol. *25* 403
Gáspár, R. jr. (1971) Proc. First Europ. Biophys. Congr. *6* 215
Gáspár, R. jr. (1972a) Acta Biochim. Biophys. Acad. Sci. Hung. *7* 275
Gáspár, R. jr. (1972b) Acta Biochim. Biophys. Acad. Sci. Hung. *7* 285
Kier, L. B. (1967) Mol. Pharmacol. *3* 487
Vasilescu, D., Lespinasse, J. N., Camous, F., Cornillon, R. (1972a) FEBS Letters *27* 335
Vasilescu, D., Camous, F., Lespinasse, J. N. (1972b) FEBS Letters *21* 179

Acta Biochim. et Biophys. Acad. Sci. Hung. Vol. 10 (1—2), pp. 83—93 (1975)

The Z line of the Flight Muscle of Honey-bee

K. TROMBITÁS, A. TIGYI-SEBES

Central Laboratory, Medical University, Pécs, Hungary

(Received May 7, 1974)

The size and arrangement of the hexagonal filament lattice in the Z line of the flight muscle of honey-bee is similar to the size and arrangement of the lattice of A filaments. Z filaments show a "tubular" structure and possess a seemingly empty inner core just like A filaments do. The Z filaments are connected with a thick network transversally. The I filaments are probably embedded in this transversal network on both sides of the Z line; they cannot be recognized inside the Z line. The filament lattice of the Z line does not exclude the possibility of the A filaments to be connected to the Z line through the connecting filaments, or continuously to pass from one sarcomer into the other.

Introduction

The structure of the Z line in the flight muscle of insects is different from the structure of the Z line of the skeletal muscle of vertebrates. The basic arrangement of filaments is hexagonal (Auber, Couteaux, 1963; Garamvölgyi, 1963; 1965; Ashhurst, 1967; 1971; Saide, Ullrick, 1973) instead of tetragonal (Knappeis, Carlson, 1962; Franzini-Armstrong, Porter, 1964; Reedy, 1964). In the opinion of Auber and Couteaux (1963) the I filaments of one sarcomer pass through the Z line and continue in the I filaments of the next sarcomer. On the level of the Z line the I filaments widen and, arranged into groups of three, they form tubules. These tubules show hexagonal arrangement. The A filaments are connected to the border of the Z line by the so-called connecting filaments, the substance of which may be the same as the amorphous intertubular substance. Garamvölgyi (1963; 1965; 1971) brought further evidences of the existence of connecting filaments. He also observed filament bands of tubular structure to be present inside the Z line; these had an arrangement corresponding to that of myosin filaments and were continuous with them. Zebe et al. (1968) also demonstrated the connecting filaments, though in their opinion an I filament within the Z line is connected to the starting point of an A filament and conversely. In the opinion of Ashhurst (1967; 1971) the Z line of insect flight muscle is constituted by I filaments and their arrangement precludes the possibility of the filaments to continue from one sarcomer into the other. He did not find evidences on the existence of connecting filaments either. Saide and Ullrick (1973) proved, that the Z line of honey-bee

is perforated with triangular-shaped tubes, ordered into a hexagonal array. Position of each Z tube corresponds to that of three thick filaments on either side of the Z line. Each Z tube incorporates 3 thin filaments from apposite sarcomers into its rims, and the thick filaments are physically continuous with the Z line.

In a previous paper (Trombitás, Tigyi-Sebes, 1974) we also supported the ideas concerning the existence of connecting filaments. In the present work we deal with the Z structure as well as the possible connection between connecting filaments and Z structure.

Materials and methods

Flight muscle of honey-bee (*Apis mellifica*) was used in the experiments. The bees were cooled to 4°C before preparation. The fresh muscle was prepared with the method of Garamvölgyi and Belágyi (1968) and fixed to a glass rod in a slightly stretched state. After preparation the muscle was immediately fixed in 1-per-cent watery solution of osmium tetroxide in 0.14 M cacodylate buffer (pH 7.4) at 0°C for 90 min. This was followed by dehydration in alcohol and embedding in araldite.

Both longitudinal and transversal sections were made from the same fibre with the aid of the special block holder of LKP. The thin sections were stained on a grid with uranyl acetate (saturated solution in absolute methanol) and lead citrate (Reynolds, 1963). The photographs were taken with a TESLA BS 613 type electron microscope at an accelerating voltage of 80 kV.

Results

In the flight muscle of honey-bee the fibrils have an I band of about 1000 Å in the state of rest (Garamvölgyi, 1965). Since, however, osmium tetroxide stimulates the muscle during fixation (Page, Huxley, 1963), the free muscle will contract during fixation, the H zone disappears and the A filaments reach the Z line, which disturbs the observation of the structure of the Z line. In order to avoid this phenomenon, the muscle was slightly stretched during fixation. We could observe sarcomers of different lengths in the same fibre (in the same section).

Fig. 1 shows a sarcomer of the length of rest and Fig. 2 one stretched to about 115 per cent. Very regular Z lines can be seen in both figures; their width is about 1000 Å. Thick bands of filaments extend parallel with the longitudinal axis of the fibril inside the Z line both at the length of rest and in the stretched sarcomer, their arrangement agrees with that of the A filaments. It seems (Figs 1, 2a and 2b) that the thick filaments are connected with these Z filaments through connecting filaments (Garamvölgyi, 1963; 1965; 1971). The fibre from which the

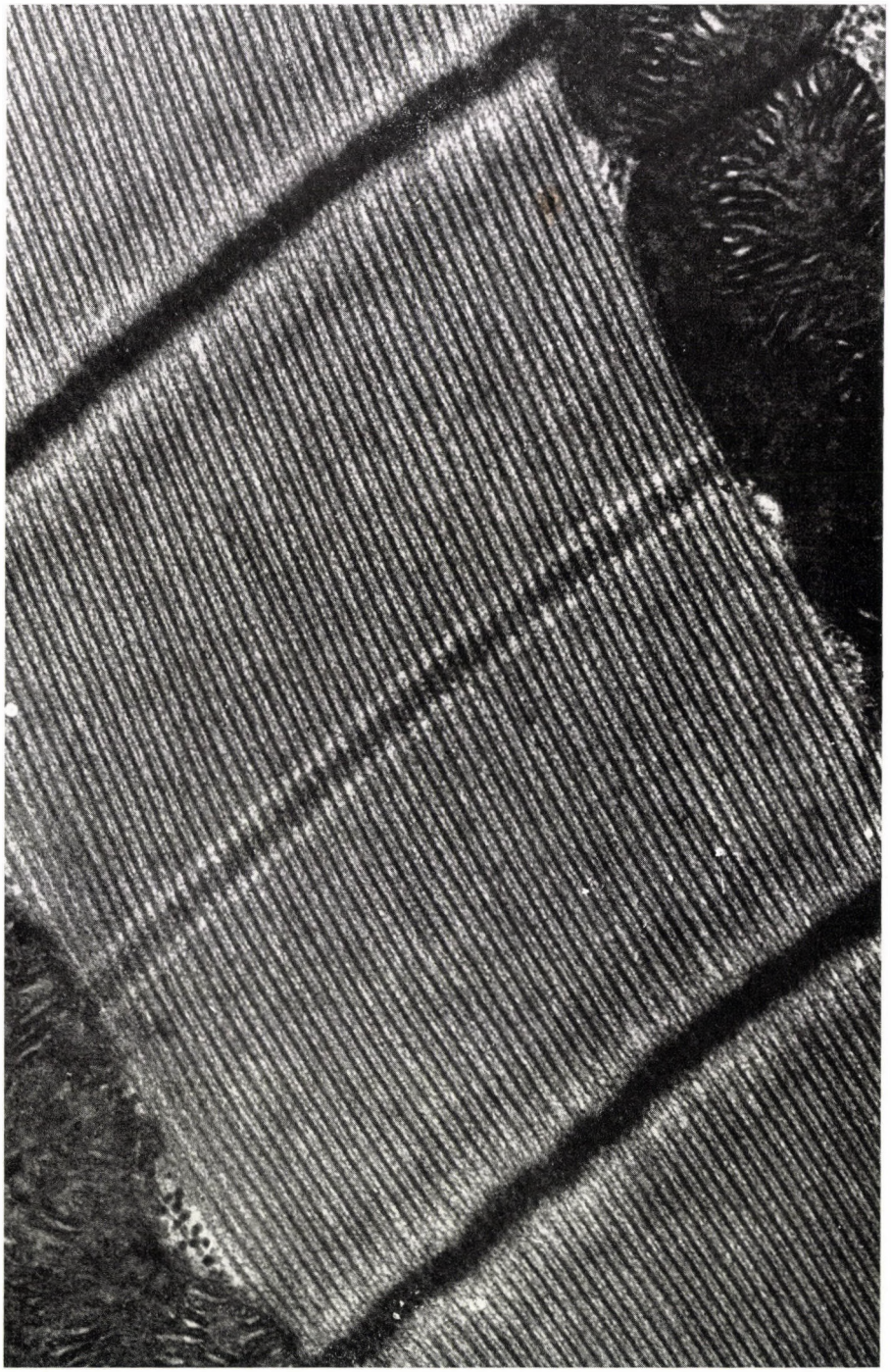

Fig. 1. A sarcomer of the flight muscle of honey-bee in the state of rest. The space between filaments is 450—480 Å. The A filaments are connected to the Z lines. Thick Z filaments can be seen in the Z lines. 40000×

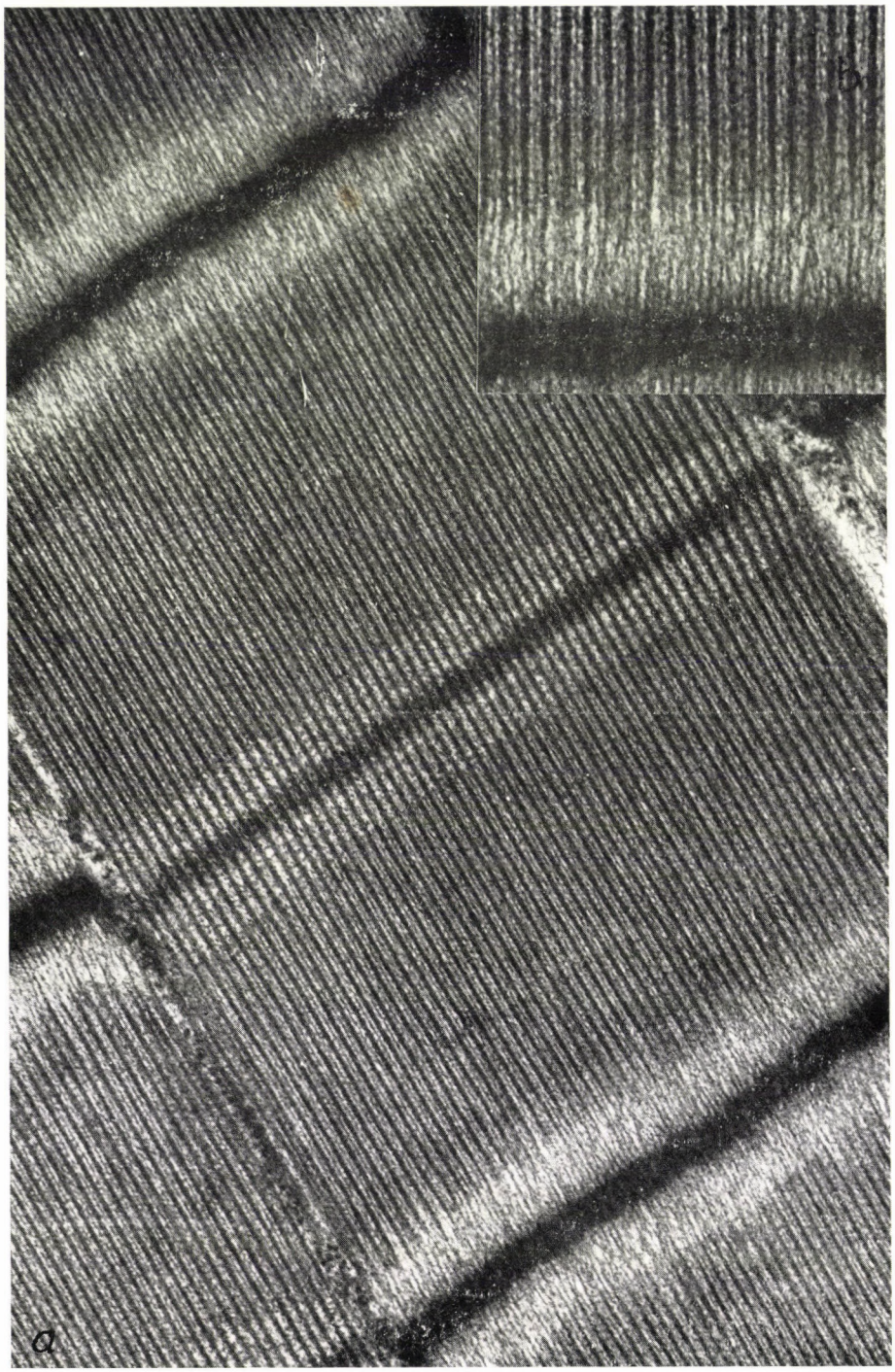

Fig. 2. a) Stretched fibril. The sarcomer is stretched to 115 per cent of the length of rest. The Z lines have the same structure as the former ones. The A filaments are connected to the Z lines. 44000×. b) The A filaments are connected to Z filaments by connecting filaments. 70000×

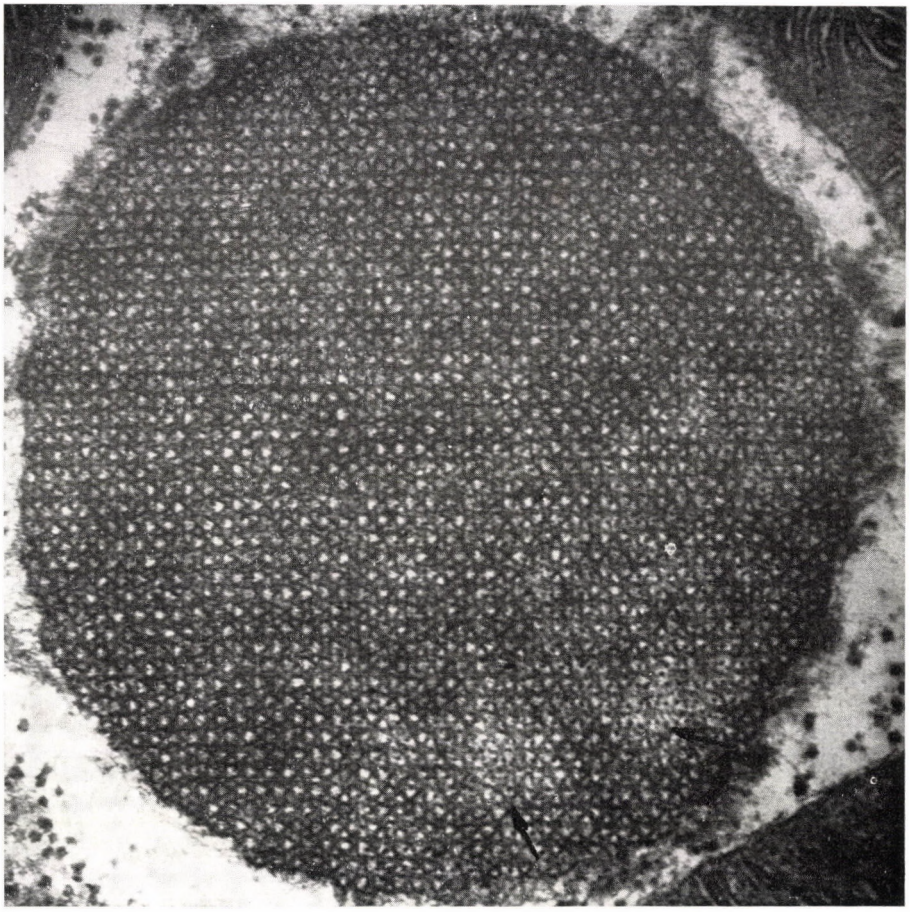

Fig. 3. Whole cross-section of the Z line. Z filaments form hexagonal filament lattice. The cross-sections of filaments are connected by thick transversal bridges. I filaments can be recognized in the light areas inside the hexagons (arrows). 60000×

above longitudinal sections had been obtained was also cut transversally with the aid of the special block holder of LKB. We succeeded in orienting a part of these cross-sections, as well as to obtain total cross-sections of the Z line. With small magnification (Fig. 3) the cross-section of the Z line shows hexagonal tubules (similarly to "the perforated plate" model, Auber, Couteaux, 1963), where the intertubular space is filled with an amorphous substance. With larger magnification (Fig. 4) this substance among the tubules can be resolved, and the Z line shows a hexagonal lattice of filaments, where the filaments have a seemingly empty core (Garamvölgyi, 1963; 1965; 1971) and are connected to one another

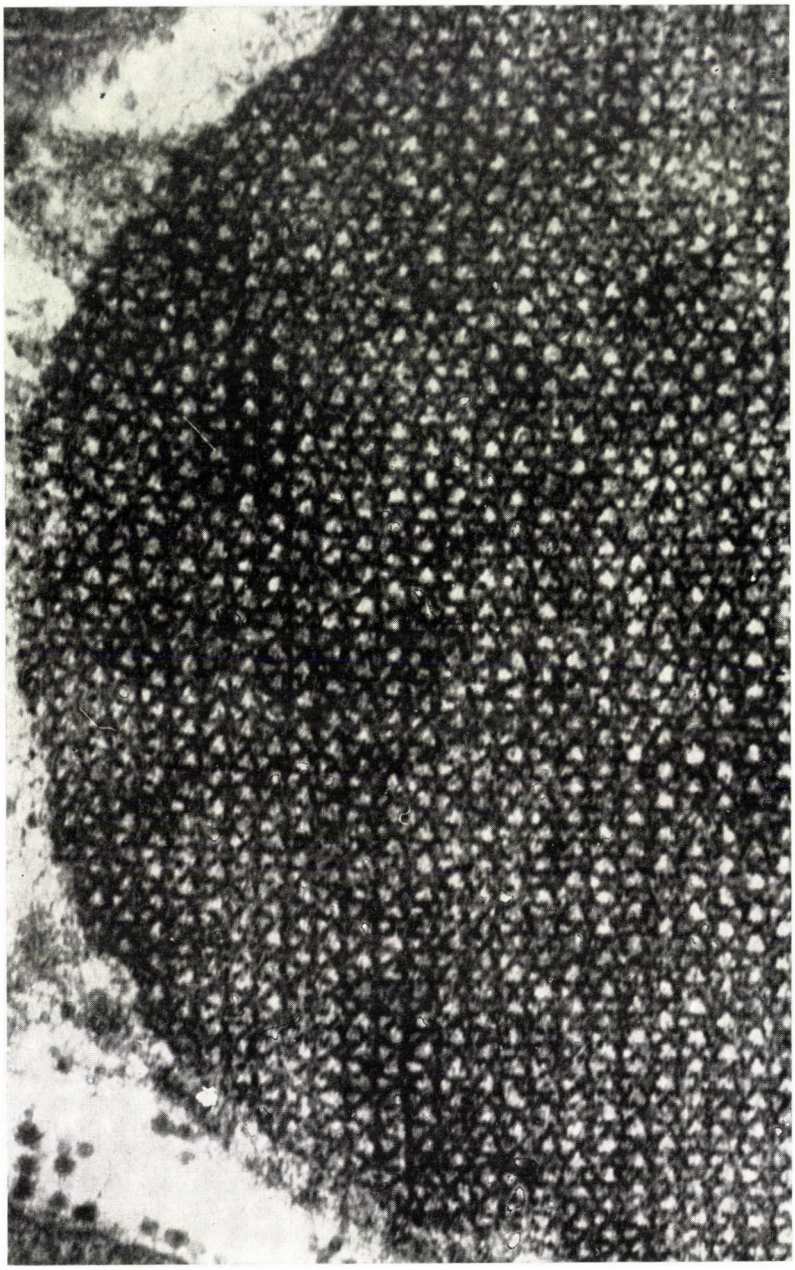

Fig. 4. The Z filaments forming hexagonal filament lattice are connected by thick transversal bridges. The Z filaments have a seemingly empty inner core. The space between filaments is 430—450 Å. In some places the I filaments can be seen inside the hexagons. 100000×

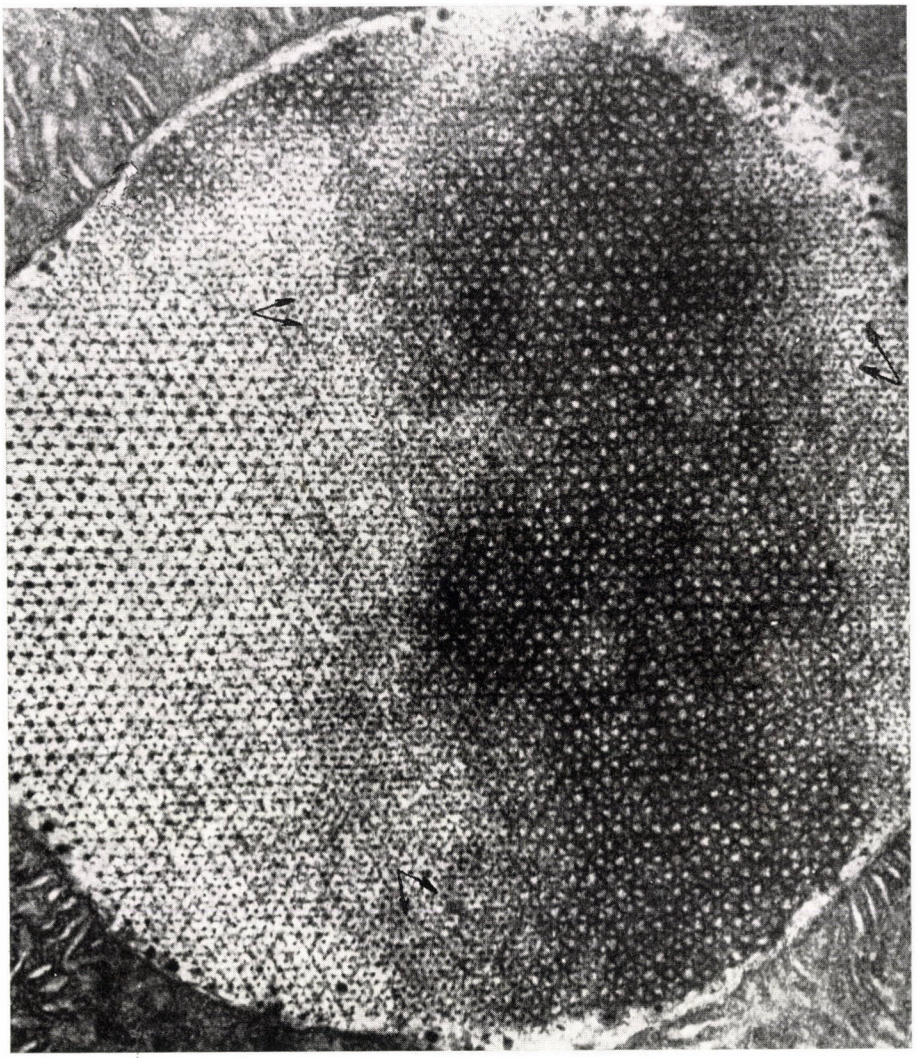

Fig. 5. Transverse section of stretched fibril through the Z line. Every second row of the filament cross-sections of the I band falls into a common straight line with a row of the Z filament cross-sections. The I filaments show hexagonal arrangement near the Z line (arrows). No I filaments can be recognized inside the Z line. 60000×

by thick transversal bridges. These cross-sections of filaments very probably are the cross-sections of thick Z filaments seen in the longitudinal sections. The space between the filaments is 430–450 Å. In the lighter parts (which places presumably show the edge of the Z line) I filaments can also be observed within the hexagons.

The transverse section shown in Fig. 5 contains a part of the A band, the I band, of the first sarcomer the Z line and a part of the I band of the next sarcomer. Every second row of the filament cross-sections of the I band (which are the continuation of the rows containing the A and I filaments alternatively) falls into the same line as the rows of the filament lattice of the Z line. The filament cross-sections appear with the same frequency in two adjacent rows of the I band. The cross-sections of I filaments can only be recognized in the layer of transitional density located on the border of the Z line but not inside the Z line. The hexagonal arrangement of I filaments can be observed near the Z line.

Discussion

Though the models of the authors mentioned in the introduction are very different, still the experimental results seem to agree well. The connecting filaments were observed by Auber and Couteaux (1963), Garamvölgyi (1963; 1965), White (1966), Zebe et al. (1968) as well as Trombitás and Tigyi-Sebes (1974). On the other hand, Ashhurst (1967; 1971) doubted the existence of connecting filaments as he had found that the adjacent rows of the I filaments contained different numbers of I filaments, i.e. "one row has twice as many I filaments as the other row" (quoted from Ashhurst, 1967). On the other hand, Ernst et al. (1969) counted the filaments in the photographs of Ashhurst (1967)] and demonstrated that the same number of cross-sections of filaments fell to areas of the same size of both the A and the I bands. So also the photographs of Ashhurst seem to prove the existence of connecting filaments both in longitudinal and in cross-sections. In the state of rest (Fig. 1) the A filaments are bound to the Z line. Notwithstanding it arose the possibility that there is no real I band in such photographs and it is the thinning ends of A filaments bridging over the apparent I band, which cause the appearance of connecting filaments (Ashhurst, 1971). If the A filaments had thinning ends of a length of 6–800 Å, corresponding to the "pseudo I bands", a zone of transitional density corresponding to these thinning ends of filaments should be seen on the I–A border in the case of greater sarcomer lengths. No such zone of transitional density was observed on the I–A border (Figs 2a and 2b), though there is no doubt of real I bands being present here. The structure of the Z line does not change in the case of such a slight stretch (cf. Figs 1 and 2) which makes it doubtless that the position of A filaments does not influence the Z structure in the state of rest (a stretch of greater degree does already influence the structure: Garamvölgyi, 1965). At the same time the connecting filaments can be well observed even in this case (Fig. 2a and 2b), though, in a thick section, this phenomenon can be produced by super-imposed filaments (Huxley, 1957; Achátz, 1968; Ashhurst, 1971). This possibility can be precluded by examining transverse sections. In Fig. 5, as opposed to the observation of Ashhurst (1967), filament cross-sections appear with the same frequency in the

rows of filaments in the I band, and the lattice of filaments is very similar to the finding of Auber and Couteaux (1963), especially near the Z line. This seems to prove that there is the same number of filaments in the I band as in the A band, i.e. that connecting filaments do exist.

Our transverse sections show that cross-sections of I filaments can be recognized only in the layer of transitional density located on the border of the Z line, but not inside the Z line. The rows containing cross-sections of connecting filaments and I filaments (which arise as the continuation of rows containing I and A filaments alternately) fall into one straight line with the rows brought about by the hexagonal lattice of filaments of the Z line on both sides of the Z line. The rest of the rows of I filaments (which arise as the continuation of the rows containing I filaments only) ends in the layer of transitional density at the border of the Z line. This finding raises the possibility that A filaments continuously pass through the Z line from one sarcomer to the next with the aid of connecting filaments and Z filaments (Garamvölgyi, 1963; 1965; 1971). Ernst and Benedetzky (1962) directly proved the passing of filaments through the Z line by demonstrating filaments continuously passing through the Z line in longitudinal section of the flight muscle of honey-bee after rinsing with distilled water.

The Z filaments shown in longitudinal section (Figs 1 and 2) show hexagonal filament lattice in whole cross-section (Figs 3 and 4) where the space between filaments is 430–450 Å. In this experiment the space between A filaments was 450–480 Å, in good agreement with the measurements of Reedy (1967).

If the Z tubes exist instead of Z filaments in the middle of the Z line (Auber, Couteaux. 1963; Saide, Ullrick, 1973), then they should be seen in the longitudinal sections. The diameter of a Z tube is about three times greater, than that of thick filament (for example Saide, Ullrick, 1973 Fig. 1.). But in longitudinal section the diameters of the Z filaments and the thick filaments are about equal.

The Z filaments are transversally connected by a thick network which can be observed in some places between the thick filaments, also in longitudinal section, though they generally form the substance of Z line which has high density and is not resolved by electron microscope. The existence of this Z transversal network is in accordance with the findings on the structure of the isolated Z plates (Ernst et al., 1958; Garamvölgyi et al., 1962). The Z plates isolated from the flight muscle of honey-bee by lactic acid showed an elaborately woven netlike surface structure; this structure may correspond to the transversal network of the Z line. If our findings are correct, the arrangement of filaments in the fibrils of the flight muscle of honey-bee can be shown by the following model (Fig. 6).

The filament lattice of the A band is the same as the one observed by Huxley and Hanson (1956) as well as Auber and Couteaux (1963) (Fig. 6a). In the I band the connecting filaments can be found at the place corresponding to the place of A filaments in the middle of hexagons consisting of I filaments (Auber, Couteaux, 1963) (Fig. 6b). In the Z line the Z filaments, connected by a thick trans-

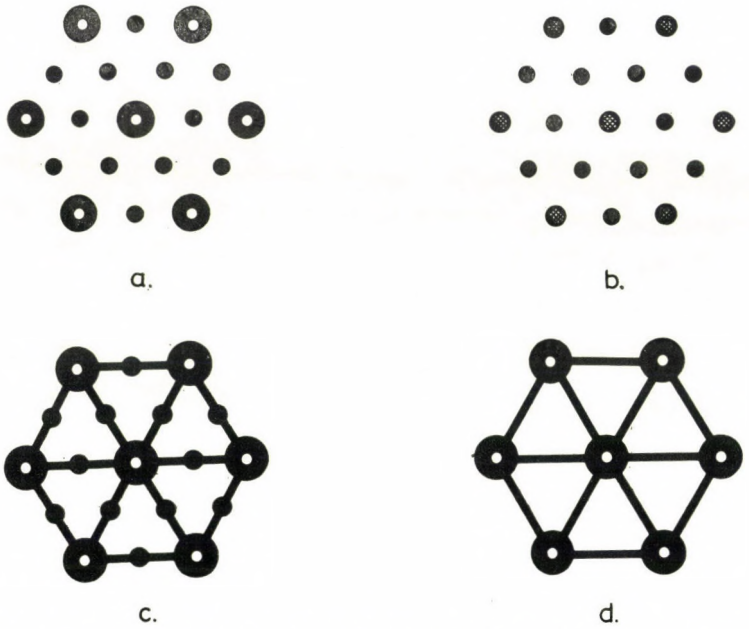

Fig. 6. The arrangement of filaments in the flight muscle of honey-bee. a) In the A band; b) in the I band; c) at the edge of the Z line; d) inside the Z line

versal network with a seemingly empty inner core, are arranged in a hexagonal lattice of filaments (Fig 6c and 6d). On both sides of the Z line I filaments are embedded in the transversal network among Z filaments (Fig. 6c). The I filaments cannot be recognized in the middle of the Z line (Fig. 6d). The distance between Z filaments is equal to the distance between A filaments.

References

Achátz, I. (1968) Acta Biochim. Biophys. Acad. Sci. Hung. *3* 183
Ashhurst, D. E. (1967) J. Mol. Biol. *27* 385
Ashhurst, D. E. (1971) J. Mol. Biol. *55* 283
Auber, J., Couteaux, R. (1963) J. Microscopie *2* 309
Ernst, E., Garamvölgyi, N., Guba, F. (1958) Acta Physiol. Acad. Sci. Hung. Suppl. *14* 40
Ernst, E., Benedetzky, St. (1962) Acta Physiol. Acad. Sci. Hung. *22* 211
Ernst, E., Kovács, K., Metzger-Török, G., Trombitás, K. (1969) Acta Biochim. Biophys. Acad. Sci. Hung. *4* 177
Franzini-Armstrong, C., Porter, K. R. (1964) Z. Zellforsch. *61* 661
Garamvölgyi, N., Metzger-Török, S., Tigyi-Sebes, A. (1962) Acta Physiol. Acad. Sci. Hung. *22* 223
Garamvölgyi, N. (1963) J. Microscopie *2* 107

Garamvölgyi, N. (1965) J. Ultrastructure Res. *13* 409
Garamvölgyi, N. (1971) "Contractile Proteins and Muscle" K. Laki (ed.), Marcel Dekker Inc. New York 1971
Garamvölgyi, N., Belágyi, J. (1968) Acta Biochim. Biophys. Acad. Sci. Hung. *3* 195
Huxley, H. E. (1957) J. Biophys. Biochim. Cytol. *32* 613
Huxley, H. E., Hanson, J. (1956) Electron microscopy. Proc. Stockholm Conf., Uppsala: Almquist and Winksel 1957, p. 202
Knappeis, G. G., Carlson, F. (1962) J. Cell. Biol. *13* 323
Page, S. G., Huxley, H. E. (1963) J. Cell. Biol. *19* 369
Reedy, M. K. (1964) Proc. Roy. Soc. B. *160* 458
Saide, J. D., Ullrick, W. (1973) J. Mol. Biol. *79* 329
Reynolds, E. S. (1963) J. Cell. Biol. *17* 208
Trombitás, K., Tigyi-Sebes, A. (1974) Acta Biochim. Biophys. Acad. Sci. Hung. *9* 243
White, D. C. S. (1966) Ph. D. Thesis (zool.) Oxford University
Zebe, E., Meinrenken, W., Rüegg, I. C. (1968) Z. Zellforsch. *87* 603

Acta Biochim. et Biophys. Acad. Sci. Hung. Vol. 10 (1—2), pp. 95—99 (1975)

Inorganic Materials in the Striated Muscle*

E. ERNST

Biophysical Institute, Medical University, Pécs, Hungary

(Received August 21, 1974)

I gladly greet the members of the European Muscle Club and would like to express my gratitude for the kind invitation giving me this opportunity to speak. Muscle is a machine, moreover, a much more excellent one than any man-made machine; it stands to reason therefore, that all the smallest parts of such a marvel of a machine are important and interesting, and that muscle has stood in the limelight of biological research for three centuries. In muscle research all natural sciences participate, and especially biochemistry and biophysics are working efficiently. These sciences friendly co-operate also at this conference: besides biochemical results also biophysical questions are treated.

Thus, in connection with the functional role of the intramuscular Ca content, the formulation comes into prominence according to which the bound Ca of the resting muscle becomes mobilized due to excitation. This hypothesis belongs to the century-old biophysical problem occupying also myself during my whole scientific activity. This problem can be formulated, generally speaking, in the following two alternatives: a) the living cell (tissue) can be considered as an *aqueous solution* in which the water and the solutes are supposed to behave according to our knowledge of solutions; b) the cell (tissue) is a *complex system* in which the water content, the organic and inorganic materials closely interlinked, perform the functions. The unchanged timeliness of these contradictory suppositions is shown by the new conference held in 1972 at the New York Academy of Sciences and organized by prof. Hazlewood (Hazlewood, 1973) with about 40 lectures and 100 participants. The results of the debates covering also questions of methods can be summarized in the formulation, agreeing also with my standpoint, as follows: *The water content and some inorganic constituents in living tissues are considerably in a bound state.*

It is certainly to be admitted that the expression "*bound state*", consistently used in the literature and also by myself, lacks a scientific definition. On the other hand, such general expressions are sometimes used in the literature, so, e.g.

* Invited lecture delivered at the 3rd conference of the European Muscle Club on September 1, 1974, Budapest.

the term "*living tissue*", although the state denoted by "living" does not have an unequivocal definition either.

1. When, however, it comes to experimental investigation of details, working with measurable values is obligatory. That was what we did twenty-five years ago, performing experiments together with Tigyi to discriminate between the two alternatives mentioned above. Our paper (Ernst et al., 1950) was entitled: "Bindungszustand des Wassers und der Elektrolyte im Muskel" ("State of Binding of Water and Electrolytes in the Muscle"); the title of the publication from the USA conference mentioned above sounds: "Physicochemical State of Ions and Water in Living Tissues." Such welcome accord can be found not only in titles but also in results.

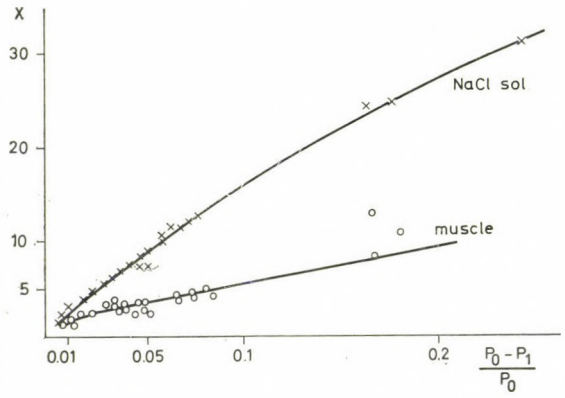

Fig. 1. Different concentration increases in muscle and in NaCl solutions at vapour-pressure equilibrium after progressive water depletion

Namely, in the question of *bound water* we described in our paper among others the following experiment: in a glass vacuum desiccator there was a balance, on one arm of which a muscle was hung, on the other a small glass basket containing 0.90 (!)* per cent NaCl solution. After evacuation, water vapour saturation was reached, and also vapour-pressure equilibrium was established between the muscle and the NaCl solution. During the experiment the balance showed that the muscle side became continuously heavier than the NaCl side, which means that in the state of vapour-pressure equilibrium the muscle had lost much less water than the NaCl solution (Fig. 1). These results prove beyond doubt that *in the course of drying, muscle binds water more strongly than does a 0.90-per-cent NaCl solution.*

* Instead of 0.72 per cent, the possibility having been taken into consideration that an increase in concentration may take place in the muscle during the time of the experiment (20°C).

In our view we treated the *boundedness of water* exactly by measuring the changes in *relative vapour-pressure lowering* in other experiments, in which, due to a continued drying, gradually less and less water remained in the muscle. Fig. 2 shows *that the relative vapour-pressure lowering of a muscle can arrive at a much higher degree than that of a NaCl solution.**

A survey of the whole literature seems to indicate that these our experimental results have shown, to this day, most unequivocally that *the water content of a muscle does not behave as a solvent but as being bound to a certain degree depending on the relative water content.*

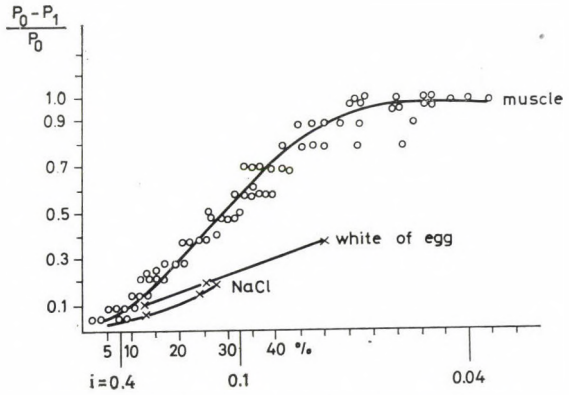

Fig. 2. Relative vapour-pressure lowering as a function of the water content of muscle

2. Having shortly discussed the question of bound water, we can deal with the problem of "*bound state*" *of the inorganic constituents* contained in muscle. According to the results of the conference in New York, some atoms bound to some organic compounds can be mobilized during activity. That is also in accordance with our conception which was formulated half a century ago in the form that a certain amount of the potassium in a resting muscle is bound and becomes released due to excitation.

Referring to the *bound K* I am obliged to admit that there is not, even today, exact evidence for it. On the other hand, the amount of K inside the fibril – if free – would mean a concentration about fifty times greater than that in its surroundings. This vast "concentration gradient" is supposed to be explained in the manner that it is continuously preserved at the expense of energy produced in metabolism. In contrast to that we have demonstrated (Ernst, Takács, 1931; see Ernst, 1963) that frog muscles perfused at the temperature of 0°C for 3–4 days did not lose more than 10–15 per cent of their original K content (Table 1),

* Ling's new paper (Ling, Negendank, 1970) shows many similarities in thinking, methods and results.

Table 1

K content of gastrocnemii perfused at 0°C for 3—4 days; n = normal, p = perfused

No.	Weight of the muscle g				Ashes, mg		K content, mg		Kloss %
	fresh		dry						
	n	p	n	p	n	p	n	p	
1	1.43	1.65	0.26	0.25	13.5	14.3	3.85	3.36	13
2	1.03	1.77	0.25	0.25	14.0	14.5	4.53	4.00	12
3	1.46	2.07	0.36	0.35	18.0	18.5	5.32	4.62	13
4	2.10	3.00	0.55	0.52	25.2	24.8	7.17	6.12	15
5	2.28	3.45	0.63	0.58	29.1	31.3	10.25	8.96	13
6	2.75	3.90	0.75	0.75	32.5	32.5	10.85	9.38	14

Table 2

K content and its specific activity in directly and indirectly stimulated muscle

No.	Simulation	Weight of muscle (mg)	Excitability (v)	Na (mg)	K (mg)	Counts/min mg K
1	indirect	410	1.0	0.22	1.12	2960
	direct	414	10.5	0.38	0.82	3502
2	indirect	422	0.9	0.24	1.24	2580
	direct	452	2.1	0.32	1.08	3100
3	indirect	462	1.0	0.28	1.18	2040
	direct	510	1.7	0.36	1.02	2860

or formulated otherwise, they *nearly retained their potassium content at a very low level of metabolism.**

Our hypothesis of *bound potassium* being mobilized during activity is based on experimental results, indicating that a significant part of the potassium has left the perfused muscle after several tetanic contractions due to electrical stimulation. This phenomenon, corroborated later in many other laboratories, can hardly be explained by considering muscle as an osmotic sac (Hill, 1930). The striated muscle is a much more complex system as was shown also by Tigyi's experimental results (Tigyi, 1959) (Table 2). According to those results, the perfused muscles which, due to activity, had *lost* a significant amount of K to the Ringer solution, had simultaneously *taken up* much more ^{42}K from the Ringer solution, as compared with the control muscles.

* This result is corroborated by the common experience that the muscles of frogs having been kept at very low temperatures in winter for many months, notwithstanding nearly retain their original K content.

But, however much I may have entered into the problem of potassium, its boundedness and mobilization, I still did not fail to take other inorganic constituents of muscle into consideration. Thus, e.g. one of our papers published twenty years ago (Ernst et al., 1954) demonstrated that the elements *K, Na and Ca* contained in muscle might take part *in a process of adsorption exchange.** Thus, I should like to call the attention of the lovers of Ca to be cautious in emphasizing, one-sidedly, the functional role of Ca in muscular activity.

Being glad to learn new fine particular results, please permit me to call attention to the *whole muscle*. Its many inorganic and organic constituents may form an interdependent collective in the resting muscle and change co-operatively in activity.

References

Ernst, E., Scheffer, L. (1928) Arch. ges. Physiol. *220* 655—671
Ernst, E., Szabolcs, J., Kovács, T. (1954) Acta Physiol. Acad. Sci. Hung. *6* 155—170
Ernst, E., Takács, I. (1931) Arch. ges. Physiol. *228* 690—699 (see Ernst, E. [1963] Biophysics of the Striated Muscle, Akadémiai Kiadó Budapest. p. 147.)
Ernst, E., Tigyi, J., Zachorcsek, A. (1950) Acta Physiol. Acad. Sci. Hung. *1* 5—26
Hazlewood, C. F. (1973) Annals of the New York Academy of Sciences *204* 6—631
Hill, A. V. (1930) Proc. Roy. Soc. B. (London) *106* 445, 447
Ling, G. N. (1962) A Physical Theory of the Living State, Ginn (Blaisdell) Waltham, Mass.
Ling, G. N., Negendank, W. (1970) Physiol. Chem. Phys. *2* 15—33
Tigyi, J. (1959) Acta Physiol. Acad. Sci. Hung. *16* 93—106 (see Kleinzeller, A., Kotyk, A. [1961] Membrane Transport and Metabolism. Publishing House Czechoslovak Acad. Praga. p. 143.)
Трошин, Х. С. (1956) Проблема клеточиой проницаемости. Изд. Акад. Наук. СССР. Москва Ленинград.
Troshin, A. S. (1966) Problems of Cell Permeability. Pergamon Press. Oxford, London.

* *The adsorption of K—Na—Ca* and its literature was treated in this paper of ours in 1954, i.e. before the publication of Troshin's or Ling's famous books (Трошин, 1956; Troshin, 1966; Ling, 1962) dealing with the adsorption of these atoms.

Acta Biochim. et Biophys. Acad. Sci. Hung. Vol. 10 (1—2), pp. 101—114 (1975)

Quantum-mechanical Studies on the Conformational Basis of Molecular Biology*

B. PULLMAN

Institut de Biologie Physico-Chimique, Laboratoire de Biochimie Théorique, Paris

The studies that I am going to describe here aim at the theoretical determination of *the conformational basis of molecular biology and pharmacology.* As is well-known, the activity of biological molecules and, in particular, of biopolymers is strongly dependent upon their conformation. In fact, the conformational criterion is frequently a prerequisite for their functioning. The understanding of the factors governing conformational stability of biomolecules and the evaluation of the preferred conformers is therefore of utmost interest for the development of quantum biochemistry.

The need for such a promotion of quantum-mechanical studies appears the more necessary as there was during the last years a prominent development of what may be called "empirical" studies in this field. These consist of partitioning the potential energy of the system into several discrete contributions, such as non-bonded and electrostatic interactions, barriers to internal rotations, hydrogen-bonding, etc., which are then evaluated with the help of *empirical formulae* deduced from studies on model compounds of small molecular weight. In the simplest approximation to these procedures (the "hard sphere" approximation), due to Ramachandran and his collaborators, the problem is even limited to the sole evaluation of allowed or forbidden contacts, with the help of Van der Waals (or similar) radii.

Interesting as such attempts are, they suffer from two obvious drawbacks. In the first place, whatever the practical justification for the partitioning of the total potential energy into a series of components, the procedure involves necessarily an element of arbitrariness and, possibly, incompleteness. Secondly, the fundamental formulae and parameters used to define the various components are far from being well-established and differ, often appreciably, from one author to another. A more rigorous deal may therefore be expected from a quantum-mechanical approach.

Possibilities of significant advances in this new direction have recently become clearly evident, due essentially to the elaboration of new methods of com-

* Lecture delivered by prof. B. Pullman as a guest of the Hungarian Academy of Sciences on August 12, 1974, Pécs.

putation which *deal simultaneously with all valence, σ and π, or even all (including inner-shell) electrons.* They are therefore able to evaluate the total molecular energy corresponding to any given configuration of the constituent atoms and thus to choose the preferred ones. Among these methods, operating all within the general scheme of the molecular orbital method, the most prominent are: *the Extended Hückel theory, the Iterative Extended Hückel Theory, the CNDO/2 and INDO methods, the PCILO method* and the *ab initio* or *non empirical* procedure.

Occasionally, all of them have been used to investigate specific conformational problems of biochemistry or pharmacology. In our laboratory we have, since about 2—3 years, developed a large program of research corresponding to *a systematic* exploration of the conformational properties of fundamental biological and pharmacological compounds with the view of assessing the role of these properties in their behaviour and function. For this sake we have used essentially the PCILO method and occasionally, when the dimensions of the system allowed it and the problem was of a particular importance, the SCF *ab initio* procedure.

I cannot insist here on the details of the methods. (For a general presentation of them see e.g. B. Pullman and A. Pullman, 1973). I would just like to illustrate here the nature and the significance of the results obtained on particularly important examples.

Proteins and their constituents

One of the principal problems in the study of the conformation of proteins is the determination of the conformational possibilities of their twenty different constituent amino-acid residues. This is done, in general, with the help of the so-called "dipeptide" model, the definitions and conventions of which are illustrated in Fig. 1 (Ramachandran, Sasisekharan, 1969; Pullman, Maigret, 1973; Pullman, Pullman, 1973).

The fundamental observation which is at the basis of this approximation is that because of the planarity of the peptide unit, the flexibility of the main backbone of the polypeptide chain originates essentially from the possibilities of rotation about the $N-C^{\alpha}$ and $C^{\alpha}-C'$ single bonds adjacent to the α-carbons. Consequently, the conformation of, say, a pair of peptide units can be specified by giving the values of the two dihedral angles Φ and Ψ around the C^{α} carbon joining these units. The conformation of the backbone of the whole polypeptide chain may be described by indicating the sequence of these angles along the chain.

The second fundamental observation indicates that, while the values assigned to one angle of a pair, Φ_i, depend markedly on the values assigned to the other angle of the same pair, Ψ_i, the interactions associated with rotations of one such pair are largely independent of the angles assumed by the neighbouring pairs Φ_{i-1}, Ψ_{i-1} and Φ_{i+1}, Ψ_{i+1}. Otherwise speaking, short-range interactions of

an amino-acid residue in a polypeptide chain which essentially involve the two peptide units directly connected with the residue represent the major determinant of its conformational possibilities. As a result of this state of affairs each pair of related rotational angles Φ and Ψ can, at least at first approximation, be treated separately from the others of the chain.

The possible values of each such pair will depend on the nature of the side chain attached to carbon α and the possible or preferred values of the side-chain rotational angles χ_1, χ_2 etc. The conformational possibilities of each of the twenty

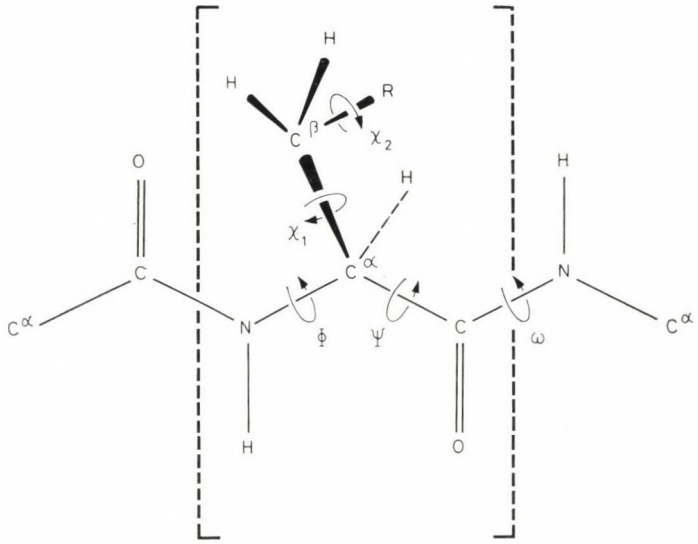

Fig. 1. Standard conventions for studying the conformation of polypeptides (Edsall et al., 1966)

residues, related to the state of the backbone, will thus be characterized by a set of associated personal values of Φ and Ψ, depending themselves on the set of χ's of the side chain.

Let us look on a few examples. Fig. 2 presents the PCILO conformational energy map for the glycyl (GLY) residue, the simplest of all residues corresponding to $R = H$ (Maigret et al., 1970). Indicated are isoenergy curves in kcal/mole with respect to the global energy minimum taken as energy zero. This energy zero (most stable conformation) is predicted for the combination $\Phi = 90°$, $\Psi = 240°$ and the symmetrical position $\Phi = 270°$, $\Psi = 120°$. Local energy minima are also seen, in particular one 2 kcal/mole above the global one at

$\Phi = \Psi = 0°$. The isoenergy curves are limited in the figure to 6 kcal/mole above the minimum, considered as a limit for stable conformations.

Fig. 3 presents similar results for the alanyl residue. (I, R = CH_3), the simplest residue containing a β carbon (Maigret et al., 1970). The most striking aspect of this map is the decrease of the conformational stability zone

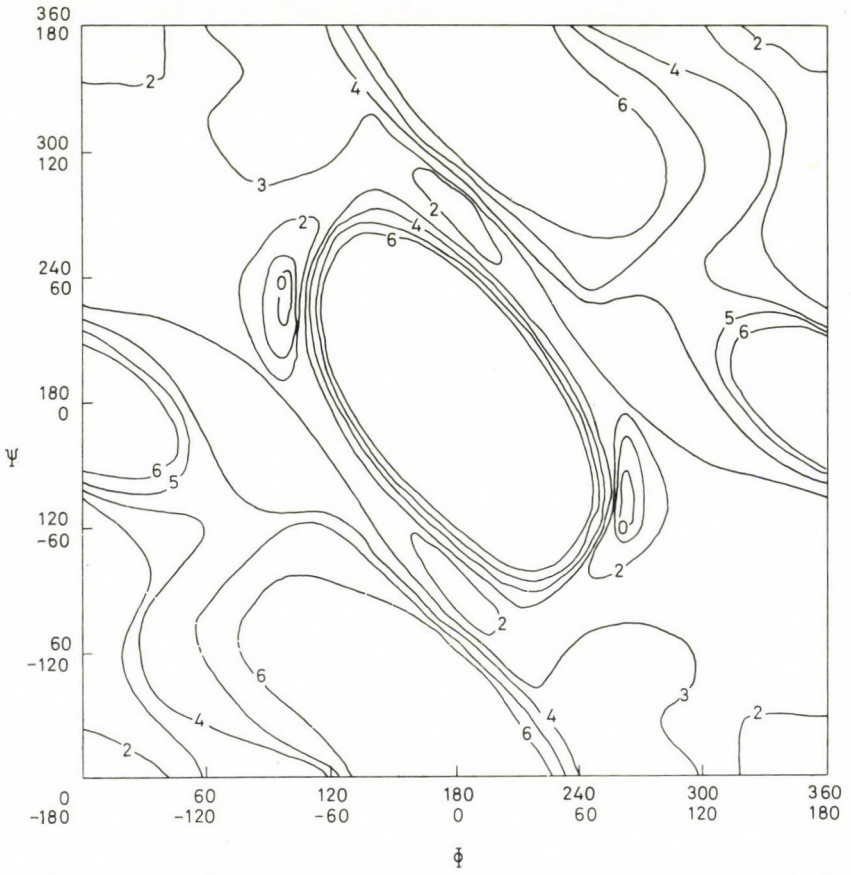

Fig. 2. PCILO conformational energy map for the GLY residue. Isoenergy curves in kcal/mole with respect to the global minimum taken as energy zero

with respect to that of the GLY residue: otherwise, we observe the same position for the nearly doubly degenerate global minimum (in this case it is only *nearly* degenerate because the residue does not have the symmetry of the GLY residue) and the presence of the local energy minimum at $\Phi = \Psi = 0°$.

The immediate question is, of course, what is the practical significance of these results for the conformation of these residues in proteins? The answer to

this question is nowadays relatively easy: it suffices to compare these theoretical indications with the experimentally observed conformations of these residues in globular proteins as given by crystal X-ray studies. A number of such proteins have been studied with sufficiently high resolution to provide information about the Φ and Ψ angles of all the constituent residues. Among such proteins are:

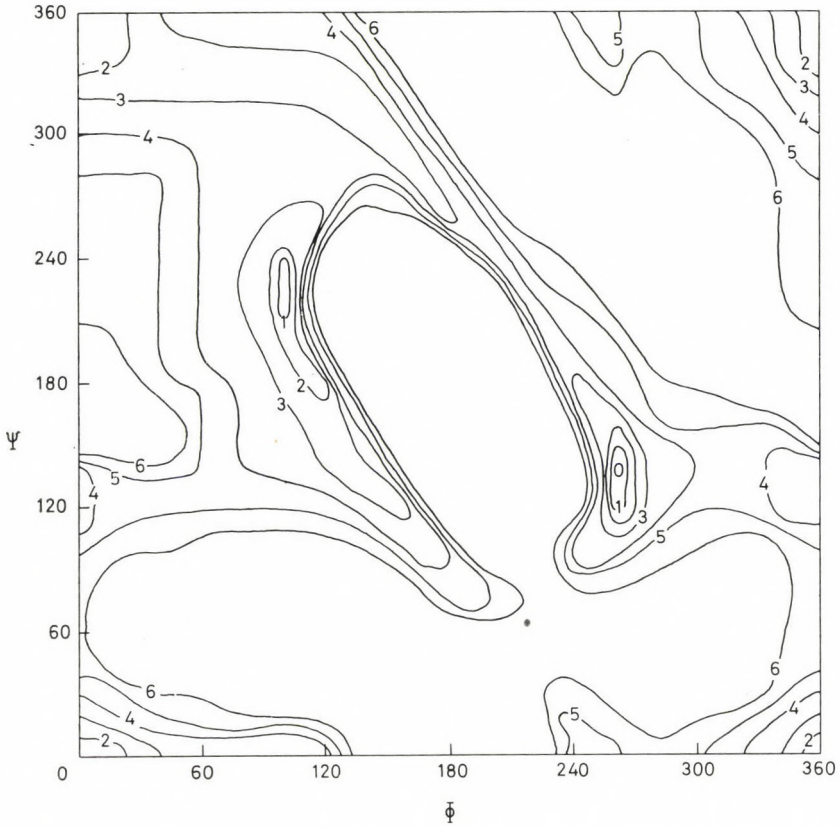

Fig. 3. PCILO conformational energy map for the ALA residue. Isoenergy curves in kcal/mole with respect to the global minimum taken as energy zero

lysozyme, myoglobin, α-chymotrypsin, carboxypeptidase, erythrocruorin, insulin, ribonuclease-S, rubredoxin, subtilisin, oxyhaemoglobin etc. They represent altogether over 2000 residues among which a large number are GLY and ALA residues. (For detailed references see B. Pullman, 1971, B. Pullman and A. Pullman, 1973.)

Fig. 4 presents:

a) the contours of the PCILO computations for the GLY residue limited at the value of 6 kcal/mole above the deepest minimum;

b) the limits of a typical "allowed" conformational space as obtained in the "hard sphere" approximation of the empirical methods (Ramachandran Sasikharan, 1969), and which is also typical of the results obtained in a large number of more developed empirical calculations using partitioned potential energy functions;

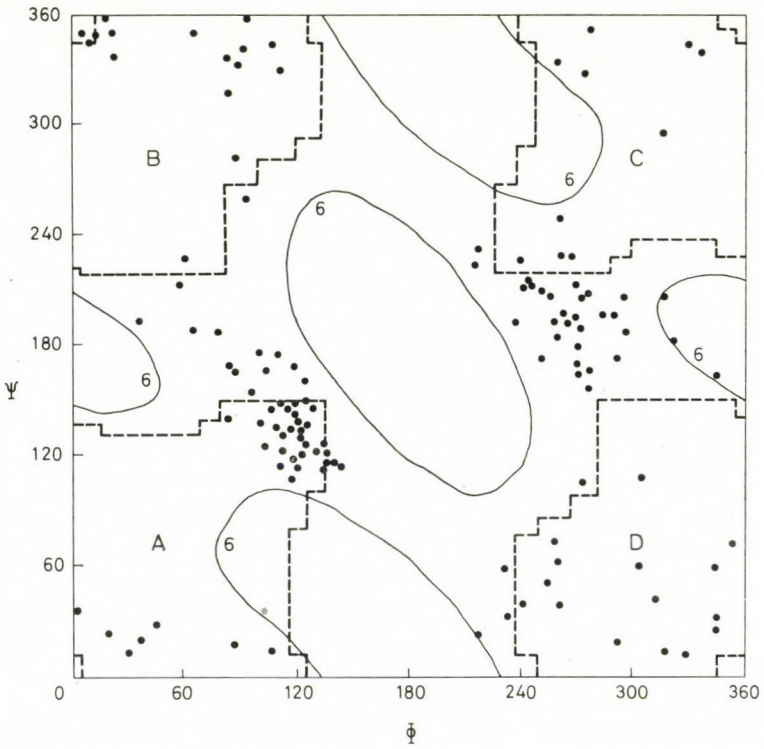

Fig. 4. Conformations of the GLY residues in globular proteins. ——— Limits of the PCILO stable zone of the GLY residue at 6 kcal/mole above the global minimum. --------- Limits of the stable zone in typical empirical computations

c) the experimental conformations of the glycyl residues in the above-mentioned globular proteins as determined by high-resolution X-ray studies.

Fig. 5 presents the same results for the ALA residue. The confrontation of the theoretical and experimental data leads immediately to two essential conclusions.

1. It is seen that in both cases the quantum-mechanical calculations impose less restrictions on the allowed or preferred conformational space than do the empirical ones.

2. The agreement between theory and experiment is much better with the quantum-mechanical calculations than with the empirical ones, many representative points lying in the space are forbidden by the latter but allowed by the former.

This situation has an important conceptual consequence: it indicates that following the quantum-mechanical computations, the "protein effect" apparently

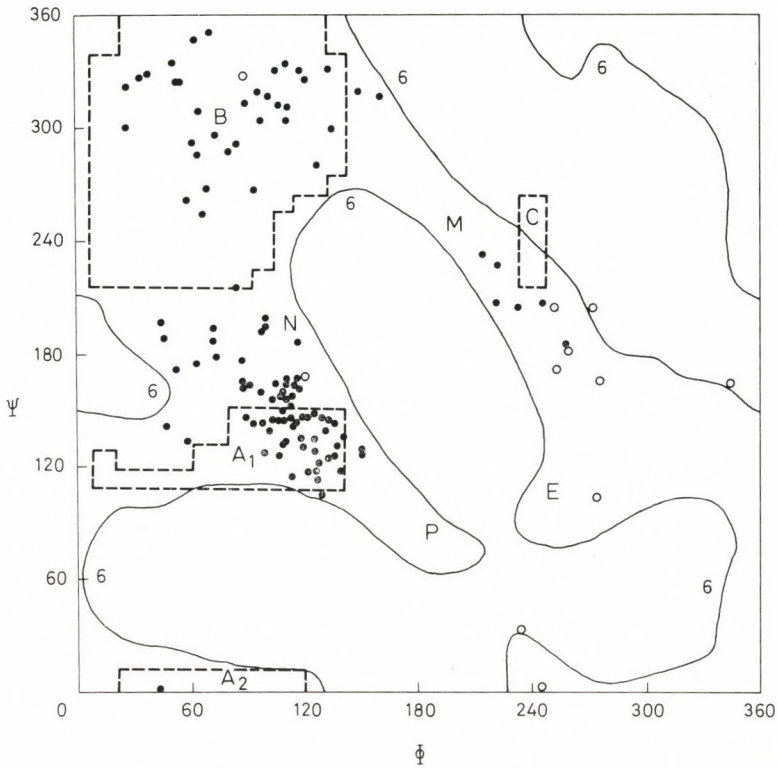

Fig. 5. Conformations of the ALA residues in globular proteins. ——— Limits of the PCILO stable zone of the ALA residue at 6 kcal/mole above the global minimum. --------- Limits of the stable zone in typical empirical computations

does not create "extraordinary" conformations, which would correspond to high-energy regions of the calculations for the "dipeptides". It just operates within the conformational stable zone of the individual residue. A different conclusion would have been drawn from the results of the empirical computations.

There is, however, also a third observation which can be made on the basis of the confrontation of the theoretical results with the conformation of the residues in globular proteins. While included within the predicted conformationally stable zone, the experimental conformations do not cluster, especially around the energy

minima of the PCILO results, in particular around the global one, but are widely scattered. The reasons for this situation are easy to determine when one considers the nature of the predicted most stable conformations. They correspond to quite particular intramolecularly hydrogen-bonded structures, *highly specific for the model dipeptide studied*: the most stable form associated with the co-ordinates $\Phi = 90°$, $\Psi = 240°$ corresponds to a seven-membered ring (Fig. 6a) called C_7 stabilized by an intramolecular hydrogen bond between $H^2 \ldots O^1$. The secondary energy minimum at $\Phi = \Psi = 0°$ corresponds to the fully extended (FE) form of the molecule stabilized by a weak intramolecular hydrogen bond formed

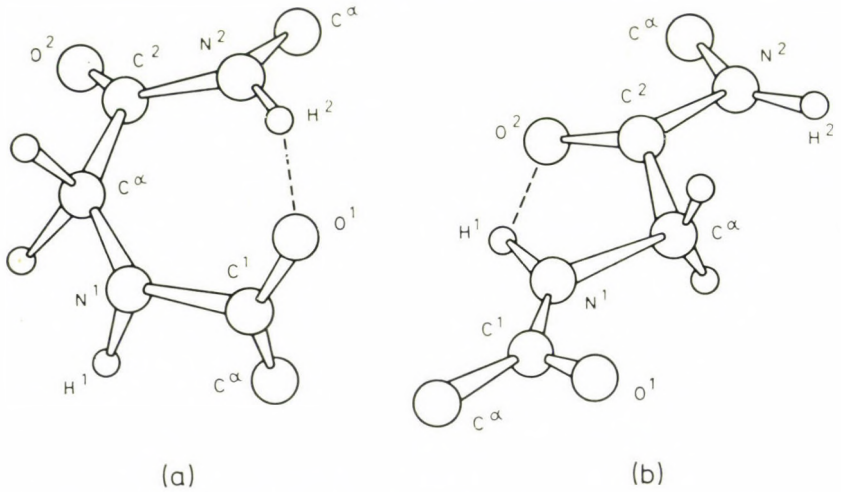

Fig. 6. The preferred conformations of the GLY and ALA dipeptides

between $O^2 \ldots H^1$ and leading to a cyclic pentagonal structure (called C_5) (Fig. 6b). These conformations are specific for the model utilized and need not be of *particular* importance in proteins where other hydrogen bonds, say between more distant residues, have a large probability to be established.

Thus, the conformational energy maps of the amino-acid residues constructed on the basis of the dipeptide model indicate correctly the overall conformational possibilities of the residues, but should not be used for the prediction of their most probable conformations in proteins. In order to make this last prediction, one needs to go beyond the dipeptide model so as to include at least medium-size interactions. Attempts in this direction have been carried out recently with promising results and PCILO computations are in press for oligopeptides including three to six amino-acid residues.

On the other hand, I would like to stress that the PCILO theoretical determination of the preferred conformations of the model dipeptides has been a success in itself. Although practically all theoretical computations whether "empirical"

or quantum-mechanical (carried out by other methods such as e.g. EHT, CNDO etc. ...) have utilized the dipeptide model, the PCILO computations are practically the only ones to have predicted the C_7 and C_5 forms as the preferred ones for these model compounds. (A group of Russian authors, using empirical methods, have predicted the importance of the C_7 forms [Popov et al., 1968].) Nowadays these predictions have been completely confirmed by NMR and infrared studies of Néel, Lascombe and co-workers (for a review see Néel, 1972; Cung et al., 1973; Avignon, Lascombe, 1973). The experiments of these authors, carried out in inert solvents (CCl_4), correspond to conditions not too far away from the isolated molecule used in the computations. The results indicate the existence of the model compounds of the GLY and ALA residues, in the very two preferred conformations predicted by the PCILO calculations: the seven-membered hydrogen-bonded ring (C_7) with angles $\Phi \approx 105°$, $\Psi \approx 130°$ and the fully extended form, involving a five-membered hydrogen-bonded ring (C_5), with angles $\Phi = \Psi = 0°$. A refinement of the experimental technique of quantitative analysis of the dipeptide leads to an approximate evaluation of the proportion of the two forms. The agreement with the theoretical predictions is again satisfactory, the C_7 form being the predominant one.

Similar results have by now been obtained for *all* the amino-acid residues of proteins and they all lead to similar individual conclusions. They indicate also, however, some general features which enable a number of extensions of the application of the procedure. Thus, one of the basic conclusions which may be drawn from these results is that the general allowed conformational space, within a fixed limit above the individual deepest minima, is similar in all these residues and similar to the general contour obtained for the alanyl residue. This situation is due to the fact that atoms situated beyond C^β of the side chain have a much smaller effect on the conformational stability than does the introduction of C^β. Naturally, there are differences among the individual residues but they all more or less conform to the pattern obtained for alanyl. What essentially distinguishes these residues from alanyl (and among themselves) is the fine structure of the conformational space and the location of the different energy minima.

Nucleic acids and their constituents

The case of the nucleic acids presents us with a different challenge. The conformational properties of polynucleotide chains depend on a series of torsion angles (Fig. 7), which may be divided into three groups:

1. the glycosidic torsion angle χ, defining the relative orientation of the purine and pyrimidine bases with respect to the sugar;
2. the torsion angles of the backbone

$$\Phi', \omega', \omega, \Phi, \Psi, \Psi'.$$

3. the torsion angles about the bonds of the sugars: $\tau_0 - \tau_4$, defining the pucker of this constituent.

In the study of nucleosides and nucleotides a special attention is frequently devoted to the orientation of the exocyclic CH_2OH or CH_2-O-PO_3H group of the sugar.

This represents a large number of degrees of freedom. Even if we put aside the torsions of the bonds of the sugars and adopt the usual empirical division of the puckering of the sugar into the classical four principal types: C(3')-endo,

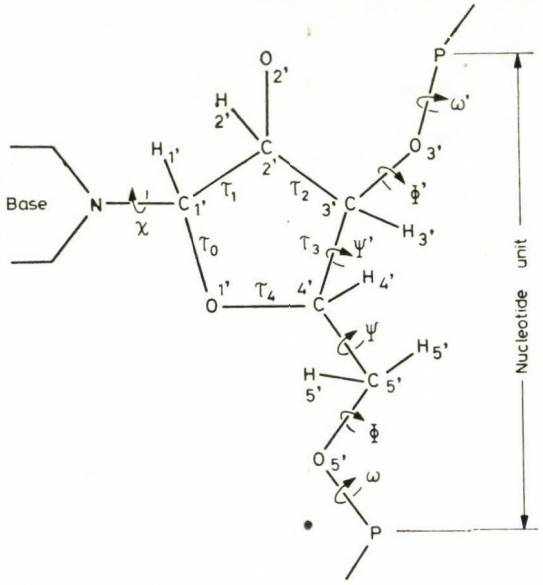

Fig. 7. The principal torsion angles in polynucleotides. Notations following M. Sundaralingam (1969, 1972)

C(2')-endo, C(3')-exo and C(2')-exo, we are still left with six essential torsion angles in the nucleotide unit. If we admit *a priori* that each of these torsions can adopt three preferred values (a reasonable *a priori* estimation), the number of possible combinations is $3^6 = 729$. Taking into account the four principal puckerings of the sugars, a dinucleoside phosphate (Fig. 8) may have about 3000 acceptable conformations. One of the goals of the theoretical work is to operate a selection of the most stable and most probable among these possible conformations so as to reduce this number.

The work, although a hard one, has been highly succesful. It has been, and continues to be carried out in steps.

The simplest to treat seems at first sight the glycosidic torsion angle χ between the base and the sugar because of its somewhat isolated position. It corresponds, in fact, to one of the most complex but also most important conforma-

tional problems in the field of nucleic acids and their constituents and which has attracted an enormous amount of theoretical and experimental investigations (Pullman, Berthod, 1973). The complexity of the problem (especially in nucleosides and nucleotides) stems from the dependence of this torsion angle upon the pucker of the sugar, the nature of the base and the orientations of the OH groups and of the exocyclic CH_2OH or CH_2O-PO_3H groups at the sugar. Different results are obtained for different possible combinations of these factors. We have explored all of them and believe to be the only ones to have done so. Contrary to the usual opinion following which the *anti* conformations are the predominant ones (opinion based on X-ray crystal studies of nucleosides and nucleotides), the real situation is a much more complex one, and a more detailed examination of experimental results in *solution* confirms, that in a number of situations the *syn* forms are abundant and important.

The essential problem appears, however, to be that of the backbone-torsion angles (Pullman et al., 1972; Perahia et al., 1973). These are too

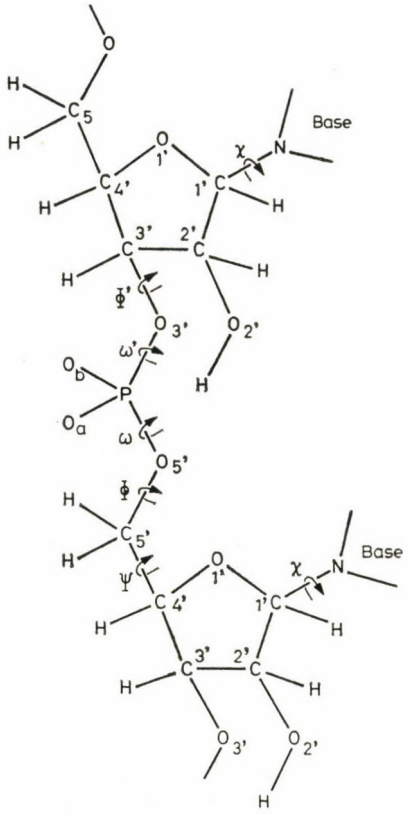

Fig. 8. The backbone of a dinucleoside monophosphate

numerous to be easily treated *en bloc*, although nowadays we could do it. The most economical treatment appears a stepwise one. Thus it is reasonable *a priori* that the strongest interdependence will exist between *adjacent* torsion angles. This means that our main goal should be to construct the conformational energy maps corresponding to the four possible combinations of two consecutive such angles: $(\omega' - \omega)$, $(\Phi' - \omega')$, $(\omega - \Phi)$, $(\Phi - \Psi)$. For this sake, preselected values have to be adopted for the torsions of the angles not involved in the particular map under consideration. These are obtained by a combination of general stereochemical arguments, by compilation of experimental indications and indica-

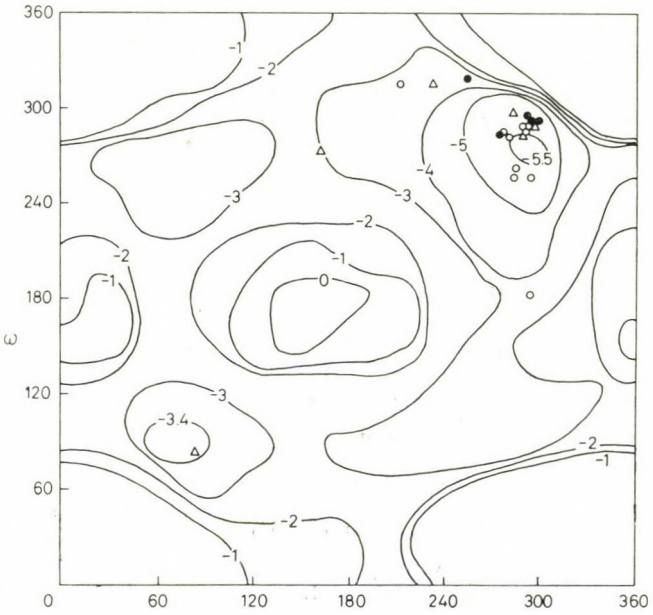

Fig. 9. PCILO ($\omega - \omega$') conformational energy map for dinucleoside monophosphates. Isoenergy curves (kcal/mole) with respect to the all trans conformation taken as energy zero

tions from available calculations by simpler empirical or quantum-mechanical method. They come out to be: 300° (preferred), 60°, and 180° for ω and ω', 60° (preferred), 180° and 300° for Ψ, 180° for Φ and 240° for Φ'. The conformational energy maps have been established for each pair of adjacent rotation angles with the appropriate combinations of these different preselected values for the remaining torsion angles. The procedure may be repeated a number of times, till self-consistency is being attained.

How do the results look like?

Let us illustrate them on the example of the $(\omega' - \omega)$ conformational energy map, which concerns what finally appear to be the two fundamental flexibility axes in polynucleotides. A representative one is given in Figure 9

(Perahia et al., 1973). It corresponds to a (3′−5′) linked diribose monophosphate with both sugars in the C(2′)-endo pucker but represents in fact the whole family of both 3′−5′ and 2′−5′ linked diribose monophosphates independently of the puckers of the sugars. Its outstanding features are the existence of two preferred stable regions corresponding to the right-handed (g^-g^-) and left-handed (g^+g^+) helices at $\omega = 270°$, $\omega' = 300°$ and $\omega = \omega' = 90°$ respectively. In Fig. 9, there is an energy difference between the two energy minima of 2.1 kcal/mole in favor of the g^-g^- conformation, which, on the other hand, is 5.5 kcal/mole more stable than the extended form ($\omega = \omega' = 180°$). The available experimental results, in crystals and in solution, confirm these predictions entirely.

We may compare our results with those obtained by the empirical computations (Sasisekharan, Lakshminarayanan, 1969). These predict the existence of seven regions of energy minima located around (ω', ω) = −60°, 60°), (60°, 180°), (180°, 60°), (180°, 180°), (180°, 300°), (300°, 180°) and (300°, 300°). Following the details of the computational procedure, some or others of these regions represent global minima: thus, when only non-bonded and torsional interactions are considered, the global minima are located at ($\omega', \omega = 60°, 60°$) and (300°, 300°); when electrostatic interactions are included in the computations with the dielectric constant $\varepsilon = 4$, the global minimum shifts to (180°, 180°); when $\varepsilon = 10$, however, the global minima move again to (60°, 60°) and (300°, 300°). These results suffer thus from the existence of too great number of local minima, some of which in regions of apparently little significance and from the difficulty in choosing unambiguously the preferred ones. More recently Olson and Flory (1972) devoted a large study to an attempt aimed at refining these empirical computations through the evaluation of the *statistical weights* of the low-energy domains of the conformational energy maps. Their effort leads to what can only be considered as very unsatisfactory results. Truly, in cases in which the older empirical computations indicated a number of equivalent local energy minima, the calculations of Olson and Flory select the most probable ones. This leads, however, in general to a pronounced disagreement with the available experimental information. In particular, one may note the occurrence of the highest statistical weights on the $\omega-\omega'$ ($\Psi'-\Psi''$ in their notations) map around the 180°−180° values of the corresponding torsion angles (*tt* conformation) for which the conformations are practically never observed.

PCILO computations have by now been completed for the remaining degrees of freedom appearing in mono- or polynucleotide units. Detailed studies have been devoted, in particular, to the orientation of the exocyclic CH_2OH group of the sugar in nucleosides (the problem of the *gg*, *gt* or *tg* conformations) (Saran et al., 1972), a comparative study of the nucleosides and nucleotides, in connection with the problem of the possible greater conformational rigidity of the latter in comparison with the former (Berthod, Pullman, 1973) and to the puckering of the ribose or deoxyribose rings (Saran et al., 1973).

Altogether and in conclusion, I feel justified to say that we seem to have today in quantum biochemistry and chemistry powerful methods for the study

of conformational problems, which may be considered as quite competitive with or, if you prefer, complementary to experimental techniques. This concerns both the possible and the preferred conformations and the barriers between them.

The next important step in these studies consists in the explicit inclusion of environmental effects. This is being investigated presently actively in our laboratory.

References

Avignon, M., Lascombe, J. (1973) in Conformation of Biological Molecules and Polymers, Proceedings of the 5th Jerusalem Symposium (E. D. Bergmann and B. Pullman eds) Academic Press, New York, p. 97

Berthod, H., Pullman, B. (1973) FEBS Letters *30* 23

Cung, M. T., Marraud, M., Neel, J. (1973) in Conformation of Biological Molecules and Polymers, Proceedings of the 5th Jerusalem Symposium (E. D. Bergmann and B. Pullman eds) Academic Press, New York, p. 69

Edsall, J. T., Flory, P. J., Kendrew, J. C., Liquori, A. M., Nemethy, G., Ramachandran, G. N., Scheraga, H. A. (1966) Biopolymers *4* 121

Maigret, B., Pullman, B., Dreyfus, M. (1970) J. Theoret. Biol. *26* 321

Neel, J. (1972) Pure and Applied Chemistry *31* 201

Olson, W. R., Flory, P. J. (1972) Biopolymers *11* 25

Perahia, D., Saran, A., Pullman, B. (1973) in Conformation of Biological Molecules and Polymers, Proceedings of the 5th Jerusalem Symposium (E. D. Bergmann and B. Pullman eds) Academic Press, New York, p. 225

Popov, E. M., Lipkind, G. M., Arkhipova, S. F., Dashevskii, U. G. (1968) Molecular Biology *2* 498

Pullman, B. (1971) in Aspects de la Chimie Quantique Contemporaine (R. Daudel and A. Pullman eds) C.N.R.S. Paris, p. 261

Pullman, B., Maigret, B. (1973) in Conformation of Biological Molecules and Polymers, Proceedings of the 5th Jerusalem Symposium (E. D. Bergmann and B. Pullman eds) Academic Press, New York, p. 13

Pullman, B., Perahia, D., Saran, A. (1972) Biochim. Biophys. Acta *269* 1

Pullman, B., Berthod, H. (1973) in Conformation of Biological Molecules and Polymers, Proceedings of the 5th Jerusalem Symposium (E. D. Bergman and A. Pullman eds) Academic Press, New York, p. 209

Pullman, B., Pullman, A. (1973) Advances in Protein Research *28* 357

Ramachandran, G. N., Sasisekharan, V. (1969) Adv. Protein Chemistry *23* 283

Saran, A., Pullman, B., Perahia, D. (1972) Biochim. Biophys. Acta *287* 211

Saran, A., Perahia, D., Pullman, B. (1973) Theoret. Chim. Acta (in press)

Sasisekharan, V., Lakshminarayanan, A. V. (1969) Biopolymers *8* 505

Sundaralingam, M. (1969) Biopolymers *7* 821

Sundaralingam, M. (1973) in Conformation of Biological Molecules and Polymers, Proceedings of the 5th Jerusalem Symposium (E. D. Bergman and B. Pullman eds) Academic Press, New York, p. 417

Acta Biochim. et Biophys. Acad. Sci. Hung. Vol. 10 (1—2), pp. 115—122 (1975)

Inactivation of Bacteriophages T7 and ΦX174 by Radiomimetics

GY. RONTÓ, M. SMOTRYAEVA, K. KRUGLYAKOVA, N. EMANUEL, I. TARJÁN

Institute of Biophysics, Semmelweis Medical University, Budapest, Hungary and Institute of Chemical Physics, USSR Academy of Sciences, Moscow, USSR

(Received October 18, 1974)

Inactivation of phages T7 and ΦX174 induced by the radiomimetics N-nitroso-N-methylurea (NMU) and N-acetylethylenimine (AEI) has been studied. In semilogarithmic scale the kinetic curves of phage inactivation were steplike in character. This was connected with the occurrence of several processes in the system. A possible kinetic model has been proposed for the process of NMU-induced phage inactivation. The model is applicable to initial phage inactivation only. From the model a kinetic curve parameter, ρ can be determined which characterizes the radiomimetic effect on different phages and determines the changes in the repair system after caffeine treatment. NMU exerted a post-inactivation effect on the phage T7. Also the NMU-induced phage T7 post-inactivation kinetic curves were of steplike character. They can be described as a sum of two exponential processes of different rate constant. The rate constant for the first stage of the post-inactivation process was close to the depurinization rate constant found in the literature.

Introduction

In recent years many chemical compounds, radiomimetics, have been found to exert effects on biological systems similar to those of radiation. These compounds are, first of all, substances having alkylating properties. N-nitroso-N-methylurea (NMU) and N-acetylethylenimine (N-AEI) are of special interest as radiomimetics.

It is well-known that NMU shows a wide range of biological effect, being an active antitumour compound (Emanuel et al., 1965; Korman et al., 1971), a carcinogene (Druckrey et al., 1964) and a supermutagene (Rapoport, 1962). The alkylating properties of these compounds have been suggested to be a basis of their action (Wheeler, 1962; Bednyak, 1970; Shooter et al., 1974; Serebryanin et al., 1969).

Since reactions of these compounds with a DNA macromolecule can play a certain role in their biological activity, NMU and N-AEI action on DNA and its components have been studied in a number of experiments *in vitro* (Schooter et al., 1974; Serebryanin et al., 1969; Rosenkranz et al., 1969; Kruglyakova et al., 1965). It was established that similarly to the effect of radiation, ethylenimine

and N-nitroso-N-alkylurea derivatives considerably changed the physico-chemical properties of the macromolecule and produced single and double strand breaks.

For studying the radiomimetic properties of NMU and N-AEI (Fig. 1) the T7 and ΦX174 free bacteriophages were used; UV inactivation of these phages has previously been studied in detail (Rontó et al., 1967; Rontó, Tarján, 1972).

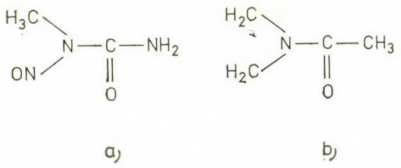

a) b)

Fig. 1. Chemical formulae of radiomimetics: N-nitroso-N-methylurea (a) and N-ac etyl ethylenimine (b)

Materials and methods

a) Bacteriophages and bacteria.

The phages T7 and ΦX174 were cultured in an M9 synthetic medium with initial titers of 5×10^8 particles /ml. *E. coli* B/r and *E. coli* C bacteria were used as host cells. The N_0 and N values (the PFU/ml in control and test samples, respectively) were determined from the mean values of 7–10 parallel experiments. 8–10 Petri dishes with 200–300 plaques were used in each experiment.

Caffeine was added to the *E. coli* B/r culture for inhibiting repair processes according to the method previously described (Sauerbier, 1964; Rontó, Tarján, 1967).

b) Treatment with radiomimetics.

The lysates of the bacteriophages T7 and ΦX174 were treated with radiomimetics in an M9 synthetic medium (pH 7) at 37°C. Solutions of the chemicals used were prepared immediately before application. The concentrations of radiomimetics employed are shown in the figures.

c) "Post-effect"

In a number of experiments NMU was removed after 15 or 60 min NMU treatment of the phages T7 by repeated dilution of phage suspensions and then the number of active phages was determined.

Results and discussion

Figures 2 and 3 show kinetic curves for inactivation of the phages T7 and ΦX174 in semilogarithmic plotting for two radiomimetics in different concentrations. As seen from the figures, the degree of phage inactivation increases with increasing mutagene concentration. Using the same concentration of NMU (0.05 M), the phage damage was more marked in the case of ΦX174. Comparison of the effect of NMU and N-AEI on phage T7 reveals N-AEI to have a stronger inactivating effect than NMU. This is the case with DNA *in vitro* (Zibina et al., 1966). In all cases the inactivation curves are of steplike character. This can be explained by the occurrence of several exponential processes in the system.

As alkylation processes are known to play a considerable role in the mechanism of action of ethylenimine and NMU derivatives on DNA (Bednyak, 1970; Shooter et al., 1974; Lawley, 1973), the phage inactivation in the initial period of time could be accounted for by these processes.

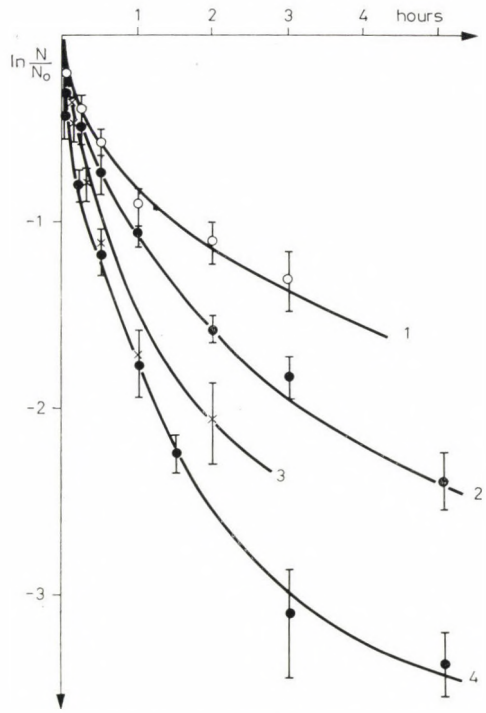

Fig. 2. Inactivation curves for phages T7 (curves 1, 2, 4) and ΦX174 (curve 3) under the action of N-nitroso-N-methylurea (1—0.025 M; 2.3—0.05 M; 4—0.075 M)

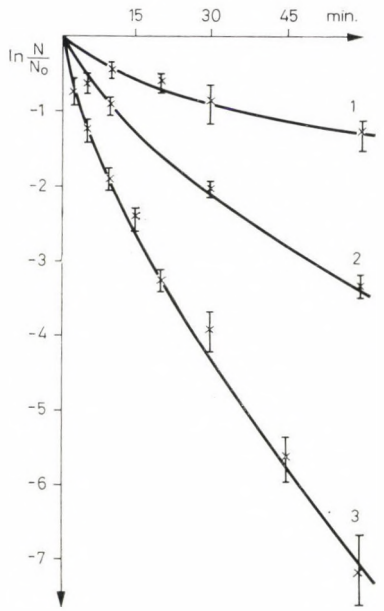

Fig. 3. Inactivation curves for phage T7 under the action of N-AEI (1—0.001 M; 2—0.003 M; 3—0.006 M)

According to Loveles and Hampton (1969), who studied the inactivation of phage T2 under the influence of NMU, the observed nature of inactivation may involve NMU decomposition. NMU is known to degrade in aqueous solutions more rapidly with increasing pH (Veleminsky, Gicher, 1970) according to the following equation:

$$C = C_0 e^{-\kappa t}, \tag{1}$$

where C_0 and C are NMU concentrations at the initial ($t = 0$) and t time, respectively, κ is the apparent decomposition rate constant. We have determined κ as 1.17×10^{-2} min^{-1} ($t = 37°$C, pH 7, medium M9) by spectrophotometry. The methyl carbon ion formed during consecutive NMU conversions is suggested to account for the NMU alkylation. Suppose the first stage of NMU decomposition to be the slowest one in the chain of consecutive NMU conversions. Then the CH_3^+ concentration would be determined by the actual NMU concentration.

If n is the mean number of alkylated sites per phage DNA molecule, then

$$\frac{dn}{dt} = K_A C_t, \tag{2}$$

where C_t is the actual NMU concentration and K_A is a value proportional to the alkylation constant. Then

$$n_t = K_A \int_0^t C_t dt, \tag{3}$$

where $D = \int_0^t C_t \, dt$.

The value of D is equivalent to an effective dose of action. As C_t decreases with time according to (1)

$$D = C_0 \int_0^t e^{-\kappa t} dt = \frac{C_0}{\kappa}(1 - e^{-\kappa t}) = \frac{C_0 - C}{\kappa} \tag{4a}$$

and

$$n = \frac{K_A(C_0 - C)}{\kappa}. \tag{3a}$$

$P(k)$ is the probability that a certain DNA molecule has k alkylated sites. This is assumed to follow a Poisson distribution. Hence the number of phages with unalkylated DNA will be

$$e^{-n} = e^{-K_A D} \tag{5}$$

Suppose that each alkylation reaction can inactivate the phage with a probability of α. Then the survival probability for a phage particle with DNA having k alkylated sites will be $(1 - \alpha)^k$. The overall survival probability (y)

for the whole population, i.e. the amount of available phages, will be

$$y = \sum_{k=0}^{\infty} P(k)\,(1 - \alpha)^k = e^{-K_A D} \tag{6}$$

Take $\rho = \alpha K_A$, then $y = e^{-\rho D}$. (6a)

As seen from the equation (6a), the value of y would depend on D, and the phage-inactivation curves corresponding to different initial C_0 concentrations should coincide. If we take into account the influence of host-cell reactivation, (6a) is to be completed in the following way

$$y_{\mathrm{HCR}} = e^{-\rho D(1-\beta_A)}, \tag{6b}$$

where β_A is the probability of repairing one alkylated site. This is shown in Fig. 4.

We actually obtained the coincidence of the curves only for the initial part until about $D = 1$ mol/min. At larger D values all the curves become descending

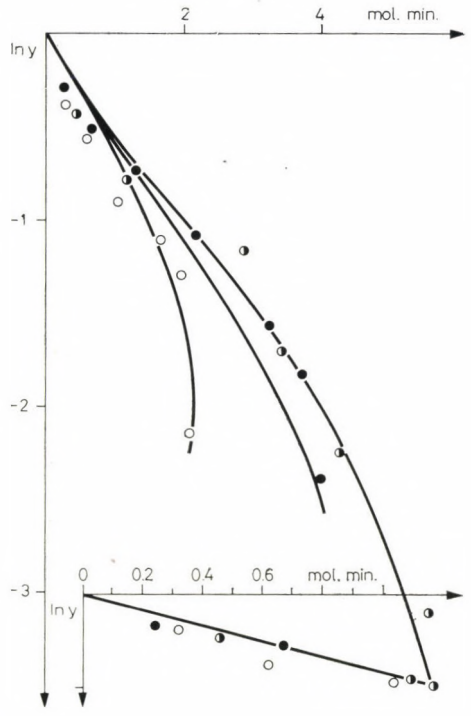

Fig. 4. Inactivation curves for phage T7 under the action of NMU as a function of the D values. 1 (○) — 0.025 M; 2 (●) — 0.05 M; 3 (◑) — 0.075 M

i.e. the phage is inactivated to a larger extent than would be expected from the model. This discrepancy might be due to additional inactivation of the phage by depurinization of the alkylated nucleotides. By the same D values this additional inactivation becomes stronger with decreasing C_0, i.e. with a longer time of NMU action.

The values of ρ and $\rho(1 - \beta_A)$ are determined from the slopes of the initial parts of the inactivation curves represented according to Fig. 4. In the case of phages T7 and ΦX174 we obtained the values of 0.85 and 1.2 mol^{-1} min^{-1} respectively.

Thus, our model describes the quantitative characteristics of the radiomimetic-induced phage inactivation in the initial period of action.

The experiments on phages T7 were evaluated with the help of *E. coli* B/r host cells capable of repairing DNA damage. Therefore, the kinetics of the phage T7 inactivation reflects the inactivation processes including the repair processes as well. As shown above, caffeine added to *E. coli* B/r cells is capable of inhibiting the cell-repair system, i.e. of repressing the DNA repair occurring after exposure of the phages to UV-light (Rontó, Tarján, 1967; Rontó et al., 1972). Repair ability of the cells (β) was found to be about 0.5. To our knowledge no data were reported on the caffeine effect in the case of treatment with various radiomimetics.

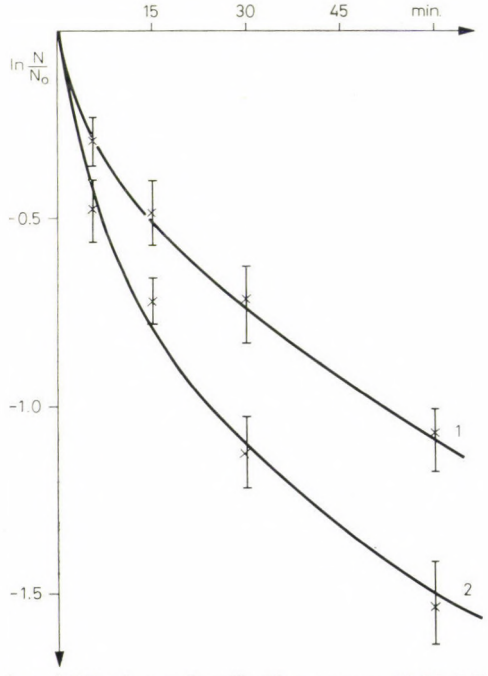

Fig. 5. The NMU-induced T7 phages inactivation curves (0.05 M) with (curve 2) and without (curve 1) caffeine treatment of host bacteria

We could show that caffeine treatment of the bacteria *E. coli* B/r after the NMU action (0.05 M) on phages T7 changed the degree of the phage inactivation similarly as UV-irradiation (Fig. 5). For the value of $\rho(1 - \beta_A)$ 1.2 $mol^{-1} \cdot min^{-1}$ was obtained. Comparing (6a) and (6b) one may write

$$\rho_{HCR+} = \rho_{HCR-}(1 - \beta_A) \tag{7}$$

For the value of β_A we obtained 0.30. This means that the host-cell reactivation capacity has similar quantitative characteristics as in the case of UV-damage repair. It has to be mentioned that the value of ρ in the case of ΦX174 inactivation represents a characteristic without influence of repair processes.

As mentioned above, the inactivation model in question seems to show that NMU-induced phage inactivation involves not only alkylation of DNA bases, but it is a multistage process.

Fig. 6 shows the "post-inactivation" of phages after 15 min (curve 1) and 60 min (curve 2) NMU treatment. One can see that they, too, are of steplike character which might be due to the occurrence of several processes in the system. Similar "post-inactivation" curves were obtained for the phage T7 under the action of another alkylating agent – monofunctional mustard gas (Lawley et al., 1969).

Our "post-inactivation" curves can be formally represented as the sum of two exponential terms:

$$\frac{N}{N_0} = Ae^{-K_1 t} + Be^{-K_2 t}$$

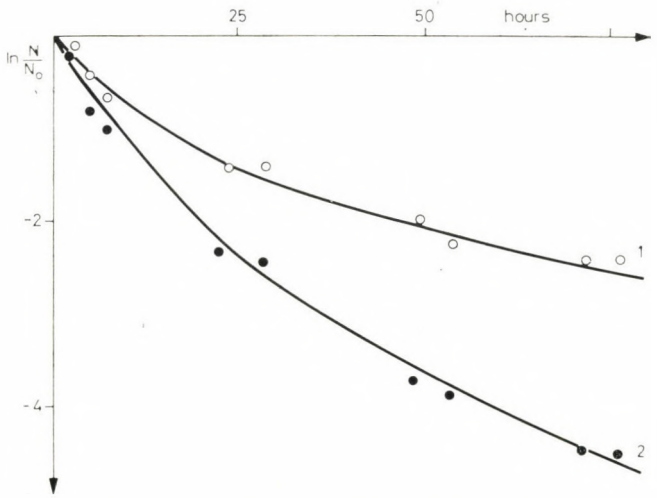

Fig. 6. "Post-inactivation" curves of phages T7 for different durations of NMU action (0.05 M). Curve 1: 15 min, Curve 2: 60 min NMU treatment

where N is the number of active phages, N_0 is the number of active phages at the time of dilution, i.e. at the time of NMU removal. The calculated post-inactivation rate constants K_1 and K_2 for the 15 and 60 min interactions of T7 phages with NMU appeared to be identical. They were: $K_1 = 0.16$ hr^{-1}; $K_2 = 0.018$ hr^{-1}. The processes differ only in preexponential factors.

It is of interest to note that the constant K_1 turned out to be close to that for depurinization of ^{14}C-guanine from the T4 phage DNA treated with NMU ($K_{\text{depurinization}} = 0.18$ hr^{-1}). Therefore, the first stage of the "post-inactivation" process is likely to involve depurinization of alkylated DNA. The second, slower "post-inactivation" process might be due to phage DNA strand breaks at the depurinization sites or to cross-links with protein amino groups of the phage head.

Thus, kinetic analysis of the experimental data on radiomimetic-induced phage inactivation yields quantitative characteristics for the inactivation of different phages under the action of radiomimetics and changes in the repair system.

The authors express their gratitude to Dr V. M. Andreev for his assistance in the treatment of experimental data, to Dr A. M. Serebryanin for the synthesis of radiomimetics, to Miss K. Aczél for helping in the experimental work and to Miss M. M. Sharina for translating the text into English.

References

Bednyak, A. E. (1970) Dokl. AN SSSR. *195* 715
Druckrey, H., Ivankovic, S., Preussmann, R. (1964) Naturwissenschaften *51* 144
Emanuel, N. M., Vermel, E. A., Rapoport, I. A., Kruglyak, S. A., Dronova, L. M., Ostrovskaya, L. A. (1965) Dokl. AN SSSR *163* 483
Kononova, S. D., Sizova, S. T., Surkov, V. V., Gumanov, L. L. (1968) "Spetsifichnos't khimicheskogo mutagenesa", M., "Nauka", (Moskva) *76*
Korman, N. P., Vermel, E. M., Milonov, B. V., Orlova, R. S. (1971) Voprosi oncologii *37*
Kruglyakova, K. E., Ulanov, B. P., Zibina, D. L., Emanuel, N. M. (1965) Dokl. AN SSSR *161* (3) 718
Lawley, P. D., Lethbridge, J. H., Edwards, P. A., Shooter, K. V. (1969) J. Mol. Biol. *39* 181
Lawley, P. D. (1973) Chem.-Biol. Interactions *7* 127
Loveles, A., Hampton, C. L. (1969) Mutation Res. *7* 1
Rapoport, I. A. (1962) Dokl. AN SSSR *146* 1418
Rontó, Gy., Tarján, I. (1967) Strahlenther. *132* 143
Rontó, Gy., Sarkadi, K., Tarján, I. (1967) Strahlenther. *134* 151
Rontó, Gy., Tarján, I. (1972) Acta Biochim. Biophys. Acad. Sci. Hung. *7* 251
Rontó, Gy., Karczag, A., Tarján, I. (1972) Studia Biophys. *33* 121
Rosenkranz, H. S., Rosenkranz, S., Schmidt, R. H. (1969) Biochim. Biophys. Acta *195* 262
Sauerbier, W. (1964) Biochim. Biophys. Res. Comm. *14* 340
Serebryanin, A. M., Smotryaeva, M. A., Kruglyakova, K. E. (1969) Izv. AN SSSR, ser. biol. *4* 607
Shooter, K. V., Howse, R., Shah, S. A., Lawley, P. D. (1974) Biochem. J. *137* 303
Veleminsky, J., Gicher, T. (1970) Mutation Res. *10* 43
Wheeler, G. P. (1962) Cancer Res. *22* 651
Zibina, D. L., Kruglyakova, K. E., Emanuel, N. M. (1966) "Supermutageni", M., "Nauka" (Moskva) *72*

Acta Biochim. et Biophys. Acad. Sci. Hung. Vol. 10 (1—2), pp. 123—128 (1975)

Photosynthetic Production and Wavelength-dependent Energy Migration

I. HORVÁTH, L. SZALAY

Department of Botany and Department of Biophysics,
József Attila University, Szeged, Hungary

(Received July 4, 1974)

If the migration of the excitation energy depends on the wavelength of the exciting light then this can be expected to influence also photosynthetic production in monochromatic light. In the present investigations we started from this assumption.

Tomato and paprika seedlings were used in the experiments.

Analysis of the results obtained on the two plants does not give a univocal answer to the question of whether the wavelength-dependent energy migration plays an inportant role in the dry-weight increase of the plants. It is beyond doubt, however, that the chlorophyll content and the dry matter increase are affected by the wavelength of the light to a considerable degree.

Introduction

The migration of the electronic excitation energy from some excited molecule to an unexcited neighbouring molecule has been extensively studied since the papers of Förster (1949) and Galanin (1955). Because of its importance in the primary process of photosynthesis, this phenomenon has been repeatedly investigated in the chlorophylls, accounts of the relevant works being given by Hoch and Knox (1968), Losev and Zenkovich (1968), Bennett and Kelley (1968), Knox (1968) and Govindjee and Mohanty (1971). These authors support the Förster energy-migration theory, although the agreement between the theory and the experimental results is not reassuring from a quantitative aspect.

It may be assumed that the poor quantitative agreement can be attributed, at least in part, to the fact that, under otherwise identical conditions, the probability of energy transfer depends on the wavelength of the exciting light. Such a dependence was first observed by Weber (1960): in essence, a molecule excited at the edge of the red band of the absorption spectrum was practically unable to transfer the excitation energy to a neighbouring unexcited molecule (red edge effect). Thus, the probability of transfer is different for different excitation frequencies. This is not accounted for by the Förster—Galanin theory. The effect was confirmed by Bauer (1969) in aromatic hydrocarbons, and by Dale and Bauer (1971) in certain other cases. Jablonski (1972) explains the phenomenon in that at an excitation frequency higher than the pure electron transfer frequency, the energy transfer occurs more often during the post-excitation period than in the equilibrium state following vibrational relaxation.

This phenomenon could be demonstrated in a mixed solution containing chlorophyll-*b* and chlorophyll-*a* (Bauer et al., 1972) and also in solutions containing carotene, chlorophyll-*a* and chlorophyll-*b* (Szabad, 1972; Szabad, Szalay, 1973). If the migration of the excitation energy depends on the wavelength of the exciting light, this can be expected to influence also photosynthetic production in monochromatic light. In the present investigations we started from this assumption.

Materials and methods

Tomato (Kecskeméti törpe variety) and paprika (Keszthelyi fehér variety) seedlings were used in the experiments. The practically monochromatic light was ensured with Zeiss metal interference filters. The filters were placed on double-walled growing-boxes, in which the plants were grown in a sand culture. The growing-boxes' double walls were perforated in an alternating manner (the facing surfaces were black), and thus the light could pass into the boxes *via* the interference filters only. The perforation was necessary because of the air exchange. A model experiment was also carried out in connection with the air exchange, in which the growing-boxes were additionally fitted with "aquarium aeraters". A 10-per-cent difference was observed in the dry weights of plants grown in the boxes with perforated walls, and those with the additional aeration. The sand culture was adjusted with Knopp solution to a water capacity of 70 per cent, and the water content was maintained by daily irrigation with distilled water to weight.

Taking into consideration the absorption spectra of chlorophyll-*a* and chlorophyll-*b*, interference filters of the following transmissions were used in the examinations: 425, 450, 475, 650, and 675 nm. The two pigments absorb energy in strongly varying proportions from the light passed through these filters.

A 1-kw halogen (iodine) lamp was used as light source, the infrared rays being filtered out with a 10 cm thick flowing water layer. The lamp caused practically no temperature increase below the water filter.

The energy of the light under these filters was constant: 7.2×10^{-3} cal cm^{-2}, cm^{-1}. Illumination was maintained for 12 hours each day. By day the temperature was ca. 28°C, and by night ca. 20°C. Three examinations were made with tomato, and four with paprika. The seedlings were processed on the 17th and 14th day after sowing, on the average, in the case of tomato and paprika, respectively. In addition to the determination of the dry weight of each organ, the chlorophyll-*a* and chlorophyll-*b* contents were measured. The pigments were extracted from 50 mg fresh material with 1 ml acetone, which was then diluted to 5 ml with petroleum ether. The amounts of chlorophyll-*a* and chlorphyll-*b* were calculated from the extinctions measured at 647 and 664 nm, according to Ziegler and Egle (1965).

Results

The results referring to dry weight are listed in Table 1. The dry weight of the storage tissues of the seed forms a significant proportion of the dry weight of the plant, and this was corrected for. The correction referred to one plant was 1.5 mg for tomato, and 4.0 mg for paprika. In this way a more realistic-seeming dry-weight increase is taken as basis.

Table 1

Dry weight and dry-weight increase

(mg/5 plants)

nm	Tomato		Paprika	
	dry weight	dry-weight increase	dry weight	dry-weight increase
425	31.5	24.0	35.0	15.0
450	22.5	15.0	26.0	6.0
475	21.5	14.0	27.5	7.5
650	30.0	22.5	42.5	22.5
675	27.5	20.0	32.5	12.5

(It should be noted that calculations were made with 5 plants, since 5 plants were grown under the interference filters and, in the following, the dry weight of 5 plants was considered for the calculation of the energy utilization.)

The results of the determination of the chlorophyll content of the cotyledon are given in Table 2.

Table 2

Chlorophyll content

(mg/g fresh weight)

nm	Tomato		Paprika	
	Chl-*a*	Chl-*b*	Chl-*a*	Chl-*b*
425	0.61	0.34	1.12	0.59
450	0.43	0.22	0.54	0.31
475	0.88	0.47	1.10	0.56
650	1.02	0.58	1.28	0.69
675	1.20	0.75	1.40	0.77

Discussion

Based on the acetone extract, the absorptions of chlorophyll-*a* and chlorophyll-*b* from the practically monochromatic light under the interference filters used were as follows.

Assuming that the numerical data given in Table 2 of the paper by Bauer et al. (1972) for the wavelength-dependent energy migration are valid, and that the energy absorbed by chlorophyll-*b* is not completely transferred (the assumed transfer at 675 nm is 50 per cent), then the photoenergy devoted to the synthesis of organic matter is characterized by the values given in column 5 of Table 3. According to these, the dry weight of the plants grown under the filters should yield the decreasing order as follows: 425, 650, 675, 450, 475 nm.

Table 3

Absorptions of chlorophyll-a and chlorophyll-b based on the acetone extract

(per cent)

nm	Absorption (per cent)		Light fraction transferred from chl-*b* to chl-*a*	Sum of columns 2 and 4
	Chl-*a*	Chl-*b*		
425	96	68	25	123
450	22	83	21	43
475	10	68	15	25
650	85	62	28	113
675	60	20	10	70

In the case of tomato the dry-weight increase (Table 1, column 3) corresponded to this order, while a somewhat different order was observed for paprika (Table 1, column 5).

As the second and fifth columns of Table 3 indicate the same order with regard to the absorbed light, it is not possible to make a clear-cut decision as to the role of the wavelength-dependent energy transfer. A further possibility of analysis arises when the amounts of chlorophyll given in Table 2 are taken into consideration and the utilizable photoenergy is expressed as the product of the extent of absorption and the amount of chlorophyll. These data are shown in Table 4.

Columns 4 and 7 of the Table 4 suggest that the following decreasing order of dry-weight increase would be expected for tomato:

650, 675, 425, 475, 450 nm,

and for paprika:

650, 425, 675, 475, 450 nm.

Table 4

Product of the extent of absorption and the amount of chlorophyll

(relative numbers)

nm	Tomato			Paprika		
	chl-*a*	chl-*b*	total	chl-*a*	chl-*b*	total
425	58	9	67	107	15	122
450	9	5	14	12	7	19
475	8	7	15	11	8	19
650	87	16	103	108	19	127
675	72	8	80	84	8	92

For paprika the sequence agrees exactly with that of the data in column 5 of Table 1, but for tomato it does not (Table 1, column 3). However, the differences in dry weight within the sequences 1 – 3 and 4 – 5 are very small. Therefore, the experimental sequence and the predicted sequence (in Table 4) are not really contradictory.

For these two plants, therefore, analysis of the results according to Tables 3 and 4 does not give an univocal answer to the question of whether the wavelength-dependent energy migration plays an important role in the dry-weight increase of the plants. It is beyond doubt, however, that the chlorophyll content and the dry-matter increase are affected by the wavelength of the light to a considerable degree.

It must be noted that the light-interference filters used did not ensure the best experimental conditions, partly because of their small size, and partly because they did not conform to the maximum and minimum photoabsorptions of chlorophyll-*a* and chlorophyll-*b*. (Of those available, the filters used approximated to this the best.) A further problem is that an *in vitro* absorption spectrum was taken as basis, thought earlier studies (Szász, Horváth, 1970) had shown the *in vivo* spectrum of chlorophyll-*b* to differ from this significantly both in the wavelength of the absorption maximum and the extent of absorption particularly in the blue wave region. In addition, it was not taken into account that also the respiration is different in lights of different "colours", although it is not probable that this difference would alter the dry-weight sequences.

The changes observed are well expressed by the energy utilization also numerically. In this calculation the energy measured under the interference filters was taken as basis, and referred to an area 4 cm in diameter. The energy value of the plant dry matter was calculated with 4000 cal per g.

The extent of the energy utilization varied between 2.0 (475 nm filter) and 12.0 per cent (425 nm filter) for tomato, and between 4.4 (450 nm filter) and 16.7 per cent (650 nm filter) for paprika.

It can also be stated that the effect is greater in paprika than in tomato.

References

Bauer, R. K. (1969) Acta Phys. Polon. *35* 101
Bauer, R. K., Szalay, L., Tombácz, E. (1972) Biophys. J. *12* 731
Bennett, R. G., Kellogg, R. E. (1968) Photochem. Photobiol. *7* 571
Dale, R. E., Bauer, R. K. (1971) Acta Phys. Polon. *40* 853
Förster, Th. (1949) Z. Naturforsch. *4* 321
Galanin, M. D. (1955) Zh. Exp. Teor. Fiz. *28* 485
Govindjee, Mohanty, P. (1971) Fluorescence News *6* 1
Hoch, G., Knox, S. (1968) Ed. A. G. Giese, Acad. Press, New York
Jablonski, A. (1972) Acta Phys. Polon. *41* 85
Knox, R. S. (1968) Physica *39* 361
Losev, A. P., Zenkovich, E T. (1968) Zh. Prikl. Spektr. *9* 144
Szabad, J. (1972) Acta Phys. Chem. Szeged, *18* 133
Szabad, J., Szalay, L. (1973) Zh. Prikl. Spektr. *19* 423
Szász, K., Horváth, I. (1970) Acta Biochim. Biophys. *5* 261
Weber, G. (1960) Biochem. J. *75* 335
Ziegler, R., Egle, K. (1965) Bestimmung. Biol. Pflanzen *41* 11

Acta Biochim. et Biophys. Acad. Sci. Hung. Vol. 10 (1—2), pp. 129—137 (1975)

Effect of Temperature on Light-absorption and Fluorescence of the Peroxidase

Z. VÁRKONYI, KATALIN KABÓK

Biophysical Institute, József Attila University, Szeged, Hungary

(Received July 26, 1974)

The absorption and fluorescence spectra of peroxidase solutions is independent of temperature in the range from 10 to 45°C. Above 45°C the absorption decreases in the visible range and increases in the ultraviolet. The intensity of fluorescence decreases with the increase of temperature. The temperature quenching of the fluorescence is accompanied by an energy transfer from tyrosine to tryptophan. The optimum enzyme activity is observed at about 40°C, at 75°C the activity ceases. The heat-induced activity change is partially reversible, the activity being restored to 40 per cent on cooling down. Enzyme activity and the activation energy of fluorescence quenching of tyrosine and tryptophan residues are given in the temperature range from 10 to 45°C. The kinetical characteristics of the processes are described.

Introduction

The temperature dependence of the light-absorption and fluorescence of horse-radish peroxidase have not yet been described, though many papers deal with the temperature dependence of the fluorescence of proteins. The changes brought about by heat in proteins result in striking changes in the fluorescence and, thus, observation of the fluorescence characteristics may provide a rapid and sensitive method for examining the state of a protein and the changes occurring in its micro-environment (Steiner, Edelhoch, 1963).

Proteins containing tryptophan have been widely studied (e.g. Gally, Edelman, 1962; Turoverov, Shchelchkov, 1970). In this group the intensity of fluorescence monotonously decreases with increasing temperature while the structures of the proteins remain unaltered. However, in the range of structural transition, the temperature-dependence does change characteristically, in many cases also the fluorescence-spectrum maximum is shifted and the band is broadening (Turoveroc, Shchelchkov, 1970).

The temperature dependence of the fluorescence of proteins containing tyrosine has been less studied. The shift of the maximum in the temperature interval of the conformational change was not observed by Turoverov and Shchelchkov (1970), who merely found a change in intensity.

Peroxidase was chosen for investigation because both tyrosine and tryptophan contribute to the fluorescence of this enzyme and, at suitable exciting wave-

lengths, their fluorescences appear well-separated (Várkonyi, Szalay, 1974). Our aim was a combined study of the absorption, the fluorescence and the enzymatic activity, as well as to draw conclusions as to the characteristics (temperature, reversibility, thermodynamic parameters) of the conformational transformation.

Materials and methods

The horse-radish peroxidase used in the experiments was a lyophilized, triply crystallized commercial preparation (Nutritional Biochemical Corporation, Cleveland). The original material had an activity of 3170 units/mg and a degree of purity RZ = 3.0. A 1×10^{-5} M solution of the recrystallized product was prepared in Tris-buffer solution of pH 7.0. Prior to measurement the solution was stored at 0–4°C for about 24 hrs. According to Klapper and Hackett (1965) the commercial peroxidase is inhomogeneous but the different fractions do not differ significantly in light absorption and enzyme activity. Therefore, the commercial sample was used without further treatment. The absorption spectra were recorded in the temperature range from 5 to 95°C. An Optical Milano Type CF 4 DR spectrophotometer was used to investigate the effects of temperature on the density and refractive index of the solution (Kortüm, 1955). The fluorescence spectra were recorded with a laboratory-built spectrofluorimeter (Várkonyi, Kovács, 1972) or with a Perkin–Elmer spectrofluorimeter, Type MPF 3, with observation normal to the exciting light using thermostated cells. The spectra were corrected for the spectral sensitivity of the photomultiplier and for reabsorption and scattered light (Murchio, Allen, 1962). The estimated effect of secondary fluorescence was negligible according to Budó (1961). The relative intensities of fluorescence were given for the same exciting-light intensity. The temperature was kept constant within ± 0.5°C and measured within the solution with a thermistor. The activity of the peroxidase was examined spectrophotometrically after Joslyn (1970) with hydrogen peroxide as a substrate and guaiacol solution by observing the optical density change at 470 nm.

Results and discussion

Between 10 and 50°C the absorption spectra are constant. Above 50°C the height of the protein peak (around 280 nm) increases, that of the haem peak (around 400 nm) decreases and also their spectral distribution is changed. If the solutions are cooled from a temperature above 50°C to any lower temperature, the absorption spectrum belonging to this lower temperature is not restored (Fig. 1). It can be concluded from this that up to 45°C the enzyme does not undergo a conformational change; at higher temperatures, however, there is an irreversible change in the conformation.

Fig. 2 shows the temperature dependence of the absorption band in detail. The changes in the extinction coefficients at 210 and 280 nm as a function of temperature are essentially similar. The absorption at 280 nm does not practically change from 10°C to 70–80°C and slightly increases above 80°C. The absorption at 210 nm steadily increases from 10 to 40–45°C; with further increase of the temperature a sudden increase occurs in the absorption. In the ultraviolet

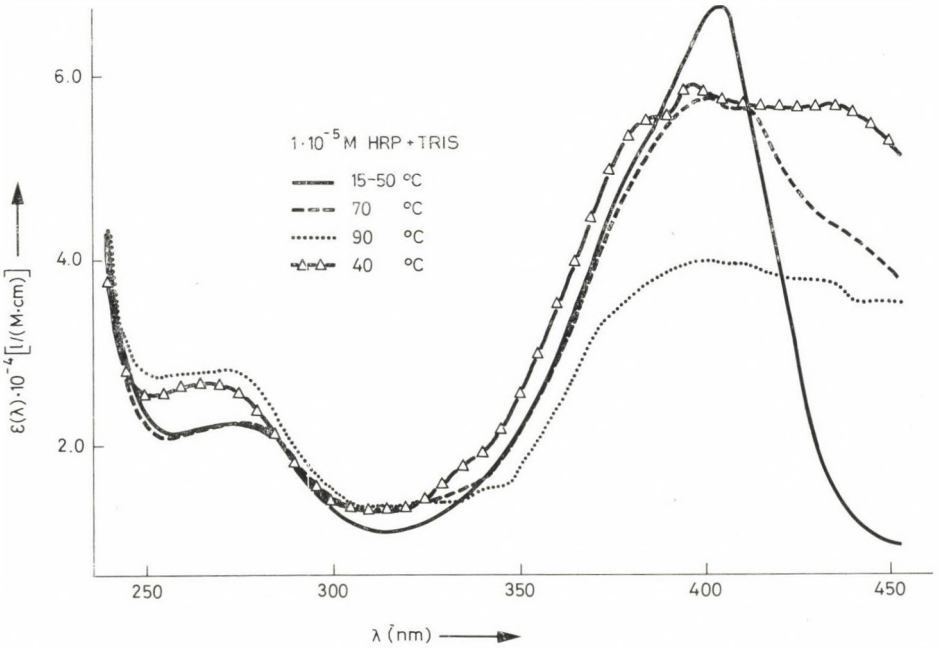

Fig. 1. Absorption spectra of 1×10^{-5} M neutral Tris-buffer solutions of peroxidase as a function of temperature in the range from 10 to 90°C, and the spectrum of a solution cooled to 40°C after heating to 90°C (———, ---------, ... data obtained by heating; △ data obtained by cooling)

absorption spectrum of β-naphthol Passerini and Ross (1967) observed an increase with increasing temperature. Similarly to the behaviour generally observed with dyes (see e.g. Hevesi and Kozma, 1966), the extinction measured at the haem peak decreases with increasing of temperature, with a sudden change around 50°C. These curves indicate that the conformational transition begins at about 40°C and is very rapid between 60 and 75°C.

Fig. 3 shows the temperature dependence of the fluorescence spectra excited at 276 and 292 nm, corresponding to the absorptions of tyrosine and tryptophan, with fluorescence maxima at 300–305 nm and 340–350 nm respectively.

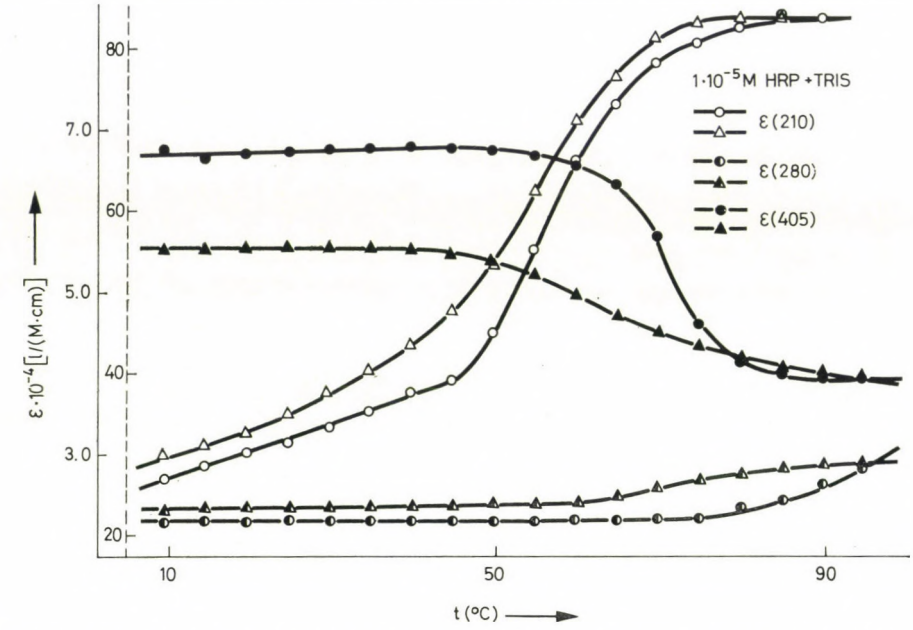

Fig. 2. Temperature dependence of absorption coefficients of neutral Tris-buffered solution of peroxidase at three wavelength characterizing the three main bands of the absorption spectrum. (The dashed curves refer to the ordinate shown by the dashed line; ○ data obtained by heating; △ data obtained by cooling)

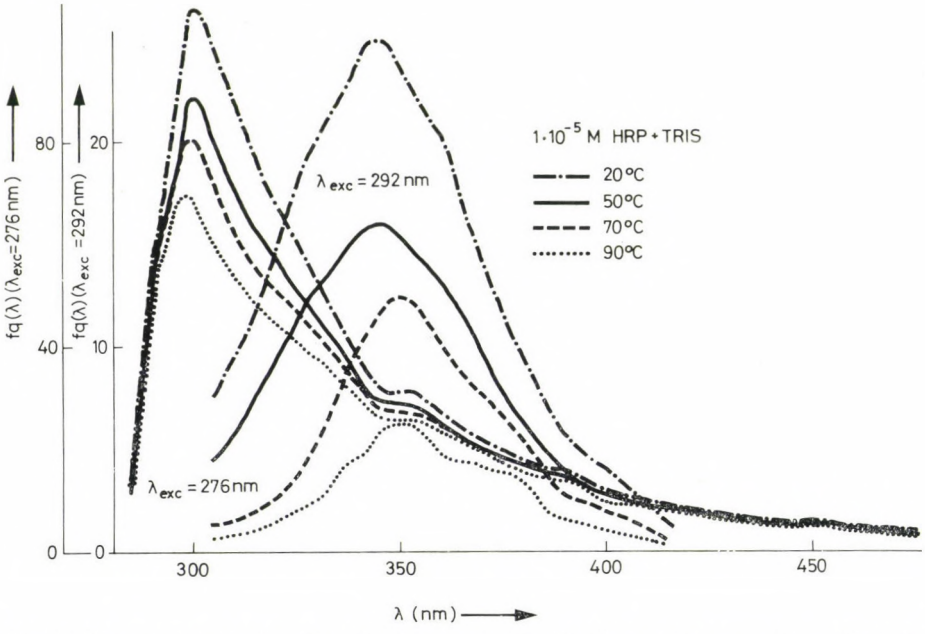

Fig. 3. Fluorescence spectra of 1×10^{-5} M neutral Tris-buffered solutions of peroxidase in the temperature range from 20 to 90°C with excitation at 276 and 292 nm

With the increase of temperature the maximum of tryptophan fluorescence is shifted towards longer waves and the band broadens, as observed by Barenboim, et al, (1968).

These changes can partly be ascribed to the accessibility for the solvent of tryptophan residues, as a consequence of the conformational transition, and partly to the rise of the vibrational energy following the temperature rise and

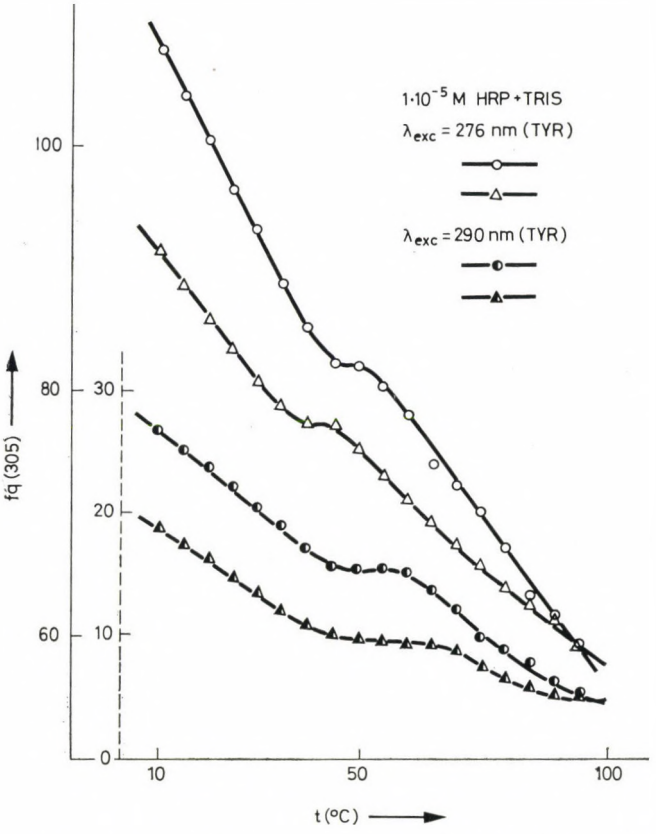

Fig. 4. Temperature-dependence of fluorescence maxima of 1×10^{-5} M neutral Tris-buffered solutions of peroxidase corresponding to the two main bands of the fluorescence spectrum (△ data obtained by heating; ○ data obtained by cooling)

leading to the weakening of intramolecular bonds. The fluorescence spectrum of tyrosine exhibits a much smaller change with the increase of the temperature.

The fluorescence spectrum of a 1×10^{-5} M solution of tryptophan in Tris-buffer (pH 7.0) between 10°C and 90°C does not depend on the temperature; the maximum is at 343 nm which is practically the same as for the room-temperature spectrum of peroxidase. This indicates that, as a result of the conformational

change, the single tryptophan residue (Welinder, Smillie, 1972) interacts more closely with a part of the protein molecule and the shift of the maximum is a consequence of this interaction.

The temperature dependence of the fluorescence intensities of peroxidase solution, as observed at 305 and 350 nm, is shown in Fig. 4. In both cases the intensity decreases with increasing temperature, showing an inflexion at about 40°C (tryptophan fluorescence) and at about 60°C (tyrosine fluorescence). A similar phenomenon observed in the case of ribonuclease was explained by

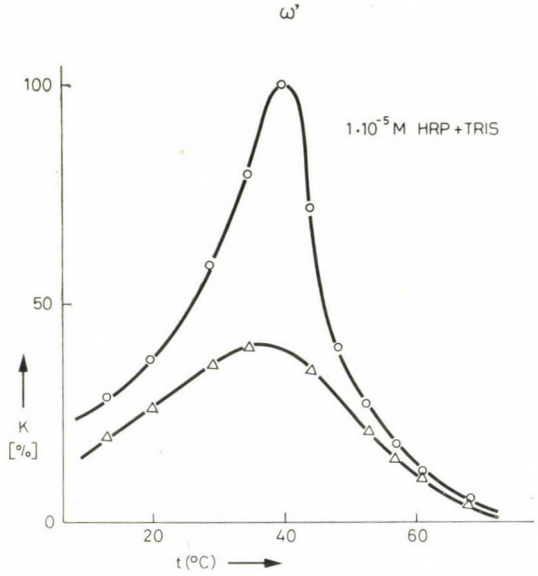

Fig. 5. Temperature dependence of activity of 1×10^{-5}, M neutral Tris-buffer solution of peroxidase (○ data obtained by heating; △ data obtained by cooling)

Barenboim et al (1968), by the splitting of the tyrosyl carboxylate hydrogen bonds. On cooling down from 90°C, the intensities of fluorescence remain below those obtained on heating, but the course of the temperature dependence is similar. If the cooling is carried out from 45°C, the intensities of fluorescence coincide with those produced on heating. This means that the intensity of the peroxidase fluorescence is subject to a "simple" temperature quenching up to ca. 45°C, and partly (and as a combined effect) undergoes a conformational change in the interval of 45–60°C. The latter, however, is partially reversible. Since the quantum yield of fluorescence around pH 7.0 does not practically depend on the pH (Cowgill, 1963; Chen et al., 1969), the decrease of the pH (from 7.0 to about 6.3) with the increase of the temperature from 10 to 90°C causes no significant change (about 2 per cent) in the intensity of fluorescence. Therefore, the observed changes are due to true temperature effect. The

temperature quenching of the fluorescence of the tryptophan solution containing Tris buffer (pH 7.0) was determined in the temperature range from 20 to 90°C. The fluorescence intensity decreases by a factor of 4.

Under similar conditions the temperature quenching of the fluorescence of the single tryptophan incorporated in peroxidase exhibits a 4fold decrease in intensity, if only the tryptophan residue is excited at 290 nm (see the dotted curves in Fig. 4). Therefore, the temperature quenching of the fluorescences of free tryptophan is more effective than that of the tryptophan bound to protein.

If the tyrosine and tryptophan in peroxidase are jointly excited at 276 nm, the temperature quenching is substantially less than the quenching when only tryptophan is excited (292 nm). The relative heights of the tyrosine and tryptophan peaks decrease at 90°C to 66 per cent and 83 per cent, respectively, of the values measured at 20°C. The ratios of the heights of the tyrosine band to that of the tryptophan band in the fluorescence spectrum measured at 20°C and 90°C are 3.3 and 2.7 respectively. This means that, on heating, a relatively greater part of the excitation energy is transferred from tyrosine to tryptophan.

Parallel with the optical measurements, also the activity of the enzyme was determined in the temperature range from 10 to 90°C. The maximum was found at about 40°C, while the activity practically ceased at 75°C (Fig. 5). On cooling, the activity was restored to about 40 per cent. The peroxidase possesses significant biological activity also after the conformational changes, in accordance with the partial reversibility of the change.

Following Turoverov (1969), the constants of the temperature quenching of fluorescence were determined with the formula $\eta_q = 1/[1 + K + k \cdot \exp(-E_a/RT)]$. Here η_q is the quantum yield of the fluorescence, E_a the activation energy, and $K = K_2/K_1$, $k = K_3/K_1 \cdot K_1$, the rate constant for deactivation of the fluorescence, K_2 that for the radiation-free and temperature-independent deactivation, and K_3 is the rate constant for temperature-dependent deactivation. Plotting $\log\left(\frac{1}{\eta_q}\right)$ against $\frac{1}{T}$ in the temperature range from 10 to 45°C, a straight line can be obtained. E_a can be determined from the slope of this straight, and k from the intercept; then K can be calculated. The values are given in Table 1. In our calculations we took into account the result published by Weber and Teale (1959), according to which $\eta_q = 0.002$ at room temperature.

The method of Raison (1973) was used for calculating the activation energy of the activity change in the temperature range investigated (10–45°C). This was 9.15 kcal/mole prior to the conformational change and 5.15 kcal/mole after the change (after cooling down and re-heating).

Comparison of the data for peroxidase with those reported by Turoverov (1969) and Chernitskii (1972) for free tyrosine and tryptophan reveals that the activation energy of the temperature quenching of the fluorescence is less for both tryptophan and tyrosine within the peroxidase than that of the free amino acid, particularly for tyrosine (3.2 kcal/mole). This can be explained by the fact

Table 1

Thermodynamic and kinetic data of the temperature quenching of fluorescence of 1×10^{-5} M neutral Tris-buffer solution of peroxidase

	Tyrosine fluorescence		Tryptophan fluorescence	
	in HRP	in free amino acid	in HRP	in free amino acid
	10=45°C	25°C	10=45°C	25°C
η_q ($T = 298$°K)	0.0087	0.21	0.002	0.22
E_a (kcal/mole)	3.2	6.2— 7.1	7.8	8.1— 8.5
$k = K_3/K_1$	10.4	10.2—13.0	8.2×10^4	15.2—14.6
$K = K_2/K_1$	114.0	0.9— 3.0	498.0	1.5— 2.3

The data for I_q of the free amino acids were taken from the literature [Weber, Teale (1959) and Chernitskii (1972)].

that in the temperature range from 10 to 45°C the tyrosine fluorescence is more easily quenched by the increase in temperature, and the energy is transferred to the tryptophan, where the difference is about 0.3 kcal/mole. For peroxidase, therefore, the fluorescence quenching involves two mechanisms: pure temperature quenching, and energy transfer.

For the tryptophan fluorescence in peroxidase the constants K_2 and K_3 can be calculated by using the value $K_1 = 1/\tau = 3.85\times10^8$ sec^{-1} of Chen et al., (1967) for tryptophan $\tau = 2.6$ nsec. Accordingly, $K_2 = 1.91\times10^{11}$ sec^{-1}, and $K_3 = 3.15\times10^{13}$ sec^{-1}. The temperature-dependent rate constant is $K_3 \cdot \exp(E_a/RT)$. Thus, at room temperature, K_3 is 2.32×10^7 sec^{-1}. From these data it can be established that the fastest process out of the three competing ones is the temperature-independent, radiation-free deactivation. K_2 is of the order of magnitude of the vibrational relaxation, two orders larger than the frequency of fluorescence, while the rate constant of the temperature-dependent deactivation is one order smaller than that of fluorescence. This explains the ready possibility for the temperature-induced change. If it were not correct, the assumption that τ of the tryptophan residue in peroxidase is the same as that of free tryptophan, the values of K_2 and K_3 would be different from those quoted, but the ratios of the differences would remain. Our data refer to 25°C, but the physiologically important temperature range is around this, and the data in this range do not differ very much from those above.

The authors wish to express their thanks to Prof. L. Szalay for his interest and helpful discussions, and to Prof. A. Garay for rendering possible the fluorescence measurements.

References

Barenboim, G. M., Sokolenko, V. A., Turoverov, K. K. (1968) Tsitologiya *10* 636—644
Budó, Á. (1961) Magyar Fizikai Folyóirat *9* 268—282
Chen, R. F., Edelhoch, H., Steiner, R. F. (1969) Physical Principles and Techniques of Protein Chemistry Ed. by S. J. Leach Acad. Press, New York and London, p. 226.
Chen, R. F., Vurek, A. A., Alexander, N. (1967) Science *156* 949—951
Chernitskii, E. A. (1972) Luminestsentsiya i strukturnaya labilnost belkov. Izd. "Nauka i tekhnika" Minsk, pp. 80
Cowgill, R. W. (1963) Arch. Biochem. Biophys. *100* 36—44
Gally, J. A., Edelman, G. M. (1962) Biochem. Biophys. Acta *60* 499—509
Hevesi, J., Kozma, L. (1966) Acta Phys. Acad. Sci. Hung. *20* 352—359
Joslyn, M. A. (1970) Enzyme Assay, in Methods in Food Analysis, Ed. by M. A. Joslyn, Acad. Press, New York and London, p. 730
Klapper, M. H., Hackett, D. P. (1965) Biochim. Biophys. Acta *96* 272—278
Kortüm, G. (1955) Kolorimetrie, Photometrie und Spektrophotometrie, Springer-Verlag, Berlin, Göttingen, Heidelberg, p. 25
Murchio, J. C., Allen, M. B. (1962) Photochem. Photobiol. *1* 259—266
Passerini, R., Ross, I. G. (1954) Chem. Phys. *22* 1012—1016
Raison, I. K. (1973) Bioenergetics *4* 285—309
Steiner, R. F., Edelhoch, H. (1963) Biochim. Biophys. Acta *66* 341—355
Turoverov, K. K. (1969) Opt. i spektr. *26* 564—570
Turoverov, K. K., Shchelchkov, B. V. (1970) Biofizika *15* 800—806 and 965—972
Várkonyi, Z., Kovács, K. (1972) Acta Biochim. Biophys. Acad. Sci. Hung. *7* 89—95
Várkonyi, Z., Szalay, L. (1974) Acta Biochim. Biophys. Acad. Sci. Hung. *9* 251—260
Weber, G., Teale, F. I. W. (1959) Disc. Faraday Soc. *27* 134—141
Welinder, K. G., Smillie, L. B. (1972) Canad. J. Biochem. *50* 44—90

Acta Biochim. et Biophys. Acad. Sci. Hung. Vol. 10 (1—2), pp. 139—141 (1975)

Inhomogeneous Detachable Technical Phantom

(Short Communication)

I. NIKL, L. BÁTKI

"Frederic Joliot-Curie" National Research Institute for Radiobiology and Radiohygiene, Budapest and X-Ray Factory of Medicor Works, Budapest, Hungary

(Received September 6, 1974)

Since the wide extension of classical image transformation of X-rays (by fluoroscopic screens and X-ray sensitive films) more and more new different types of image transformers, photofluorographs and image intensifiers are available for the radiologist performing examinations. In the course of practice the radiologist compares the quality of the picture obtained by the new image transformers with that of the conventional radiographs. In course of some years this comparison proved to be subjective. Accordingly, the mode of evaluation of the new image transformers is not reliable. A more and more critical attitude to the up-to-date image transformers has become predominant recently. As a rule, the users object to the quality of the picture mainly if the patient is corpulent or if the X-ray contrast due to the body contrast on the examined field shows but minor differences. It should be admitted that proportional deteriorations are met with also on the classical radiographs in similar cases. However, radiologists are already familiar and reckon with them. With the new image transformers the deterioration of picture quality appears in other dimensions and so renders the correct evaluation of the picture uncertain. The methods applied in industry (as e.g. image resolution by test patterns, etc.) for the characterization are rather unfamiliar to the radiologist and hardly applicable to the radiographs occurring in medical practice. In technical practice, the living human body cannot be applied as a measurement object to find the means of radiation protection. On the other hand, both as to the human body or anatomical phantoms simulating it, the same difficulties arise when the contrast differences formed on the image transformer — neither as object, nor as image contrast — do not appear in discrete, pre-scheduled form, but over a wide range, from which conclusions are difficult to draw. Accordingly, the industry turning out such devices and the radiologists have no common reference object that would be acceptable for both parties. By developing a technical phantom, we attempted to produce a device that would satisfy the aspects of both parties concerned.

In the phantom Mix-D material represents the soft tissues and N-1 material the bone tissues. Mix-D was produced according the well-known formula (Jones, Raine, 1949), while the compound of N-1 material (60 per cent bone powder, 30 per cent paraffin, 5 per cent LE wax and 5 per cent pine-resin) was developed

by ourselves. The density of the N-1 material is 1.47 g/cm^3. Density of skeleton with bone-marrow is approximately 1.5 g/cm^3 (Snyder et al., 1969). The half-value layers (HVL) of N-1 have been compiled in Table 1.

Table 1

Half-value layers (HVL) of N-1 material at two X-ray qualities

kV	HVL of Al	HVL of N-1
	mm	
80	1.56	2.62
100	1.96	3.34

The geometrical dimensions of the phantom simulate those of an average pelvis. It consists of a detachable basic part (Fig. 1) that comprises two bone-steps having the dimensions of the sacrum. One of these is linear (Fig. 1/1) and the other exponential (Fig. 1/2). Related to each other, the two bone-steps may be used in two different arrangements. The two steps can be fitted into a medium representing soft tissues (Fig. 1/3). The basic part can be completed by Mix-D phantom layers of various thicknesses so as to represent any body thickness.

The single steps within the two steps representing the bone tissue have separate intra-step circular contrast steps. The geometrical dimensions of the two steps and of the circular contrast steps are such that the shadows of contrast differences in pictures taken from the phantom by various image transformers should still be comprised by the measuring fields of micro- or macro-densitometers.

The phantom is, in general, suitable for use in all cases where the exact and reproducible measurement of either X-rays or, indirectly, of image contrast is required. It is also suitable for the measurement of electrical charge contrast. Owing to the two various steps (linear and exponential), it is possible to evaluate the image-transferring capacity of the various image-transformer systems or chains participating in image transformation.

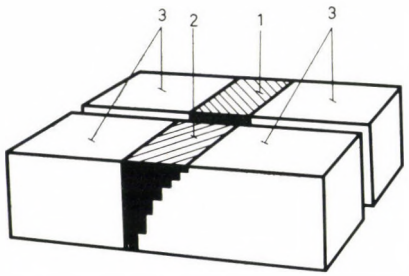

Fig. 1. Detachable basic phantom that comprises bone steps fitted into Mix-D material

Decidedly more image-transformer chains are involved in the newer image-transforming systems (e.g. X-ray TV) than in classical image transformation (film, human eye). Also, they are more complex. Whatever should the system be, the aim is identical in compliance with the nature of image-transforming system, the optimum X-ray contrast pattern of the given object should reach the input. The phantom system is suitable for similar examinations.

References

Jones, D. E. A., Raine, H. C. (1949) British J. Radiology *12* 549
Snyder, W. S., Ford, M. R., Warner, G. G., Fisher, H. I. (1969) MIRD Pamphlet No. 5, J. Nucl. Med. 10 Suppl. *3*

Book Review

Methodische Bedingungen für den histochemischen Nachweis anorganischer Ionen mit besonderer Berücksichtigung des anorganischen Orthophosphats.
Methodological conditions of the histochemical detection of inorganic ions with special regard to inorganic orthophosphates. K. J. Halbhuber (Ergebnisse der experimentellen Medizin, Bd. 14, Edited by C. Pfeiffer) VEB Verlag Volk und Gesundheit, Berlin, 1973.

The booklet (102 pages, 31 figures) deals with methods for the light- and electron-microscopic visualisation of free inorganic orthophosphates present in the liver cells largely as water-soluble free anions, i.e., in a highly diffusible form. The critical analysis of Tandler's method which yields a massive reaction in the nucleoli indicates that lead phosphate has a high affinity to nuclear structures. Thus, owing to diffusion and to special non-specific binding conditions of the reaction products, this method will lead to erroneous location of orthophosphates.

A newly developed method, — quick freezing ("Gefrierstop") in liquid nitrogen at — 79°C and freeze substitution with lead acetate containing methanol —, eliminates or minimizes diffusion and affinity artifacts.

In the case of liver cells the method results in a homogeneous distribution of the reaction, the nucleus exhibiting weaker reactivity than the cytoplasm.

Testing the specificity of the method clearly revealed that, besides orthophosphates, bicarbonates anddiphosphoesters were also visualized. Electron microscopy of the freeze-substituted tissues showed a few superficial cell layers with well-preserved structures. In these cells the reaction was found to be localized in the hyaloplasm and the mitochondria.

The book gives evidence of careful work and devotion to the subject. It contains an extensive collection of literature and can warmly be recommended to research workers dealing with this or similar questions.

G. KELÉNYI

Aufgabensammlung zur Biophysik für das Grund- und Fachstudium in Medizin, Tierproduktion — Veterinärmedizin und Biowissenschaften. Von Prof. Dr. W. Beier and Dr. rer. nat. S. Wunderlich, VEB Georg Thieme, Leipzig 1973. Mit 53 Abbildungen, 13 Tabellen und einer Formelsammlung.

The collection of exercises consists of three parts. The first part contains examples which are suitable for exercising the application of physical notions and laws for solving medical-biological problems. The six Chapters treat the examples, in nearly 220 pages, throwing light upon the general physical bases (1), the whole organism (2), organs and systems of organ (3), cellular and subcellular systems (4), the organism and the environment (5) as well as their interaction and activity. Chapter six deals with the medical application of technique.

The authors' aim was to make it possible for those who listened to biophysical and medical-physical lectures to practice the

application of the learnt basic notions and laws.

The authors best approached this aim in Chapters 3, 4, 5, and 6 of the first part, as it arises from the nature of the matter.

A large number of the exercises within each theme makes possible a better understanding of the lectures held by the authors, as emphasized also in the foreword.

The exercises of the subjects can be divided into three groups on the basis of their degree of difficulty. The first group contains exercises which can be solved with the aid of the simple knowledge of the material. The exercises of the second, and especially the third, category already need special knowledge and a creative way of thinking.

The second part of the book contains very useful tables, and the third part introduces the most important formulas.

At the end of the book we can find a list of references and subject index.

The book can be favourably used as a handbook in teaching medical students and students of biology.

S. DAMJANOVICH

Fortschritte der experimentellen und theoretischen Biophysik. Band 18. V. K. Vransky (Sofia). Zellelektrophorese. VEB Georg Thieme, Leipzig, 1974. 97 pages, 20 figures, 3 tables

With the aid of cell- or micro-electrophoresis one can determine the migration speed of charged particles in electric field. It also enables us to obtain information on the composition, structure and characteristics of the surface layer of cells, nuclei of cells, mitochondria or not biological particles. The apparatuses of this almost 100 year-old method were continually improved technically from the thirties, so that also membrane characteristics modified by biological, chemical, physical influences can be studied today, in addition to exact and reproducible measurements.

The monograph treats our present knowledge concerning the theories and results of the method in four Chapters.

Chapter 1 deals with the electric double-layer (surface charge, electrokinetics, zeta potential). It recites and documents the necessary basic physical principles of the theory of the method in such a way as making it easily understandable also for those who are not experts in the theme; mathematical deductions are not neglected either.

Chapter 2 summarizes the practical points of view of methodology, stressing that this is the only method even today by which the shift of the particle in an electric field can be directly observed and, at the same time, the migration speed can be measured (surface charge). It mentions the characteristics of apparatuses, cells of different structure, the requirements towards microscope and electrical source, the relation between migration speed and pH as well as ionic strength of the medium.

Chapter 3 summarizes the results obtained up to now and deals with the prospect of the method. It shows by the example of erythrocytes that their surface charge is different in different species; so the structural arrangement of the cell membrane cannot be taken for basis of classification of different cells. At the same time, the method is appropriate for the relative determination of the dissociating components in the outside layer of the cell. It is stated that no connection exists between the increased sedimentation of the erythrocytes and the zeta-potencial of the cell. The change of surface charge upon the effect of various drugs is demonstrated on thrombocytes; and that upon the effect of ionizing radiation on ascites cells. It is mentioned that the antigen—antibody reaction can also be tested with this method. It deals with the mobility of pathological, first of all, tumorous cells, different from normal; these data must be still evaluated with some reservations from a diagnostic point of view.

Chapter 4 summarizes, first of all, the data concerning erythrocytes and sperm-cells, and then the results of investigations on different human cells. It is stated that the mobility of almost every kind of animal cells is determined by the neuramic acid content of the membrane surface. Observations on microbes, fungi and algae are also reported.

The monograph is completed by 232 references. It is an enjoyable piece of reading for biologists, and physicians interested in the arrangement and analysis of the surface structure of the cell. The exquisite make-up of the work is a credit to the publisher.

K. JOBST

Dan F. Keller: *Glucose-6-Phosphate Dehydrogenase Deficiency*. Chemical Rubber Company Monoscience Series, Butterworth London 1971.

The question of glucose-6-phosphate dehydrogenase (G6PD) deficiency is equally interesting for clinical hematologists, specialists dealing with blood transfusion, geneticists, and biochemists working in enzymology or on biomembranes. The short monograph of D. F. Keller summarizes the fundamental aspects of the field in a manner that makes the book a useful reading working on G6PD deficiency.

First, the history of the discovery of G6PD deficiency is described, then the properties and function of G6PD in the red blood cells are discussed. To emphasize its importance, the authors deals with the pathophysiology of G6PD deficiency and the correlation between oxidative injury and red cell G6PD in, separate parts.

In the second part the genetic aspects are examined. The author gives detailed tables of the known genetic variants and of the ethnic distribution of the illness.

It is reasonable that the third part of the book is more detailed where the author describes the clinical manifestations of the deficiency, as G6PD deficiency is a disease in the first place and only secondly a problem for basic research.

The last part deals with the laboratory investigation methods. The author did not forget that at many places there are no facilities available for spectrophotometric measurement of enzyme activity and therefore gives simple methods, which can be used above all as screening tests. He deals with cytochemical methods, too, and finally, he gives a critical summary of the available procedure.

A short Addendum and an excellent list of references complete the book.

O. RÁCZ

INTERNATIONAL COLLOQUIUM ON LIPOPROTEINS AND HYPERLIPIDEMIES

In September 3–6th 1975 will be held in Lisbon an International Colloquim on lipoproteins and hyperlipidemies.

The principal themes of the meeting shall be:
1 – Structure and metabolism of lipoproteins
2 – Methods of study of lipoproteins
3 – Classification of hyperlipidemies
4 – Primary and secondary hyperlipidemies
5 – Risk factores – a biochemical approach
6 – Free themes

All correspondence related to the meeting should be addressed to:

Prof. M. J. HALPERN
Dept. of Biochemistry
Faculty of Medicine of Campo Santana
Lisbon Portugal

Printed in Hungary

A kiadásért felel az Akadémiai Kiadó igazgatója Műszaki szerkesztő: Zacsik Annamária

A kézirat nyomdába érkezett; 1975. I. 14. — Terjedelem: 13,30 (A/5) ív, 64 ábra

75.1315 Akadémiai Nyomda, Budapest — Felelős vezető: Bernát György

Walter de Gruyter
Berlin · New York

R. C. Allen — H. R. Maurer
(Editors)

Electrophoresis and Isoelectric Focusing in Polyacrylamide Gel

Advances of Methods and Theories, Biochemical and Clinical Applications

1974. Large-octavo. 316 pages. With 115 illustrations and 19 charts.
Bound DM 105,— ISBN 3 11 004344 0

This book presents the most recent advances of the methods of electrophoresis (PAGE) and isoelectric focusing (PAGIF) in polyacrylamide gel which have gained wide use in fields of biology and medicine. Described in detail are new findings on the physicochemical properties of the gel itself (Morris, Richards), theory and practice of optimization, standardization and evaluation of polyacrylamide gel electrophoresis (Maurer, Robard, Chrambach, Allen), isoelectric focusing and isotachophoresis in polyacrylamide gel (Vesterberg, Pogacar, Griffith, Catsimpoolas), quantification methods (Allen, Kling, Catsimpoolas), preparative methods (Nees, Grässlin), micro methods (Grossbach, Neuhoff, Ruchel, Dames, Maurer, Giebel), biochemical applications for isozymes and nucleic acids (Uriel, Richards, Staynov, Phillips), clinical applications (Hunter, Hoffmeister, Abraham, Felgenhaurer, Allen, Utterman). The various chapters in this volume are comprised of papers presented at a conference held at Tübingen, Germany October 6-7, 1972. This conference was arranged to bring together a group of specialists in the field in order to assess the state of the art, to discuss problems of standardization and optimization of separations, to relate theoretical considerations to practical application, as well as to discuss the limitations and future potential of these techniques in biology and medicine. This volume should serve as a usefull reference to investigators and students who wish to, or who are already employing PAGE and PAGIF in their work.

Lehrbuch der anorganischen Chemie

Begründet von **A. F. Holleman**

Von Dr. Dr. h. c. Dr. h. c. **Egon Wiberg,** Professor an der Universität München

71. — 80., völlig umgearbeitete und stark erweiterte Auflage
mit einem Anhang Chemiegeschichte, Raumbilder-Erläuterungen, einem Tabellen-Anhang, sowie 216 Figuren und einer Beilage von 37 Struktur-Bildern in stereoskopischer Darstellung.
Groß-Oktav. XXXII, 1209 Seiten. 1971. Balacron DM 58,—

Der Text der 71. — 80. Auflage des Lehrbuches wurde völlig umgestalltet und stark erweitert, so daß ein neues Werk entstanden ist, das sie jetzt nicht mehr — wie bisher — nur an den Anfänger, sondern auch an die Fortgeschrittenen der Chemie wendet.

Das Buch gliedert sich in vier große Hauptteile:

A: Atom und Molekül
B: Hauptgruppen des Periodensystems
C: Nebengruppen des Periodensystems
D: Lanthaniden und Actiniden

Den Abschluß des Buches bilden: ein chemiegeschichtlicher Anhang, ein Anhang mit Erläuterungen zur angefügten Raumbilder-Beilage und ein Tabellen-Anhang. Die Atomgewichte, Elementhäufigkeiten, physikalische Daten und atomaren Konstanten entsprechen dem neusten Stand.

Die Anzahl der Abbildungen, Tabellen und tabellarischen Überblicke wurde beträchtlich erhöht. Die Raumbilder-Beilage wurde um 6 Atomstrukturen vermehrt.

Walter de Gruyter & Co · Berlin 30

Reviews of the Hungarian Academy of Sciences are obtainable at the following addresses:

AUSTRALIA

C. B. D. Library and Subscription Service
Box 4886, G. P. O.
Sydney N. S. W. 2001

Cosmos Bookshop
145 Acland St.
St. Kilda 3182

AUSTRIA

Globus
Höchstädtplatz 3
A–1200 Wien XX

BELGIUM

Office International de Librairie
30 Avenue Marnix
1050–Bruxelles

Du Monde Entier
162 Rue du Midi
1000–Bruxelles

BULGARIA

Hemus
Bulvar Ruszki 6
Sofia

CANADA

Pannonia Books
P. O. Box 1017
Postal Station "B"
Toronto, Ont. M5T 2T8

CHINA

C N P I C O R
Periodical Department
P. O. Box 50
Peking

CZECHOSLOVAKIA

Mad'arská Kultura
Národní třida 22
115 66 Praha

PNS Dovoz tisku
Vinohradská 46
Praha 2

PNS Dovoz tlače
Bratislava 2

DENMARK

Ejnar Munksgaard
Nörregade 6
DK–1165 Copenhagen K

FINLAND

Akateeminen Kirjakauppa
P. O. Box 128
SF–00101 Helsinki 10

FRANCE

Office International de Documentation et Librairie
48 Rue Gay-Lussac
Paris 5

Librairie Lavoisier
11 Rue Lavoisier
Paris 8

Europeriodiques S. A.
31 Avenue de Versailles
78170 La Celle St. Cloud

GERMAN DEMOCRATIC REPUBLIC

Haus der Ungarischen Kultur
Karl-Liebknecht-Strasse 9
DDR–102 Berlin

Deutsche Post
Zeitungsvertriebsamt
Strasse der Pariser Kommüne 3–4
DDR–104 Berlin

GERMAN FEDERAL REPUBLIC

Kunst und Wissen
Erich Bieber
Postfach 46
7 Stuttgart S

GREAT BRITAIN

Blackwell's Periodicals
P. O. Box 40
Hythe Bridge Street
Oxford OX1 2EU

Collet's Holdings Ltd.
Denington Estate
London Road
Wellingborough Northants NN8 2QT

Bumpus Haldane and Maxwell Ltd.
5 Fitzroy Square
London W1P 5AH

Dawson and Sons Ltd.
Cannon House
Park Farm Road
Folkestone, Kent

HOLLAND

Swets and Zeitlinger
Heereweg 347b
Lisse

Martinus Nijhoff
Lange Voorhout 9
The Hague

INDIA

Hind Book House
66 Babar Road
New Delhi 1

India Book House
Subscription Agency
249 Dr. D. N. Road
Bombay 1

ITALY

Santo Vanasia
Via M. Macchi 71
20124 Milano

Libreria Commissionaria Sansoni
Via Lamarmora 45
50121 Firenze

JAPAN

Kinokuniya Book-Store Co. Ltd.
826 Tsunohazu 1-chome
Shinjuku-ku
Tokyo 160–91

Maruzen and Co. Ltd.
P. O. Box 5050
Tokyo International 100–31

Nauka Ltd.–Export Department
2–2 Kanda
Jinbocho
Chiyoda-ku
Tokyo 101

KOREA

Chulpanmul
Phenjan

NORWAY

Tanum-Cammermeyer
Karl Johansgatan 41–43
Oslo 1

POLAND

Węgierski Instytut Kultury
Marszalkowska 80
Warszawa

BKWZ Ruch
ul. Wronia 23
00–840 Warszawa

ROUMANIA

D. E. P.
Bucureşti

Romlibri
Str. Biserica Amzei 7
Bucureşti

SOVIET UNION

Sojuzpechatj – Import
Moscow
and the post offices in each town

Mezhdunarodnaya Kniga
Moscow G–200

SWEDEN

Almqvist and Wiksell
Gamla Brogatan 26
S–101 20 Stockholm

A. B. Nordiska Bokhandeln
Kunstgatan 4
101 10 Stockholm 1 Fack

SWITZERLAND

Karger Libri AG.
Arnold-Böcklin-Str. 25
4000 Basel 11

USA

F. W. Faxon Co. Inc.
15 Southwest Park
Westwood, Mass. 02090

Stechert-Hafner Inc.
Serials Fulfillment
P. O. Box 900
Riverside N. J. 08075

Fam Book Service
69 Fifth Avenue
New York N. Y. 10003

Maxwell Scientific International Inc.
Fairview Park
Elmsford N. Y. 10523

Read More Publications Inc.
140 Cedar Street
New York N. Y. 10006

VIETNAM

Xunhasaba
32, Hai Ba Trung
Hanoi

YUGOSLAVIA

Jugoslovenska Knjiga
Terazije 27
Beograd

Forum
Vojvode Mišića 1
21000 Novi Sad

Contents

28. V. 1975 Index : 26.030

VOLUME 10
NUMBER 3
1975

Acta biochimica et biophysica

ACADEMIAE SCIENTIARUM HUNGARICAE

AKADÉMIAI KIADÓ, BUDAPEST

ABBPAP 10 (3) 147–261 (1975)

Acta Biochimica et Biophysica

Academiae Scientiarum Hungaricae

Szerkeszti:

STRAUB F. BRUNÓ és ERNST JENŐ

Technikai szerkesztők:

SAJGÓ MIHÁLY és NIEDETZKY ANTAL

Szerkesztőség postai címe: 1502 Budapest, Pf. 7 (biokémia)
7643 Pécs, Pf. 99 (biofizika)

Az *Acta Biochimica et Biophysica* a Magyar Tudományos Akadémia idegen nyelvű folyóirata, amely angol nyelven (esetleg német, francia vagy orosz nyelven is) eredeti tanulmányokat közöl a biokémia és a biofizika — fehérjék (struktúra és szintézis), enzimek, nukleinsavak, szabályozó és transzport-folyamatok, bioenergetika, izom-összehúzódás, radiobiológia, biokibernetika, funkcionális és ultrastruktúra stb. — tárgyköréből.

A folyóirat negyedévenként jelenik meg, a négy füzet évente egy kb. 400 oldalas kötetet alkot. Kiadja az Akadémiai Kiadó.

Megrendelhető az Akadémiai Kiadónál (1363 Bp. Pf. 24.), a külföld részére pedig a Kultúra Könyv és Hírlap Külkereskedelmi Vállalatnál (1389 Budapest 62, P.O.B. 149).

The *Acta Biochimica et Biophysica*, a periodical of the Hungarian Academy of Sciences, publishes original papers, in English, on biochemistry and biophysics. Its main topics are: proteins (structure and synthesis), enzymes, nucleic acids, regulatory and transport processes, bioenergetics, excitation, muscular contraction, radiobiology, biocybernetics, functional structure and ultrastructure.

The Acta Biochimica et Biophysica is a quarterly, the four issues make up a volume of some 400 pages per annum. Manuscripts and correspondence with the editors and publishers should be sent to

Akadémiai Kiadó, Budapest 24, P.O.B. 502.

The subscription rate is $32.00 per volume. Orders may be placed with *Kultúra* Trading Co. for Books and Newspapers (1389 Budapest 62, P.O.B. 149) or with its representatives abroad, listed on p. 3 of the cover.

Acta Biochimica et Biophysica — журнал Академии Наук Венгрии, публикующий на английском языке (возможно и на немецком, французском и русском языках) оригинальные статьи по проблемам биохимии и биофизики — белков (структура и синтез), энзимов, нуклеиновых кислот, процессов регуляции и транспорта, биоэнергетики, мышечного сокращения, радиобиологии, биокибернетики, функциональной структуры и ультраструктуры и т. д.

Журнал выходит ежеквартально, выпуски каждого года составляют том объемом около 400 сшпаниц. Журнал выпускает Издательство Академии Наук Венгрии.

Рукописи и корреспонденцию просим направлять по следующему адресу:

Akadémiai Kiadó, Budapest 24, P.O.B. 502.

Подписная цена — $ 32.00 за том. Заказы принимает:

Предприятие по внешней торговле книгами и газетами «Kultúra» (1389 Budapest 62, P.O.B. 149) или его заграничные агентства.

Acta Biochim. et Biophys. Acad. Sci. Hung. Vol. 10 (3), pp. 147—152 (1975)

Increased Synthesis of Nuclear RNA in Regenerating Rat Liver after γ-Irradiation

ANNA FÓNAGY, E. J. HÍDVÉGI, LARISZA GUETH, L. D. SZABÓ

"Frédéric Joliot-Curie" National Research Institute for Radiobiology and Radiohygiene, 1775 Budapest, Hungary

(Received April 30, 1975)

Nine hours after partial hepatectomy rats were whole-body, ^{60}Co-γ-irradiated with exposures of 50, 100, 200, 500, 1000 and 2000 *R*, respec tively. RNA was prepared from isolated nuclei of rat liver 12 hours after partial hepatectomy. Animals were injected with ^{14}C-orotic acid 20 minutes before killing. The isolated labelled nuclear RNA was fractionated by sucrose density gradient centrifugation. The specific radioactivity of RNA was correlated with that of the specific radioactivity of nucleotide pool of the liver homogenates.

RNA synthesis was found to increase after each dose applied as compared to the rate of RNA synthesis in 12 hours regenerating liver. The increment depended on the dose delivered: 10% at 50 *R*, 50% at 500 *R* and 30% at 2000 *R*. Nuclear RNA synthesis also increased in the liver of non-hepatectomized rats 3 hours after 500 *R* γ-irradiation, but the increment was only 20—30% above the non-hepatectomized and unirradiated control.

The regenerating liver, as a partially synchronized cell system, is a feasible experimental tool for studying the events of macromolecular syntheses after irradiation. The intensity of synthesis of certain species of RNA depends on which intervention has been used earlier and on the duration of time between hepatectomy and irradiation (Ord, Stocken, 1956; Beltz et al., 1957; Welling, Cohen, 1960; Bucher, 1963; Uchiyama et al., 1965, 1966; Berg, Goutier, 1967; Fausto, Van Lancker, 1969; Fónagy et al., 1975; Markov et al., 1975).

It has already been described that the intensity of RNA synthesis increases in liver a few hours after whole-body X-irradiation alone (Hídvégi et al., 1965, 1970; Cammarano et al., 1969; Popov et al., 1971). It is also well known that shortly after partial hepatectomy RNA synthesis in the liver increases (Fujioka et al., 1963; Muramatsu, Busch, 1965).

The present paper describes an increased synthesis of nuclear RNA in regenerating liver when the irradiation was applied in the late G_1-phase after hepatectomy.

Abbreviations used: rRNA, ribosomal RNA; mRNA, messenger RNA; pre-rRNA, precursor of rRNA; RNase, ribonuclease.

Materials and methods

6-^{14}C-orotic acid, specific radioactivity 62 mCi/mmol, was purchased from The Radiochemical Centre, Amersham. Diethyl pyrocarbonate was the product of Bayer Werke, Leverkusen. Sucrose for density-gradient centrifugation was purchased from Schwarz (Mann, Orangeburg) and Darco G 60 activated charcoal from Serva, Heidelberg. All other chemicals were the products of Reanal, Budapest.

F_1 hybrids of Wistar R/Amsterdam × Long-Evans (Chester Beatty hooded) male rats were used, weighing 180–200 g. The animals were starved for 24 hours before being killed. Partial hepatectomy consisted in the removal of about two-thirds of the liver (left lateral and medial lobes) (Higgins, Anderson, 1931). Surgery was done under ether anesthesia in the evening hours. Nine hours after hepatectomy the animals were irradiated with γ-rays from a ^{60}Co-source, at exposure rate of 129 *R*/min. Doses of 50, 100, 300, 500, 1000 and 2000 *R* were delivered to the whole body.

Either whole livers of three control animals or five livers of hepatectomized rats were pooled. Twenty minutes before being killed the animals were injected intravenously with 2 μCi of ^{14}C-orotic acid. Three hours after irradiation the rats were killed and the livers were immediately perfused with ice cold physiological saline. The livers were homogenized at 0°C in 2.1 M sucrose solution containing 3.3 mM $CaCl_2$. All sucrose solutions were treated with diethyl pyrocarbonate to destroy RNase activity. The homogenate was then ultracentrifuged at 0°C at 40 000 × *g* for one hour in the No. 30 rotor of the Beckman model L2-65B ultracentrifuge.

The pellet of clean nuclei was suspended in 0.05 M acetate buffer (pH 5.1) containing 0.3% sodium-dodecyl-sulphate and 0.14 M NaCl. The RNA was extracted by phenol containing 0.1% 8-hydroxyquinoline at 60°C for 10 minutes (Steele et al., 1965; Steele, Busch, 1966). The RNA was precipitated by adding 2.5 volumes of ethanol containing 2% potassium acetate.

The whole nuclear RNA was fractionated on a 10–45% (w/w) linear sucrose density gradient containing 1 mM EDTA and 0.1 M NaCl in 0.01 M acetate buffer (pH 5.1). 200 μg of RNA was layered on a 36 ml-gradient and ultracentrifuged in the SW 27 rotor at 26 000 rpm for 16 hours. The gradient was continuously recorded at 254 nm and fractionated with an ISCO model 640 fractionator. The radioactivity of 1 ml fractions was measured in a Packard Tri-Carb model 3375 liquid scintillation spectrometer.

From a small part of the liver homogenate the specific radioactivity of the acid-soluble nucleotide pool was determined. 1 M perchloric acid was added to a final concentration of 0.5 M to the liver homogenate. The sample was kept in ice for 30 minutes and then centrifuged. From the samples of the supernatant the labelled nucleotides were adsorbed to Darco G 60 and eluted with 50% ethanol containing 2.5% NH_3. The optical density at 254 nm and the radioactivity of the eluate were measured.

Results

First the incorporation of ^{14}C-orotic acid into whole nuclear RNA was measured after irradiation with various doses. The value of incorporation is given as specific radioactivity of whole nuclear RNA (Fig. 1*A*).

The relative specific radioactivity of the whole nuclear RNA (Fig. 1*B*) was determined by relating the specific radioactivity of the whole nuclear RNA to the specific radioactivity of the nucleotide pool. The radiosensitivity of the synthesis of whole nuclear RNA was investigated 3 hours after irradiation of non-hepa-

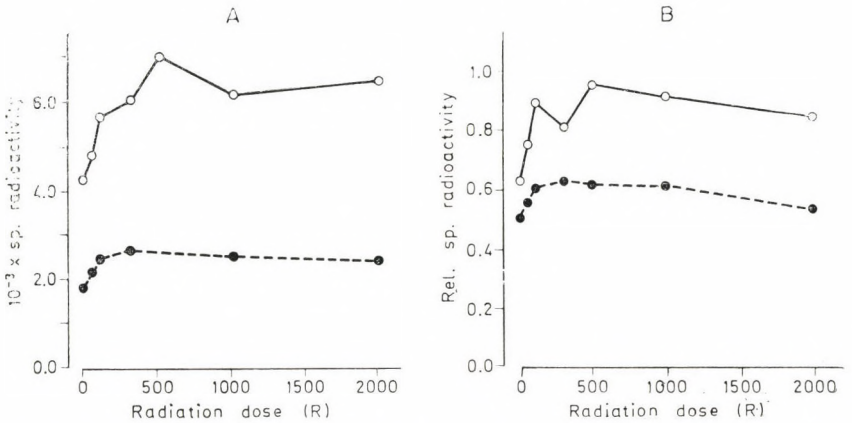

Fig. 1. Radiation dose dependence of increased synthesis of whole nuclear RNA isolated from normal and regenerating liver. *A*, Specific radioactivity of whole nuclear RNA; *B*, Relative specific radioactivity of whole nuclear RNA. The lower curves (● — ●) show the radioactivity of nuclear RNA isolated from non-hepatectomized animals 3 hours after irradiation. The upper curves (○ — ○) show the radioactivity of nuclear RNA isolated 12 hours after partial hepatectomy from rats which were irradiated at the 9th hour of the regeneration process. 2 μCi of ^{14}C-orotic acid was administered intravenously 20 minutes before sacrifice. Specific radioactivity of RNA and of nucleotides: dpm/E_{260} nm. Relative specific radioactivity of RNA is related to the specific radioactivity of the acid-soluble nucleotide pool of the homogenate

tectomized rats (Fig. 1*A* and *B*, lower curves) and 3 hours after irradiation of partially hepatectomized, rats, i.e. the animals were irradiated in the 9th hour and sacrificed in the 12th hour of the regeneration process (Fig. 1*A* and *B*, upper curves).

In both cases an increase in the radioactivity of nuclear RNA was established and the difference from the control already reached its maximum at a dose of 500 *R*. The increase in radioactivity of rat liver nuclear RNA of irradiated animals was about 20 — 30% (Fig. 1*A* and *B*, lower curves), and 50 — 60% when both hepatectomy and irradiation were applied together (Fig. 1*A* and *B*, upper curves). A comparison of Fig. 1*A* with Fig. 1*B* indicates that the specific radioactivity

of the nuclear RNA and its relative specific radioactivity change similarly as a function of the dose. This means that the specific radioactivity of the nucleotide pool changes only slightly under the effect of irradiation either in intact or in regenerating liver.

For a further characterization of the effect of radiation on RNA synthesis the whole nuclear RNA was fractionated by sucrose density gradient centrifugation. The major radioactivity peak coincided with the 45 *S* optical density peak.

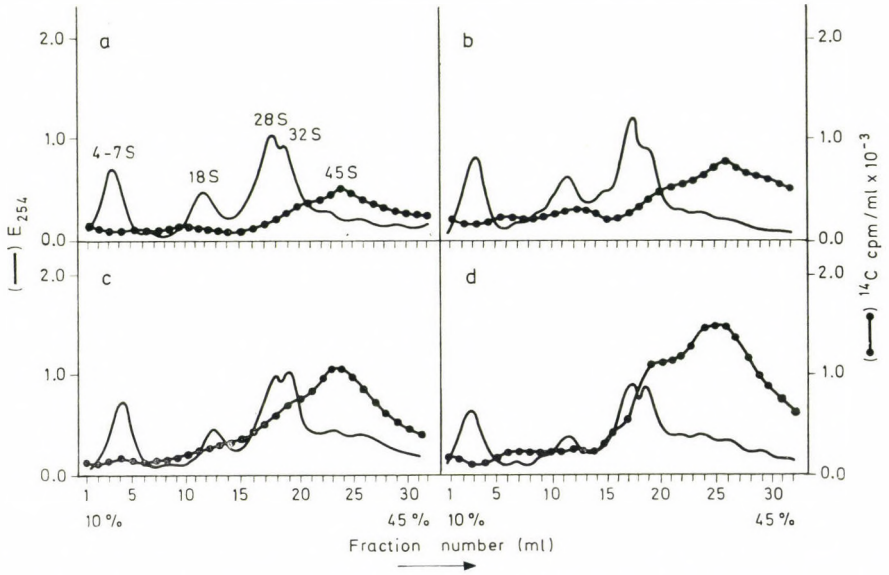

Fig. 2. Sucrose density gradient profile of whole nuclear RNA isolated from rat liver. Rats were injected with 2 μCi of ^{14}C-orotic acid 20 minutes before sacrifice. 200 μg of whole nuclear RNA were applied to 36 ml of a 10–45% (w/w) linear gradient and centrifuged at 0° C at 26 000 rpm for 16 hours in an SW 27 rotor. The full line represents the optical density recorded at 254 nm and the dotted line the radioactivity of 1 ml fractions. The numbers above the peaks indicate the approximate sedimentation coefficients. *a*, non-hepatectomized and unirradiated control; *b*, 3 hours after 500 *R* irradiation; *c*, 12 hours after partial hepatectomy; *d*, 12 hours after partial hepatectomy and irradiated with 500 *R* at the 9th hour after partial hepactectomy

20 minutes after injection of ^{14}C-orotic acid (Fig. 2). In the liver of irradiated rats (Fig. 2*b*) there was a slight increase of incorporation into each fraction of nuclear RNA as compared to the control (cf. Fig. 2*a* and *b*). In the regenerating liver (Fig. 2*c*) there was a marked increase in the amount of 45 *S* and 32–35 *S* RNA of whole nuclear RNA (Fig. 2*c* continuous line). Relative to the amount of 4–7 *S* RNA in the whole nuclear RNA of regenerating liver the amount of 28 *S*, 32–35 *S* and 45 *S* fractions increased by approx. 20, 50 and 150%, resp. The increased synthesis of 32–35 *S* and 45 *S* RNA was also reflected in the markedly

increased incorporation of ^{14}C-orotic acid into these RNA fractions (Fig. 2*c* dotted line).

In the liver of partially hepatectomized and irradiated animals (Fig. 2*d*) there was very high incorporation into the 32–35 *S* and 45 *S* RNA fractions.

A comparison of the increase in radioactivity of either the whole nuclear RNA (Fig. 1) or their fractions, caused by irradiation or hepatectomy alone, with that induced by irradiation of hepatectomized rats suggests that the increased RNA synthesis of regenerating liver further increases after irradiation.

Discussion

In the present experiments the labelling of the acid-soluble nucleotide pool of liver homogenate was measured and the relative specific radioactivity of nuclear RNA was compared with the specific radioactivity of the nucleotide pool. In accordance with others (Bucher, 1963; Bucher, Swaffield, 1969; Ord, Stocken, 1972) our results showed that partial hepatectomy increased the specific radioactivity of the nucleotide pool. On the other hand there was no change in the specific radioactivity of the nucleotide pool of liver homogenates 3 hours after irradiation either in normal or in regenerating liver. Even between 3–24 hours after irradiation there was not found any change by other investigators (Ord, Stocken, 1956; Maass, Timm, 1964; Hídvégi et al., 1970). Accordingly, in studies the dose function of irradiation, the specific radioactivity of nuclear RNA, i.e. the degree of incorporation into nuclear RNA should be taken into account for estimating differences in the rate of RNA synthesis. To compare the intensity of RNA synthesis at various time intervals after hepatectomy, however, the relative specific radioactivity of RNA should be used.

Inhibition of DNA synthesis after X-irradiation is well established in regenerating liver (Holmes, Mee, 1953; Ord, Stocken, 1956; Beltz et al., 1957). There are conflicting data, however, concerning RNA synthesis. Upon irradiation incorporation of precursors into nuclear RNA of regenerating livers either decreased (Uchiyama et al., 1965; Welling, Cohen, 1960; Berg, Goutier, 1967), remained unchanged (Beltz et al., 1957), increased slightly (Ord, Stocken, 1956) or increased definitively (Markov et al., 1975). According to the available data and on the basis of our own experiments (Fónagy, Hídvégi, 1975) the contradictory data could be explained and certain conclusions might be drawn. Nuclear RNA synthesis in regenerating liver is highly reduced if the irradiation has been performed in the first few hours after hepatectomy (Welling, Cohen, 1960) or very shortly before hepatectomy (Berg, Coutier, 1967). When the irradiation intervened later, i.e. 6–12 hours after hepatectomy and the regeneration process had already started, RNA synthesis was not inhibited but stimulated (Ord, Stocken, 1956; Markov et al., 1975). In agreement with findings of several investigators the experiments described in this paper show that the radioactivity of nuclear RNA increased after hepatectomy (Fujioka et al., 1963; Muramatsu, Busch, 1965) and/or irradiation (Hídvégi et al., 1965, 1970; Cammarano, 1969; Popov et al., 1971; Ord, Stocken,

1956; Markov et al., 1975). These results suggest that irradiation increases rather than decreases the rate of RNA synthesis in regenerating livers in the G_1-phase.

The different types of RNAs responded in a different way to irradiation. The synthesis of rRNA was stimulated both after hepatectomy (Muramatsu, Busch, 1965) and irradiation (Hídvégi et al., 1965, 1970; Cammarano et al., 1969). Parallel to the increase in the rRNA content of the cells the synthesis of low molecular weight nuclear RNA increased after irradiation (Fónagy, Hídvégi, 1975a) and in regenerating liver (Stevely, White, 1970; Fónagy, Hídvégi, 1975a). The synthesis of mRNA was affected by irradiation in normal and in regenerating liver in an opposite way. In normal liver radiation caused an early stimulatory effect, whereas in regenerating liver the synthesis of mRNA was inhibited (Markov et al., 1975). In the present experiments RNA was extracted from isolated nuclei and the RNA was not degraded during the isolation procedure as demonstrated by sedimentation analyses of nuclear RNA (Fig. 2). Both the amount and radioactivity of 32–35 *S* and 45 *S* RNA increased in regenerating liver after irradiation. This observation and a report on the inhibition of mRNA synthesis (Markov et al., 1975) suggest that mainly the synthesis of pre-rRNA and certain species of low molecular weight nuclear RNA increased after irradiation in regenerating liver.

References

Beltz, R. E., Van Lancker, J. L., Potter, V. R. (1957) Cancer Res. *17* 688
Berg, T. L., Goutier, R. (1967) Arch. Int. Physiol. Bioch. *75* 49
Bucher, N. L. R. (1963) Int. Rev. Cytol. *15* 245
Bucher, N. L. R., Swaffield, M. N. (1969) Biochim. Biophys. Acta *174* 491
Cammarano, P., Pons, S., Chinali, G., Gaetani, S. (1969) Radiat. Res. *39* 289
Fausto, N., Van Lancker, J. L. (1969) Arch. Biochem. Biophys. *135* 231
Fónagy, A., Hídvégi, E. J. (1975) Proc. 9th FEBS Meet., Vol. 33A, p. 181, Hídvégi E. J. (editor), North-Holland, Amsterdam and Akadémiai Kiadó Budapest
Fónagy, A., Hídvégi, E. J. (1975a) Biochem. J. *146* 357
Fujioka, M., Koga, M., Lieberman, I. (1963) J. Biol. Chem. *238* 3401
Hídvégi E. J., Kálmán, E., Lónai, P., Bölöni, E., Holland, J., Várterész, V. (1965) Proc. 2nd FEBS Meet., Vienna, p. 324, Verlag der Wiener Medizinischen Akademie
Hídvégi, E. J., Bölöni, E., Holland, J., Antoni, F., Várterész, V. (1970) Biochem. J. *116* 503
Higgins, G. M., Anderson, R. M. (1931) Arch. Pathol. *12* 186
Holmes, B. E., Mee, L. K. (1953) Brit. Emp. Cancer Campaign, 31st Annual Report, p. 249
Maass, H., Timm, M. (1964) Strahlentherapie *123* 64
Markov, G. G., Dessev, G. N., Russev, G. C. Tsanev, R. G. (1975) Biochem. J. *146* 41
Muramatsu, M., Busch, H. (1965) J. Biol. Chem. *240* 3960
Ord, M. G. Stocken, L. A. (1956) Biochem. J. *63* 3
Ord, M. G., Stocken, L. A. (1972) Biochem. J. *129* 175
Popov, P. G., Valeva-Dimitrova, L. I., Hadjiolov, A. A. (1971) Z. Naturforsch. *26 b* 1282
Steele, W. J., Okamura, N., Busch, H. (1965) J. Biol. Chem. *240* 1742
Steele, W. J., Busch, H. (1966) Biochim. Biophys. Acta *119* 501
Stevely, W. S., White, M. (1970) Biochem. J. *119* 59
Uchiyama, T., Fauasto, N., Van Lancker, J. L. (1965) Arch. Biochem. Biophys. *110* 191
Uchiayma, T., Fausto, N., Van Lancker, J. L. (1966) J. Biol. Chem. *241* 991
Welling, W., Cohen, J. A. (1960) Biochim. Biophys. Acta *42* 181

Acta Biochim. et Biophys. Acad. Sci. Hung. Vol. 10 (3), pp. 153–159 (1975)

Properties of Skeletal Muscle Phosphorylase–Protein Complexes

P. GERGELY, GY. VEREB, GY. BOT

Institute of Medical Chemistry, University of Medicine, Debrecen, Hungary

(Received April 18, 1975)

Frontal gel filtration studies on muscle extract and mixture of purified enzymes have verified the existence of a protein-complex between phosphorylase (alpha-1,4-glucan: orthophosphate glycosyltransferase EC 2.4.1.1.) and phosphorylase kinase. The complex has an apparent molecular weight of 750 000 daltons. The complex formation depends on the protein concentration and the presence of Ca^{2+}. Removal of Ca^{2+} with EGTA results in the dissociation of the complex. A regulatory role may be attributed to Ca^{2+} since the concentration of free Ca^{2+} changes in skeletal muscle through the effect of hormonal or electrical stimulation. Strong association was also detected between phosphorylase kinase and phosphorylase phosphatase. The transient inhibition of phosphorylase phosphatase can be explained by this interaction.

Introduction

The observation that a protein–glycogen complex can be isolated from rabbit skeletal muscle is a strong indication that such a complex represents the structural and functional unit of the cell (Meyer et al., 1970). It was shown that the properties of the enzymes in the protein–glycogen complex are different from those of the purified enzymes (Heilmeyer et al., 1970; Haschke et al., 1970). An important finding was that the modified properties of enzymes in the complex could probably be attributed to a protein component and not to the presence of glycogen (Haschke et al., 1972). Moreover the dephosphorylation of phosphorylase *a* by phosphorylase phosphatase is inhibited during "flash activation" in concentrated suspension of the protein–glycogen complex as reported by Haschke et al. (1972). No clear explanation has been offered for the transient inhibition of phosphorylase phosphatase, though Gratecos and Fischer (1974) postulate a complex formation between the enzymes of the protein–glycogen complex.

According to our latest report frontal gel filtration is a useful tool for the demonstration of protein interactions in the phosphorylase system (Gergely et al., 1974). It was found that phosphorylase *b* associates with phosphorylase kinase in crude muscle extract, furthermore purified phosphorylase kinase has an inhibitory effect on the activity of phosphorylase phosphatase (Bot et al., 1975).

Therefore it is of interest to investigate the reversibility of the complex formation between these enzymes and the factors which can influence such complex formations *in vivo*.

Materials and methods

Phosphorylase *b* was prepared from rabbit skeletal muscle, recrystallized three times and dissolved in 0.04 M glycerophosphate – 0.01 M mercaptoethanol (pH 6.8) buffer (Fischer, Krebs, 1962). AMP was removed by Norit-cellulose treatment (Fischer, Krebs, 1958) reaching a ratio of $A_{260} : A_{280} \leq 0.58$.

Phosphorylase *a* was prepared from crystalline phosphorylase *b* with phosphorylase kinase according to the method of Fischer and Krebs (1962). After Norit-cellulose treatment the ratio of $A_{260} : A_{280}$ was 0.52. Phosphorylase activity was assayed by the procedure of Illingworth and Cori (1953). Specific activity of phosphorylase *b* ranged from 50 – 55 units mg^{-1} in the presence of 1 mM AMP and 16 mM glucose 1-phosphate. Specific activity of phosphorylase *a* was 59.5 units mg^{-1} in the presence of 16 mM glucose 1-phosphate and in the absence of AMP.

Phosphorylase kinase was prepared from rabbit skeletal muscle (DeLange et al., 1968), its activity was assayed according to the method of Cohen (1973). The specific activity of kinase was 6.90 units mg^{-1} at pH 8.2. The ratio of activity at pH 6.8 to 8.2 was 0.02, therefore phosphorylase kinase could be considered as a nonactivated one (Krebs et al., 1964).

Phosphorylase phosphatase activity was assayed by incubating phosphorylase *a* with phosphorylase phosphatase at 30°C and measuring residual phosphorylase *a* reported by Varsányi and Bot (1973).

Protein was determined by the biuret-procedure (Lowry et al., 1951), or by measuring the absorbance at 280 nm using an absorbance index of phosphorylase $A_{280}^{1\%} = 12.5$ (Sevilla, Fischer, 1969) and of phosphorylase kinase $A_{280}^{1\%} = 12.4$ (Cohen, 1973).

Frontal analysis gel filtration was chosen as a method for the demonstration of complex formation between enzyme-proteins (Chiancone et al., 1968; Földi et al., 1973; Gergely et al., 1974). Frontal gel filtration was performed on a Sepharose 4B column, 1.2×60 cm (LKB), operated in ascending manner at 23 ± 0.2°C. The column, equilibrated with 0.1 M sucrose (pH 6.8) was calibrated with thyroglobulin (Mw. 670 000), catalase (Mw. 240 000) and phosphorylase *b* (Mw. 190 000). Molecular weights were calculated according to Fischer (1969) from the inflection points of the sigmoidal elution profiles. The void volume (V_0) was determined with Blue Dextran 2000. The elution profiles were followed by monitoring the enzyme activities of the components in the effluent.

Crude muscle extract was prepared from fresh minced rabbit skeletal muscle with 1 volume of 0.1 M sucrose (adjusted with 0.1 M Tris to pH 6.8) and centrifuged for 20 min at $10\,000 \times g$, 4°C. The supernatant fluid was allowed to stand for 1 hour at 30°C and the precipitated protein was collected by centrifugation. The clear supernatant, referred to as muscle extract, was applied to the column.

The "pH 6.1 acid precipitate" was obtained from muscle extract by adjusting the pH value to 6.1 with 1 M acetic acid. Thereafter it was allowed to stand for 30 min at 4°C, the precipitate was collected by centrifugation and dissolved in 0.1 M sucrose pH 6.8 (final protein concentration 12–14 mg per ml). This solution ("pH 6.1 acid precipitate") contains phosphorylase kinase and phosphorylase phosphatase but it is free from phosphorylase *b*.

Results and discussion

In our preceding paper a complex formation between phosphorylase *b* and phosphorylase kinase was demonstrated. The existence of the complex was observed in a muscle extract as well as in the mixture of purified enzymes (Gergely et al., 1974).

First we studied the effect of protein concentration and Ca^{2+} on the formation of the phosphorylase *b* and kinase complex. In these experiments a mixture of crystalline phosphorylase *b* and purified kinase was used for frontal gel filtration on a Sepharose 4B column (Fig. 1).

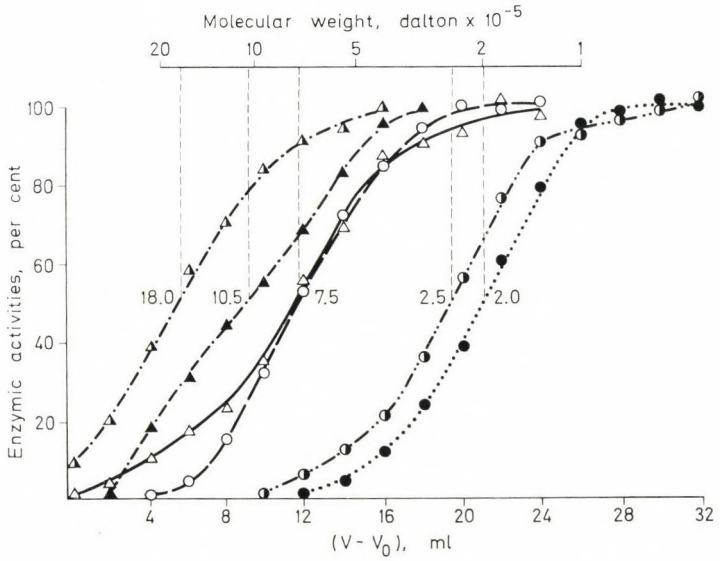

Fig. 1. Effect of protein concentration and Ca^{2+} on the complex formation between phosphorylase *b* and phosphorylase kinase. Frontal gel filtration was performed as described in Methods. The activities of phosphorylase *b* and kinase are expressed in per cent of activities in the sample applied to the column. The enzyme activities are plotted against the corrected elution volumes ($V - V_0$). Elution profiles of crystalline phosphorylase *b* and purified kinase in: "undiluted mixture": ○—○ phosphorylase *b* and △—△ kinase activity (enzyme concentrations 2.0 and 0.4 mg per ml, respectively); "10-fold diluted mixture": ●—● phosphorylase *b* and ▲—▲ kinase activity (0.2 and 0.04 mg per ml, respectively); "EGTA treated *undiluted* mixture": ◑—◑ phosphorylase *b* and ◭—◭ kinase activity (2.0 and 0.4 mg per ml, respectively; final concentration of EGTA was 0.005 M)

It can be seen from the profile of "undiluted mixture" that the activities of phosphorylase *b* and kinase ran parallel which indicates the complex formation (Gergely et al., 1974). The apparent molecular weight of the complex is about 750 000 daltons which is lower than the sum of the components. This discrepancy cannot be explained though it is known that phosphorylase kinase is constituted

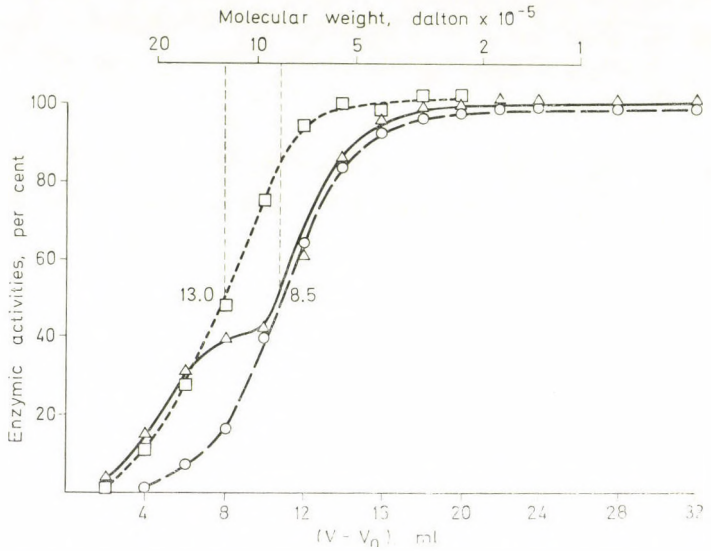

Fig. 2. Complex formation between phosphorylase kinase, phosphorylase phosphatase and phosphorylase *b* in muscle extract. Conditions are described in Methods. Enzyme activities are expressed in per cent of the activities in the sample applied to the column: ○—○ phosphorylase *b*, △—△ kinase and □—□ phosphatase activity (total protein concentration 40 mg per ml, phosphorylase *b* 1.05, kinase 0.35 mg per ml)

of 12 subunits (Hayakawa et al., 1973; Cohen, 1973), therefore the dissociation of kinase to lower molecular weight species cannot be excluded under these conditions. Another interpretation may be a strong interaction between phosphorylase kinase of high concentration and Sepharose matrix resulting in a retardation (Jennissen et al., 1973).

In order to test whether the dissociation of the protein-complex is affected by the concentration of the components, the mixture was diluted 10-fold. As shown in Fig. 1, "10-fold diluted mixture", the activities of phosphorylase *b* and kinase ran *separately*. After dilution phosphorylase *b* emerged from the column in later fractions than in the case of the undiluted mixture and the apparent molecular weight of phosphorylase *b* corresponds to 200 000 daltons in good agreement with other data of the literature (DeVincenzi, Hedrick, 1967; Seery et al., 1967). The profile of kinase also changed upon dilution, and we detected the presence of kinase in fractions which did not contain phosphorylase yet. The elution profile

is complex: it seems that a fraction of kinase is eluted with a very high molecular weight, whereas its major part has a smaller one. The average apparent molecular weight of phosphorylase kinase is 1.05×10^6 daltons which does not differ essentially from the molecular weight of purified enzyme (1.33×10^6 daltons according to Hayakawa et al., 1973). In the light of the foregoing we may say that the dilu-

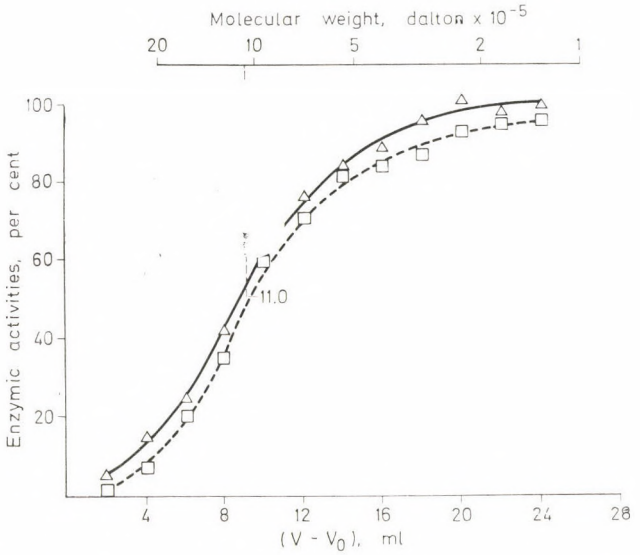

Fig. 3. Elution profiles of phosphorylase phosphatase and phosphorylase kinase in "pH 6.1 acid precipitate". Conditions are described in Methods. Enzyme activities are expressed in per cent of the activities in the sample applied to the column: △—△ phosphorylase kinase and □—□ phosphatase activity (total protein concentration 12.5 mg per ml)

tion abolishes the interaction between phosphorylase *b* and kinase, furthermore, high enzyme concentrations are required for the protein interactions.

In "*EGTA treated undiluted mixture*", when Ca^{2+} was removed with EGTA, the activities of phosphorylase *b* and kinase ran *separately* again (see Fig. 1). It is well known that phosphorylase kinase has a Ca^{2+} requirement for its catalytic function (Ozawa et al., 1967; Krebs et al., 1968; Brostrom et al., 1971), and according to our observations Ca^{2+} is needed for the complex formation, too. The apparent molecular weight of kinase after EGTA treatment is about 1.8×10^6 daltons which could probably be attributed to a self-association in the absence of Ca^{2+}.

It may be mentioned here that a complex formation (and disruption upon dilution or EGTA) between phosphorylase *a* and phosphorylase kinase was also observed (not documented). It was concluded from the data that the complex of phosphorylase *a* and kinase does not differ considerably from that of phosphorylase *b* and kinase.

In order to obtain other component(s) of the protein-complex, muscle extract was applied to the Sepharose 4B column (Fig. 2).

It is seen from the profiles that the activity of phosphorylase phosphatase ran parallel with kinase of high molecular weight. (The low plateau of kinase elution profile after the void volume was discussed earlier by Gergely et al., 1974.) The apparent molecular weight of phosphorylase phosphatase–kinase (and phosphorylase *b*) complex is much higher (1.3×10^6 daltons) than that of phosphatase alone. The molecular weight of partially purified phosphatase is about 32 000 daltons (Gratecos et al., 1974), therefore the high molecular weight of the complex also indicates the association. It is known from the literature that the separation of phosphorylase kinase from phosphatase is not a perfectly solved problem, purified kinase always contains phosphatase impurities (e.g. Haschke et al., 1970; Cohen, Antoniw, 1973). These data support the assumption that a strong interaction may exist between phosphorylase kinase and phosphorylase phosphatase.

Fig. 3 shows the elution profile of "pH 6.1 acid precipitate". The activities of kinase and phosphatase ran parallel (apparent molecular weight approximately 1.1×10^6 daltons) which proves the strong association. Removal of Ca^{2+} with EGTA does not cause the dissociation of phosphorylase kinase and phosphatase complex. It may be supposed that Ca^{2+} has no role in the complex formation between these enzymes.

It seems that a biological function can be attributed to the kinase–phosphatase complex since Bot and his co-workers (1975) reported on the regulatory role of phosphorylase kinase in the activity of phosphatase, i.e. in the conversion of phosphorylase *a* to *b*. According to their results nonactivated phosphorylase kinase inhibits the activity of phosphorylase phosphatase. The inhibition could be achieved through protein–protein interaction which would be supported by the above experiments.

The findings that interactions may exist between phosphorylase and its related enzymes suggest an "ordered structure" of the enzymes in glycogen metabolism. The purpose of further studies is to demonstrate the existence of other enzymes in this complex and to focus attention on its physiological importance.

References

Bot, Gy., Varsányi, M., Gergely, P. (1975) FEBS Letters *50* 351–354

Brostrom, C. O., Hunkeler, F. L., Krebs, E. G. (1971) J. Biol. Chem. *246* 1961–1967

Chiancone, E., Gilbert, L. M., Gilbert, G. A., Kellett, G. L. (1968) J. Biol. Chem. *243* 1212–1219

Cohen, P. (1973) Eur. J. Biochem. *34* 1–14

Cohen, P., Antoniw, F. J. (1973) FEBS Letters *34* 43–47

DeLange, R. J., Kemp, R. G., Riley, W. D., Cooper, R. A., Krebs, E. G. (1968) J. Biol. Chem. *243* 2200–2208

DeVincenzi, D. L., Hedrick, J. L. (1967) Biochemistry *6* 3489–3497

Fischer, E. H., Krebs, E. G. (1958) J. Biol. Chem. *231* 65–71

Fischer, E. H., Krebs, E. G. (1962) in Methods in Enzymology (Colowick, S. P., Kaplan, N. O. eds), Vol. 5, pp. 369–373, Academic Press, New York

Fischer, L. (1969) in Laboratory Techniques in Biochemistry and Molecular Biology (Work, T. S., Work, E. eds), pp. 157–200, North-Holland Publishing Company, Amsterdam
Földi, J., Szabolcsi, G., Friedrich, P. (1973) Acta Biochim. Biophys. Acad. Sci. Hung. *8* 263–265
Gergely, P., Vereb, Gy., Bot, Gy. (1974) Acta Biochim. Biophys. Acad. Sci. Hung. *9* 223–226
Gratecos, D., Fischer, E. H. (1974) Biochem. Biophys. Res. Comm. *58* 960–967
Gratecos, D., Detwiler, T., Fischer, E. H. (1974) in Metabolic Interconversion of Enzymes 1973 (Fischer, E. H., Krebs, E. G., Neurath, H., Stadtman, E. R. eds), pp. 43–52, Springer-Verlag, Berlin
Hayakawa, T., Perkins, J. P., Walsh, D. A., Krebs, E. G. (1973) Biochemistry *12* 567–573
Haschke, R. H., Heilmeyer, L. M. G., Meyer, F., Fischer, E. H. (1970) J. Biol. Chem. *245* 6657–6663
Haschke, R. H., Grätz, K. W., Heilmeyer, L. M. G. (1972) J. Biol. Chem. *247* 5351–5356
Heilmeyer, L. M. G., Meyer, F., Haschke, R. H., Fischer, E. H. (1970) J. Biol. Chem. *245* 6649–6656
Illingworth, B., Cori, G. T. (1953) in Biochemical Preparations (Snell, E. E. ed), Vol. 3, pp. 1–9, John Wiley et Sons, Inc., New York
Jennissen, H. P., Hörl, W. H., Heilmeyer, L. M. G. (1973) Hoppe-Seyler's Z. Physiol. Chem. *354* 236–238
Krebs, E. G., Love, D. S., Bratvold, G. E., Trysaer, K. A., Meyer, W. L., Fischer, E. H. (1964) Biochemistry *3* 1022–1033
Krebs, E. G., Huston, R. B., Hunkeler, F. L. (1968) in Advances in Enzyme Regulation (Weber, G. ed), Vol. 6, pp. 245–255, Pergamon Press, Oxford
Lowry, O. H., Rosebrough, N. J., Farr, A. L., Randall, R. J. (1951) J. Biol. Chem. *193* 265–273
Meyer, F., Heilmeyer, L. M. G., Haschke, R. H., Fischer, E. H. (1970) J. Biol. Chem. *245* 6642–6648
Ozawa, E., Hosoi, K., Ebashi, S. (1967) J. Biochem. (Tokyo) *61* 531–533
Seery, V. L., Fischer, E. H., Teller, D. C. (1967) Biochemistry *6* 3315–3327
Sevilla, C. L., Fischer, E. H. (1969) Biochemistry *8* 2161–2171
Varsányi, M., Bot, Gy. (1973) Acta Biochim. Biophys. Acad. Sci. Hung. *8* 23–31

Acta Biochim. et Biophys. Acad. Sci. Hung. Vol. 10 (3), pp. 161—169 (1975)

Inhibitory Effect of Prostaglandin E_2 on the Incorporation of ^{3}H-thymidine into the DNA of Thymus Cells

M. TÓTH, T. ZAKÁR, F. ANTONI

First Institute of Biochemistry, Semmelweis University Medical School, Budapest, Hungary

(Received March 25, 1975)

When rat thymic cells suspended in a simple salt–glucose–albumin medium were incubated with 10 μg/ml Prostaglandin E_2 (PGE_2) an inhibition of incorporation of ^{3}H-thymidine into DNA was observed. PGE_1 had a similar effect, while PGB_2 and arachidonic acid proved to be ineffective. This inhibitory effect of PGE_2 could be detected after a lag period of about 30 min but in the second hour of incubation the rate of incorporation of ^{3}H-thymidine decreased to about 60 per cent of the control value. The extent of inhibition was found to be proportional to the $\log_{10}$ of the PGE_2 concentration.

Autoradiography showed that PGE_2 had no influence on the number of DNA synthesizing cells.

As an effect of PGE_2 an early transient increase in the labeling of thymidine triphosphate was observed while the levels of labeled thymidine in the cells were not found to be significantly different in the presence of PGE_2.

Introduction

Prostaglandin E_1 and E_2 have been found to stimulate the proliferation of certain cell types in culture including thymus cells of the rat (Whitfield et al., 1972, 1972a) and hemopoietic stem cells of the mouse (Fehér, Gidáli, 1974), while in a number of other cell types these compounds have been shown to be inhibitory (Otten et al., 1972; Prasad, 1972; Kram et al., 1973; Thomas et al., 1974). It is of particular interest that addition of PGE_1 *in vitro* to cultured thymus cells of the rat results during the ensuing 2 hours in a twofold increase in the number of cells which incorporate labelled thymidine into their DNA (Whitfield et al., 1972, 1972a). This finding suggests that PGE_1 may relieve a block imposed at the transition from G_1 to S phase or in the S phase to the cell cycle of some of the thymus cells.

Considering the relatively short period necessary to detect an effect of PGE_1 on the DNA synthesis in thymus cells, we regarded these cells as especially suitable to study the influence of the variation of experimental conditions on the action of PGE compounds on DNA synthesis. With this idea in mind we carried out experiments in which the effect of PGE_2 on DNA synthesis was investigated using simple incubation media instead of the sophisticated mixture in which the stimulatory effect of PGE_1 on DNA synthesis has been observed. In preliminary experi-

ments we found that PGE_1 and PGE_2 had an inhibitory effect on the incorporation of ^{3}H-thymidine into thymus cell DNA. This finding raised the possibility that, depending on the presence of some constituents in the incubation mixture, DNA synthesis in rat thymic cells may respond differently to treatment with a PGE compound. In order to obtain more insight into this effect of PGE on DNA synthesis, we performed experiments to reveal how PGE compounds influence (*i*) the cellular uptake, (*ii*) the conversion to thymidine phosphates and (*iii*) the rate of incorporation into DNA of ^{3}H-thymidine in thymus cells suspended in a salt-glucose-albumin medium. The results of these experiments are the subject of this paper.

Experimental procedure

Minced thymus glands (obtained from adult male Sprague-Dawley rats of 200—250 g body weight) were placed into the slightly modified medium of Goldfine et al. (1972) (Medium A: NaCl 120 mM; KCl 5 mM; $CaCl_2$ 1 mM; $MgCl_2$ 2.5 mM; NaH_2PO_4 1.5 mM; glucose 11 mM; bovine serum albumin 20 mg/ml; Tris-HCl, pH 7.5 50 mM) and then carefully squashed with a hand driven glass pestle against the walls of a loose fitting tube. Cells released by this treatment were separated from debris by filtering through 2 layers of gauze.

Albumin included into medium A as described by Goldfine et al. (1972) was to prevent the cells from mechanical damage during preparation and incubation. Omission of albumin from the medium resulted regularly in a loss of thymidine incorporating activity of thymus cells but had no influence on the PGE effect studied.

Cell suspensions ($1-2\times10^8$ cell/ml) freshly prepared under sterile conditions, were incubated at 37°C with 2.5 μCi/ml ^{3}H-thymidine (Institute for Research, Production and Utilization of Radioisotopes, Prague; 20 Ci/mmole) by continuous shaking. Unless specified otherwise, the cells were not preincubated without ^{3}H-thymidine. PGE_2 (Chinoin Chemical and Pharmaceutical Works, Budapest) was applied by drying it onto the bottom of the incubation flask from ethanolic solutions while from the control flask an appropriate amount of ethanol was evaporated. By adding ^{3}H-PGE_2 (Isotope Institute, Budapest; 100 Ci/mmole) to unlabelled PGE_2 we were able to show that about 80 per cent of the PGE_2 dried onto the incubation flask was redissolved within 30 sec upon addition of the incubation medium. Labelled prostaglandins were extracted from the incubation mixtures (Unger et al., 1971) at various times of incubation and analyzed for derivatives by thin layer chromatography (Shaw, Ramwell, 1969). This type of experiments revealed that no substantial metabolization or degradation of PGE_2 took place in this suspension of thymus cells during incubation. This was in agreement with the finding of Schaumburg (1973).

Incubation was stopped by adding ice-cold perchloric acid (PCA) to 0.2 N final concentration. After several washings of the acid precipitate with 0.2 N PCA, DNA was hydrolyzed in 0.4 N PCA at 90°C. Most of the PCA was removed from

the hydrolysate in the form of $KClO_4$ and the DNA content (Dische, 1955) and radioactivity were then measured from separate aliquots.

Before autoradiography cells were washed with 0.9% NaCl containing 0.5 mM thymidine, suspended in 0.9% NaCl, dropped on slides and left to dry. Fixation was achieved using first an ethanol–chloroform–acetic acid mixture (6 : 3 : 1 v/v/v) for 10 min and then ethanol for 2×10 min. Autoradiography was performed by means of the dipping technique using Ilford K5 emulsion. After 14 days of exposure the autoradiograms were developed in ORWO A-49 developer and stained with haematoxylin-eosin. Labeled nuclei ($15-50$ silver grains per nucleus) among $1-2 \times 10^3$ nuclei were counted under a light microscope.

Free ^{3}H-thymidine levels in the cells were determined in some experiments by subtracting the radioactivity bound to thymidine phosphates from the radioactivity found in the neutralized acid extract of cells. In these experiments the cells were washed with medium A prior to the addition of PCA. Thymidine phosphates were separated by anion exchange chromatography on Dowex 1X8 formate columns. A stepwise gradient of ammonium formate in 4 M formic acid allowed the recovery of the various thymidine phosphates (dTMP, dTDP, dTTP) in 12 ml eluent each. The eluent was evaporated by heating, the residue was dissolved in water and after the addition of a scintillation cocktail, the radioactivity was measured. Radioactivity determinations were made by adding the sample dissolved in 0.5 ml water to 10 ml of scintillation cocktail containing 0.8% PPO, 0.01% POPOP, 6.0% naphthalane in dioxane–methylcellosolve–toluene (10 : 2 : 1, v/v/v) and using a Packard TriCarb, Model 2425 spectrometer.

Results

It was found in ten separate experiments that in the presence of 10 μg/ml PGE_2 and during an incubation period of 3 hours, the amounts of ^{3}H-thymidine incorporated into the DNA of thymus cells decreased to 77 ± 4.5% (mean ± S.D.) of the control values (which varied in the range of $3 \times 10^4 - 4 \times 10^4$ cpm/mg DNA). We tested PGE_1, PGB_2 and arachidonic acid in similar concentrations as PGE_2 and found that among these compounds only PGE_1 had a similar effect on the incorporation of ^{3}H-thymidine into DNA (77 ± 3.2% of control).

The kinetics of the effect of PGE_2 on the incorporation of labeled thymidine is shown in Fig. 1. No inhibition of incorporation could be observed in the first 30 min of the incubation. After the first hour of incubation, however, the rate of incorporation of ^{3}H-thymidine decreased in PGE treated cells to about 60% of the control value. Fig. 2 demonstrates that in the range of $0.01-10$ μg/ml (3×10^{-8} M $- 3 \times 10^{-5}$ M) PGE_2 concentration the extent of inhibition was proportional to the $\log_{10}$ of the prostaglandin concentration.

In order to decide whether a reduced number of DNA synthesizing cells or a decreased rate of DNA labeling (or both) was responsible for the observed effect of PGE_2 on the incorporation of ^{3}H-thymidine into DNA, we carried out

autoradiography. As shown in Table 1 the labeling index in PGE_2-treated and in control suspensions was very similar. This suggests that PGE_2 decreased the rate of DNA labeling in S phase cells rather than the number of these cells. Although the labeling index was lower than the values reported from other laboratories

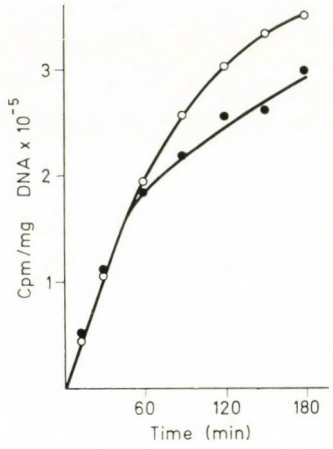

Fig. 1. Effect of PGE_2 on the incorporation of ^{3}H-thymidine into DNA as a function of the time of incubation. Thymus cells were incubated at a cell density of 10^8 cells/ml, under the standard conditions in the absence (— ○ — ○ —) or in the presence (— ● — ● —) of 10 μg/ml PGE_2. At the times indicated on the abscissa, aliquots of the reaction mixtures were transferred into ice-cold 0.2 N PCA and the label recovered in the DNA fraction was determined

Table 1

Comparison of the labeling index of thymus cell nuclei following incubation of thymus cells with ^{3}H-thymidine in the absence or in the presence of 10 μg/ml PGE_2

Thymus cells were incubated at 1.2×10^8 cells/ml cell density under the standard conditions. Preincubation was carried out exactly as the incubation with the only exception that ^{3}H-thymidine had been omitted from the mixture

Time of pre-incubation (min)	Time of incubation with ^{3}H-thymidine (min)	Radioactivity (cpm/mg DNA)		Labeling index (%)	
		$-PGE_2$	$+PGE_2$	$-PGE_2$	$+PGE_2$
—	20	10000	12260	4.6	4.3
60	60	14950	8150	3.9	4.0
120	60	—	—	3.6	3.6

(Wagner et al., 1967; McManus et al., 1971; Whitfield et al., 1972a; Fabrikant, Foster, 1972), it showed only a slight decrease during incubation, indicating that at least a fraction of the competent thymus cells was capable of DNA synthesis even in the poor incubation medium applied in this study. Nevertheless, as shown

by the time course of the incorporation of ^{3}H-thymidine into thymus cells (Fig. 1) the rate of DNA synthesis decreased during incubation.

In a series of experiments the cellular levels, the conversion to thymidine phosphates and the incorporation into DNA of ^{3}H-thymidine were determined

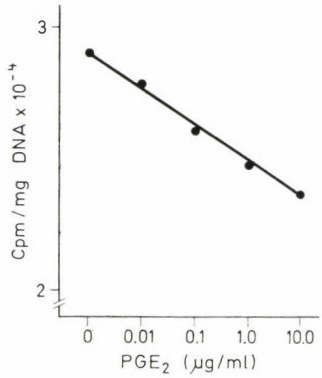

Fig. 2. Effect of various concentrations of PGE_2 on the incorporation of ^{3}H-thymidine into DNA. Thymus cells were incubated at 2×10^8 cells/ml cell concentration under the standard conditions for 3 hours

Table 2

Effect of PGE_2 on the incorporation of ^{3}H-thymidine into thymidine phosphates and DNA and on the levels of labeled thymidine in the cells

Thymus cells ($1-2\times10^8$ cells/ml) were incubated with or without 10 μg/ml PGE_2 in the standard reaction mixture for 20, 40, 90 and 180 minutes, respectively. The data are expressed relative to the control value (control value = 1). The mean value ± the standard deviation of the results obtained with different suspensions are presented

Time of incubation (min)	cpm/mg DNA in PGE_2 treated* / cpm/mg DNA in control			n
	dTTP	DNA	free ^{3}H-thymidine	
20	3.4 ± 0.9	0.98 ± 0.04	0.91 ± 0.1	4
40	0.59 ± 0.06	0.92 ± 0.01	1.00 ± 0.003	4
90	0.76 ± 0.05	0.75 ± 0.02	0.92 ± 0.15	3
180	0.77 ± 0.07	0.72 ± 0.03	0.96 ± 0.05	5

* Radioactivity values: in DNA = $3\times10^4 - 4\times10^5$ cpm/mg DNA in dTTP = $5\times10^2 - 3\times10^3$ cpm/mg DNA, in thy = $1.5\times10^4 - 2.5\times10^4$ cpm/mg DNA

in thymus cells incubated for various periods with or without PGE_2. Both in the control and in the PGE_2 treated cells ^{3}H-dTTP was found as the predominant phosphorylated derivative of ^{3}H-thymidine at any time during incubation. A rep-

resentative pattern of analysis of thymidine phosphates is shown in Fig. 3. The effects of PGE_2 on the relative labeling rates[1](control value = 1) of dTTP, DNA and on the relative levels of free ^{3}H-thymidine in thymus cells are summarized in Table 2.

After 20 min incubation PGE_2 caused an about threefold rise in the labeling of dTTP and this was followed by a drop below the control value in the nex

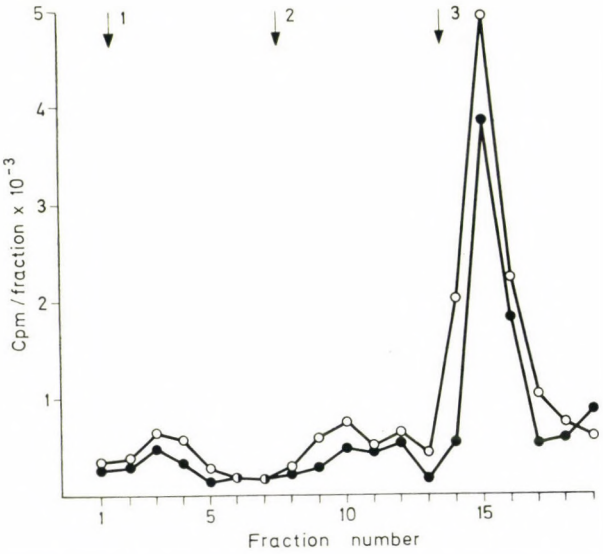

Fig. 3. Chromatography of labeled thymidine phosphates. Portions of a thymus cell suspension (10^8 cells/ml) were incubated under the standard conditions, in the absence (○—○—) or in the presence (—●—●—) of 10 μg/ml PGE_2 for 3 hours. The neutralized acid extract of the cells was passed through a 0.7×7 cm Dowex 1X8 column which was in the formate form. The resin was then successively washed with 20 ml water and 25 ml of 2 M formic acid. The thymidine phosphates were recovered with the following eluents: 1. dTMP — 0.2 M ammonium formate, 4 M formic acid. 2. dTDP — 0.5 M ammonium formate, 4 M formic acid. 3. dTTP — 1.0 M ammonium formate, 4 M formic acid. Fractions of 2 ml volume each were collected in counting vials, the eluents were evaporated by heating and radioactivity in the residues was determined

20 min. At 90 and 180 min of incubation the labeling of dTTP was found below the control value. These experiments showed again that administration of PGE_2 led to a decrease of the labeling rate of DNA. This effect could be seen first in suspensions incubated for 40 min. The levels of free ^{3}H-thymidine were very similar in control and PGE-treated cells, which suggested that the rate of uptake of labeled thymidine by these cells was not influenced by PGE_2.

Discussion

Under our experimental conditions PGE_2 had no influence on the number of DNA synthesizing (S phase) thymus cells but inhibited the incorporation of ^{3}H-thymidine into DNA. PGE_1 showed a similar effect as PGE_2. These findings seem to be at variance with previous reports on the early increase in the number of S phase cells among cultured thymocytes exposed to PGE_1 (Whitfield et al., 1972, 1972a). It appears that the choice of the incubation medium may be critical to the type of PGE effect, since an increase in the number of S phase cells has been demonstrated using MAC-1 medium (MacManus et al., 1971) which is much more complex in composition than the salt–glucose–albumin mixture used in our experiments. One disadvantage of this medium may be the inclusion of albumin which does disturb the concentration of calcium ions and of prostaglandins. It should be noted, however, that in contrast with mitosis, the stimulatory effect of PGE_1 on DNA synthesis of thymus cells has not been found to be dependent on the presence of calcium ions (Whitfield et al., 1972a) and the binding of PGE_2 to albumin (Raz, 1972, 1972a) is weak enough to leave a high proportion of PGE_2 free in the medium.

Our results clearly show that during the first two hours of incubation a definite portion of thymus cells is able to incorporate labelled thymidine into their DNA even in a simple incubation medium and the presence of either PGE_1 or PGE_2 leads to an inhibition of this process. It is important to note that this finding and those experiments in which PGE_1 proved to be stimulatory to the proliferation of thymus cells incubated in "complete" medium are not mutually exclusive. In fact we consider PGE compounds as agents which act in a different way on cells blocked at their transition from phase G_1 to phase S (or, alternatively, in phase S) of their cycle and on cells which are already actively engaged in DNA synthesis. We propose that the former effect (stimulation of the initiation or resumption of DNA synthesis) can be detected only in "complete" media, while the latter (inhibition of DNA synthesis) manifests itself mainly in "incomplete" media like the one used in our experiments. This idea directs the attention to a search for chemical agents the presence of which is indispensable for the stimulation of DNA synthesis in blocked thymus cells and the absence of which is crucial when the demonstration of inhibition of DNA synthesis in S phase thymus cells is desired.

It has been demonstrated by Schaumburg (1973) that rat thymocytes contain about 300 sites per cell which can bind PGE_1 with high affinity. Half saturation of these sites was found at 2 nM PGE_1 concentration at 37°C. On the other hand, we found a definite inhibitory effect on thymidine incorporation at a much higher PGE concentration (about 10^{-5} M) which was certainly manyfold in excess of the physiological levels of PGE in the cells. The linear log dose – response relationship also shows that this effect of PGE is pharmacological in nature rather than physiological. It is striking that the proliferative effect of PGE_1 has been found in a similar concentration range (Whitfield et al., 1972a). Moreover, similar concentrations of PGE_1 have been shown to stimulate adenylate cyclase activity in thymo-

cytes (Franks et al., 1971; Whitfield et al., 1972, 1972a) as well as in several other cells in culture (Perry et al., 1971; D'Armiento et al., 1972; Otten et al., 1972; Maganiello, Vaughan, 1972; Sheppard, 1972). The lag period we found before the effect on DNA labeling could be detected is compatible with the accumulation of a substance which can mediate the PGE effect to DNA synthesis.

It is of interest to note that prior to its effect on DNA labeling, PGE_2 seems to enhance the rate of phosphorylation of thymidine. Taking into account that the exchange of dTTP in the pool must be very rapid (see data on absolute counts in Table 1) it is easy to realize that at a given rate of DNA synthesis a few per cent increase in the rate of phosphorylation of thymidine would be sufficient to attain a considerable increase in the amounts of label in dTTP after 20 min of incubation. It is not known whether this increased incorporation of label is parallel to an expansion of the dTTP pool in the cell, but if so, then the changes in the DNA precursor nucleotide levels should be taken into account as a factor which may lead to a decreased rate of DNA labeling with ^{3}H-thymidine (Reichard, 1972).

We are indebted to the "Frédéric Joliot-Curie" National Institute for Radiobiology and Radiohygiene, Budapest, for the initiation and support of these investigations.

We should like to express our thanks to the Chinoin Chemical and Pharmaceutical Works Budapest, for providing us with the prostaglandins used in these experiments.

The expert and skillful technical assistance of Miss Irén Szabó is gratefully acknowledged.

References

Dische, Z. (1955) in The Nucleic Acids (eds.: Chargaff, E., Davidson, J. N.), Academic Press, New York, Vol. 1, p. 285

D'Armiento, M., Johnson, G. S., Pastan, I. (1972) Proc. Nat. Acad. Sci. (USA) *69* 459

Fabrikant, J. I., Foster, B. R. (1972) Johns Hopkins Med. J. *130* 208

Fehér, I., Gidáli, J. (1974) Nature *247* 550

Franks, O. J., MacManus, J. P., Whitfield, J. F. (1971) Biochem. Biophys. Res. Commun. *44* 1177

Goldfine, I. D., Gardner, J. D., Neville, D. M. Jr. (1972) J. Biol. Chem. *247* 6919

Kram, R., Mamont, P., Tomkins, G. M. (1973) Proc. Nat. Acad. Sci. (USA) *70* 1432

MacManus, J. P., Whitfield, J. F., Youdale, T. (1971) J. Cell. Physiol. *77* 103

Maganiello, V., Vaughan, M. (1972) Proc. Nat. Acad. Sci. (USA) *69* 269

Otten, J., Johnson, G. S., Pastan, I. (1972) J. Biol. Chem. *247* 7082

Perry, C. V. Johnson, G. S., Pastan, I. (1971) J. Biol. Chem. *246* 5785

Prasad, K. M. (1972) Nature New Biol. *236* 49

Raz, A. (1972) Biochem. J. *130* 631

Raz, A. (1972a) Biochim. Biophys. Acta *280* 602

Reichard, P. (1972) in Advances of Enzyme Regulation (ed.: Weber, G.), Pergamon Press, Oxford—New York, Vol. 10, p. 3

Schaumburg, B. P. (1973) Biochim. Biophys. Acta *326* 127

Shaw, J. E., Ramwell, P. W. (1969) in Methods of Biochemical Analysis (ed.: Glick, D.), Interscience, New York, Vol. 17, p. 325

Sheppard, J. R. (1972) Nature New Biol. *236* 14

Thomas, D. R., Philpott, G. W., Jaffe, B. M. (1974) Exp. Cell Res. *84* 40
Unger, W. G., Stamford, I. F. Bennett, A. (1971) Nature *233* 336
Wagner, H. P., Cottier, H., Cronkite, E. P. Cunningham, L., Jansen, C. R., Rai, K. R. (1967) Exp. Cell Res. *46* 441
Whitfield, J. F., MacManus, J. P., Braceland, B. M., Gillan, D. J. (1972) Horm. Metab. Res. *4* 304
Whitfield, J. F., MacManus, Braceland, B. M., Gillan, D. J. (1972a) J. Cell. Physiol. *79* 353

Acta Biochim. et Biophys. Acad. Sci. Hung. Vol. 10 (3), pp. 171–176 (1975)

Inhibition by Quinaldate of Dehydrogenases

T. Kőnig, Beatrix Kocsis, Éva Pocskay

Second Institute of Biochemistry, Semmelweis University Medical School, Budapest, Hungary

(Received March 7, 1975)

Quinaldate (quinoline-2-carboxylate) inhibits pyridine-, and flavin nucleotide-dependent dehydrogenases, both inside the mitochondria and in isolated form. Other mitochondrial functions and some other isolated enzymes (with one exception) are not influenced by quinaldate at all. Thus, quinaldate can be regarded as a specific "dehydrogenase inhibitor". The inhibition of alcohol dehydrogenase (EC 1.1.1.1) and lactate dehydrogenase (EC 1.1.1.27) by quinaldate is of mixed type, both with respect to NAD^+ and ethanol or lactate, respectively. The K_i for alcohol dehydrogenase is 4.5 mM, that of lactate dehydrogenase 7.5 mM. It can be assumed that the inhibition by quinaldate of dehydrogenases is a consequence of its binding to that part of the active centre which takes part in the dehydrogenation itself and might possess very similar structure in all dehydrogenases.

Introduction

In a recent paper we have shown that quinaldate (quinoline-2-carboxylate) in millimolar concentrations inhibits reversibly mitochondrial oxidation at the substrate dehydrogenase level (Kőnig, 1975). The fact that the mitochondrial respiratory chain, oxidative phosphorylation and substrate translocation were not influenced by quinaldate at all, pointed to some specificity of the inhibition. The finding that both NAD and flavin nucleotide linked dehydrogenases having substrates of very different chemical structure were inhibited by quinaldate led us to suggest that quinaldate inhibits dehydrogenases by interacting with that part of their active centre which is involved in the catalytic process.

In this paper experiments with isolated enzymes are presented providing additional evidence to the specificity and type of inhibition by quinaldate of dehydrogenases.

Materials and methods

All chemicals used were the purest commercially available. Alcohol dehydrogenase (alcohol: NAD^+ oxidoreductase EC 1.1.1.1) was a crystallized lyophilized preparation from yeast, lactate dehydrogenase (L-lactate: NAD^+ oxidoreductase EC 1.1.1.27) a 3 times crystallized suspension in ammonium sulphate from pig striated muscle. Both enzymes were obtained from Reanal.

Both dehydrogenase reactions were studied at room temperature in 3 ml reaction mixtures. Alcohol dehydrogenase activity was measured in a standard reaction medium containing 100 mM Na-pyrophosphate buffer, pH 9.0, lactate dehydrogenase activity measurements were performed in a standard reaction medium containing 100 mM Tris-HCl buffer, pH 7.2. The concentrations of the other reaction components are given in the legends to the figures. Quinaldate was used in the form of its Tris-salt. Reactions were started by the addition of ethanol or lactate, respectively. Reaction rates were measured by following the formation of NADH at 340 nm using a Beckman DB-GT recording spectrophotometer. Reaction velocity was calculated from the initial slope of the curves.

Results

In Table 1 qualitative data are collected on the sensitivity of different enzymes to quinaldate. The results obtained with mitochondria (Kőnig, 1975) are also included. It can be seen that all dehydrogenases tested (whether extramitochondrial or mitochondrial) are inhibited by quinaldate. On the other hand, enzymes catalyzing reactions of other types, with the sole exception of subtilisin, and mitochondrial functions other than dehydrogenation, including electron transfer by cytochromes, are not inhibited. (The effect of quinaldate on subtilisin was, however, considerably smaller than on dehydrogenases: even 20 mM quinaldate showed only a 30% inhibition.) Thus, it appears that quinaldate is a quite specific inhibitor of dehydrogenases.

As to the mechanism of inhibition by quinaldate it seemed necessary to examine the kinetics of inhibition with isolated dehydrogenases as well using both substrates. For this purpose alcohol dehydrogenase (EC 1.1.1.1) and lactate dehydrogenase (EC 1.1.1.27) were chosen. Since the former one contains functionally essential metal ions (Zn^{2+}) (Vallee, Hoch, 1955; Oppenheimer et al., 1967), whereas the latter one does not (Pfleiderer et al., 1958), comparison of the characteristics of inhibition by quinaldate of these two dehydrogenases offers also a possibility to establish whether quinaldate acts by chelating metal ions. As it can be seen from the Lineweaver–Burk plots, both alcohol dehydrogenase and lactate dehydrogenase show a mixed-type inhibition by quinaldate with respect to substrate (Figs 1a, 2a). This is in agreement with our previous finding with mitochondrial 3-hydroxybutyrate oxidation (Kőnig, 1975). Moreover, a mixed inhibition by quinaldate was found also with respect to NAD (Figs 1b, 2b). Thus, our earlier conclusion that quinaldate acts on the "dehydrogenating part" of dehydrogenases (Kőnig, 1975) is now supported in kinetic terms. The Dixon-plots (Figs 1c, 2c) indicate that alcohol dehydrogenase and lactate dehydrogenase have K_i values of the same order of magnitude, 4.5 mM and 7.5 mM, respectively.

Table 1

Effect of quinaldate on mitochondrial dehydrogenation, on other mitochondrial functions and on isolated enzymes

	Inhibited reaction	Non-inhibited reaction
In mitochondria*:	Pyruvate + malate dehydrogenation 2-oxoglutarate dehydrogenation 3-hydroxybutyrate dehydrogenation Glutamate + malate dehydrogenation Succinate dehydrogenation Palmitoyl carnitine dehydrogenation NADH oxidation (after ultrasonic treatment)	Cytochrome *c* oxidation and reduction Cytochrome a + a_3 oxidation and reduction Penetration of substrates Oxidative phosphorylation Uncoupling of oxidative phosphorylation
Isolated enzymes	L-lactate: NAD^+ oxidoreductase (EC 1.1.1.27) (rabbit muscle)[a] Alcohol: NAD^+ oxidoreductase (EC 1.1.1.1) (yeast)[b] D-3-hydroxybutyrate: NAD^+ oxidoreductase (EC 1.1.1.30) (*Rhodopseudomonas sphaeroides*)[c] D-glyceraldehyde-3-phosphate: NAD^+ oxidoreductase (phosphorylating) (EC 1.2.1.12) (pig muscle)[d] D-amino acid: oxygen oxidoreductase (deaminating) (EC 1.4.3.3) (pig kidney)[e] Subtilisin (EC 3.4.21.14)[f]	ATP-phosphohydrolase (EC 3.6.1.3) (myosin)[g] α-Chymotrypsin (EC 3.4.21.1) (beef pancreas)[h]

* Taken from Kőnig (1975)

[a,b] See Materials and methods

[c] 100 mM Tris-HCl buffer, pH 7.2; 10 mM DL-3-hydroxybutyrate; 2 mM NAD; 14 μg enzyme; 5—40 mM quinaldate

[d] 100 mM glycine-NaOH buffer, pH; 8.5; 10 mM Na_2HPO_4; 2 mM D-glyceraldehyde-3-phosphate; 2 mM NAD; 3 μg enzyme; 5—10 mM quinaldate

[e] 100 mM Tris-HCl buffer, pH 8.3; 50 mM DL-alanin; 4 μM FAD; 1.5 mg enzyme; 5—20 mM quinaldate

[f] 100 mM phosphate buffer, pH 7.5; 0.2 mM p-nitrophenylacetate; 0.01 mM enzyme; 20 mM quinaldate

[g] 32 mM KCl, 0.4 mM EDTA, 8 mM Tris-HCl buffer, pH 7.2; 10 mM $CaCl_2$; 2 mM ATP-Na; 1.7 mg enzyme; 11 mM quinaldate

[h] 100 mM phosphate buffer, pH 7.5; 0.2 mM p-nitrophenylacetate; 0.01 mM enzyme; 30 mM quinaldate

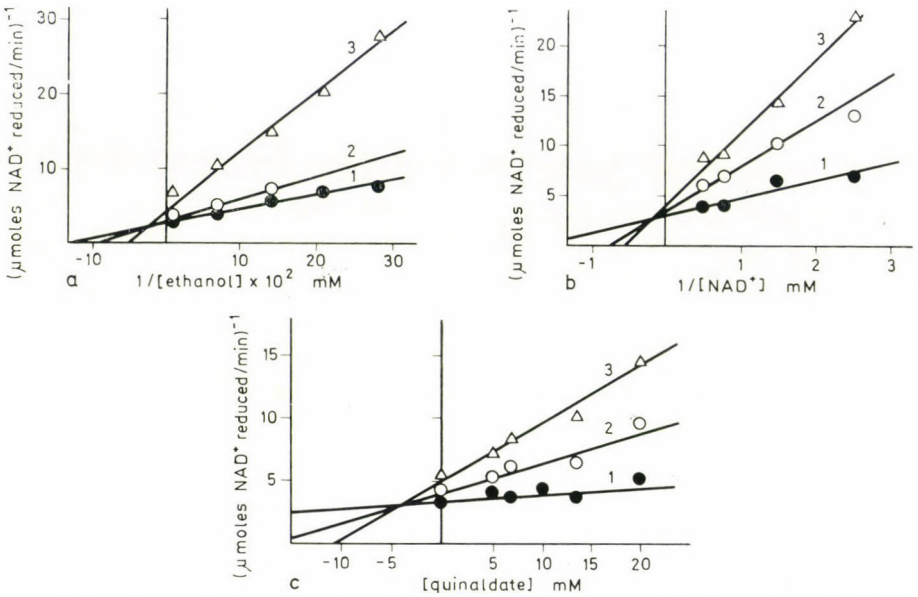

Fig. 1. Inhibition of alcohol dehydrogenase by quinaldate. The reaction mixtures contained 0.201 U of enzyme: a. Lineweaver–Burk plot. NAD^+ concentrations were 2 mM. Ethanol concentrations varied from 3.59 mM to 71.8 mM. 1) no inhibitor, 2) 5 mM quinaldate, 3) 20 mM quinaldate; b. Lineweaver–Burk plot. Ethanol concentrations were 71.8 mM. NAD^+ concentrations varied from 0.4 mM to 2 mM. 1) no inhibitor, 2) 10 mM quinaldate, 3) 20 mM quinaldate; c. Dixon plot. NAD^+ concentrations were 2 mM. Quinaldate concentrations varied from 0 to 20 mM. 1) 71.8 mM ethanol, 2) 14.3 mM ethanol, 3) 7.18 mM ethanol

Discussion

The results presented in this paper give additional experimental support concerning the specificity and mechanism of inhibition by quinaldate of dehydrogenases, as suggested earlier (Kőnig, 1975). Since all dehydrogenases tested are inhibited by quinaldate without exception, and enzymes catalyzing reactions of other types and other mitochondrial functions are not inhibited, it appears that quinaldate can be regarded as a specific "dehydrogenase inhibitor". To explain the weak inhibitory effect of quinaldate on subtilisin, detailed kinetic studies are required.

Since all dehydrogenases tested were inhibited by quinaldate, a common mechanism of inhibition seems very probable. Thus chelation of metal ions by quinaldate is improbable, since there are dehydrogenases which do not contain metal at all. But also dehydrogenases containing functionally essential metal ions seem to be inhibited by a mechanism other than chelation of metal ions by quinaldate. This can be concluded from a comparison of the inhibition characteristics of alcohol dehydrogenase and lactate dehydrogenase. In this context it is worth

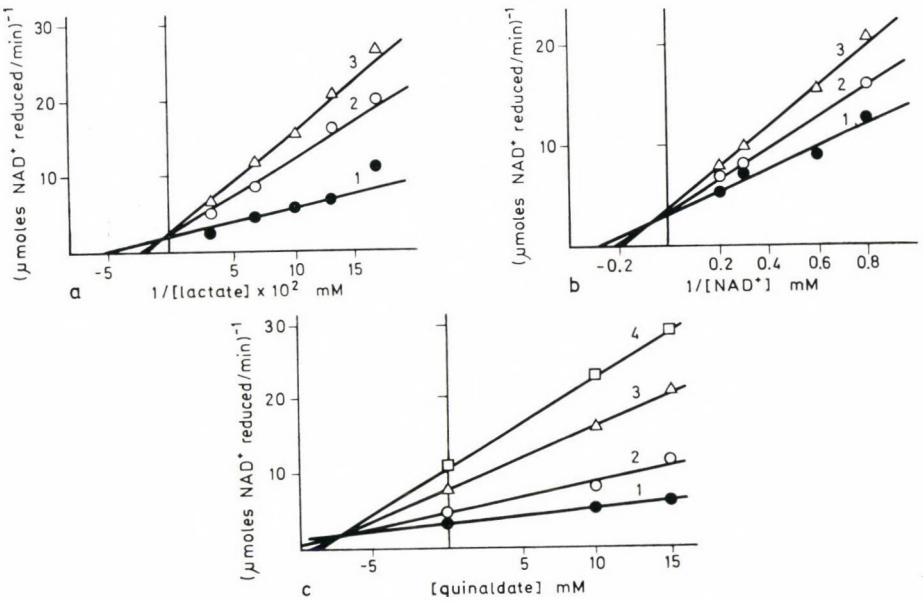

Fig. 2. Inhibition of lactate dehydrogenase by quinaldate. The reaction mixture contained 0.224 U of enzyme. a. Lineweaver–Burk plot. NAD^+ concentrations were 5 mM. Lactate concentrations varied from 6 mM to 30 mM. 1) no inhibitor, 2) 10 mM quinaldate, 3) 15 mM quinaldate. b. Lineweaver–Burk plot. Lactate concentrations were 30 mM. NAD^+ concentrations varied from 1.25 to 5 mM. 1) no inhibitor, 2) 5 mM quinaldate, 3) 10 mM quinaldate. c. Dixon plot. NAD^+ concentrations were 5 mM. Quinaldate concentrations varied from 0 to 15 mM. 1) 30 mM lactate, 2) 15 mM lactate, 3) 7.5 mM lactate, 4) 6 mM lactate

mentioning that according to others, heterocyclic nitrogen bases known to be good chelators of Zn^{2+} inhibit yeast alcohol dehydrogenase by binding to the pyridinium ring region of the NAD^+ binding site of the enzyme rather than to its Zn^{2+} ions. These compounds are known to inhibit alcohol dehydrogenase competitively with respect to NAD^+ (Anderson et al., 1966; Anderson, Reynolds, 1966). The inhibition by quinoline of alcohol dehydrogenase was also found to be competitive with respect to NAD^+ suggesting its binding at the above-mentioned region (Anderson et al., 1966; Anderson, Reynolds, 1966). However, our finding that flavin nucleotide-linked dehydrogenases are also inhibited by quinaldate makes it improbable that inhibition of dehydrogenases by quinaldate is due to its interaction with the pyridinium-binding site of the enzymes. Thus, it appears that by introducing a carboxyl group into quinoline the characteristics of its binding to dehydrogenases are altered.

From our results obtained with mitochondria we have concluded that it is not the substrate binding site of dehydrogenases quinaldate is interacting with (Kőnig, 1975). The finding that the inhibition by quinaldate of the isolated dehy-

drogenases examined is of a mixed type with respect to substrate rather than competitive, provides new evidence to support this conclusion.

Since inhibition by quinaldate of the dehydrogenases examined is of a mixed type with respect to both NAD^+ and their other substrate, it seems very probable that quinaldate acts on the "dehydrogenating part" of their active centre hindering also sterically the binding of both NAD^+ and substrate. The analogies found in the amino acid sequence of peptides containing the reactive residues of different NAD-linked dehydrogenases indicate a structural similarity of their active centre (Keleti, 1970; Ohlsson et al., 1974). As flavin nucleotide dependent dehydrogenases are also inhibited by quinaldate, it seems probable that a common structural principle prevails in the active centre of all dehydrogenases.

Thanks are due to Prof. P. Elődi, Prof. T. Keleti, Drs L. Polgár and T. Vajda for performing some of the qualitative experiments and for invaluable discussions.

References

Anderson, B. M., Reynolds, M. L. (1966) Arch. Biochem. Biophys. *114* 299
Anderson, B. M., Reynolds, M. L., Anderson, C. D. (1966) Biochim. Biophys. Acta *113* 235
Keleti, T. (1970) in H. Sund (ed.): Symposium on Pyridine Nucleotide-Dependent Dehydrogenases. Springer-Verlag, Berlin, p. 103
Kőnig, T. (1975) Acta Biochim. Biophys. Acad. Sci. Hung. *10* 17
Ohlsson, I., Nordström, B., Brändén, C. I. (1974) J. Mol. Biol. *89* 339
Oppenheimer, H. L., Green, R. W., McKay, R. H. (1967) Arch. Biochem. Biophys. *119* 552
Pfleiderer, G., Jeckel, D., Wieland, Th. (1958) Biochem. Z. *330* 296
Vallee, B. L., Hoch, F. L. (1955) Proc. Nat. Acad. Sci. U.S.A. *41* 327

Acta Biochim. et Biophys. Acad. Sci. Hung. Vol. 10 (3), pp. 177—179 (1975)

Distribution of Pyrimidine Oligonucleotides in DNA Fractions of *Escherichia coli*, Separated on Methylalbumin-Kieselguhr Columns

(Short Communication)

IBOLYA KISS, A. UDVARDY, P. VENETIANER

Institute of Biochemistry, Biological Research Center, Hungarian Academy of Sciences, Szeged, Hungary

(Received January 27, 1975)

Methylalbumin-Kieselguhr (MAK) chromatography has been widely used for the fractionation of both double-stranded and single-stranded DNA (Kothari, 1970; Rudner et al., 1969), still the chemical basis of the separation is not yet fully understood. Rudner and her co-workers separated the denatured DNA of *B. subtilis* (Rudner et al., 1972) and *E. coli* (Rudner, LeDoux, 1974) into two fractions by intermittent gradient elution and analyzed the overall base composition and the pyrimidine oligonucleotide distribution of these fractions. We reported earlier that in the case of *E. coli* (and also *S. typhimurium*) DNA, the number of separable fractions can be chosen at will by applying stepwise elution, and that the overall Py/Pu ratio of the fractions increases with the salt concentration required for elution (Udvardy, Venetianer, 1973). In order to elucidate further the mechanism of this separation, it seemed to us worthwhile to analyze the distribution of pyrimidine clusters (isostichs) among the fractions obtained by stepwise elution.

^{32}P-labelled DNA from *Escherichia coli* MRE 600 (RNase I$^-$) was prepared, denatured and fragmented as described earlier (Udvardy, Venetianer, 1971, 1973; Venetianer, 1969). Details of the stepwise elution MAK chromatography have also been described (Udvardy, Venetianer, 1973).

DNA fractions were depurinated with formic acid and diphenylamine according to Burton (1967). Pyrimidine oligonucleotides were separated according to chain length on DEAE-cellulose at pH 5.5 as described by Rudner et al. (1972). The position of the chromatographic peaks indicated the chain lengths. These assignments were verified by repeated chromatography of each isostich fraction on DEAE-cellulose at pH 3.5 (Kizer, Saunders, 1972). Under these conditions the isostichs can be separated according to base composition. The number of separated components in all cases agreed with the number predicted on the basis of chain length. The base compositions of these fractions were determined by their UV spectra (Spencer, Chargaff, 1963).

All the quantitative data presented here are based on ^{32}P radioactivity measurements. These were carried out in a Beckman LS-200 liquid scintillation spectrometer, using the Tcherenkov effect.

We analyzed the distribution of pyrimidine isostichs in 7 individual DNA fractions of denatured fragmented *E. coli* DNA, eluted from MAK between 0.70 and 0.96 M NaCl. By our method we were able to detect pyrimidine isostichs up to a chain length of 11. However, the amount of the two longest isostichs was so low that the quantitative evaluation was unreliable. For this reason the data in the last two rows of Table 1 are of doubtful significance. This table summarizes the results of one complete isostich analysis. The data show that although

Table 1

Distribution of pyrimidine isostichs among separated DNA fraction obtained by MAK-chromatography

The data show the percentage distribution of the various isostichs within each DNA fraction, calculated from the distribution of ^{32}P radioactivity. P_i = represents the radioactivity recovered as inorganic phosphate originating from the digested purine tracts

		Concentration of eluting NaCl (M)							Unfractionated DNA
		0.70	0.73	0.76	0.79	0.82	0.85	0.96	
Py isostich chain length	I.	26.33	27.97	24.76	25.03	24.26	25.75	26.00	27.12
	II.	31.32	29.21	30.42	30.24	29.82	28.06	28.26	26.56
	III.	17.77	17.39	17.15	16.67	16.74	15.83	14.38	17.32
	IV.	10.04	10.70	11.33	10.58	10.66	10.91	10.42	12.01
	V.	6.15	6.70	7.03	7.33	7.41	7.64	7.62	6.86
	VI.	3.25	3.61	3.92	4.24	4.33	4.75	4.94	3.74
	VII.	1.94	2.01	2.08	2.62	2.77	2.75	2.84	2.04
	VIII.	1.18	1.24	1.44	1.44	1.69	1.69	2.09	1.33
	IX.	0.61	0.65	0.69	0.75	0.87	0.97	1.39	0.77
	X.	0.75	0.53	0.87	0.52	0.54	0.76	0.86	0.68
	XI.	0.64	1.00	0.31	0.60	0.92	0.90	1.21	0.59
% of recovered DNA		13.08	15.25	21.71	20.49	17.35	7.80	4.31	
P_i, %		29.66	25.85	25.65	23.50	23.42	22.80	22.33	28.06
Py/Pu ratio		0.85	0.94	0.97	1.02	1.03	1.04	1.07	

the overall Py/Pu ratio increases steadily with the concentration of the eluting salt, this tendency is clearly not reflected in the distribution of the shorter pyrimidine isostichs. The proportion of isostichs I–III is slightly decreasing with increasing salt concentration and isostich IV remains constant. On the other hand the proportion of isostichs V–IX is steadily increasing in fractions eluted with higher salt concentrations.

Thus it seems likely that the main contributing factor in the MAK-fractionation of randomly sheared denatured bacterial DNA is not simply the Py/Pu ratio of the fragments, but the distribution of the longer (over chain length 5) pyrimidine (consequently also purine) isostichs. The higher the proportion of these longer pyrimidine clusters in a given fragment, the stronger is the binding to the MAK column. These findings are in full agreement with the results of Rudner and LeDoux (1974), but extend their validity from two DNA fractions obtained by intermittent gradient elution to seven or more separate fractions obtained by stepwise elution.

References

Burton, K. (1967) in Methods in Enzymology, Vol. XIIA, p. 222 (Eds: Grossman, L. and Moldave, K.), Academic Press, New York—London
Kizer, P. E., Saunders, G. F. (1972) Biochemistry *11* 1562
Kothari, R. M. (1970) Chromatog. Rev. *12* 127
Rudner, R., Karkas, J. D., Chargaff, E. (1969) Proc. Nat. Acad. Sci. (USA) *63* 152
Rudner, R., LeDoux, M., Nazellis, A. (1972) Proc. Nat. Acad. Sci. (USA) *69* 2745
Rudner, R., LeDoux, M. (1974) J. Biochem. *13* 118
Spencer, J. H., Chargaff, E. (1963) Biochim. Biophys. Acta *68* 9
Udvardy, A., Venetianer P. (1971) Eur. J. Biochem. *20* 513
Udvardy, A., Venetianer, P. (1973) Biochim. Biophys. Acta *308* 234
Venetianer, P. (1969) J. Mol. Biol. *45* 375

Acta Biochim. et Biophys. Acad. Sci. Hung. Vol. 10 (3), pp. 181–184 (1975)

Electron Spin Resonance Spectra of Chicken Hepatoma and Liver Tissue

G. ELEK,* K. LAPIS,* A. ROCKENBAUER,** T. TIBAY**

*First Institute of Pathology, Semmelweis Medical University and **Central Research Institute of Chemistry of the Hungarian Academy of Sciences, Budapest, Hungary

(Received November 13, 1974)

When studied by electron spin resonance (ESR) (Swartz et al., 1972), tumorous tissues differ from their normal equivalents in the following aspects:

1. In tumorous tissues the signal measured in the vicinity of the $g = 2$ region of the spectrum is of a smaller amplitude or completely absent (Commoner et al., 1954; Commoner, Ternberg, 1961; Mallard, Kent, 1964; Dodd, 1973).

2. Signals attributed to certain paramagnetic metal ions are also decreased (Nebert and Mason, 1963; Swartz et al., 1973). New lines may exceptionally appear, too (Mallard, Kent, 1966).

So far mostly human and mammalian tumours (hepatoma and liver tissue) induced by carcinogens have been studied. The aim of the present work was to extend these observations to a fowl tumour of viral origin.

The tissues studied were from the liver of one-month-old and freshly hatched Hunnia hybrid chickens and from 16-day-old Duke embryos as well as transplantable hepatomas induced by the MC-29 chicken *leukosis* virus (Lapis et al., 1973, 1974, 1975; Langlois et al., 1974; Elek et al., 1975). The 50th subcutaneous tumour passage was used for comparisons. ESR spectra of freezed samples were recorded by the modified method of Kovalenko et al. (1971; Elek et al., 1974) in a JES-ME-3X spectrometer.

The spectrum of liver tissue from one-month-old chickens was dominated by a 100 gauss wide signal localized at approximately $g = 2.25$ (Fig. 1). This singlet was absent from the hepatoma spectrum, otherwise it was strikingly similar to that of whole blood.

In the case of Morris hepatoma, Nebert an Mason (1964) observed a decrease of the signal of microsomal haem iron which is localized in the same region. The underlined section indicating the $g = 2$ region is shown in Fig. 2, in a higher resolution. The lowest curve, added for the sake of comparison, represents the spectrum of the liver of a one-month-old Swiss mouse, with the signals of the Mn control included in order to demonstrate the magnitude of the magnetic field. The signals observed in the spectrum of chicken liver appeared at the places where mammalian liver tissue also exhibited paramagnetic absorption ($g = 1.94; 1.97; 2.03$ and the Mn lines, cf. Vanin et al., 1968; Vanin and Chetverikov, 1968). These spectrum components were already recognizable in the liver of 16-day-old chicken embryos. The $g = 2$ signal evolving from free radical(s), part of which is given by

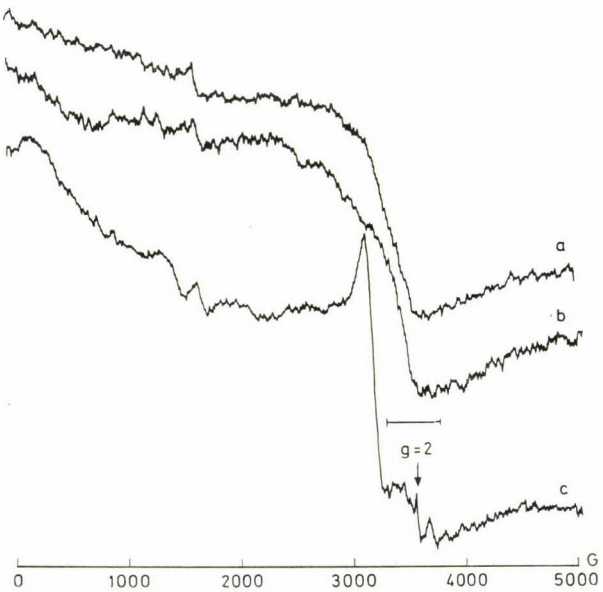

Fig. 1. X-banded ESR spectrum of frozen chicken tissue. The tissue sample was frozen immediately after killing the animals and stored in liquid air. Paramagnetic resonance signals as a function of the magnitude of the magnetic field were recorded between 0 and 5000 gauss. The arrow indicates the $g = 2$ region corresponding to free radicals. a) Signal given by chicken blood clot; b) signal given by a 10-day-old MC-29 hepatoma; c) signal given by the liver of a one-month-old chicken. The three spectra were recorded under identical conditions. Microwave power: 100 mW; modulation: 12.5 gauss; amplification: 1000-fold; time constant (τ): 1 sec; recording time 5 minutes

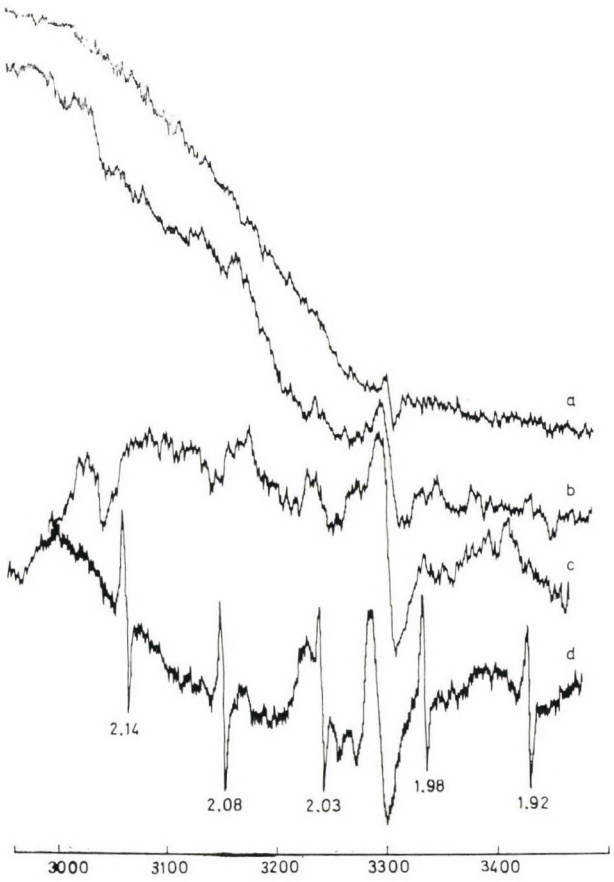

Fig. 2. X-banded ESR spectrum of frozen chicken tissue in the vicinity of $g = 2$. For a detailed description of sample preparation see the legends to Fig. 1. Abscissa: magnetic field in the range of 2970—3470 gauss. a) Signal given by a MC-29 hepatoma; b) signal given by the liver of a 14-day-old chicken embryo; c) signal given by the liver of a one-month-old chicken; d) signal given by the liver of a one-month-old mouse and by the $Mn^{2+}MgO$ standard. The numbers under the Mn lines of the last spectrum represent values of g. All spectra were recorded under identical conditions. Power: 10 mW; modulation: 12.5 gauss; amplification: 2500-fold; $\tau = 1$ sec; $t = 5$ minutes

the blood content of the tissue, also decreased in the tumour (chicken blood clot gave a small free radical signal).

The experiment was repeated three times and on each occasion identical results were obtained. Thus one may generalize by saying that in malignancy ESR signals decrease or disappear not only in mammals but in fowls as well.

The authors express their gratitude to Dr István Földes for providing them with chicken embryos and to Dr Ferenc Tüdős for his advice on ESR measurements.

References

Commoner, B., Townsend, K., Pake, G. E. (1954) Nature *174* 689
Commoner, B., Ternberg, J. L. (1961) Proc. Nat. Acad. Sci. (USA) *47* 137
Dodd, N. J. F. (1973) Brit J. Cancer *28* 257
Elek, G., Turcsányi, B., Holland, R., Ladányi, L. (1974) Acta Biochim. Biophys. Acad. Sci. Hung. *9* 15
Elek, G., Földes, I., Jókay, I., Karczag, E., Lapis, K. (1975) Acta microbiol. Acad. Sci. hung. *22* 341
Kovalenko, O. A., Anfalova, T. V., Sokolov, V. J., Chibrikin, V. M. (1971) Biofisica (Moscow) *16* 663
Langlois, A. J., Lapis, K., Ishizaki, R., Beard, J. W., Bolognesi, D. P. (1974) Cancer Res. *34* 1457
Lapis, K., Beard, D., Beard, J. W. (1973) Orvostudomány *24* 229
Lapis, K., Beard, D., Beard, J. W. (1974) Orvostudomány *25* 151
Lapis, K., Beard, D., Beard, J. W. (1975) Cancer Res. *35* 132
Mallard, J. R., Kent, M. (1964) Nature *204* 1192
Mallard, J. R., Kent, M. (1966) Nature *210* 588
Nebert, D. W., Mason, H. S. (1963) Cancer Res. *23* 833
Nebert, D. W., Mason, H. S. (1964) Biochim. Biophys. Acta (Amst) *86* 415
Swartz, H. M., Bolton, J. R., Borg, D. C. (1972) Biological Application of Electron Spin Resonance, Wiley—Interscience, New York—London
Swartz, H. M., Mailer, C., Ambegaonkar, S., Antholine, E. W., McNellis, D. E., Sneller, S. J. (1973) Cancer Res. *33* 2588
Vanin, A. F., Chetverikov, A. G., Blumenfeld, L. A. (1968) Biofisica (Moscow) *13* 66
Vanin, A. F., Chetverikov, A. G. (1968) Dokl. Akad. Nauk SSSR *178* 949

Acta Biochim. et Biophys. Acad. Sci. Hung. Vol. 10 (3), pp. 185–199 (1975)

Some Structural Features of Rabbit Muscle Aldolase as Derived from its Limited Proteolysis

MAGDA SOLTI, ETELKA BISZKU, M. SAJGÓ, GERTRUD SZABOLCSI

Enzymology Department, Institute of Biochemistry, Hungarian Academy of Sciences, Budapest, Hungary

(Received July 15, 1974; in revised form November 10, 1974)

The peptides released during the limited tryptic proteolysis of rabbit muscle aldolase (Biszku et al., 1973) were located in the primary structure. The pattern of peptide liberation, peptide bond splitting and activity decrease is compatible with two structural models for the truncated tetrameric product, named aldolase-T. According to the more probable model aldolase-T has the structure $A^+A^+B^{++}B^{++}$. Subunits B^{++} are deprived of the segments comprising residues 1–27, 42–71 and 306–364 of the intact enzyme and are inactive. The fragment comprising residues 28–41 is non-covalently attached to these subunits. Subunits A^+ are depleted only of peptides 1–27 and 324–332 and retain 70% activity. In these subunits the fragment comprising residue 333–364 remains non-covalently bound. The molecular weights of the truncated subunits, determined with polyacrylamide-gel electrophoresis in the presence of sodium dodecylsulfate support the above conclusions.

Aldolase-T can be reversibly denatured at pH 2 or in 4 M urea. The recovery of enzymatic activity after decreasing urea or acid concentration indicates the non-covalent rebinding of fragment 333–364. This fragment is named the "T-peptide" of trypsin-treated aldolase. It is suggested that segments 1–27 and 324–364 are not necessary for the renaturation process. Since aldolase-T is a tetramer it seems that large parts of the N- and C-terminal regions of the enzyme are not involved in the intersubunit interactions.

The C-terminal region of aldolase, starting around residue 324, appears to be necessary to the structure of the active site. In contrast to this, the N-terminal region up to residue 27 and probably to residue 60, is not part of the active center.

Introduction

Earlier we found that during the limited tryptic digestion of rabbit muscle aldolase (fructose-1,6-bisphosphate: D-glyceraldehyde-3-phosphate lyase [EC 4.1.2.13]) nine different peptides were split off from the enzyme, while the activity decreased to and remained constant at 35% of the original value (Biszku et al., 1973). The salient feature of the mechanism proposed for the limited proteolysis was that the four subunits of the enzyme were damaged in a non-uniform way, from which it was deduced that the structure of aldolase should be of type AABB. It appeared that from one kind of subunits only two peptides were cut out, whereas from the other subunit-pair seven further peptides were removed.

Abbreviations: TCA, trichloroacetic acid; SDS, sodium dodecylsulfate

The activity decrease during the limited proteolysis could be adequately described by two consecutive processes. Namely, the splitting off of a particular tyrosine-containing peptide from all four subunits gave rise to a 70% active intermediate and the consecutive cleavage of a bond adjacent to a cysteinyl residue, found previously to be essential for enzymatic activity (Szajáni et al., 1970), inactivated subunits type B. The truncated product, named aldolase-T, i.e. trypsin treated aldolase, proved to be a homogeneous, tetrameric protein.

In the present paper we report the location of the released peptides in the primary structure of aldolase and a more detailed study of the structure of aldolase-T. These data allow us to draw conclusions about the structure and the active site of native aldolase.

Materials

Aldolase was prepared from rabbit skeletal muscle and recrystallized three times according to Taylor et al. (1948). Protein concentration was determined spectrophotometrically by using $A^{0,1\%}_{280} = 0.81$, based on the amino acid composition derived from the sequence of aldolase (Sajgó, Hajós, 1974). The specific activity of the preparations was 80 to 100 AU $\times$ mg^{-1} protein, by the dinitrophenyl hydrazine test and 12 to 14.5 μmoles NADH min^{-1} $\times$ mg^{-1} protein by the coupled aldolase-α-glycerophosphate dehydrogenase test (cf. aldolase assay). Calculations were based on a molecular weight of 158 000 for the tetrameric enzyme (Kawahara, Tanford, 1966; Závodszky, Biszku, 1967).

Trypsin, Calbiochem B grade, twice recrystallized, was a chymotrypsin-free preparation, as tested with N-benzoyl-L-tyrosine ethyl ester substrate. Tryptic activity was assayed at 20° according to Schwert and Takenaka (1955) and one unit (*TU*) was defined as the amount of trypsin which gave an increase in absorbance at 253 nm of 1.0 min^{-1}, as described previously (Biszku et al., 1973).

Aldolase-T was routinely prepared from aldolase treated with 2 moles of *p*-mercuribenzoate per subunit, in 0.1 M sodium phosphate buffer pH 7.5 at 20°, and isolated as described previously (Biszku et al., 1973). The preparations were stored freeze-dried. Protein concentration of isolated aldolase-T was determined spectrophotometrically by using $A^{0,1\%}_{280} = 0.835$, based on the structure presented in Fig. 1. The specific activity of the preparations was 45 $\pm$ 5 AU $\times$ mg^{-1} protein, i.e. 5.5 $\pm$ 0.6 μmoles NADH min^{-1} $\times$ mg^{-1}.

Trypsin inhibitor was a Worthington preparation.

Fructose-1,6-bisphosphate was a Reanal preparation. The solution of the sodium salt was purified by repeated charcoal treatment.

p-Chloromercuribenzoate (British Drug Houses) was further purified according to Boyer (1954). The *p*-mercuribenzoate content in solutions of pH 7.5 was determined at 232 nm, by using a millimolar extinction coefficient of 16.7 mM^{-1} $\times$ cm^{-1} (Boyer, 1954).

Porcine pancreatic amylase was prepared according to Hatfaludi et al. (1966). The molecular weight was taken as 52 000 (Závodszky, Elődi, 1970).

Myoglobin (Calbiochem) was a sperm whale preparation. The molecular weight was taken as 17 200, based on the amino acid sequence (Edmundson, 1965).

Sodium dodecylsulfate. A Reanal preparation was used after recrystallization from ethanol.

All other reagents were commercial preparations of reagent grade.

Methods

Aldolase assay

Since aldolase-T was prepared from a mercury derivate of aldolase, enzyme activity was routinely assayed by the dinitrophenyl-hydrazine test of Swenson and Boyer (1957) as described earlier (Biszku et al., 1973). One unit of aldolase activity (AU) is defined as a change of 0.1 min^{-1} is the absorbance at 520 nm. Specific activity is given as $AU \times mg^{-1}$ protein.

The activity of the preparations was also assayed by a coupled enzyme reaction with an excess of α-glycerophosphate dehydrogenase in 0.1 M Tris-HCl buffer pH 7.5 at 20°. Specific activity is given as μmoles of NADH oxidized by 1 mg aldolase per minute.

Titration of peptide bonds split during tryptic digestions

Aldolase gelfiltered on a Sephadex G-25 column equilibrated with 0.1 M KCl was treated with 2 moles of *p*-mercuribenzoate per mole of subunit as described previously (Biszku et al., 1973). The mercury derivate had the same specific activity as the native enzyme. The digestion of about 160 mg protein, performed in 0.1 M KCl solution pH 7.5 at 20°, was followed by recording the alkali uptake under continuous nitrogen flow with a TTTI autotitrator equipped with a recorder, as described earlier (Biszku, Szabolcsi, 1964), except that much smaller amounts of trypsin (0.02 to 0.5 TU per ml) were used in order to slow down the reaction.

For aldolase activity assay digestion was stopped at time intervals by an about 400-fold dilution with 0.1 M sodium phosphate buffer pH 7.5. For analytical studies proteolysis was arrested at appropriate times by the addition of either trypsin inhibitor or trichloroacetic acid.

Polyacrylamide-gel electrophoresis in the presence of sodium dodecylsulfate

This was performed according to Weber and Osborn (1969), as described previously (Biszku et al., 1973). For molecular weight determination the gels were calibrated with a mixture of aldolase, amylase and myoglobin. Relative mobility was calculated as the distance travelled by the protein divided by the distance travelled by the dye bromophenol blue.

Determination of released tyrosine, tryptophan and cysteine

These were performed as described previously (Biszku et al., 1973).

Urea denaturation

1 – 5 mg/ml samples of aldolase and aldolase-T in 0.1 M sodium phosphate buffer pH 7.5 were treated with urea, final concentration 4 M, for 30 minutes at 20°. The solutions were diluted with 0.1 M phosphate buffer or with buffer containing 4 M urea, to about 0.1 mg per ml enzyme and activity was assayed with the dinitrophenylhydrazine test. In some experiments urea-treated aldolase-T was dialysed in the cold against 0.1 M phosphate buffer pH 7.5 overnight or gel-filtered on a Sephadex G-25 column equilibrated with the same buffer. For the determination of T-peptide release (cf. text) 15 to 20 mg per ml aldolase-T was dissolved in 0.1 M sodium phosphate buffer containing 4 M urea and precipitated with trichloroacetic acid, final concentration 6.6%. Tyrosine was determined spectrophotometrically in the acid supernatant (Biszku et al., 1973).

Reversible acid denaturation

This was performed as described by Stellwagen and Schachman (1962).

Peptide analytical methods

Separation and purification of the peptides liberated during the limited proteolysis were performed as described earlier (Biszku et al., 1973).

Cyanogen bromide cleavage of aldolase, fractionation and tryptic digestion of the fragments* were performed as described previously (Sajgó, 1971; Sajgó, Hajós, 1974). Digestion with chymotrypsin (Calbiochem, A grade) was carried out in 0.1 M ammonium bicarbonate pH 8.2 for two hours at 37°. Enzyme–substrate ratio 1 : 50, by weight. Digestion was arrested by addition of diisopropyl-phosphofluoridate. To obtain large overlapping fragments we used the tryptic digest of the citraconylated fragment CB2. Citraconylation was performed according to Dixon and Perham (1968).

Peptides were separated and purified by paper electrophoresis and chromatography in buffer and solvent systems applied previously (Sajgó, 1969).

N-terminal sequences were determined by the dansyl-Edman method (cf. Hartley, 1970), C-terminal sequences by the micro-method of Sajgó and Dévényi (1972).

* The alignment of the cyanogen bromide fragments of aldolase is: CB1 = residues 1–158, CB3 = residues 159–224, CB4 = residues 225–242, and CB2 = residues 243–364 (Lai, 1968; Sajgó, 1971).

Amino acid analyses were carried out according to the single column procedure of Dévényi (1969) with a Beckman Unichrom analyzer.

Amides were located on the basis of electrophoretic mobilities.

Results and discussion

Location of the liberated peptides in the primary structure of aldolase

We described previously that nine different peptides were isolated as split products during the formation of aldolase-T. These peptides were denoted as Nt-27,* CB1-1, CB1-2, TYR-B, CB2-1, P(TRP), TYR-A, P(CYS) and TYR-C. At that stage of the sequence analytical work we could locate peptide Nt-27 as the N-terminal 1–27 residues of the enzyme and P(CYS) and TYR-C as comprising the C-terminal 32 residues of aldolase (Biszku et al., 1973). By elucidating the complete sequence of aldolase (Sajgó, Hajós, 1974a), now we can present the position of all the nine peptides liberated during the formation of aldolase-T.

The amino acid composition, partial or total sequence of peptides CB1-1, TYR-B and CB1-2 shows that these peptides comprise residues 42–56, 57–59 and 60–71, respectively (Sajgó, Hajós, 1974, 1974a) (Table 1).

On the other hand, peptides CB2-1, P(TRP), TYR-A, P(CYS) and TYR-C originate from the C-terminal region of aldolase (Biszku et al., 1973). The amino acid composition and alignment of these peptides are presented in Tables 2 and 3, respectively. These peptides were also isolated and sequenced from the tryptic digest of the C-terminal cyanogen bromide fragment of the enzyme (residues 243–364). To overlap these peptides we used bridge-peptides isolated from the chymotryptic digest of this fragment. In addition, we also obtained a large overlapping peptide comprising peptides P(TRP) and TYR-A from the tryptic digest of the citraconylated C-terminal cyanogen bromide fragment.

In our previous paper (Biszku et al., 1973), based on kinetic considerations, we tentatively located peptide CB2-1 between peptides TYR-A and P(CYS). According to the analysis of the C-terminal cyanogen bromide fragment peptide CB2-1 precedes peptide P(TRP). In addition to the evidence given by the chymotryptic bridge-peptide we should also note that the C-terminal cyanogen bromide fragment contains only two tryptophan residues. One of them is located in peptide P(TRP) while the sequence around the other tryptophan is . . . Lys-Pro-Trp-Ala-Leu . . . (Sajgó, Hajós, 1974a). Thus the overlap presented in Table 3 seems to be sufficient to localize peptides CB2-1 and P(TRP) as adjacent peptides.

As we already mentioned we found that during the formation of aldolase-T the subunits of the enzyme were attacked by trypsin in a non-uniform way. In the present state of the sequence studies we could not reveal any difference as possible reason for this phenomenon.

* According to our recent analysis (Sajgó, Hajós, 1974) the peptide denoted earlier as Nt-26 in fact comprises 27 amino acid residues.

Table 1

Analytical data of peptides CB1-1, TYR-B and CB1-2 released during the formation of aldolase-T

The arrows show the direction of sequencing by dansyl-Edman method or carboxypeptidase A + B treatment. Regions in parentheses were not sequenced. We present within brackets the corresponding peptides isolated from the tryptic digest of the N-terminal cyanogen bromide fragment CB1 (cf. Sajgó, Hajós, 1974)

Peptide	Composition (μmoles)	Sequence
CB1-1	Asx (1.9) Thr (1.8) Ser (0.8) Glx (4.1) Gly (1.1) Ile (0.7) Leu (0.9) Lys (1.0) Arg (2.1)	Lys-Leu-Glx-Ser-Ile-Gly-Glx(Thr, Asx, Thr, Glx, Glx, Asx)Arg-Arg [42 56] [Lys-Leu-Gln-Ser-Ile-Gly-Glx-Thr-Asx-Thr-Glx-Glx-Asx-Arg-Arg]
TYR-B	Tyr (0.8) Phe (1.0) Arg (1.1)	Phe-Tyr-Arg [57 59] [Phe-Tyr-Arg]
CB1-2	Asx (1.9) Glx (1.1) Pro (1.9) Gly (1.1) Ala (1.0) Val (0.6) Ile (0.7) Phe (1.1) Lys (1.0) Arg (1.0)	Ala-Phe-Pro-Glx(Asx, Asx, Gly, Arg, Pro)Val-Ile-Lys [60 71] [Ala-Phe-Pro-Glu-Asp-Asn-Gly-Arg-Pro-Val-Ile-Lys]

Table 2

Amino acid composition of peptides CB2-1, P(TRP), TYR-A and P(CYS)

The corresponding tryptic (T) and chymotryptic (CT) peptides were isolated from the digest of fragment CB2

Peptide	CM-Cys	Asp	Thr	Ser	Glu	Pro	Gly	Ala	Val	Ile	Leu	Tyr	Phe	Lys	His	Arg	Trp
CB2-1	—	—	—	0.7	1.1	—	—	2.9	—	—	2.1	—	—	1.0	—	—	—
T1	—	—	—	0.8	1.1	—	—	3.0	—	—	1.9	—	—	0.9	—	—	—
CT1	—	—	—	0.7	1.0	—	—	2.8	—	—	0.9	—	—	1.0	—	—	+
P(TRP)	—	1.0	—	—	1.1	—	2.1	0.9	—	—	1.0	—	—	3.1	—	—	+
T2	—	—	—	—	—	—	2.0	0.9	—	—	—	—	—	1.1	—	—	++
T3	—	—	—	—	—	—	1.9	1.1	—	—	—	—	—	1.9	—	—	++
T4	—	0.9	—	—	1.0	—	—	—	—	—	1.1	—	—	2.1	—	—	—
T5	—	1.1	—	—	1.0	—	—	—	—	—	1.1	—	—	0.9	—	—	—
CT2	—	1.0	—	—	0.9	—	2.1	—	—	—	0.9	—	—	2.1	—	—	—
TYR-A	—	—	—	—	3.1	—	—	1.9	0.7	—	—	0.8	—	0.8	—	1.1	—
T6	—	—	—	—	3.0	—	—	1.8	0.6	—	—	0.9	—	0.9	—	1.0	—
CT3	—	—	—	—	2.9	—	—	1.9	—	—	—	0.7	—	1.0	—	—	—
TCi*	—	0.9	—	—	4.1	—	1.9	2.9	0.5	—	1.0	0.8	—	3.8	—	1.0	+
CT4	—	—	—	—	—	—	—	1.8	0.7	—	0.9	—	—	0.7	—	1.1	—
P(CYS)	0.5	1.0	—	0.8	1.1	—	1.1	3.1	—	—	1.9	—	—	1.0	—	—	—
T7	0.7	0.9	—	0.7	1.0	—	1.2	2.9	—	—	2.0	—	—	0.9	—	—	—
CT5	0.6	—	—	—	0.9	—	1.0	1.1	—	—	—	0.8	—	1.1	—	—	—

* Isolated from the tryptic digest of the citraconylated fragment CB2.

Correlation between peptide release and peptide bond cleavage during the formation of aldolase-T

In order to visualize the sequence of events leading to the formation of aldolase-T we have to be able to give a quantitative account of peptide bonds hydrolyzed in terms of peptide release. In the knowledge of the alignment of the released peptides, their order of appearance in the digest and the total number of peptide bonds split, we should be able to follow the formation of the truncated enzyme, moreover to depict a probable structure of aldolase-T.

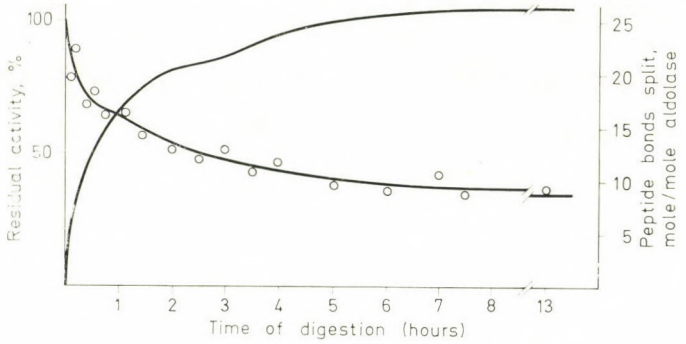

Fig. 1. Time course of peptide bond splitting and activity decrease during the formation o f aldolase-T. The digestion mixture contained 164 mg of aldolase treated with 2 molar equivalents of *p*-mercuribenzoate per subunit in a 15 ml solution of 0.1 M KCl pH 7.5. Trypsin (3 TU) was added in a volume of 10 µl. Temperature 20°. For activity determination digestion was stopped by a 400-fold dilution with 0.1 M phosphate buffer pH 7.5. The continuous line represents the peptide bond splitting calculated from the consumption of 0.02 N NaOH automatically recorded. (○) Activity decrease. The solid line represents the theoretical curve of a two-step consecutive reaction. The activity of an intact subunit is taken as 1. Step *a*, the activity of all four subunits decreases to 0.7, $k_a = 0.1\ min^{-1}$. Step *b*, two of the subunits are inactivated, $k_b = 0.006\ min^{-1}$ (cf. Biszku et al., 1973)

During the formation of aldolase-T, in agreement with our earlier results (Biszku, Szabolcsi, 1964) we measured the splitting of 25 ± 1.5 peptide bonds per mole aldolase. A typical experiment is presented in Fig. 1. The activity decrease as well as the release of the peptides analyzed earlier followed the same kinetics in 0.1 M KCl pH 7.5, used as titration medium, as in 0.1 M phosphate buffer pH 7.5, the medium routinely used for the preparation of aldolase-T. Namely, peptides Nt-27 and TYR-A were liberated from all four subunits, and peptides TYR-B, P(TRP), P(CYS) and TYR-C were released from only two polypeptide chains (Biszku et al., 1973). Peptides CB1-1, CB1-2 and CB2-1 do not contain such residues which would allow the direct and quantitative monitoring of their appearance in the digest (cf. Tables 1 and 3). However, the balance of peptide release and peptide bond cleavage helps to establish the molar ratio in which they are liberated from the enzyme.

The possible correlations between peptide release and peptide bond splitting are presented in Table 4. Two models can be constructed which are compatible

Table 3

Alignment of peptides, CB2-1, P(TRP), TYR-A, P(CYS) and TYR-C (residues 306—364)

The arrows show the direction of sequencing by dansyl-Edman method or by carboxypeptidase A, B and A+B digestion. Regions in parentheses were not sequenced. Peptides signed with T and CT were isolated from the tryptic and chymotryptic digest of the cyanogen bromide fragment CB2, respectively. The large fragment TCi was isolated from the tryptic digest of the citraconylated fragment CB2. The alignment of peptides P(CYS) and TYR-C was shown previously (Biszku et al., 1973)

Peptide	Sequence
CB2-1	Ala-Leu-Glx(Ala, Ser)Ala-Leu-Lys
T1	Ala-Leu-Gln-Ala-Ser-Ala-Leu-Lys
CT1	Gln-Ala-Ser-Ala-Leu-Lys-Ala-Trp
P(TRP)	Ala-Trp-Gly-Gly-Lys(Lys, Glu, Asn)Leu-Lys
T2	Ala-Trp-Gly-Gly-Lys
T3	Ala-Trp-Gly-Gly-Lys-Lys
T4	Lys-Glu-Asn-Leu-Lys
T5	Glu-Asn-Leu-Lys
CT2	Gly-Gly-Lys-Lys-Glu-Asn-Leu
TYR-A	Ala-Ala-Glx(Glx, Glx)Tyr-Val-Lys-Arg
T6	Ala-Ala-Gln-Glu-Glu-Tyr-Val-Lys-Arg
CT3	Lys-Ala-Ala-Gln-Glu-Glu-Tyr
TCi	Ala-Trp-Gly-Gly-Lys-Lys-Glu-Asn-Leu-Lys-Ala-Ala-Gln-Glu-Glu-Tyr-Val-Lys-Arg
CT4	Val-Lys-Arg-Ala-Leu
P(CYS)	Ala-Leu-Ala-Asx(Ser, Leu, Ala, Cys)Gln-Gly-Lys
T7	Ala-Leu-Ala-Asn-Ser-Leu-Ala-Cys-Gln-Gly-Lys
CT5	Ala-Cys-Gln-Gly-Lys-Tyr

```
          310        315        320        325        330        335        340
Ala-Leu-Gln-Ala-Ser-Ala-Leu-Lys-Ala-Trp-Gly-Gly-Lys-Lys-Glu-Asn-Leu-Lys-Ala-Ala-Gln-Glu-Glu-Tyr-Val-Lys-Arg-Ala-Leu-Ala-Asn-Ser-Leu-Ala-Cys-Gln-Gly-Lys
<---------- CB2-1 ---------->
          <---------- P(TRP) ---------->
                               <---------- TYR-A ---------->
                                                  <---------- P(CYS) ---------->

          345        350        355        360
Tyr-Thr-Pro-Gly-Ala-Ser-Gln-Ser-Gly-Ala-Ala-Ala-Gln-Leu-Phe-Ile-Ser-Asn-His-Ala-Tyr
<---------- TYR-C ---------->
```

Table 4

Correlation between peptide release and peptide bond cleavage during the formation of aldolase-T

Experimental conditions as in legends to Fig. 1. Digestion was arrested at time intervals and a) the residual aldolase activity was assayed, b) the amounts of tyrosine, tryptophan and cysteine were determined in the deproteinized digest and c) the peptides released were isolated and identified. A and B stand for the two kinds of subunits which exhibit differential susceptibility towards trypsin. The subunits which are inactivated during the process, i.e. those which lose peptide P(CYS), are arbitrarily denoted as B

Peptides split off, in order of liberation			Subunits affected			Calculated number of peptide bonds split	Calculated activity of the subunits[b]	
Peptide	Position of the sequence	Pseudo first order rate constant[a]	Amount[a]	Model 1	Model 2		A	B
		k, min^{-1}	mole per mole aldolase			per mole aldolase	1.0	1.0
TYR-A	324–332	0.1	4	AABB	AABB	8	0.7	0.7
TYR-B	57– 59	0.03	2	AA	BB	4		
CBl-1	42– 56	—	(2)	AA	BB	2		
P(TRP)	314–323	0.015	2	AA	BB	2		
P(CYS)	333–343	—	~2	BB	BB	2		0.0
TYR-C	344–364	0.004	2	AA	BB	0		
CB2-1	306–313	—	(2)	AA	BB	2		
CB1-2	60– 71	—	(2)	AA	BB	2		
Nt-27	1– 27	—	4	AABB	AABB	4	0.7	0.0
						26	0.35	
							Overall activity	

[a] For the kinetic analyses, the correlation between tyrosine, tryptophan and cysteine release and the amounts of peptides liberated cf. Biszku et al. (1973). The figures in parentheses are suggested values compatible with the total number of peptide bonds hydrolyzed.

[b] The activity of an intact subunit is taken as 1. For time course of activity decrease cf. Fig. 1, for the kinetic analysis Biszku et al., (1973).

[c] Peptide TYR-C is released in a three-step consecutive reaction, the rate constants being $k_1 = 0.1$ min^{-1}, $k_2 = 0.006$ min^{-1} and $k_3 = 0.004$ min^{-1} (Biszku et al., 1973). k_1 equals the rate constant of the liberation of peptide TYR-A. According to the sequence analysis k_2 would characterize the splitting off of peptide P(CYS) and k_3 the release of the non-covalently bound peptide TYR-C.

with the measured number of cleaved peptide bonds. Both fulfil the following requirements: (i) aldolase consists of two pairs of subunits which exhibit differential susceptibility towards trypsin. (ii) One pair of subunits, those from which peptide P(CYS) is split off, are inactivated during the formation of aldolase-T. These are arbitrarily denoted as B. The other subunit pair is denoted as A. (iii) The

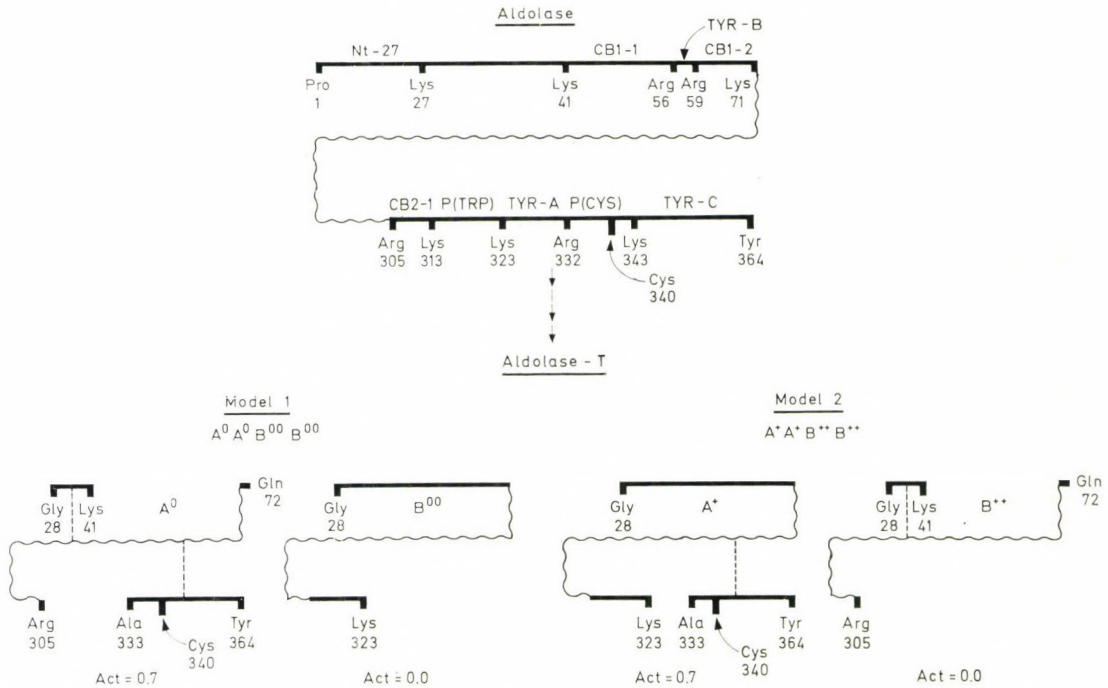

Fig. 2. Tentative models for the structure of aldolase-T. The structure of the mutilated tetrameric enzyme is $A^\circ A^\circ B^{\circ\circ} B^{\circ\circ}$ (Model 1) and $A^+A^+B^{++}B^{++}$ (Model 2). A° and A^+ as well as $B^{\circ\circ}$ and B^{++} represent the two kinds of differently truncated subunits in the two models, respectively. The activity of an intact subunit is taken as 1. The straight lines on the scheme are proportional with the length of the polypeptide chain. The dotted lines represent the interactions which prevent the release of non-covalently bound segments in aldolase-T. The position of the dotted lines is arbitrary. For the sequence of residues 1—71 and 306—364 cf. Sajgó and Hajós, (1974, 1974a) and Table 3, respectively

models should agree with the determined molecular weight of the subunits (see below).

From the models presented in Table 4 we could deduce that peptides CB1-1, CB1-2 and CB2-1 had to be split off from only two of the subunits of aldolase. Were they liberated from all four polypeptide chains we would arrive to a model which requires the cleavage of 38 peptide bonds per mole aldolase and peptide TYR-B had to be split off from all four subunits.

The schematic representation of the structure of aldolase-T according to Models 1 and 2 is given in Fig. 2. Model 1 seems to us rather improbable. It is unlikely that a subunit truncated to such an extent as that denoted A° should retain 70% activity. We are inclined to propose Model 2 for the structure of aldolase-T, which means that all the peptides liberated from only two polypeptide chains would derive from the subunits denoted B. In the following we shall refer to the structure of aldolase-T as that presented in Model 2.*

The structure of aldolase-T

On the scheme of Fig. 2 two fragments are shown to be non-covalently bound to aldolase-T. The tetradecapeptide Gly-28 – Lys-41 in subunits B^{++} and the large fragment Ala-333 – Tyr-364 in subunits A^{+}. Neither of these fragments has ever been found in the deproteinized digest. However, if digestion was arrested at an intermediate stage the fragments comprising residues 1 – 41 and 333 – 364 could be detached from the impaired protein by urea-treatment in the following way: the protein fraction of the digest was isolated by gelfiltration and following treatment with (^{14}C)-bromoacetate in the presence of 6 M urea was gelfiltered again but now in the presence of urea. The fragment denoted as Nt-41 could be isolated from the small molecular weight fraction and was sequenced. From this we concluded that (*a*) the peptide bond between residues 41 – 42 is split prior to that between 27 – 28 and (*b*) in the absence of urea the fragment between residues 28 – 41 remains bound to the protein, probably through hydrophobic forces, since the fragment contains mostly non-polar residues (Sajgó, Hajós, 1974, 1974a).

We could not yet isolate the large peptide from the C-terminal. On the paper electrophoretogram of the small molecular weight fraction besides peptide Nt-41, only a streaking radioactive band was found near the origin. Due to the strong adsorption we could not elute the radioactive component from the paper. If, however, the small molecular weight fraction of the gelfiltration profile was pooled and digested with trypsin it yielded peptides (^{14}C)-CM-P(CYS) and TYR-C in addition to the tryptic subfragments of peptide Nt-41, i.e. peptides 1 – 12, 14 – 27, 28 – 41 and free lysine.

* A third model similar to Model 2 can also be visualized. In this model peptides CB2-1 and P(TRP) would be split off from subunits A^{+}. However this model is not supported by the molecular weight determination (see below).

In addition to these experiments, the trichloroacetic acid supernatant of urea-treated aldolase-T was tested for tyrosine content. We found 3.9 ± 0.3 moles of tyrosine per mole aldolase-T, which is what was expected, since fragment 333–364 contains two tyrosyl residues in position 344 and 364 (cf. Table 3).

The validity of the models illustrated in Fig. 2 was also tested by the molecular weight determination by polyacrylamide-gel electrophoresis. We already reported that during polyacrylamide-gel electrophoresis in the absence of sodium dodecylsulfate aldolase and aldolase-T migrated as single, homogeneous proteins, whereas in the presence of sodium dodecylsulfate aldolase-T gave rise to two bands migrating faster than the intact aldolase subunit (Biszku et al., 1973). According to the relative mobilities of the subunits in the presence of sodium dodecylsulfate the molecular weights of the two truncated subunits are 31 000 and 25 000. This is in good agreement with the values calculated on the basis of peptide release (Model 1 or Model 2, cf. Fig. 2), assuming that in sodium dodecylsulfate the non-covalently bound fragments 28–41 and 333–364 are detached from the rest of the polypeptide chains (Table 5).

Table 5

Molecular weights of aldolase, aldolase-T and their polypeptide chains

The calculated data are based on amino acid (Lai, 1968) and sequence analysis (Sajgó, Hajós, 1974a). In the case of aldolase-T the calculated data refer to the models in the scheme of Fig. 2

Enzyme	Molecular weight	
	Measured	Calculated
	dalton × 10^{-3}	
Aldolase	158[a]	157.12
	159 ± 3[b]	
Aldolase, in 6 M guanidine	37–41[a]	39.28
Aldolase-T	125 ± 3[b]	119.43
Aldolase-T		
Subunit A^{+} or $B^{\circ\circ}$	—	35.24
Subunit B^{++} or A°	—	26.72
Aldolase-T, in SDS		
Subunit A^{+} or $B^{\circ\circ}$	31	32.00[c]
Subunit B^{++} or A°	25	25.40[c]

[a] Sedimentation equilibrium (Kawahara, Tanford, 1966)
[b] Sedimentation equilibrium (Závodszky, Biszku, 1967)
[c] It is assumed that in SDS the subunits lose the non-covalently bound fragments (cf. Fig. 2)

The mechanism of formation and properties of aldolase-T permit us to assume that the C-terminal region of the enzyme, starting somewhere around residue 324, plays a key role in the structure of the active site. Moreover, the peptide bonds between residues 323–324 and/or 332–333 are hypersensitive towards

trypsin in both kinds of subunits. It is already known that in the C-terminal region of the enzyme there are two residues necessary for enzymatic activity, namely Cys-340 (Szajáni et al., 1970) and Tyr-364 (Drechsler et al., 1959; Rutter et al., 1961). It was also shown that acetylation of some internal tyrosyl residues produces similar changes in the catalytic properties of aldolase as the removal of the C-terminal tyrosine (Pugh, Horecker, 1967, 1967a). It is to be seen whether these are identical with Tyr-329 and/or Tyr-344.

In contrast to the C-terminal region, residues 1 – 27 or even the residues up to 60 are not part of the structure of the active site. Namely, peptide 1 – 27 is released at the end of the limited proteolysis and its splitting off does not alter the residual activity of the impaired subunits A (cf. Table 4). The release of peptides CB1-1 and TYR-B (residues 42 – 59) from the 70% active subunits type B precedes the annihilation of enzymic activity of these subunits. Whether residues 60 – 71, which correspond to peptide CB1-2, are essential for enzyme activity cannot be deduced from our data as this peptide is split off from the already inactivated subunits B. That the N-terminal region is not required for catalysis is compatible with the fact that the functionally important residues identified so far are located in more remote parts of the polypeptide chain. A lysine residue was found to be at the phosphate binding site of the enzyme (Shapiro et al., 1968) and the sequence of the tryptic peptide that contains it, was reported (Anai et al., 1973). According to our analysis of fragment 1 – 158 (Sajgó, Hajós, 1974) this residue can be located at position 105. Lys-105 should be sterically near to Cys-340, of which we found that it is also involved in the phosphate binding of aldolase (Szajáni et al., 1970). As shown by Lai et al. (1971), under certain conditions, this cysteinyl residue may form a disulfide bridge with another cysteinyl residue located somewhere in the N-terminal portion of the chain. This residue is Cys-84 (cf. Sajgó, Hajós, 1974). Thus the structure of the active site of aldolase is formed by a folding back of at least one sixth of the chain from the C-terminal towards the center of the chain whereby Cys-340, Tyr-364, Lys-221, the Schiff's base forming lysine (Lai et al., 1965; Sajgó, 1971), Lys-105 and Cys-84 become juxtaposed.

Reversible denaturation of aldolase-T. The "T-peptide" of the enzyme

It is known that native aldolase is reversibly inactivated in 4 M urea (Swenson, Boyer, 1957). Stellwagen and Schachman (1962) have shown that in 4 M urea or in 0.01 N HCl aldolase is dissociated into random coil polypeptide chains. Following reconstitution the chains refold, and the tetramer is reformed with the concomitant recovery of about 70% activity. Table 6 shows that following reconstitution of acid or urea treated aldolase-T, enzymatic activity is also recovered. However, after dialysis or gelfiltration of urea-treated aldolase-T the crippled enzyme is inactivated.

These results suggest that the truncated subunits can refold and even reconstitute the active center provided that fragment 333 – 364 is present. By analogy

Table 6

Reversible denaturation of aldolase and aldolase-T

Treatment	Specific activity		Tyrosine in the TCA supernatant of aldolase-T[a]	
	Aldolase	Aldolase-T	Without carboxy-peptidase-A treatment	Following carboxy-peptidase-A treatment
	AU × mg^{-1}		mole/mole aldolase-T[b]	
None	100	48	0.0	2.1
0.01 N HCl, followed by reconstitution	67	30	—	—
4 M urea	1[c]	0.0[c]	3.9	—
4 M urea, followed by dilution with buffer	62	25	—	—
4 M urea, followed by dialysis or gel filtration	60	0.0	0.0	0.0

[a] The TCA supernatant of the native and urea-treated aldolase did not contain tyrosine
[b] The molecular weight of aldolase-T was taken as 120 000
[c] The activity assay mixture also contained urea

to the *S-peptide* of subtilisin-treated ribonuclease (Richards, Withayathil, 1959), we named the non-covalently bound fragment to "*T-peptide*" of trypsin-treated aldolase.

We have not yet studied in detail the events leading to the reconstitution of aldolase-T. We assume that subunits A^+, which in urea seem to consists of residues 28–323, are capable of renaturation. However, the structure of the active site is only formed by the non-covalent rebinding of the T-peptide. Thus it appears that the N-terminal portion 1–27 and perhaps even the C-terminal portion 324–364 are not required for the renaturation process.

The data presented also corroborate our previous suggestion that intact aldolase consists of two kinds of subunits. Further structural studies should reveal whether the different susceptibility towards trypsin is due to some not yet revealed differences in the primary structure or to some asymmetry in the position of the subunits within the tetramer. In any case, although the limited tryptic attack has rather severely damaged two of the subunits, this has not effected the forces which hold the polypeptide chains together. Thus, it seems that large portions of the N- and C-terminal regions of these chains are not parts of the intersubunit surfaces.

The authors thank Professor F. B. Straub for his continued interest during the work and Mrs Klára Majzik and Mrs Klára Lendvay for the excellent technical assistance.

References

Anai, M., Lai, C. Y., Horecker, B. L. (1973) Arch. Biochem. Biophys. *156* 712–717
Biszku, E., Szabolcsi, G. (1964) Acta Physiol. Acad. Sci. Hung. *25* 169–175
Biszku, E., Sajgó, M., Solti, M., Szabolcsi, G. (1973) Eur. J. Biochem. *38* 283–292
Boyer, P. D. (1954) J. Am. Chem. Soc. *76* 4331–4336
Dévényi, T. (1969) Acta Biochim. Biophys. Acad. Sci. Hung. *4* 297–299
Dixon, H. B. F., Perham, R. N. (1968) Biochem. J. *109* 312–314
Drechsler, E. R., Boyer, P. D., Kowalsky, A. G. (1959) J. Biol. Chem. *234* 2627–2634
Edmundson, A. B. (1965) Nature *205* 883–887
Hartley, B. L. (1970) Biochem. J. *119* 805–822
Hatfaludi, F., Strashilow, T., Straub, F. B. (1966) Acta Biochim. Biophys. Acad. Sci. Hung. *1* 39–44
Kawahara, K., Tanford, C. (1966) Biochemistry *5* 1578–1584
Lai, C. Y. (1968) Arch. Biochem. Biophys. *128* 201–211
Lai, C. Y., Hoffee, P., Horecker, B. L. (1965) Arch. Biochem. Biophys. *112* 567–579
Lai C. Y., Chen, C., Smith, J. D., Horecker, B. L. (1971) Biochem. Biophys. Res. Commun. *45* 1497–1505
Pugh, E. L., Horecker, B. L. (1967) Biochem. Biophys. Res. Commun. *26* 360–365
Pugh, E. L., Horecker, B. L. (1967a) Arch. Biochem. Biophys. *122* 196–203
Richards, F. M., Withayathil, P. J. (1959) J. Biol. Chem. *234* 1459–1465
Rutter, W. J., Richards, O. C. Woodfin, B. M. (1961) J. Biol. Chem. *236* 3193–3197
Sajgó M. (1969) Acta Biochim. Biophys. Acad. Sci. Hung. *4* 385–389
Sajgó, M. (1971) FEBS Lett. *12* 349–351
Sajgó, M., Dévényi, T. (1972) Acta Biochim. Biophys. Acad. Sci. Hung. *7* 233–236
Sajgó, M., Hajós, Gy. (1974) FEBS Lett. *38* 341–344
Sajgó, M., Hajós, Gy. (1974a) Acta Biochim. Biophys. Acad. Sci. Hung. *9* 239–241
Schwert, G. W., Takenaka, Y. (1955) Biochim. Biophys. Acta *16* 570–575
Shapiro, S., Enser, M., Pugh, E. L., Horecker, B. L. (1968) Arch. Biochem. Biophys. *128* 554–562
Stellwagen, E., Schachman, H. K. (1962) Biochemistry *1* 1056–1068
Swenson, A. D., Boyer, P. D. (1957) J. Am. Chem. Soc. *79* 2174–2179
Szajáni, B., Sajgó, M., Biszku, E., Friedrich, P., Szabolcsi, G. (1970) Eur. J. Biochem. *154* 171–178
Taylor, J. F., Green, A. A., Cory, G. T. (1948) J. Biol. Chem. *173* 591–604
Weber, K., Osborn, H. (1969) J. Biol. Chem. *244* 4406–4412
Závodszky, P., Biszku, E. (1967) Acta Biochim. Biophys. Acad. Sci. Hung. *2* 109–112
Závodszky, P., Elődi, P. (1970) Acta Biochim. Biophys. Acad. Sci. Hung. *5* 225–229

Acta Biochim. et Biophys. Acad. Sci. Hung. Vol. 10 (3), pp. 201–206 (1975)

Effect of Detergents and Sucrose Derivatives on the Modified Protein Determination of Lowry

D. GAÁL, L. HOLCZINGER

Oncopathological Research Institute, Department of Biochemistry, Budapest, Hungary

(Received December 20, 1974)

The effect on the protein determination method of Lowry, as modified by Hartree, of widely used detergents (sodium deoxycholate, sodium laurylsulphate, Triton X-100 and Triton WR-1339) and of sugar derivatives often used for preparing concentration gradients (sucrose, dextran, Ficoll and Metrizamide) was examined.

Each of the compounds studied gave rise to a coloured product in the test; however, the correlation between concentration and optical density was usually nonlinear.

The majority of these substances — especially Ficoll, Metrizamide and dextran — interfere with the procedure even at low concentrations, thus their elimination from the sample before protein determination is inevitable.

Introduction

The protein determination method developed by Lowry et al. (1951) has been modified several times (Miller, 1959; Chou, Goldstein, 1960; Hartree, 1972; Schacterle, 1973). Many compounds may interfere with the protein determination based on the use of the Folin reagent (Lowry et al., 1951; Chou, Goldstein, 1960; Zondag, van Boetzelaer, 1960; Rieder, 1961; Diamant et al., 1967; Robson et al., 1968) and the interference of certain substances (e.g. carbohydrates) is higher under the conditions of the modified system (Gerhardt, Beevers, 1968; Bonitati et al., 1969).

In the experiments presented here we examined how some substances used as preparing gradients or as detergents influenced the results of the protein determination method of Lowry as modified by Miller and later by Hartree.

Materials and methods

Folin-Ciocalteu phenol reagent (Merck) and bovine serum albumin (Bovine Albumin powder, fraction V. from bovine plasma; Armour Pharmaceutical Co.) as protein standard were used in the experiments. The compounds examined were sodium deoxycholate (Reanal, analytical grade), sodium laurylsulphate (SDS; Reanal, analytical grade), Triton X-100 (Serva Feinbiochemica, Heidelberg), Triton WR-1339 (Winthrop Laboratories, Newcastle Upon Tyne,

England), sucrose (Reanal, analytical grade), Ficoll (Pharmacia, Uppsala, Sweden), dextran (Reanal, analytical grade) and Metrizamide [2(3-acetamido-5-N-methyl-acetamido-2,4,6-triiodobenzamido)-2-deoxy-D-glucose] (Nyegaard and Co., A/S, Oslo, Norway).*

The following comparative measurements were carried out in the experiments:

a) Formation of coloured products by the compounds studied, measured by Hartree's method.

b) Measurement by Hartree's method of the mixture of protein-detergent and protein-sugar derivatives against blanks of distilled water and of solutions containing increasing concentrations of the substance examined.

Optical density was measured in a Spektromom 203 spectrophotometer (Hungarian Optical Works, Budapest) at 650 nm in 1 cm cuvettes. In order to determine the absorption maximum, measurements were made in the range of 540 – 860 nm.

The degree of interference or inhibition was expressed on the basis of corrected or uncorrected data. Data that were not corrected were obtained by measuring O.D. against distilled water, while corrected data are the results of measurements against blanks containing detergents or sugar derivatives. In both cases the differences were expressed as percentages of the absorption of the albumin standard.

Results and discussion

According to the method of Hartree the absorption maximum was found near 750 nm. Optical densities, however, were measured at 650 nm, since – in agreement with the data of Hartree (1972) – linearity in the widest range (between 25 and 125 μg) was observed at this wavelength.

Each detergent and sugar derivative tested gave coloured products by this method. Colour intensity was insignificant at low concentration, but more expressed at higher concentrations. The optical density, however, was not linearly proportional with the concentration. The absorption of the substances developing the highest colour intensities (Ficoll, Metrizamide and dextran) is shown in Fig. 1.

The effects of detergents and sugar derivatives on the intensity of colour produced by albumin are summarized in Table 1. The optical densities read against distilled water indicate that each compound – with the exception of sucrose and SDS – considerably increased the colour yield given by the protein alone. Especially high values were obtained for Ficoll, Metrizamide and dextran.

Measurements of colour intensities against blanks containing detergents or sugar derivatives at the corresponding concentrations resulted in highly variable values depending on the nature and concentration of the interfering compound (see Table 1, corrected data).

* Metrizamide was a gift of Nyegaard and Co., A/S, Oslo, Norway.

Table 1

Effect of detergents and sucrose derivatives on the intensity developed by albumin

Compound	Concentration % (w/v)	Relative colour intensity (percentage of that exhibited by standard albumin)	
		Uncorrected	Corrected
50 μg albumin			
+ Na-deoxycholate	0.05	100	
	0.1	110	104
	0.4	112	105
	0.8	114	107
+ Na-laurylsulphate (SDS)	0.1	101	98
	0.25	101	98
	0.5	102	97
	1.0	100	93
	2.0	99	90
+ Triton X-100	0.01	107	101
	0.02	111	104
	0.025	115	108
	0.04	127	86*
	0.05	153	71*
+ Triton WR-1339	0.01	105	99
	0.03	113	93
	0.04	118	58*
	0.05	126	43*
+ sucrose	1.7 (0.05 M)	100	96
	3.4 (0.1 M)	99	90
	6.8 (0.2 M)	103	85
	17.1 (0.5 M)	101	73
	34.2 (1.0 M)	95	56
+ Ficoll	0.1	121	95
	0.5	173	96
	1.0	203	86
	2.0	258	81
	5.0	420	92
+ dextran	0.25	98	88
	0.5	134	88
	2.0	155	89
	5.0	212	106
	10.0	240	108
+ Metrizamide	0.1	118	97
	0.5	164	104
	1.0	272	116
	1.5	335	118

* The solution was turbid

The anionic sodium deoxycholate and the non-ionic Triton X-100, as well as Metrizamide and dextran (at higher concentrations) gave rise to a slight increase rather than decrease of the absorption of the protein. The rest of the substances, however, inhibited colour development characteristic of the protein. In the case of sucrose and SDS, comparison of the corrected data with the uncorrected ones shows that both compounds inhibited colour development by albumin; however,

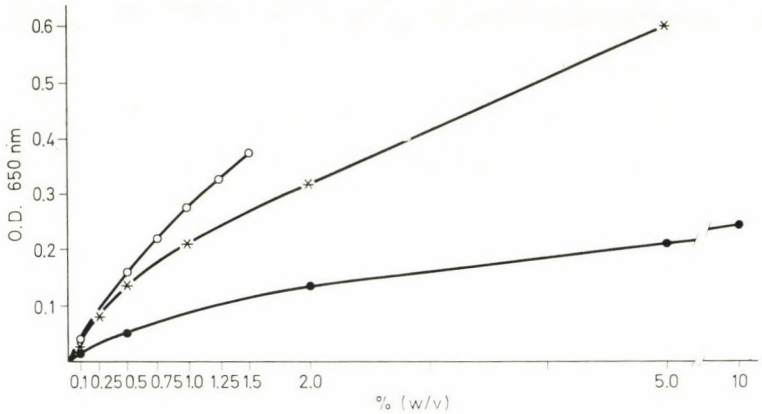

Fig. 1. Absorption of dextran, Ficoll and Metrizamide against distilled water in the absence of protein. Optical densities are the averages of 5 independent determinations, 3 parallels in each. Deviation from the mean value is below 1.5% (this refers to O. D. values in Fig. 2 and Table 1, too). ●—●, dextran; ★—★, Ficoll; ○—○, Metrizamide

this inhibition was compensated by the colour developed by these substances themselves.

When applied above certain concentrations, the two non-ionic detergents (Triton X-100 and Triton WR-1339) formed insoluble complexes with the reagents in the absence of protein under our experimental conditions, thus rendering O.D. measurements impossible.

The influence of Ficoll on protein determination as a function of Ficoll concentration is shown in Fig. 2. The slopes of the curves decrease parallel with increasing concentrations.

Since the influence of sucrose on protein determination by the biuret reaction, in which no phenol reagent is used, has already been described (Hinton et al., 1969), it seemed advisable to examine the effect of Ficoll (2%) and of Metrizamide (1%) in an experimental set-up in which these substances were added to the system after the phenol reagent. In this case optical densities were measured immediately or after 10 minutes of incubation. Under such conditions Metrizamide had no significant effect on the absorption of the protein, while Ficoll interfered with the measurement. In contrast to the increase of 258% shown in Table 1, however, the colour intensity relative to that of the albumin standard increased to 145%

only. Without incubation a negligible increase was observed. When the reaction was performed in water, Metrizamide proved to be ineffective again, the effect of Ficoll was 11 % of its original effect, independently of incubation. On the basis of this observation it seems likely that the interference of the substances in question are decisively influenced by complex formation with the copper reagent. Concentrations of the copper tartarate reagent higher than the usual (5-fold excess) had no effect on the interference by Ficoll and Metrizamide.

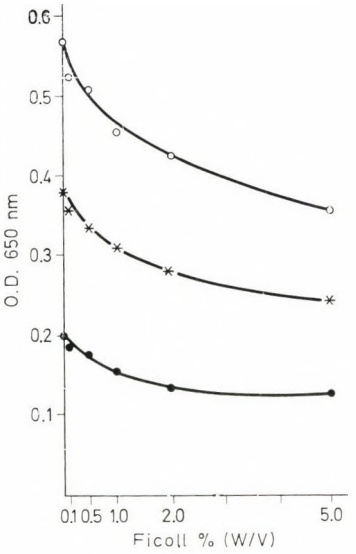

Fig. 2. Inhibition by Ficoll of protein determination as a function of protein concentration. ●—●: albumin, 50 μg; ★—★: albumin, 100 μg; ○—○: albumin, 150 μg

Elimination of sucrose widely used in biochemical fractionations and of the detergents in question is a relatively simple task. Elimination from the system of Metrizamide which has a low molecular weight can be easily achieved, too: according to recent results (Rickwood et al., 1974) Metrizamide exhibiting a very high UV absorption even at low concentrations is reversibly bound to proteins and when the excess of Metrizamide is removed from the system, the Metrizamide–protein complex dissociates.

In contrast to sucrose Ficoll, an artificial polysaccharide of high molecular weight, cannot be removed by simple dialysis. For this reason the strong inhibition of protein determination by Ficoll should be taken into consideration when performing the Lowry test in the presence of this compound. It is advisable to use the methods described for the elimination of the interfering substances (Benett, 1967; Kuno, Kihara, 1967; Arora, 1971).

The influence of dextran is also worth mentioning since dextran gels are widely used in various separation techniques. In almost every case the washing fluid of large pore dextran gels contains measurable amounts of dextran and this alters the results of protein determinations from the eluate.

Since the effect of these substances on protein determination depends upon their concentration, in biological systems in which the concentration of interfering compounds cannot be accurately determined, corrections cannot be made either. In these cases elimination of these compounds from the system is inevitable before protein determination starts.

References

Arora, D. J. S. (1971) Canad. J. Biochemistry *49* 139
Bennett, T. P. (1967) Nature *213* 1131
Bonitati, J., Elliott, W. B., Miles, P. G. (1969) Anal. Biochem. *31* 399
Chou, S. C., Goldstein, A. (1960) Biochem. J. *75* 109
Diamant, B., von Redlich, D., Glick, D. (1967) Anal. Biochem. *21* 135
Gerhardt, B., Beevers, H. (1968) Anal. Biochem. *24* 337
Hartree, E. F. (1972) Anal. Biochem. *48* 422
Hinton, R. H., Burge, M. L. E., Hartman, G. C. (1969) Anal. Biochem. *29* 248
Kuno, H., Kihara, H. K. (1967) Nature *215* 974
Lowry, O. H., Rosenbrough, N. J., Farr, A. L., Randall, R. J. (1951) Biol. Chem. *193* 265
Miller, G. L. (1959) Anal. Chem. *31* 964
Rickwood, D., Hell, A., Birnie, G. D., Gilhuss-Moe, C. (1974) Biochim. Biophys. Acta *342* 367
Rieder, H. P. (1961) Clin. Chim. Acta *6* 188
Robson, R. M., Gall, D. E. Templet, M. J. (1968) Anal. Biochem. *24* 33
Schacterle, G. (1973) Anal. Biochem. *51* 654
Zondag, H. A., van Boetzelaer, G. L. (1960) Clin. Chim. Acta *5* 155

Acta Biochim. et Biophys. Acad. Sci. Hung. Vol. 10 (3), pp. 207–215 (1975)

Electron Microscopic Observations on the Poly(A)-RNP Component of the Pre-mRNA Containing Nuclear Complexes

L. KOMÁROMY, J. MOLNÁR, A. TIGYI

Institute of Biology, University Medical School, Pécs, Hungary

(Received December 9, 1974)

The nuclear ribonucleoprotein particles containing polyadenylic acid were prepared from rat liver nuclear extract by treatment with RNase I. The sedimentation coefficient of the particles was approximately 14 *S*. These particles represent a component of the pre-mRNA containing ribonucleoprotein complexes of the nucleus. The submicroscopic morphology of the particles was examined in preparations pretreated by platinum-palladium shadowing and by various negative staining methods as well as in ultrathin sections. The 14 *S* particles are globular structures, 120–140 Å in diameter. The particles are characterized by a strong tendency to aggregation. The results are discussed with respect to mRNA transport.

Introduction

As shown by Samarina and co-workers, pre-mRNA bound to the macroglobular informofer protein is present in the nucleus in the form of polysome-like complexes (Samarina et al., 1968). It has been also revealed by biochemical studies, that following pre-mRNA synthesis, a polyadenylic acid containing ribonucleoprotein is bound to these polyparticles at the 3'-terminal (Darnell et al., 1972; Samarina et al., 1973a). If no RNase inhibitor is added during the extraction of RNP particles, the pre-mRNA containing nuclear polyparticles decomposes to 30 *S* particles containing pre-mRNA and to polyadenylic acid RNP particles sedimenting in the 14 *S* zone of the nuclear extract (Samarina et al., 1973b). The latter differs from the 30 *S* nuclear particles described earlier also by their different protein composition (Molnár, Samarina, 1975).

In our present study the ultrastructural characteristics of the 14 *S* particles containing polyadenylic acid-RNP (abbreviated as 14 *S* particles) were analysed by various methods. Our results show that the poly(A)-RNP particles can be isolated after the incubation of the nuclear extract with RNase I. Submicroscopically these particles appear as globules, 120–140 Å in diameter and exhibit a strong tendency to form aggregates.

Abbreviations used: pre-mRNA, heterogeneous nuclear RNA; 14 *S* particles, nuclear RNP component containing polyadenylic acid; 30 *S* particle, nuclear particle containing pre-mRNA in a complex with informofer protein.

Materials and methods

Rats of both sexes from the CFY strain were used for the experiments. Nuclear fraction was prepared from the liver by the modified Chauveau method (Samarina et al., 1968). The extraction medium did not contain RNase inhibitor. The nuclear extract obtained in this way was divided in two parts. One of these was treated with pancreatic RNase I (Reanal, Budapest) at concentration of 10 μg/ml at 37°C for 30 min. The second part was not treated with RNase. Following the incubation the extract treated with RNase was cooled to 4°C, then both extracts were ultracentrifuged in 15–30% (w/w) linear sucrose gradients in the SW 27 rotor of a Beckman Model L2-65B ultracentrifuge at 24 000 rpm at 3°C. Fractions of 14 drops were collected and absorbances were measured at 226 and 260 nm.

Fractions of 30 *S* and 14 *S* zones of the sucrose gradient were pooled and prepared for electron microscopic investigations as described earlier (Komáromy et al., 1974). The samples were divided into three parts. The first one was placed on electron microscopic grids covered by parlodium carrier membrane and stained with a 2% aqueous solution of uranyl acetate or with a 4% aqueous solution of silicotungstate. The second part of the material was prepared according to the basic-protein film technique (Lang and Mitani, 1970), and shadowed in platinum-palladium vapour at an angle of 6°20′ in a Zeiss Jena HBA 120/2 instrument (Bradley, 1965). The amount of platinum-palladium alloy applied was 20 mg (platinum/palladium ratio 3 : 1). The third part of the material was sedimented in a VAC 601 ultracentrifuge for 4 hours at 200 000 × *g*. The pellet was fixed first in 2.5% glutaraldehyde for 2 hours and then in 2% buffered osmium tetroxide. The dehydrated material was then embedded in Durkupán ACM (Fluka). Ultrathin sections were prepared with an LKB ultramicrotome and stained with uranyl acetate and lead citrate (Reynolds, 1963).

Electron microscopic preparations were examined in a JEM 100-B and TESLA BS 613 electron microscope (accelerating voltage 80 kV).

Results

The sedimentation pattern of the nuclear extract ultracentrifuged in a 15–30% (w/w) sucrose gradient revealed the appearance of the 30 *S* nuclear particles containing pre-mRNA (Fig. 1 *A*). The 14 *S* zone is also shown on the sedimentogram. Fractions of the 14 *S* zone are characterized by a high poly(A) content (Samarina et al., 1973a, 1973b). The following experiment was performed to concentrate 14 *S* particles.

When a nuclear extract treated with RNase I was ultracentrifuged in a 15–30% sucrose gradient, the sedimentogram obtained was significantly different from that of the control (Fig. *A* 1 and *B*). The amount of the 30 *S* particles decreased considerably, with a concomitant appearance of a peak in the 14 *S* region.

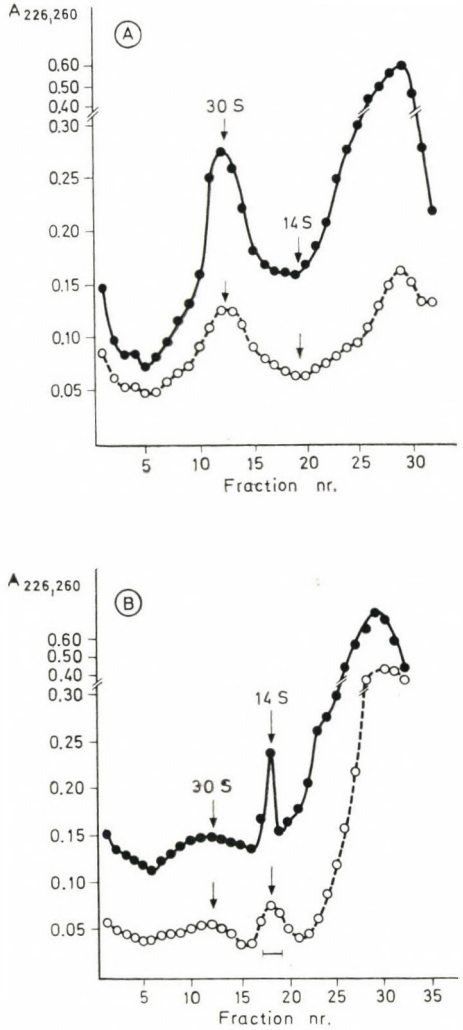

Fig. 1. Sedimentation profile of rat liver nuclear extract in sucrose gradient. The nuclear extract was layered on top of a 15—30% (w/w) linear sucrose gradient and centrifuged at 3°C for 16 hours in the SW 27 rotor of a Beckman Model L2-65B preparative ultracentrifuge at 24 000 rpm. Fractions of 14 drops were collected. Direction of sedimentation: from the right to left. *A*. Sedimentogram of a nuclear extract prepared without RNase inhibitor. The arrows indicate the 30 *S* and 14 *S* region. *B*. Sedimentogram of a nuclear extract prepared without RNase inhibitor, pretreated with RNase I (10 μg/ml). The zones of the 30 *S* nuclear particles and of the 14 *S* poly(A)-RNP particles are marked. —○—○—: A_{260}, —●—●—: A_{226}

RNase treatment caused aggregation of a part of 30 *S* particles as described previously (Molnár, Komáromy, 1974). Another part of the particles was dissociated and the RNA content of these particles appeared in the light zone of the gradient.

Thus the distance between the 30 *S* peak shown in Fig. 1*A* and the light zone increased, the background decreased and a peak corresponding to the poly(A)-RNP particles appeared (Fig. 1*B*). In such cases the adenine content of the fractions containing the 14 *S* particles can reach values as high as 60% (Molnár, Samarina 1975).

According to our electron microscopic observations, the 14 *S* RNP particles displaying a high poly(A) content appeared in different forms. In preparations

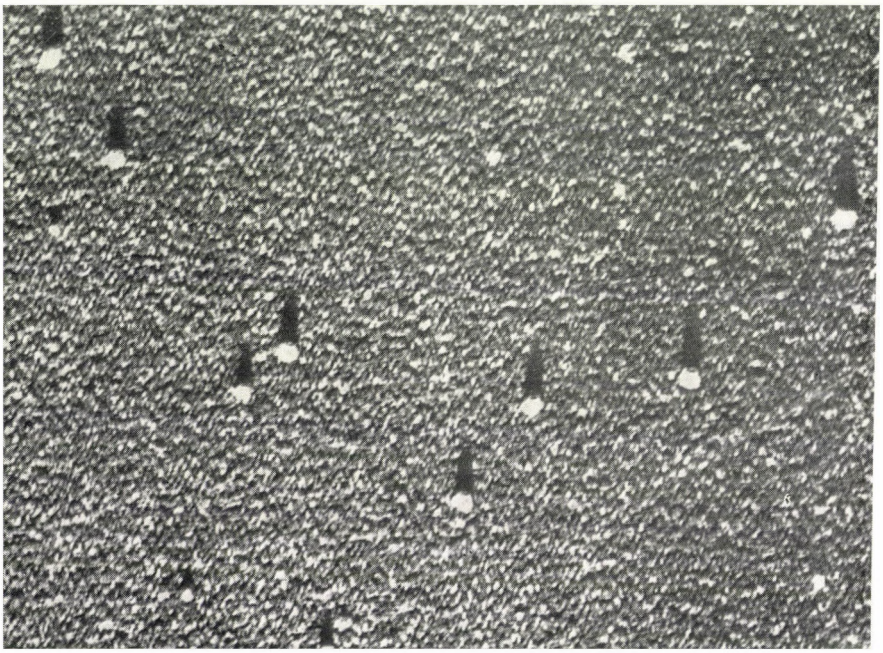

Fig. 2. Electron micrograph of the nuclear poly(A)-RNP particles. Single particles, approx mately 130 Å in diameter are shown. Platinum-palladium shadowing. Magnification × 60 000

shadowed in platinum-palladium vapour single particles of 120–140 Å in diameter were most frequently seen. These particles were globular (Fig. 2). The size of particles was calculated from the shadow length (Fig. 3). The diameter of the poly(A)-RNP particles was in the range of 90–170 Å; most frequently observed particles had a diameter of 120–140 Å. The mean value of the diameters was 132 Å.

In addition to single particles, dimer and trimer formations were often observed in the poly(A)-RNP particle preparations (Fig. 4*A*.) Aggregates or chain-like complexes consisting of 5, 6 or more monomers were sometimes observed, too (Fig. 4*B*).

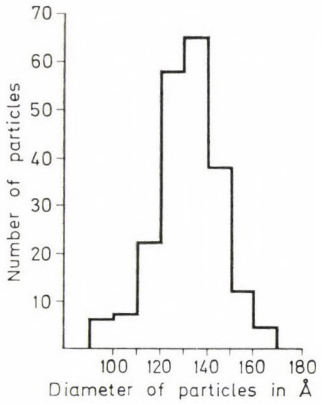

Fig. 3. Size distribution of the poly(A)-RNP particles of the nucleus. The diameters were determined on an electron micrograph (magnification ×60 000) of a preparation shadowed by platinum-palladium and their distribution drawn in a column diagram

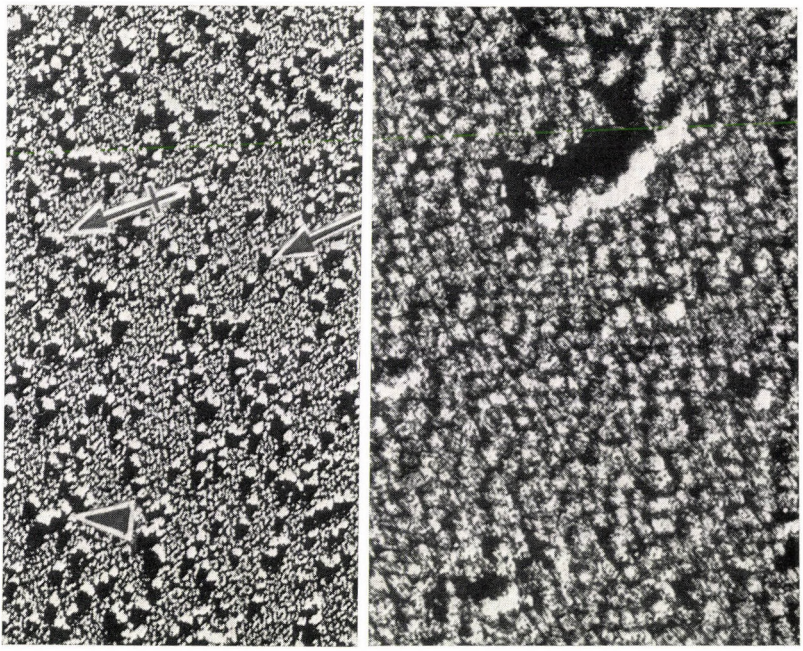

A *B*

Fig. 4. Electron micrographs of the poly(A)-RNP particles of the nucleus. *A.* Platinum-palladium shadowing. Magnification ×25 000. ◀— single particle, ◀—/— dimer structure, ◀ trimer structure. *B.* Platinum-palladium shadowing. Chain-like complex containing several monomers. Magnification ×81 600

In preparations negatively stained with uranyl acetate or silicotungstate the 14 *S* poly(A)-RNP particles appeared as single or complex particles (dimer, trimer, etc.) similarly to the shadowed ones (Fig. 5).

Fig. 6 shows the submicroscopic appearance of the 30 *S* particles prepared by shadowing with platinum-palladium (Fig. 6*A*) or by negative staining (Fig. 6*B*)

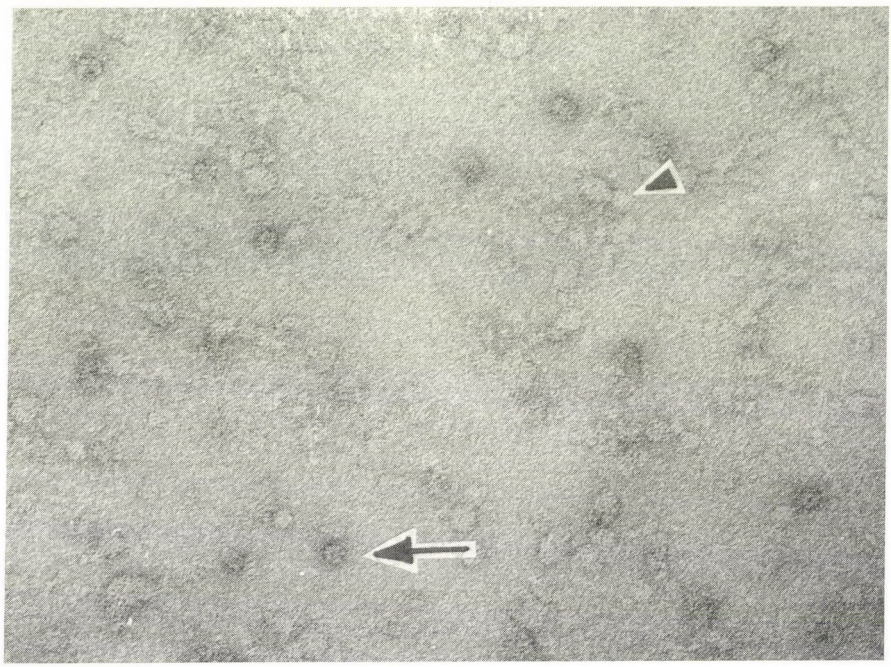

Fig. 5. Electron micrograph of the poly(A)-RNP particles of the nucleus. Stained with 4% silicotungstate. ◀— single particle, ◀ complex structure consisting of several particles. Magnification × 200 000

These micrographs indicate that, in contrast to the 14 *S* poly(A)-RNP particles, the diameter of the 30 *S* particles is 190 – 200 Å as described previously (Komáromy et al., 1974). Similarly to the 14 *S* particles, the 30 *S* particles are of a globular shape.

On the ultrathin sections of the poly(A)-RNP particles globular structures resembling those observed in the shadowed and negatively stained preparations were seen. In addition to the globular structures aggregates appeared (Fig. 7*A*). In contrast to the 14 *S* particles, electron micrographs of the ultrathin sections of the 30 *S* particles containing pre-mRNA revealed globules of larger diameter (Fig. 7*B*).

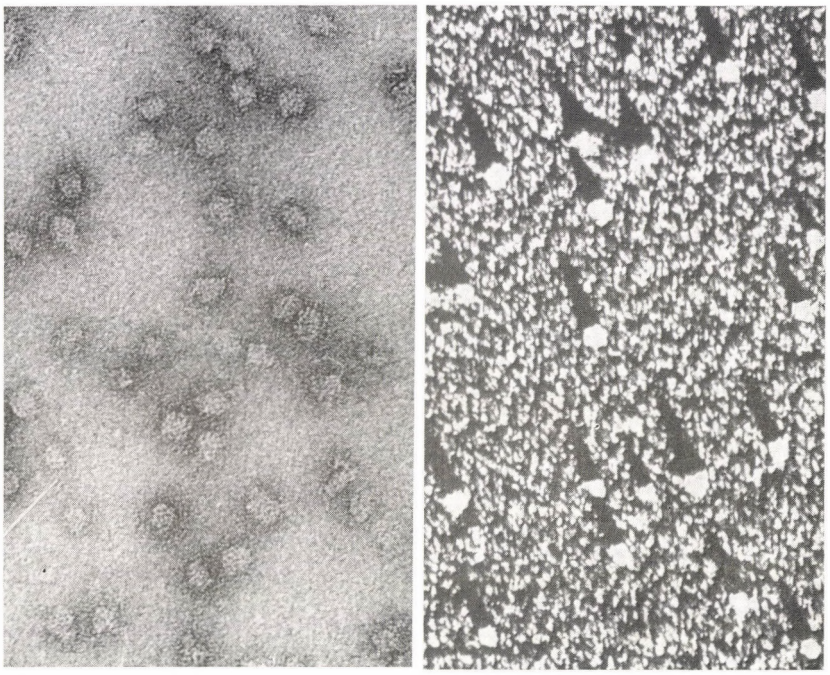

A *B*

Fig. 6. Electron micrograph of the 30 *S* nuclear particles containing pre-mRNA. *A*. Platinum-palladium shadowing. Magnification ×60 000. *B*. Stained with 1% aqueous solution of uranyl acetate. Magnification ×200 000

Discussion

As shown in several laboratories, the 30 *S* nuclear particles contain pre-mRNA in complex with informofer (Samarina et al., 1968; Niessing, Sekeris, 1971; Georgiev, Samarina, 1971; Martin et al., 1973; Pederson, 1974). These pre-mRNP particles are present in the nucleus in the form of polyparticles and following transcription a poly(A)-containing fragment is attached to the 3' end of pre-mRNA (Mendeczki et al., 1972; Samarina et al., 1973a, 1973b; Martin et al., 1973; Georgiev et al., 1973).

In the present experiments the poly(A)-component of the nuclear pre-mRNA containing RNP complexes was isolated and purified for electron microscopic investigations by means of treating the nuclear extract by RNase I. Pancreatic RNase I does not affect the polypurine sequences of the RNA molecule, thus the isolation of the poly(A)-RNP fragment is possible. Another way of isolation and purification of the nuclear 14 *S* particles was the following: a) sedimentation of the nuclear extract in a 15–30% (w/w) sucrose gradient and concentration by precipitation of the 14 *S* fraction in ammonium sulphate; b) dissolution of the

precipitate, followed by incubation with RNase; c) resedimentation in 15–30% (w/w) sucrose gradient. By this method particles containing as much as 75% adenine could be prepared. These particles represent pure poly(A)-RNP particles (Molnár, Samarina, 1975). However, preparations obtained by this method are not quite

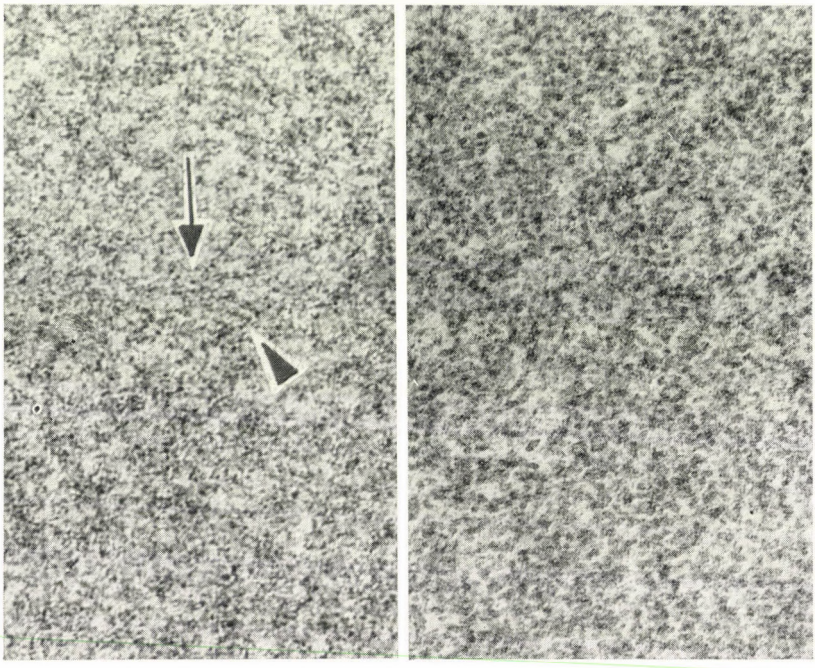

A *B*

Fig. 7. Electron micrograph of ultrathin section of a nuclear poly(A)-RNP particle (*A*) and that of a 30 *S* nuclear particles containing pre-mRNA (*B*). *A*. Fixed in 2.5% glutaraldehyde and 1% OsO_4. Magnification × 126 000. ◀— single particles, ◀ fibril-like aggregates. *B*. Fixed in 2.5% glutaraldehyde and 1% OsO_4

suitable for electron microscopy because of the high extent of aggregation brought about by the precipitation step.

The diameter of the poly(A)-RNP particles of our material ranges from 90 to 170 Å. This shows a certain extent of heterogeneity of the particles. It has been reported that the poly(A) particles of the nucleus are heterogeneous with respect to both their sedimentation behaviour and protein composition (Quinlan et al., 1974). According to these data two types of poly(A) particles, 15 *S* and 17 *S*, respectively, were observed. It may be presumed that the heterogeneity in the diameters is related to different RNA chain lengths in the different particles (Darnell et al., 1971).

It seems worth mentioning that the submicroscopic structure of the poly(A)-

containing fragment of the polysomal mRNP of the rat liver bears a striking resemblance to that of the nuclear 14 *S* particles (Tomcsányi et al., 1974).

We regard the single particles, 120–140 Å in diameter, as the *in situ* form of the poly(A) fragment of the pre-mRNA polyparticles. The other complexes – dimeric, trimeric and others forms – are probably derived from the single particles due to the strong tendency to aggregation of the poly(A)-RNP fragment.

The authors wish to thank Drs G. P. Georgiev, O. P. Samarina, P. P. Juhász and T. Tomcsányi for their valuable advice and Mrs Erzsébet Studinger and Mrs Erzsébet Berta for devoted technical assistance.

References

Bradley, D. E. (1965) in Kay, D. (ed.) Techniques for Electron Microscopy, p. 96. Blackwell Scientific Publications, Oxford
Darnell, J. E., Wall, R., Tushinski, R. J. (1971) Proc. Nat. Acad. Sci. USA *68* 1321
Georgiev, G. P., Samarina, O. P. (1971) Advanc. Cell. Biol. *2* 47
Georgiev, G. P., Varshavsky, A. J., Ryskov, A. P., Church, R. B. (1973) Cold Spring Harbor Symposia on Quantitative Biology *38* 869
Komáromy, L., Molnár, J., Tigyi, A. (1974) Acta Biochim. Biophys. Acad. Sci. Hung. *8* 135
Lang, D., Mitani, M. (1970) Biopolymers *9* 373
Martin, T., Billings, P., Levey, A., Ozarslan, S., Quinlan, T. (1973) Cold Spring Harbor Symposia on Quantitative Biology *38* 921
Mendecki, I., Lee, S. Y., Brawerman, G. (1972) Biochemistry *11* 792
Molnár, J., Komáromy, L. (1974) Acta Biochim. Biophys. Acad. Sci. Hung. *7* 299
Molnár, J., Samarina, O. P. (1975) Mol. Biol. Reports *2* 1
Niessing, J., Sekeris, C. E. (1971) Biochim. Biophys. Acta *247* 383
Pederson, T. (1974) J. Cell Biol. *83* 163
Phylipson, L., Wall, R., Glickman, G., Darnell, I. (1971) Proc. Nat. Acad. Sci. USA *68* 2806
Quinlain, T. J., Billings, P. B., Martin, T. E. (1974) Proc. Nat. Acad. Sci. USA *71* 2632
Reynolds, E. S. (1963) J. Cell Biol. *17* 208
Samarina, O. P., Lukanidin, E. M., Molnár, J., Georgiev, G. P. (1968) J. Mol. Biol. *33* 251
Samarina, O. P., Lukanidin, E. M., Georgiev, G. P. (1973a) in Karolinska Symposia on Research Methods in reproductive Endocrinology. 6th Symp. Prot. Synthesis in Reproductive Tissue, p. 130
Samarina, O. P., Aitkozhina, N. A., Besson, J. (1973b) Mol. Biol. Reports *1* 193
Tomcsányi, T., Komáromy, L., Solymosy, E., Tigyi, A. (1974) Abstr. Commun. 9th Meet. Fed. Europ. Biochem. Soc.

Acta Biochim. et Biophys. Acad. Sci. Hung. Vol. 10 (3), pp. 217—220 (1975)

The Effect of Cold and Fasting on the Carnitine Concentration in the Brown Adipose Tissue of Rats

I. ALKONYI, J. KERNER, A. SÁNDOR

Biochemical Institute, University Medical School, Pécs, Hungary

(Received September 18, 1974)

The ratio of acetylcarnitine to carnitine was unchanged in the interscapular brown fatty tissue of rats which were kept at 5°C. The quantity of total acid soluble carnitine relative to the fat-free dry weight was also unchanged.

On the other hand a small decrease of the environmental temperature from 23°C to 18°C and 20°C resulted in a significant increase in the acetylcarnitine to carnitine ratio.

A number of data point to a close connection between carnitine content and rate of degradation of fat: carnitine markedly increases the oxidation of fatty acids in various tissue preparations (Fritz, 1959; Fritz, Yue, 1963; Bremer, 1962), and the amount of carnitine esters rises considerably under various conditions characterized by enhanced degradation of fat (Pearson, Tubbs, 1964; Bohmer et al., 1966; Delisle, Radomski, 1968). Carnitine must play a role also in the metabolism of brown adipose tissue, as here only lipids are oxidized and the oxidation is significantly accelerated in the case of thermogenesis, for example under the effect of cold (Cameron, Smith, 1964; Hull, Segall, 1965). Indeed, it has been shown that the oxygen consumption and fatty acid oxidation of the mitochondria of brown adipose tissue are markedly increased *in vitro* by carnitine (Hittelman et al., 1969; Drahota et al., 1970). Although the amount of carnitine and the activity of carnitine acetyltransferase (CAT) in brown adipose tissue are high as compared to other tissues (Marquis, Fritz, 1965), it has not yet been studied how these change during the transition from the resting into the thermogenetic phase. Delisle and Radomski (1968) measured the concentration of carnitine and its esters in rats exposed to cold, but omitted from the tissues examined the brown adipose tissue.

We have shown in our earlier work that CAT activity increased 2 to 2.5-fold in rat brown adipose tissue during cold adaptation (Kerner et al., 1973). In the present study we examined the concentration of carnitine, acetylcarnitine and long-chain fatty acid carnitine esters under the same experimental conditions.

Materials and methods

Male Wistar rats weighing 250–300 g were used. The animals were exposed to temperatures of 4°, 18° and 20°C for various time periods or they were fasted. The controls were kept at 23 to 24°C. The animals were killed by decapitation, the interscapular brown adipose tissue was frozen in dry ice–acetone mixture. In the experiments each group consisted of 5 to 6 animals. The tissue was extracted with perchloric acid, and carnitine and acetylcarnitine were determined in the extract (Pearson et al., 1970). The esterified carnitine was liberated by alkaline hydrolysis both in the acid extract (total acid-soluble carnitine) and in the pellet (carnitine esterified with long-chain fatty acids), and was determined as free carnitine. Dry weight was measured after desiccation at 90°C. For lipid-free dry weight determinations lipids were extracted with petroleum ether. The reagents used were CoA, citrate synthetase, malate dehydrogenase, carnitine acetyltransferase (Boehringer, Mannheim, West Germany) NAD, Na-EDTA, Tris, Na-desoxycholate, K_2HPO_4 (Reanal, Budapest, Hungary). DL-acetylcarnitine was prepared according to Friedman and Fraenkel (1957) from DL-carnitine hydrochloride (Schuchard, Munich, West Germany).

Results and discussion

After exposing the animals to 4°C for various times there is no increase either in the concentration of long-chain fatty acylcarnitine or in the amount of acetylcarnitine relative to free carnitine (Table 1). The change in the ratio of carnitine ester/free carnitine is an indication of a similar change in the correspond-

Table 1

Effect of cold (+4°C) on the concentration of carnitine and carnitine esters in the brown adipose tissue of rats

Duration of cold exposure	No. of animals	Moles/g wet tissue		Acetylcarnitine/ free carnitine ratio ± S.E.	Non-fat dry materia in % of wet tissue ± S.E. (No. of animals)
		long-chain FA carnitine ester ± .S.E.	acid soluble* total carnitine ± S.E.		
Control					
0 min	6	36±7.25	602±19.55	0.29±0.018	11.0±0.04 (5)*
30 min	11	23±4.08	580±30.15	0.28±0.025	
1 hour	5	23±8.18	565±40.05	0.32±0.031	
4 hours	5	40±9.20	550±42.18	0.31±0.035	
1 week	15	28±5.85	936±28.20	0.34±0.025	17.6±0.05 (5)
2 weeks	5	27±7.87	993±49.20	0.27±0.042	16.8±0.04 (5)
4 weeks	10	30±6.12	1083±35.02	0.24±0.034	17.0±0.03 (5)

* The total amount of free carnitine and acetylcarnitine is not significantly lower than that of total acid-soluble carnitine

Table 2

Effect of temperature and starvation on the concentration of carnitine and carnitine esters in the brown adipose tissue of rats

Group of animals	No. of animals	Moles/g wet tissue			Acetylcarnitine / free carnitine ratio ±S.E.
		acetylcarnitine ±S.E	free l-carnitine ±S.E	long-chain FA-carnitine ester ±S.E.	
Control 23°–24°C	6	132±12.21	450±19.32	36±7.25	0.29±0.018
20°C, 7 days	5	237±19.4	396±24.12	46±6.85	0.60±0.022 $p < 0.01$
18°C, 7 days	5	298±17.20	395±22.08	48±8.4	0.75±0.022 $p < 0.001$
18°C, 3 days	5	234±15.13	360±20.28	40±7.18	0.65±0.019 $p < 0.001$
20°C, 7 days 1 h + 4°C	5	150±18.22	460±21.46	20±6.80	0.32±0.020
48 h starvation	6	176±15.44	324±18.25	20±8.08	0.54±0.015 $p < 0.01$
48 h starvation 1 h + 4°C	6	125±14.89	380±20.42	5.0±7.05	0.32±0.022

ing CoA ester/free CoA ratio (Pearson, Tubbs, 1964; Bremer, Wojtczak, 1972). Thus the accumulation of a given carnitine ester means that the corresponding CoA ester is being formed faster than it is further metabolized. In particular, the elevated concentration of acetylcarnitine shows that the rate of fatty acid oxidation is enhanced to a greater extent than is the oxidizing capacity of the citrate cycle. Delisle and Radomski (1968) have found that after exposure to 4°C both the long-chain fatty acyl- and the acetylcarnitine contents increase in the liver, although this organ plays no fundamental role in thermogenesis. At the same time in heart and skeletal muscle only the relative amount of acetylcarnitine rises. The fact that in brown adipose tissue none of the carnitine esters increases as a result of exposure to 4°C suggests that the degradation products, such as acetyl-CoA, of fatty acids are metabolized. Furthermore, it is seen in Table 1 that the total amount of carnitine increases only if calculated on a wet tissue basis, whereas on a lipid-free dry material basis the increase is insignificant.

Under the effect of moderate cold and fasting the acetylcarnitine/carnitine ratio increases (Table 2), i.e. under such conditions the rate of fatty acid oxidation is greater than the metabolizing capacity of the citrate cycle. This is conceivable as the reduced coenzymes exert a more pronounced inhibitory effect on the citrate cycle than on fatty acid oxidation (Bremer, Wojtczak, 1972) and the inhibition of the enzymes of the citrate cycle by ATP is also known (LaNoue et al., 1972). If the fasted animals are exposed to 4°C for 1 hour before killing, the acetyl-

carnitine/carnitine ratio decreases (Table 2). This observation indicates that in this tissue the ability to oxidize acetylcarnitine or acetyl-CoA markedly increases, since the formation of acetyl-CoA is also enhanced owing to the increased lipid oxidation.

As shown above it is possible to induce such conditions in the brown adipose tissue when the oxidation of fatty acids, i.e. substrate supply, is greater than can be coped with by the respiratory chain. This suggests that, *in vivo*, in the non-thermogenetic state, the mitochondria of brown adipose tissue are not completely uncoupled, as the respiration of mitochondria derived from this tissue is limited by substrates in the uncoupled state (Drahota et al., 1970; Gray et al., 1970).

References

Bohmer, T., Norum, K. R., Bremer, J. (1966) Biochim. Biophys. Acta *84* 244
Bremer, J. (1962) J. Biol. Chem. *237* 3627
Bremer, J., Wojtczak, Anna B. (1972) Biochim. Biophys. Acta *280* 515
Cameron, I. L., Smith, R. Em. (1964) J. Cell Biol. *23* 89
Delisle, G., Radomski, M. W. (1968) Canad. J. Physiol. Pharmacol. *46* 71
Drahota, Z., Alexandre, A., Rossi, C. R. (1970) Biochim. Biophys. Acta *205* 491
Friedman, S., Fraenkel, G. (1957) in Vitamins and Hormones, Karris, R. S., Marrian, G. F., Thimann, K. V. (editors), Academic Press, New York, Vol. 15, p. 85
Fritz, I. B. (1959) Am. J. Physiol. *197* 297
Fritz, I. B., Yue, K. T. N. (1963) Lipid Res. *4* 279
Grav, H. J., Pederson, J. I., Christiansen, E. N. (1970) Eur. J. Biochem. *12* 11
Hittelman, K. J., Lindenberg, O., Cannon, B. (1969) Eur. J. Biochem. *11* 183
Hull, D., Segall, M. M. (1965) J. Physiol. (London) *181* 468
Kerner, J., Sándor, A., Alkonyi, I. (1973) Acta Physiol. Acad. Sci. Hung. *3* 227
Marquis, N. R., Fritz, I. B. (1965) J. Biol. Chem. *240* 2193
LaNoue, Kathrin, F., Bryla, J., Williamson, J. R. (1972) J. Biol. Chem. *247* 667
Pearson, D. J., Tubbs, P. K., Chase, J. F. A. (1970) in Methoden der enzymatischen Analyse, Bergmeyer, H. U. (ed.), Akademie-Verlag, Berlin Vol. III, pp. 1710–1723.
Pearson, D. J., Tubbs, P. K. (1964) Biochim. Biophys. Acta *84* 772

Acta Biochim. et Biophys. Acad. Sci. Hung. Vol. 10 (3), pp. 221–227 (1975)

Sigmoidal Substrate Saturation Curves in Michaelis–Menten Mechanism as an Artefact

ÉVA FISCHER, T. KELETI

Enzymology Department, Institute of Biochemistry, Hungarian Academy of Sciences, Budapest, Hungary

(Received July 2, 1975)

The conditions under which sigmoidal substrate saturation curves are to be expected in the simple Michaelis–Menten mechanism and the Michaelis–Menten mechanism combined with the concomitant partial inactivation of the enzyme have been determined. The differential equations describing these mechanisms were solved numerically for different sets of rate constants by computer simulation on the basis of the second order Runge–Kutta method.

In order to simulate the real experimental conditions, the substrate saturation curves have also been derived from velocity values in the quasi-steady state, by using the non-linear least squares fitting method.

In the framework of the Michaelis–Menten mechanism there is a sigmoidal relationship between initial velocity and substrate concentration only in the case of a Van Slyke mechanism, i.e. if $k_2 \gg k_{-1}$ and therefore $K = k_2/k_1$ is a "kinetic constant" if the velocity is determined in the quasi-steady state.

If the enzyme is inactivated during the course of velocity measurement in the quasi-steady state, a sigmoidal or a degenerated hyperbolic saturation curve is obtained.

A sigmoidal saturation curve can be obtained in the case of the Van Slyke mechanism, independent of the rate constant of the inactivation of the enzyme, or in the case of Michaelis–Menten or Briggs–Haldane mechanism, if k_3 is sufficiently high. The inflexion point of such substrate saturation curves is determined by the rate constants, i.e. $S_0 \lesssim k_3/k_1$ and k_{-1}/k_1 and/or k_2/k_1. The higher the value of k_3 the more pronounced is the sigmoidicity.

The Michaelis constant can precisely be determined only if the velocities are measured in the very steady state at all substrate concentrations used. If the measurements are made in the quasi-steady state, the K_M is always underestimated.

Introduction

The allosteric and cooperative properties of oligomeric enzymes, which frequently result in sigmoidal saturation curves, are considered to be the most effective mechanisms of regulation of enzyme activity.

However, a number of experimental data and theoretical considerations prove that non-allosteric, monomeric enzymes may also exhibit sigmoidal saturation curves under certain conditions, e.g. if they are present in several (2 or more) isomeric forms and the steady state assumption holds (Keleti, 1968; Frieden, 1970; Rübsamen et al., 1974; Ricard et al., 1974). Similarly, if oligomeric enzymes

reversibly dissociate, the saturation curves may also be sigmoidal (Kurganov, 1967, 1968, 1974; Kurganov, Yakovlev, 1973; Kurganov et al., 1974). Moreover, experimental results show that if an enzyme is unstable and is gradually inactivated during the activity assay, the saturation curve may have sigmoidal shape (Harding, 1969; Dennis, 1969).

We simulated two types of mechanisms and analysed the conditions which lead to sigmoidal saturation curves. The mechanisms studied were the following:

1. The simple Michaelis–Menten mechanism:

$$E + S \underset{k_{-1}}{\overset{k_1}{\rightleftharpoons}} ES \xrightarrow{k_2} E + P \qquad \text{(I)}$$

where E is the enzyme, S the substrate, ES the enzyme–substrate complex, P the product and k_1, k_{-1} and k_2 are the rate constants.

2. The Michaelis–Menten mechanism in the case of an unstable enzyme, i.e. the Michaelis–Menten mechanism combined with the concomitant inactivation of the free enzyme:

$$\begin{array}{ccccc} E & + & S \underset{k_{-1}}{\overset{k_1}{\rightleftharpoons}} & ES & \xrightarrow{k_2} & E + P \\ \downarrow{\scriptstyle k_3} & & & & & \downarrow{\scriptstyle k_3} \end{array} \qquad \text{(II)}$$

where k_3 denotes the first order rate constant of enzyme inactivation. It is assumed that the substrate completely stabilizes the enzyme, i.e. the rate constant of the inactivation of ES equals zero.

These mechanisms were simulated by solving numerically the equations describing the reactions with different sets of rate constants.

Methods

The steady state assumption in the Michaelis–Menten mechanisms results in a first degree hyperbola in the plot initial velocity *vs.* $[S]$. However, in mechanism II, the inactivation of the enzyme may formally be taken as a quasi-irreversible inhibition, if the enzyme reaction fulfils the steady state assumption. This means that $[E]_T$, which is usually constant, becomes a time-dependent function. The general form of the equation describing this mechanism is a second degree hyperbola in $[S]$ (Botts, Morales, 1953; Botts, 1958; Keleti, 1968). Therefore the following second degree hyperbola:

$$y = a_1 \frac{a_2 x'^2 + a_3 x'}{a_2 x'^2 + a_4 x' + a_5} \qquad (1)$$

was fitted to the velocity values by least square fitting *programme RF15.*

In this equation x' is the substrate concentration, y the velocity of product formation, a_1 to a_5 are constants containing the products, sums and ratios of rate constants if steady state holds. In the quasi-steady state a_1 to a_5 are the functions of rate constants. The values of a_1 to a_5 were calculated by parameter estimation for each set of experiment simulated. The y-values were weighted by their inverse squares. Error calculations were carried out by assuming Gaussian error propagation.

Programme IQF2 solves numerically the differential equations that describe mechanisms I and II by using a second order Runge–Kutta method (Mc Cracker, Dorn, 1965). As input data the initial concentrations of enzyme and substrate, the rate constants and the time steps must be given. The time step can be changed within a calculation. The programme computes the concentrations of the enzyme, substrate, enzyme–substrate complex and product as a function of time in each time step. The velocity of product formation is also calculated. The time needed to reach the steady state, i.e. the exact time at which maximum velocity of product formation occurs, can also be obtained.

The computing programmes were written in FORTRAN IV and carried out in an ICL 1905 computer.

Calculation procedure

The time course of the reactions and the rate of product formation were calculated for different sets of rate constants at various initial substrate concentrations. Initial velocities were calculated not only for the steady state but also for the quasi-steady state for the following reason. The exact steady state (i.e. $d\,[ES]/dt = 0$) only prevails for an infinitesimal time period and therefore is currently not amenable to experimental techniques. In the routine work, measurements are usually carried out later, in the quasi-steady state phase. By using the quasi-steady state approximation an error is introduced in the estimation of initial velocity. The choice of the period of the quasi-steady state was made according to Walter (1974).

By applying the unit-free parameters A, B and dimensionless observables (Endrényi et al. 1971):

$$A = a_5 \cdot a_2/a_4^2;\ B = a_3/a_4;\ V_{rel} = y/a_1 = v_0/V_{max};\ x = (a_4/a_5)x'$$

we obtain the generalized, dimensionless form of equation (1):

$$V_{rel} = \frac{Ax^2 + Bx}{Ax^2 + x + 1} \tag{2}$$

and this function is more convenient to handle. It can be shown that in this function an inflection point and therefore sigmoidicity occurs if $A > B$, $B < 1$. If $A = B\,(1-B)$ the expression is reduced to a first degree hyperbola.

Results and discussion

1. Velocity determined in the steady state

If the curves were fitted to points corresponding to the maximum of $[ES]$, i.e. velocities were calculated in the *exact* steady state, no sigmoidicity was found either in mechanism I or in mechanism II. In the case of mechanism I this is theoretically expected. In mechanism II, which theoretically yields a second degree hyperbola, in the *exact* steady state still an ordinary or only a slightly degenerated first degree hyperbola can be fitted to the calculated velocity values in all cases, since *up to the steady state* the amount of inactivated E_0 is negligible, unless $k_3 \gg k_1 S_0$.

2. Velocity determined in the quasi-steady state. Deviations from the first degree hyperbolic behaviour

Mechanism I

If the velocities were calculated in the quasi-steady state the points could be fitted to a first degree hyperbola only if $S > E$ and $E < K_M$ or K_S. As shown in Table 1, deviations from the rectangular hyperbola occur in any of the mechanisms, if $[S]$ is varied from values starting from $[S] \leq [E]$, which is needed for the precise determination of parameters A and B. However, in this case the basic assumption of the Michaelis–Menten kinetics $[S] \gg [E]$ is not satisfied and therefore one cannot expect a first degree hyperbolic saturation curve.

Table 1

Unit-free constants for Eq. (2) in mechanism I

In all cases $k_1 = 0.1$, $E_0 = 1.0$, and time is in arbitrary units. For the precise determination of A and B, S_0 was varied between 0.01 and 2000. The sigmoidal saturation curve ($A > B$ and $B < 1$) was obtained only if $k_2 \gg k_{-1}$ (cf. Fig. 1).

k_2	0.03	0.03	3.0	3.0	0.375
k_{-1}	0.06	6.0	0.06	6.0	0.625
A	0.68	0.095	3.75	0.34	0.45
B	0.85	0.10	0.61	0.65	0.74

The rectangular hyperbola is distorted giving rise to a sigmoid saturation curve in the case of Van Slyke mechanism (Van Slyke, Cullen, 1914; Webb, 1963), i.e. if $k_2 \gg k_{-1}$ and therefore K is a "kinetic constant", $K = k_2/k_1$ (Table 1).

Mechanism II

If the enzyme is unstable and velocities are determined in the quasi-steady state, the distortion of the rectangular hyperbola is more readily observable.

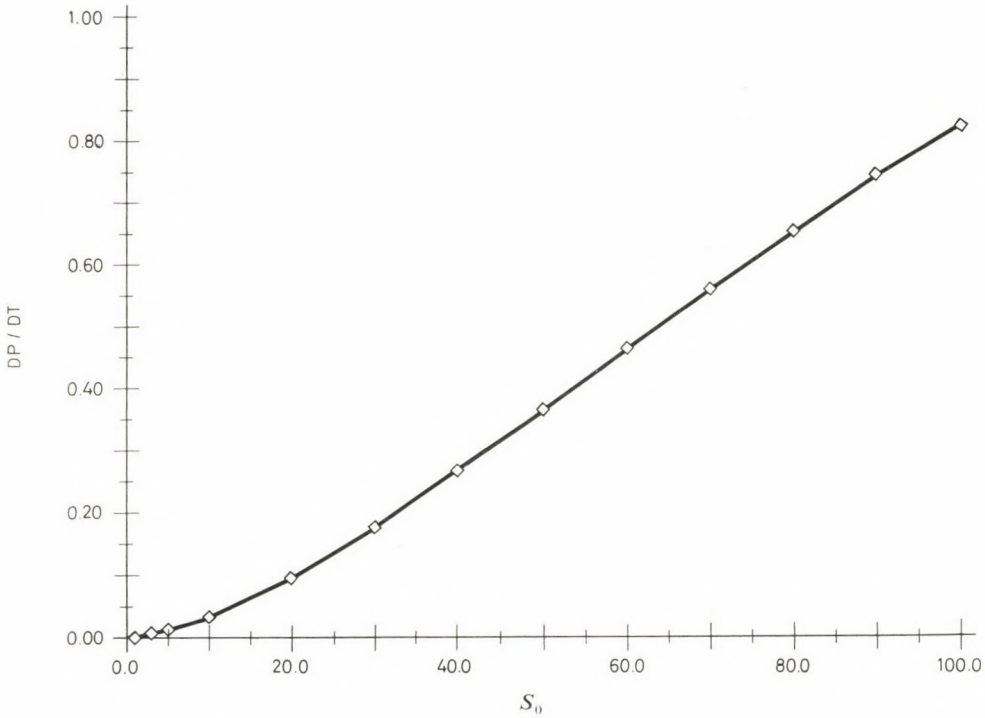

Fig. 1. Computer output of the saturation curve. The position of the inflexion point

$k_1 = 0.1$, $k_{-1} = 0.06$, $k_2 = 3.0$, $E_0 = 1.0$, $A = 3.75$, $B = 0.61$. The points represent the values of the rate of product formation calculated in the quasi-steady state by programme IQF2, the solid line corresponds to equation (1) fitted by programme RF15

Table 2

Unit-free constants for Eq. (2) in mechanism II

Conditions see in Table 1

	k_2	0.03	0.03	3.0	3.0	0.375
k_3	k_{-1}	0.06	6.0	0.06	6.0	0.625
	A	0.64	0.15	2.94	0.40	0.31
0.01	B	0.71	0.16	0.63	0.42	0.68
	A	0.37	0.41	1.27	0.23	0.29
0.1	B	0.69	0.43	0.23	0.09	0.77
	A	0.68	0.67	0.6	0.67	0.65
1.0	B	0.27	0.27	0.04	0.26	0.37

1. A sigmoidicity is observable ($A > B$) at any relationship between k_2 and k_{-1} if k_3 is sufficiently high.

2. In the case of the Van Slyke mechanism, the sigmoidicity is always detectable, independent of the value of k_3. The position of the inflexion point is at a substrate concentration determined by the rate constants, i.e. $S_0 \lesssim k_3/k_1$ and k_{-1}/k_1 and/or k_2/k_1.

The data of Tables 1 and 2 demonstrate that velocity determinations in the quasi-steady state may produce deceptive saturation curves. This is all the more hazardous since the values of the rate constants are generally not known when the saturation curves are determined. Moreover velocity measurements practically cannot be performed in the exact steady state, although most investigations imply this assumption. The values of steady-state times for the experiments simulated are collected in Table 3.

It is seen that if the substrate concentration is varied within a broad range, the duration of the pre-steady state may vary more than one order of magnitude.* Since in the routine experimental work the exact time of the steady state is never known for each substrate concentration, the saturation curves determined from velocity measurements in the quasi-steady state become degenerated hyperbolas or even sigmoidal curves. These sigmoidal saturation curves may be regarded as artefacts.

Table 3

The time needed to reach the steady state in mechanism I

Conditions see in Table 1

	k_2 3.0	3.0	0.375	0.03	0.03
S_0	k_{-1} 0.06	6.0	0.625	0.06	6.0
0.01	1.45	0.37	3.4	14	1.1
0.03	1.45	0.37	3.4	14	1.1
0.1	1.45	0.37	3.4	14	1.1
3.0	1.3	0.33	3.0	6.7	0.62
30	1.2	0.33	1.2	2.2	0.59
75	0.5	0.26	0.9	1.2	0.42
100	0.34	0.2	0.9	0.95	0.28
200	0.22	0.18	0.31	—	—
500	0.136	0.08	0.156	0.2	0.12
1000	0.098	0.05	0.088	0.1	0.07

*Footnote, see next page

It should be emphasized that even the K_M values cannot be evaluated precisely unless from velocities determined in the steady state. During the time course of an enzyme reaction the following relationships hold:

(a) pre-steady state: $k_1[S][E] > (k_2 + k_{-1})[ES]$, i.e. $[S][E]/[ES] > (k_2 + k_{-1})/k_1$
(b) steady state: $[S][E]/[ES] = (k_2 + k_{-1})/k_1$
(c) quasi-steady state; $[S][E]/[ES] < (k_2 + k_{-1})/k_1$

Since $(k_2 + k_{-1})/k_1 = K_M$ this means that in case (c) the value of K_M is underestimated. Since the time period of the quasi-steady state is the function of $[S]$, if $k_3 = 0$, and of $[S]$ and k_3 if $k_3 \neq 0$, a narrow but relatively high substrate concentration range should be used for the determination of both the saturation curve and K_M.

The authors are indebted to Dr G. Szabolcsi for the valuable criticism and suggestion during the preparation of the manuscript.

* At very low substrate concentrations the duration of the pre-steady state is practically independent of $[S_0]$. This is in accordance with the fact that τ, which is related to the duration of the pre-steady state, is practically independent of $[S_0]$ at low initial substrate concentration: $\tau = 1/(k_1[S_0] + k_2 + k_{-1})$. If $k_1[S_0] \ll (k_2 + k_{-1})$ the expression of τ will be: $\tau' = 1/(k_2 + k_{-1})$.

References

Botts, D. J., Morales, M. (1953) Trans. Faraday. Soc. *49* 696–707
Botts, D. J. (1958) Trans. Faraday. Soc. *54* 593–604
Dennis, D. T. (1969) Biochim. Biophys. Acta *191* 719–721
Endrényi, L., Chan, M. S., Wong, I. T. F. (1971) Canad. J. Biochem. *49* 581–598
Frieden, C. (1970) J. Biol. Chem. *245* 5788–5799
Harding, W. M. (1969) Arch. Biochem. Biophys. *129* 57–61
Keleti, T. (1968) Acta Biochim. Biophys. Acad. Sci. Hung. *3* 247–258
Kurganov, B. I. (1967) Mol. Biol. *1* 17–27
Kurganov, B. I. (1968) Mol. Biol. *2* 166–179
Kurganov, B. I. (1974) Mol. Biol. *8* 525–535
Kurganov, B. I., Yakovlev, V. A. (1973) Mol. Biol. *7* 429–447
Kurganov, B. I., Kagan, Z. S., Dorozhko, A. I., Yakovlev, V. A. (1974) J. Theor. Biol. *47* 1–41
Mc Cracker, D. D., Dorn, W. S. (1965) Numerical Methods and FORTRAN Programming. John Wiley and Sons Inc., New York
Ricard, J., Meunier, J. C., Buc, J. (1974) Eur. J. Biochem. *49* 195–208
Rübsamen, H., Khandker, R., Witzel, H. (1974) Hoppe–Seyler's Z. Physiol. Chem. *355* 687–708
Van Slyke, D. D., Cullen, G. E. (1914) J. Biol. Chem. *19* 141
Walter, C. (1974) J. Theor. Biol. *44* 1–5
Webb, J. L. (1963) Enzyme and Metabolic Inhibitors, Vol. I. Acad. Press, N. Y. p. 20

Acta Biochim. et Biophys. Acad. Sci. Hung. Vol. 10 (3), pp. 229–231 (1975)

Proposed Preferred Conformation of ACTH

(Preliminary Communication)

M. LŐW, L. KISFALUDY, S. FERMANDJIAN*

Research Laboratory of Chemical Works of G. Richter Ltd. Budapest, Hungary and *Département de Biologie, Service de Biochemie, Gif-Sur-Yvette, France

(Received July 25, 1975)

In spite of several investigations concerning ACTH conformation, no evidence was been given for a preferred conformation of this important peptide (Lindestrøm-Lang, 1956; Blout, 1962; Craig et al., 1965, 1972; Squire, Bewley, 1965; Schwyzer, Sieber, 1966; Eisinger, 1969; Edelhoch, Lippold, 1969; Patel, 1971; Schiller 1972). In contrast, from our recent circular dicroism studies (Fermandjian et al., 1975) with human $ACTH_{1-32}$ and its fragments (Kisfaludy et al. 1972), the most important phenomenon observed is helix formation induced by trifluoroethanol (TFE). The spectrum in the peptide region (250 to 180 nm) of human $ACTH_{1-32}$ in aqueous solution at pH 6 showed one broad negative band at 195 nm, whereas in TFE two negative bands located at 223 nm and 205 nm and one positive band at 192 nm were observed. Human $ACTH_{1-32}$ shows a linear random coil–helix transition when the percentage of water decreases. These results, together with the CD studies of different fragments, clearly indicate that the ACTH molecule, similarly to gastrointestinal peptides (Bodanszky et al., 1974), also have an active architecture. It is flexible only in water solution whereas in TFE, which according to Urry et al. (1971) mimics the natural environment of membrane proteins, has an ordered conformation. We then calculated which part of the molecule has a tendency to form secondary structures, according to Chou and Fasman (1974). These calculations showed that the appearance of a helix can be expected at the 3–9 and 27–35 regions, residues 23–26 tend very strongly to form a β-turn, while no section of the molecule is favourable for β-sheet formation. The suggested secondary structure (Fig. 1) is in accordance with the CD studies mentioned above.

From the above considerations the following conclusions can be drawn: (1) The different ACTH-s have very similar conformational properties, which is not unexpected in the case of mammalian species, where the difference is only one amino acid, but in the case of the evolutionally very distant dogfish ACTH, where the primary structure differs in eleven amino acids, it is rather surprising. The conformation of the molecule seems to be conserved during evolution, so it can be regarded as a characteristic property of ACTH like the active core or the binding site. (2) It seems that the acidic C-terminal part of the molecule can effectively protect the basic core against trypsin-like enzymes only in the proposed preferred

conformation. Namely, the C-terminal helix, directed by the β-turn, can cover and protect the basic residues in positions 15–18. For instance, in the first stage of the biological life of ACTH, when it is released from proACTH (Gewirtz et al., 1974), the basic core may be thus protected, whereas the Lys-Ser or Arg-Ser binding at the N-terminus of the "small" ACTH is accessible to the converting enzyme. (3) It can also be assumed that during the transport mechanism the ACTH molecule also has a similar preferred conformation in which it is more resistant to proteolytic attack. It is known that the biological half life of shorter ACTH

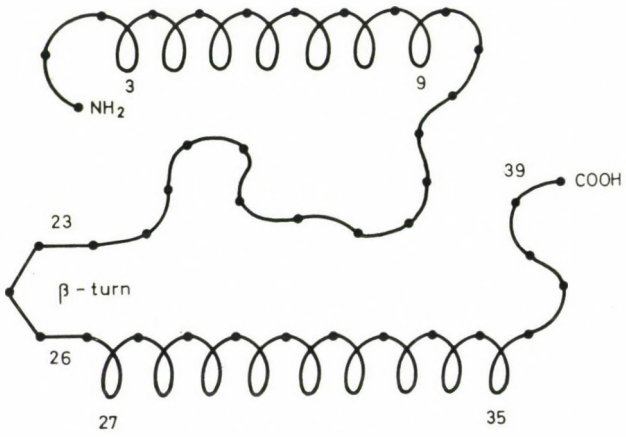

Fig. 1. Schematic diagram of helical and β-turn regions predicted in ACTH (each helical loop represents a single helical residue and not a single turn consisting of 3.6 residues)

fragments (Reisert et al., 1966) is about half or one third of the total molecule. Similarly, the biological potency of shorter fragments does not exceed 100 U/mg, whereas the human $ACTH_{1-32}$ studied, which contains the important β-turn segment and the main part of the helicophilic 27–35 segment, has a potency of 180 U/mg. Furthermore, the significance of the β-turn is demonstrated by the fact that the deaminated ACTH (Asp^{25}-ACTH) also has a lower biological potency (Gráf et al., 1973). (4) When the ACTH molecule reaches the receptor cells, the protective effect is not required any longer and the conformation proposed above, may disturb the binding. This was confirmed by Lowry's experiments (Lowry, McMartin, 1974) who found that on isolated receptor cells the 1–24 fragment is sevenfold more potent than the intact ACTH. We think that this observation confirms the above assumption, since it is inconceivable that a structural part which only inhibits the hormone action could resist the evolutional progress.

References

Blout, E. R., quoted by Li, C. H. (1962) in Recent Progr. in Hormone Res. *18* 1—32
Bodanszky, M., Bodanszky, A., Klausner, M. S., Said, S. I. (1974) Bioorganic Chemistry *3* 133
Chou, P. Y., Fasman, G. D. (1974) Biochemistry *13* 222
Craig, L. C., Fischer, J. D., King, T. P. (1965) Biochemistry *4* 311—318
Craig, L. C., Kac, H., Chen, H. C., Printz, M. P. (1972) in Structure–Activity Relationship of Protein and Polypeptide Hormones (ed. by Margoulies, M., Greenwood, F. C.) pp. 176—179, Excerpta Medica, Amsterdam
Edelhoch, H., Lippoldt, R. E. (1969) J. Biol. Chem. *244* 3876—3883
Eisinger, J. (1969) Biochemistry *8* 3902—3908
Fermandjian, S., Greff, D., Lőw, M., Kisfaludy, L. (1975) Biochemistry; submitted for publication
Gewirtz, G., Schneider, B., Krieger, D. T., Jalow, R. S. (1974) J. Clin. Endocrinol. Metab. *38* 227—230
Gráf, L., Hajós, G., Patthy, A., Cseh, G. (1973) Hormone Metab. Res. *5* 142—143
Kisfaludy, L., Lőw, M., Szirtes, T., Schőn, I., Sárközi, M., Bajusz, S., Turan, A., Juhász, A., Beke, R., Gráf, L., Medzihradszky, K. (1972) in Chemistry and Biology of Peptides (ed. by Meienhoffer, J.) pp. 299—303) Ann. Arbor, Mich.
Linderstrøm-Lang, K. V., quoted by Li, C. H. (1956) in Adv. in Prot. Chem. *11* 101—120
Lowry, P. J., McMartin, C. (1974) Biochem. J. *142* 287—294
Patel, D. J. (1971) Macromolecules *4* 215—254
Reisert, P. M., Haun, G., Rindfleisch, H. (1966) Symp. Deut. Ges. Endokrinol. *12* 270—273
Schiller, P. W. (1972) Proc. Nat. Acad. Sci. (USA) *69* 975—979
Schwyzer, R., Sieber, P. (1966) Helv. Chim. Acta *49* 134—158
Squire, P. G., Bewley, T. (1965) Biochim. Biophys. Acta *109* 234—240
Urry, D. W., Masotti, L., Krivacic, J. R. (1971) Biochim. Biophys. Acta *241* 600—612

Acta Biochim. et Biophys. Acad. Sci. Hung. Vol. 10 (3), pp. 233–242 (1975)

Orientation Dependence in the Epr Spectra of Spin Labels in Glycerinated Muscle Fibres

J. BELÁGYI

Central Laboratory, Medical University, Pécs, Hungary

(Received October 3, 1974)

Glycerinated muscle fibres labelled with a set of five-membered maleimide spin labels revealed a complex type epr spectra, which showed a reduced rate of anisotropic motion. The spectra can be interpreted in terms of the ratio of the two down-field peaks and of the hyperfine coupling constant. The spectra clearly indicated that the preferred orientation of the $2p\pi$ molecular orbital of the odd electron is perpendicular rather than parallel to the long axis of the muscle fibres. Increasing chain length between the maleimide ring and pyrrolidine nitroxide ring reduces the orientational anisotropy. Thermal denaturation destroys the orientation dependence of the epr spectra of spin labels. The Mg-ATP induced shortening of the fibres influences the spectral parameters. The fibres which had been contracted showed a modified orientation dependence of epr spectra.

Introduction

Nitroxide spin labelling proved to be a useful tool in studies on contractile proteins of muscle and model systems (Seidel et al., 1970; Stone et al., 1970; Seidel, Gergely, 1971, 1973; Tokiwa, 1971). The electron paramagnetic resonance (epr) spectrum is sensitive to the orientation of spin labels with respect to the laboratory magnetic field and depends on the rotational mobility of the spin labels (Hamilton, McConnel, 1968; Griffith, Waggoner, 1969; McConnell, McFarland, 1970). The pronounced anisotropy of the striated muscle and glycerinated muscle fibres reflects an arrangement of the molecular structure which plays an important role in physiological processes (Ernst, 1963). With a structural probe such as spin label it may be possible to test the molecular structure around the label and to study the orientation dependence which is evoked by the anisotropic distributions of label orientation. Cooke and Morales (1969) were the first to study the epr spectrum on glycerinated fibres labelled with six-membered maleimide spin label.

It has been the aim of the present work to investigate the orientation dependence of epr spectrum on glycerinated muscle fibres with SH-directed spin labels in order to obtain information on the local order of the contractile system and to look for possible changes after Mg-ATP induced shortening and thermal denaturation. We confirm and extend the earlier experiments and try to give a possible interpretation.

Materials and methods

The preparation followed was essentially that of Huxley (1963). The fibre bundles prepared from psoas muscle of the rabbit were glycerinated for three weeks or longer in refrigerator at $-16°C$. After washing the fibre bundles in 0.1 M KCl, 0.001 M $MgCl_2$ and 0.07 M phosphate buffer (pH 7.0) at room temperature to remove the glycerol, the preparations were kept in the same solution containing the spin label. The reaction of spin label with glycerinated muscle fibres was carried out on ice.

The following spin labels were used:

(i) 3-maleimido-2,2,5,5-tetramethyl-1-pyrrolidinyloxyl as label I,
(ii) 3-(maleimidomethyl)-2,2,5,5-tetramethyl-1-pyrrolidinyloxyl as label II,
(iii) 3-(3-maleimidopropyl)carbamoyl-2,2,5,5-tetramethyl-1-pyrrolidinyloxyl as label III,
(iv) 4-maleimido-2,2,6,6-tetramethylpiperidinooxyl as label IV,
(v) 4-(2-iodoacetamido)-2,2,6,6-tetramethylpiperidinoxyl as label V.

All the spin labels were purchased from Synvar Associates. The glycerinated muscle fibres have reacted with $0.3-0.5$ or $1.5-1.6$ M of spin label per 10^5 g of protein for 60 or 180 min in the case of maleimide spin labels or for 24 hours with iodoacetamide spin label. The unreacted label was removed by washing the fibre bundles in a large amount of salt solution for 16 hours at 4°C.

Thermal denaturation was carried out in thermostat at 50 ± 1 °C for 20 min. The shortening of the muscle fibre bundles was elicited in a medium containing 4 mM ATP and 4 mM $MgCl_2$. All chemicals used in the experiments were analytical grade and obtained from Reanal (Budapest).

The electron paramagnetic resonance spectra were taken at room temperature using a Zeiss Model ER 9 spectrometer operating at 9 kMc/s. The temperature within the cell was 23°C. The orientation of the glycerinated muscle fibres with respect to the applied field was obtained by appropriate alignment of short segments of the fibres in a flat cell. The epr spectra were characterized by the ratio of the two down-field peaks [denoted by $I_{+1}(A)/I_{+1}(B)$] where A means the spectral component due to a strong immobilization of the attached label, while B the spectral component due to a label with greater degree of rotational freedom, the weakly immobilized spin labels and the hyperfine coupling parameter $2A_{zz}$ measured between the outermost hyperfine extrema. It should be noted that the $I_{+1}(B)$ peak is strongly influenced by the orientational anisotropy of the strongly immobilized spin labels; therefore, the ratio of the two down-field peaks can reflect the change in the degree of orientation of spin labels. This can cause some difficulty in the interpretation of epr spectra, especially after MgATP-induced modification. Spectra were recordced twice and were found to be very well reproducible. Field calibration was done by using peroxylamine disulphonate ion radicals in low concentration.

Results

The epr spectrum of glycerinated muscle fibres labelled with maleimide spin labels showed both strongly and weakly immobilized spin labels. When the molar ratio of spin label added to 10^5 g of contractile protein was increased an increasing ratio of $I_{+1}(A)/I_{+1}(B)$ was observed in agreement with earlier findings (Cooke, Morales, 1969; Seidel et al., 1970). The epr spectra revealed that maleimide labels reacted on at least two different sites of contractile proteins which can be distinguished by the degree of rotational freedom of the spin label. We have observed

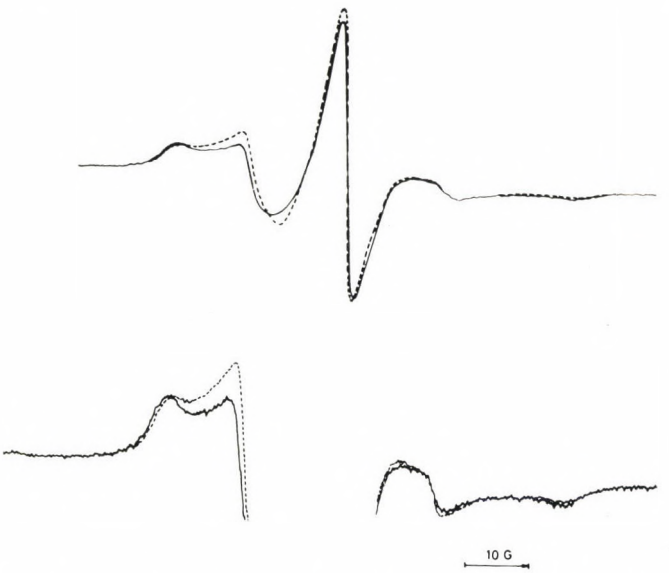

Fig. 1. Epr spectra of spin-labelled glycerinated muscle fibres at two different orientations with respect to the laboratory field. Solid line: long axis of the fibres perpendicular to the magnetic fields; dotted line; long axis of the fibres parallel to the magnetic field. 0.3 M maleimide label (label I) reacted with 10^5 g of protein. The inserts show the low- and high-field components at higher gain setting

some difference between the five-membered and six-membered maleimide spin labels (label I and label IV, respectively) as also demonstrated by McConnell and co-workers (Ogawa et al., 1968) and Taylor (Taylor et al., 1969). Labelling the protein system with label I resulted in a more pronounced immobilization of the spin label molecules in comparison with label IV; therefore, the former one was preferred during the experiments.

Fig. 1 shows the epr spectra of glycerinated muscle fibres labelled with label I in two different orientations with respect to the magnetic field applied. The solid line indicates the epr spectrum obtained in experiments in which the long axis

of the fibre bundle was oriented perpendicular to the external magnetic field. The dotted line shows the parallel orientation of the same preparation. It can be seen that there is a small but definite change in the various spectral features. The amount of label was 0.3 M of maleimide spin label (label I) added to 10^5 g of protein. The protein content of the muscle fibre was assumed to be 20 % of the wet weight. The comparison of the spectral features is given in Table 1 on the basis of the parameters introduced to characterize the epr spectra.

Table 1

Spectral parameters of spin-labelled glycerinated muscle fibres at different orientations to the laboratory magnetic field

Orientation	$I_{+1}(A)/I_{+1}(B)$	$2A_{zz}(G)$	Molar ratio of label to protein
$a \perp H_0$	0.95	61.3	0.33
$a \parallel H_0$	0.66	61.4	
$a \perp H_0$	1.60	61.6	
$a \parallel H_0$	1.14	61.4	1.5
minced	1.40	61.4	

In the table a denotes the long axis of the muscle fibres and H_0 the laboratory magnetic field. The spin label added to muscle protein was label I. The values are the mean of several determinations.

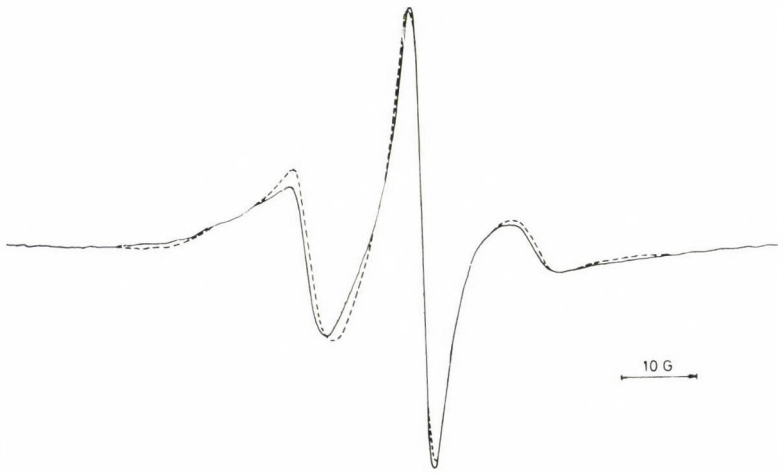

Fig. 2. Epr spectra of oriented glycerinated muscle fibre labelled with label II at two different orientations. 0.37 M label II reacted with 10^5 g of protein

The experiments described here utilized two other kinds of five-membered maleimide spin labels with increasing chain length between the pyrrolidine nitroxide ring and the maleimide ring (label II and label III, respectively) in order to check the environment of the combining sites. Fig. 2 shows the epr spectra of glycerinated muscle fibres at two different orientations of the long axis to the laboratory field. The solid line is the spectrum obtained in experiments in which the long axis was oriented perpendicular to the field applied. The dotted line indicates the parallel orientation of the same fibre bundle. As it can be seen from Fig. 2 there occurred both strongly and weakly immobilized spin labels. But the spin labels with increasing chain length give a decreasing ratio of $I_{+1}(A)/I_{+1}(B)$ and, at the

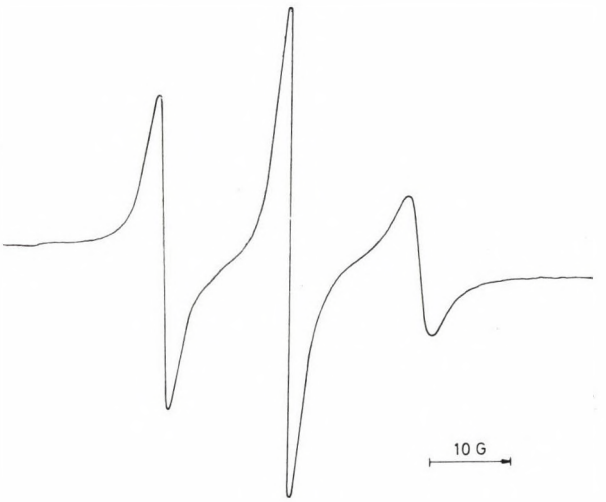

Fig. 3. Epr spectrum of glycerinated muscle fibre labelled with label III. No effect of orientation was observed. 0.23 M label was added to 10^5 g of protein

same time, the difference in the spectral feature between the two orientations becomes smaller. No difference could be observed with label III (Fig. 3). The experimental results referring to label II are summarized in Table 2.

Only a small orientation effect was obtained in the spectra of iodoacetamide-spin-labelled glycerinated fibres. When the fibre bundles were aligned parallel to the laboratory field the ratio of $I_{+1}(A)/I_{+1}(B)$ was reduced by 10 %.

It is of interest to study how the orientation dependence of the epr spectrum of spin labels is influenced by thermal-induced modification of the contractile system. After heat denaturation a significant change appeared in the epr spectrum. Details of the spectral changes were published in an earlier paper (Belágyi, Damerau, 1974). The thermal treatment is followed by a strong increase of the more mobile component at the expense of the strongly immobilized form (Fig. 4). After thermal treatment we did not observe any difference between the spectra of differ-

Table 2

Spectral parameters of spin-labelled muscle fibres at different axis orientations to the magnetic field

Orientation	$1_{+1}(A)/(I_{+1}(B)$	$2A_{zz}(G)$	Molar ratio of label to protein
$a \perp H_0$	0.43	61.3	0.37
$a \parallel H_0$	0.35	61.3	
$a \perp H_0$	0.46	61.3	1.5
$a \parallel H_0$	0.37	61.3	

The spin label added to muscle protein was label II.

ent orientations with regard to the laboratory magnetic field. The spectra of a fibre bundle in different orientations were the same, independent of the degree of labelling and the time of incubation. In contrast, when the molar ratio of spin label added to 10^5 g of protein was increased a greater ratio of $I_{+1}(A)/I_{+1}(B)$ was found in both directions also after thermal treatment. The value of $I_{+1}(A)/I_{+1}(B)$ rose from 0.71 up to 1.24 at higher concentration of label (1.6 M label I 10^5 g protein). Table 3 shows the spectrum parameters of spin-labelled muscle fibre denatured by thermal treatment. The correlation time was calculated according to an equation given by Kusnetsov et al. (1971). The effect of thermal denaturation was independent of the method of spin-labelling. The spectral changes were the same whether the label was reacted with the glycerinated fibre bundle before or after heat denaturation.

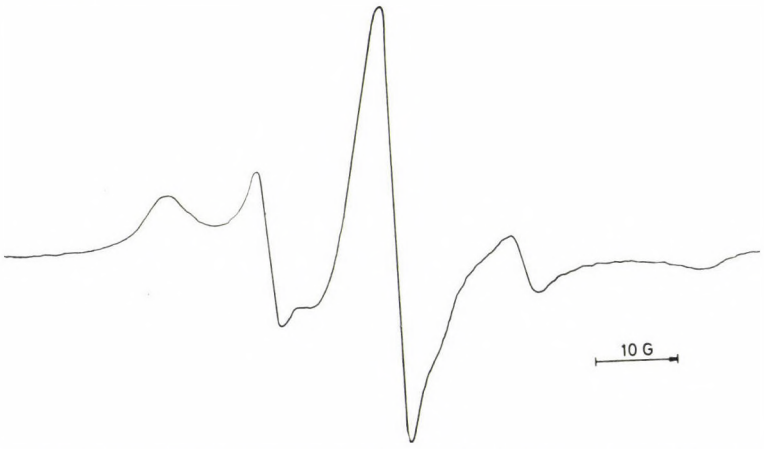

Fig. 4. Epr spectrum of glycerinated muscle fibre labelled with label I after heat denaturation. No effect of orientation was observed. 0.33 M label was added to 10^5 g of protein

Table 3

Effect of heat denaturation on epr spectra of oriented muscle fibres labelled with label I

Orientation	$I_{+1}(A)/I_{+1}(B)$	τ_c (nsec)
$a \perp H_0$	0.71	1.5
$a \parallel H_0$	0.73	1.5

The molar amount of label I added to 10^5 g of protein was 0.33. The values are the means of four determinations.

When the spin-labelled (label I) glycerinated muscle fibres were reacted with Mg-ATP and allowed to shorten, significant changes were observed in the epr spectra (Fig. 5). After addition of Mg-ATP both the ratio of $I_{+1}(A)/I_{+1}(B)$ and the parameter $2A_{zz}$ markedly increased. This increase may reflect a further immobilization of spin labels bound to protein, furthermore, a conversion of a small fraction of labels from weakly immobilized to highly constrained state or a change in the degree of orientation of spin labels. The former statement is in agreement with the experimental results of Cooke and Morales (1969) using six-membered maleimide label. The difference in the epr spectra with respect to the two orienta-

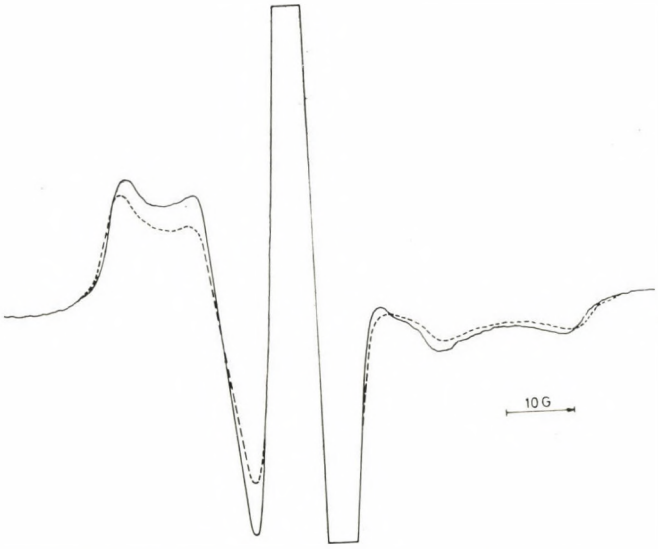

Fig. 5. Epr spectra of glycerinated muscle fibre labelled with label I before and after Mg-ATP induced shortening. Spectra were taken in orientation parallel to the fibres. Solid line: spectrum before shortening; dotted line: after shortening. 1.5 M label I reacted with 10^5 g of protein

tions remained small but significant after shortening; this is demonstrated in Fig. 6. The results of calculations for the effect evoked by Mg-ATP shortening are given in Table 4.

Table 4

Effect of ATP on epr spectra of oriented muscle fibres

Orientation	$I_{+1}(A)/I_{+1}(B)$		$2A_{ZZ}(G)$	
	addition		addition	
	none	ATP	none	ATP
$a \perp H_0$	1.60	1.63	61.6	62.8
$a \parallel H_0$	1.14	1.45	61.4	62.8
minced	1.40	1.48	61.4	62.3

The amount of spin label (label I) added to 10^5 g of protein was 1.5 mol.

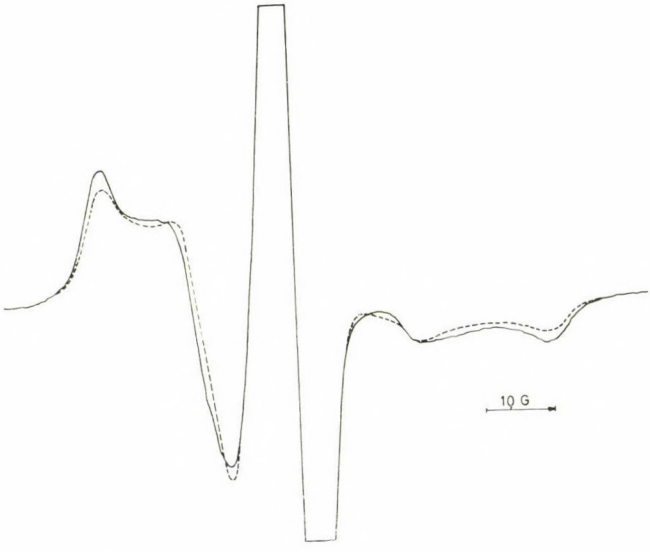

Fig. 6. Orientation dependence of epr spectra after shortening. Solid line: long axis of fibres perpendicular to the magnetic field; dotted line: long axis of the fibres parallel to the magnetic field

Discussion

Labelling the glycerinated muscle fibre bundle prepared from psoas muscle of the rabbit with five-membered maleimide spin label resulted in a complex epr spectrum. The maleimide label preferentially reacts with −SH groups (Hamilton, McConnell, 1968); therefore, the strongly immobilized label can be assumed to

arise from labels attached to the so-called fast reacting groups (S_1 thiol groups) on myosin (Kielley, Bradley, 1956) and the sulfhydryl groups on actin (Stone et al., 1970; Tonomura et al., 1969). The conclusions are limited by the fact that one part of the spin labels is located on the thick filaments and the other part of them reacts with sites on the thin filaments. We must assume some contribution in the epr spectra due to spin labels attached to the slowly reacting groups on myosin (S_2 thiol groups) and/or to other groups, especially at increasing ratio of spin label added to 10^5 g of protein.

It is immediately apparent from Fig. 1 that the feature of the epr spectra varies when the samples have different orientation to the magnetic field applied. This is doubtless a direct evidence for the anisotropy; the labels covalently attached to the contractile proteins are not fully randomly oriented. Epr spectra of oriented lipid films (Libertini et al., 1969; Jost et al., 1971; Israelachvili et al., 1974) and nerve fibres (Hubbell, McConnell, 1969) or single crystals (Griffith et al., 1965; Snipes et al., 1974) reveal a strong dependence on the orientation of label with respect to the direction of the laboratory field. The change in orientation effects the ratio of the two down-field peaks and $I_{+1}(A)/I_{+1}(B)$ decreases when the position of fibres is changed from perpendicular into parallel state. This fact leads to the conclusion that the $2p\pi$ orbital of spin labels possesses an orientation rather perpendicular than parallel to the long axis of the muscle fibres. The spectrum of glycerinated muscle fibres labelled with six-membered maleimide or iodoacetamide spin labels showed also other characteristics which can be explained by the different orientation of the piperidine and pyrrolidine nitroxide ring with respect to the fibre axis. Nevertheless, it can also be assumed that iodoacetamide spin label can be bound to other groups than can maleimide spin labels.

Labelling the glycerinated muscle fibres with five-membered maleimide label having increasing chain length between the pyrrolidine nitroxide ring and maleimide ring results in progressive decrease of the ratio of $I_{+1}(A)/I_{+1}(B)$ with increasing chain length, as seen from Figs 2 and 3. The maleimide labels can be assumed to be bound to the same sites independent of the chain length. When the chain length exceeds the effective depth of the combining site, the nitroxide ring will partially be free for rotation; thereby the ratio of $I_{+1}(A)/I_{+1}(B)$ decreases and the anisotropic motion of the label will be markedly reduced.

Thermal denaturation destroys the orientation dependence of epr spectra (see Table 3). This can be ascribed to the greater sensitivity of the environment of the spin-labelled sites to thermal treatment and, therefore, the preferred orientation of $2p\pi$ orbitals will cease to exist.

When the fibres were shortened the epr spectra revealed changes both in the ratio of $I_{+1}(A)/I_{+1}(B)$ and $2A_{zz}$ parameter. After shortening the orientation dependence of epr spectra persisted, but had a modified feature as it can be seen in Table 4. The ratio of $I_{+1}(A)/I_{+1}(B)$ indicates only a small increase when the long axis of the fibre bundles was oriented perpendicular to the magnetic field, but its change was more pronounced when the long axis of the fibres coincided with the field direction. The difference controlled by t-test is significant at $p = 0.01$

level. The increase of $2A_{zz}$ parameter shows a further immobilization of a small fraction of spin labels evoked by shortening of the fibre bundle. However, the comparison of the post-shortening changes in the ratio of $I_{+1}(A)/I_{+1}(B)$ in both orientations to the laboratory magnetic field reveals that any remarkable increase only appears in parallel orientation; therefore, one can conclude that a small change can exist in the degree of orientation of spin labels.

As to the physiological importance of the changes obtained in the experiments we have not yet any reasonable hypothesis to interpret these phenomena; therefore, further experiments are needed to explore the relation between muscle structure and spin label epr spectra.

The author wishes to thank Mrs. J. Brucker for her technical assistance.

References

Belágyi, J., Damerau, W. (1974) Acta Biochim. Biophys. Acad. Sci. Hung. *9* 367
Burley, R. W., Seidel, J. C., Gergely, J. (1971) Arch. Biochem. Biophys. *146* 597
Cooke, R., Morales, M. F. (1969) Biochemistry *8* 3188
Ernst, E. (1963) Biophysics of the Striated Muscle. Akadémiai Kiadó, Budapest
Griffith, O. H., Cornell, D. W., McConnel, H. M. (1965) J. Chem. Phys. *43* 2909
Griffith, O. H., Waggoner, A. S. (1969) Act. Chem. Res. *2* 17
Hamilton, C. L., McConnell, H. M. (1968) Spin labels. In Structural Chemistry and Molecular Biology. (Eds. Rich, A. and Davidson, N.), p. 115, Freeman, W. H. and Co., San Francisco
Huxley, H. E. (1963) J. Mol. Biol. *7* 281
Israelachvili, J., Sjösten, J., Eriksson, L. E. G., Ehrström, M., Gräslund, A., Ehrenberg, A. (1974) Biochim. Biophys. Acta *339* 164
Jost, P., Libertini, L. J., Hebert, V. C. (1971) J. Mol. Biol. *59* 77
Kielley, W. W., Bradley, L. B. (1956) J. Biol. Chem. *218* 653
Kusnetsov, A. N., Wassermann, A. M., Volkov, A.U., Korst, N. N. (1971) Chem. Phys. Letters *12* 103
Libertini, L. J., Waggoner, A. S., Jost, P. C., Griffith, O. H. (1969) Proc. Nat. Acad. Sci. (USA) *64* 13
McConnell, H. M., McFarland, B. G. (1970) Quart. Rev. Biophys. *3* 91
Ogawa, S., McConnell, H. M., Horwith, A. (1968) Proc. Nat. Acad. Sci. (USA) *61* 401
Seidel, J. C., Chopek, M., Gergely, J. (1970) Biochemistry *9* 3265
Seidel, J. C., Gergely, J. (1971) Biochem. Biophys. Res. Comm. *44* 826
Seidel, J. C., Gergely, J. (1973) Arch. Biochem. Biophys. *158* 853
Snipes, W., Cupp, J., Cohn, G., Keith, A. (1974) Biophys. J. *14* 20
Stone, D. B., Prevost, S. C., Botts, J. (1970) Biochemistry *9* 3937
Taylor, J. S., Leigh, J. S., Cohn, M. (1968) Proc. Nat. Acad. Sci. (USA) *64* 219
Tokiwa, T. (1971) Biochem. Biophys. Res. Comm. *44* 471
Tonomura, Y., Watanabe, S., Morales, M. F. (1969) Biochemistry *8* 2171

Acta Biochim. et Biophys. Acad. Sci. Hung. Vol. 10 (3), pp. 243–249 (1975)

Osmosis without Solute

E. ERNST

Biophysical Institute, Medical University, Pécs, Hungary

(Received January 28, 1975)

Van't Hoff's misconception of the kinetics of solutes in a solution was long ago displaced by the thesis about osmotic water migration caused by the difference in chemical potential on the two sides of the semipermeable membrane. Consequently the osmotic process was now investigated when *normal* water and *heavy* water were separated by the "semipermeable" membrane. Due to the difference between the chemical potentials a substantial osmotic pressure was measured on the side of the heavy water simultaneously with a significant migration of water on both sides.

Introduction

Preparing my lecture on osmosis in 1933, I was not able to accept Eucken's (1926) thesis: "In principle, osmotic pressure would be measurable simply manometrically in a completely closed space." This was an excessive formulation of van't Hoff's conception considering the gas-like behaviour of the solute as the driving force in the osmotic migration of the solvent. Against this – according to Helmholtz – not understandable "gas-theory" of osmosis, there appeared, nearly simultaneously, the conception describing the difference in vapour pressure of the solvent on the two sides of the semipermeable membrane as the driving force. As an experimental demonstration of this thesis some papers could be considered (Lipmann, 1907; Aubert, 1912; see also Kohnstamm, 1911) emphasizing the possibility that osmotic water migration could be brought about by a temperature difference causing a difference in vapour pressure on the two sides of the membrane. The phenomenon was named *thermoosmosis* (cf. Freundlich, 1922; Eastman, 1926).

The papers quoted above contained ambiguous descriptions often mixing up thermoosmosis and thermodiffusion, therefore my co-workers and I, beginning in 1933, tried to prepare an apparatus demonstrating thermal osmosis unambiguously (e.g. Ernst, Homola, 1952*; Vető, 1967). We succeeded in demonstrating

* This paper describing (pp. 492–93): "the increase in the fluid mobilization due to that of temperature difference can pass for a fundamental phenomenon of thermoosmosis" remained, unfortunately, unknown for Sollner (Carr, Sollner, 1962; Sollner, 1969). Notwithstanding, his statement (pp. 616, 75): "the rate of thermoosmosis is proportional to the temperature difference across the membrane" is in full agreement with our experimental results.

e.g. that blood serum heated on the one side of a membrane and cooled on the other became concentrated and diluted, respectively, which process could be considered as a model of the production of saliva.

The question of thermoosmosis is dealt with in Katchalsky and Curran's excellent work (1965) treating the thermodynamics of irreversible processes in general and especially emphasizing the thesis (pp. 41, 48, 49) that "a difference in *chemical potential* provides the driving force for the flow of matter (water)". On the other hand, another book on thermodynamics (Pitzer, Brewer, 1961) directly interlinks the chemical potential and espacing tendency, fugacity, vapour pressure of water, all of which increase with increasing temperature. Thus thermoosmosis can be considered as a scientifically evidenced phenomenon.

Consequently, the question arises why thermoosmosis plays so little a role in the international biological literature in contrast to osmosis, the importance of which is perhaps even overestimated in some fields. One of the most probable explanations is that the original wrong conception of osmotic pressure, as ascribed to a gas-like behaviour of the solutes, still survives. That is clearly shown by an otherwise good book (Hillel, 1971), which described the role of the chemical potential of water in osmotic pressure exactly and, notwithstanding, uses the phrase: "the osmotic pressure of a *nonvolatile solute*".* In reality the osmotic pressure of a watery solution is caused – as known – by the migration of water from the side of higher chemical potential of the solvent to the lower as shown by the formula

$$\pi = \frac{1}{v}(\mu_0 - \mu_1) = \frac{1}{v} RT \ln \frac{p_0}{p_1},$$

where π = osmotic pressure, v = partial mole volume of water, μ_0 and μ_1, further p_0 and p_1 are the chemical potentials and the vapour pressures of water in standard state and in the solution, respectively.

To liberate ourselves from the misconception of ascribing osmotic pressure to a gas-like behaviour of the solute, experiments were performed in which *normal and heavy water* were on the two sides of a $Cu_2Fe(CN)_6$-membrane. Namely, in this case when there is not any solute present and the volume and shape of both molecules are equal, but their self-diffusion coefficients and their vapour pressures are different at the same temperature, a significant osmotic pressure could be expected on the side of heavy water.

Method

Heavy water (obtained from the Soviet Union and West Germany) and twice distilled water were used in these experiments.

The osmometer is in principle similar to that described earlier (Ernst, Homola, 1952): the "semipermeable" membrane of $Cu_2Fe(CN)_6$ was prepared in

* My italics.

the wall of a clay cylinder (Fig. 1, C). This cylinder was closed during the experiment by a rubber plug (P_1)* with two borings containing two glass tubes (1 and 2) for filling the cylinder and measuring the increase in pressure or volume. This cylinder was put into a glass vessel (G) with a larger rubber plug (P_2) with two borings also containing two glass tubes (3 and 4).

The clay cylinder was filled with heavy water, the glass cylinder with bidistilled water. The taps of glass tubes 1 and 3 were closed, the menisci of the fluids

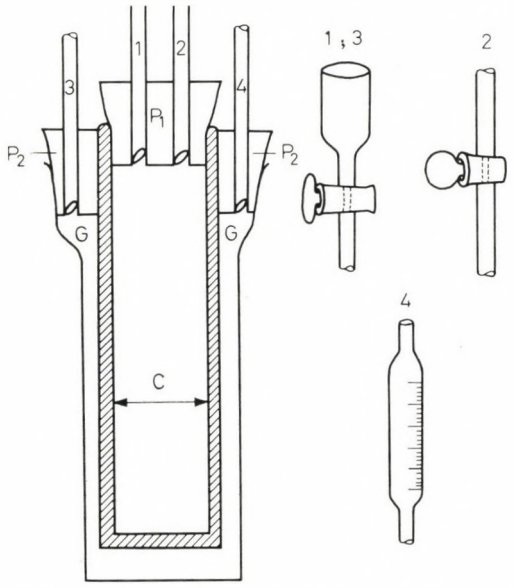

Fig. 1. Osmometer, C = clay cylinder; G = glass vessel; P_1, P_2 = rubber plugs in C and G, respectively; 1, 2, 3, 4 = glass tubes for filling C and G, and measuring the changes of pressure or volume

in tubes 2 and 4 observed in order to determine the increase and decrease in the volumes inside and outside.

The pressure inside (tube 2) was measured by two methods: (a) tube 2 was filled with water and linked together with a manometer (diameter of the lumen ~1 mm) filled with mercury. In this case the transfer of normal water into the heavy water, even in a very low volume of say 0.1 ml, caused a pressure increase of about 200 mm Hg. (b) In tube 2 the meniscus of the heavy water stood e.g. 20 mm below the tap, which was afterwards closed; in this case the pressure against which normal water migrated into heavy water could be computed from the decrease of the space over the meniscus. If the volume of this closed space decreased

* The stands of the plugs are fixed for the term of an experiment.

from 20 to 10 units, i.e. $\frac{v_2}{v_1} = \frac{1}{2}$, the pressure increased from the original 1 atm to $\frac{p_2}{p_1} = 2$ atm, hence $\Delta\pi = 1$ atm.

To control this value of osmotic pressure tube 2 was, in a separate experiment, linked together with an aneroid manometer connected to a syringe of e.g. 50 ml. At the stage of the experiment, when e.g. $\Delta\pi = 0.5$ atm, a pressure of 0.5 atm can be brought about by the syringe; then the tap of tube 2 is opened, and the meniscus can rise further during continuation of the experiment.

Results

Over 20 experiments have been carried out on 13 osmotic apparatuses as described above. According to the aim of the present paper only two examples will be described below.

1. Osmotic pressure. Depending on the specific qualities of the single osmotic devices, osmotic pressures of different magnitudes were measured always on the side of the heavy water. The measured pressure ranged from a few cm of water to 1.5 atm. Table 1 contains some data of an experiment (clay cylinder No. 3, apparatus 7).

Table 1

V_0 = volume decrease in tube 4; V_i = position of the meniscus in tube 2; Δs = relative volume changes of the space over the meniscus in tube; P = total pressure in this closed space; P_m = pressure shown by the aneroid manometer (atm)

Time	°C	V_o, cm³ −	V_i, cm +	Δs	P, atm
9h 40′	19.0	0.0	0.0	—	—
10h 15′	19.5	0.1	0.2	20/18	1.1
11h 15′	19.7	0.2	0.6	20/14	1.4
12h 15′	20.2	0.3	1.0	20/10	2.0
14h 40′	20.0	0.3	1.1	20/9	2.2
1.12 atm of artificial pressure, tap 2 is opened					
					P_m
18h 15′	20.0	0.9	3.0		1.08
21h	19.0	1.2	3.7		1.07

It is evident from Table 1 that the *transfer of normal water to heavy water occurred continuously even against a pressure of e.g. 1 atm*, and the transfer went on for many days.

2. The volume of transfer. Column V_0 shows that the volume of the outside compartment decreased by 1.2 ml (and V_i increased). The real transfer was neces-

sarily much greater, because the heavy water concentration inside had decreased from the original value of 99.8% to 45%, as shown by the determination of the refraction of the fluid of 85 + 3.5 ml inside. The real total transfer can be computed by the formulae

$$v_{i0} = v_{0i} - 3.5$$

and

$$\frac{v_{0i}}{V_i - v_{0i}} = \frac{55}{45},$$

where v_{0i} and v_{i0} are the volumes of fluids transferred from outside to inside and from inside to outside, respectively. Thus

$$\frac{v_{0i}}{V_i - v_{0i} + 3.5} = \frac{55}{45},$$

therefore $v_{0i} \sim 48.5$ ml and $v_{i0} \sim 45$ ml; accordingly, 45 ml of the 85 ml of heavy water had migrated from inside to outside, hence 48.5 ml of normal water had imigrated to inside.* In contrast to this simplified computation, the transfer consists, in reality, of a complex process during which a migration of fluids connuously goes on in both directions while the heavy water becomes continuously diluted inside, and the heavy water concentration of the fluid outside continuously increases.

Discussion

1. The fundamental biological importance of water makes it desirable to consider the question of water transport more closely. First of all a few data of H_2O and D_2O should follow. The diameters of both molecules are equally 2.7 Å, and also the electric charges are equal. In the diffusion coefficient

$$D = \frac{kT}{6\pi\eta r}$$

the viscosity (g cm^{-1} $s^{-1} \times 10^{-2}$, at 20°C) is

$$\eta_{H_2O} = 1.002 \text{ and } \eta_{D_2O} = 1.243,$$

therefore

$$D_{H_2O} > D_{D_2O}.$$

* Control: $\frac{100}{45} = \frac{88.5}{40}$ is approximately right ($\Delta \sim 0.5\%$).

Further, the vapour pressure (torr, at 20°C) is

$$p_{H_2O} = 17.53 \text{ mm Hg and } p_{D_2O} = 14.93 \text{ mm Hg}$$

accordingly, the difference between their chemical potentials is

$$-(\eta_{D_2O} - \eta_{H_2O}) = RT \ln \frac{p_{H_2O}}{p_{D_2O}}.$$

2. It is common knowledge that a significant part of the evaporation heat of water is used for disrupting from each other the molecules bound by their dipoles and much more by H-bonds. Now, heavy water is more bound than normal water, which is indicated, among others, by the fact that the evaporation heats (cal mol^{-1}, 100°C) are

$$Q_{H_2O} \sim 9\,700 \text{ and } Q_{D_2O} \sim 11\,000.$$

A certain degree of binding of water can be established doubtless already in pure water, but *bound water* is encountered in every case when water gets in any connection with other substances forming water-containing multicomponent systems. Only as a single example a watery solution can be considered in which the fact that water is bound to a certain degree is indicated by lowering of the vapour pressure of the water in the solution, in consequence of which the osmotic pressure caused by migration of the water of greater vapour pressure is:

$$\pi = \frac{1}{v} RT \ln \frac{p_1}{p_2}.$$

Quite the same formula is valid for the *swelling pressure* (Katz, 1918), which is brought about by the water migrating from outside into the structure of the swelling system.

Bound water can be established also in connection with porosity and capillarity and therefore it gains special importance for biological systems containing similar structures. Generally, in every case when there are cell compartments containing differently bound water there are also adequate devices for transfer of water.

References

Aubert, M. (1912) Ann. Chim. Physic. Sér. 8. *26* 145
Carr, C. W., Sollner, K. (1962) J. Electrochem. Soc. *109* 616–622
Eastman, E. D. (1926) J. Amer. Chem. Soc. *48* 1482
Ernst, E. (1970) Acta Biochim. Biophys. Acad. Sci. Hung. *5* 57
Ernst, E., Homola, L. (1952) Acta Physiol. Acad. Sci. Hung. *3* 487
Eucken, A. (1926) In Müller–Pouillet's Lehrbuch der Physik III. 1. Friedrich Vieweg, Braunschweig, p. 626
Freundlich, H. (1922) Kapillarchemie. Akad. Verlagsges. mbH, Leipzig, pp. 371, 378

Hillel, D. (1971) Soil and Water. Academic Press, New York, pp. 35, 45, 54
Katchalsky, A., Curran, P. F. (1965) Nonequilibrium Thermodynamics in Biophysics. Harvard University Press, Cambridge, Mass.
Katz, J. R. (1918) Kolloidchem. Beihefte *9* 1
Kohnstamm, Ph. (1911) Proc. Acad. Wetensch. Amsterdam *19* 658
Lipmann, G. M. (1907) C. R. Acad. Sci. Paris *145* 104
Pitzer, R. S., Brewer, L. (1961) Thermodynamics, II. ed. McGraw-Hill Book Company, New York
Sollner, K. (1969) J. Macromol. Sci.Chem. Part *A3* (1) pp. 1—86
Vető, F. (1967) Acta Biochim. Biophys. Acad. Sci. Hung. *2* 441

Acta Biochim. et Biophys. Acad. Sci. Hung. Vol. 10 (3), pp. 251--257 (1975)

Dielectric Dispersion Measurements of Dimeric and Monomeric Forms of Phosphorylase *b*

J. FITORI, J. NAGY

Biophysical Institute, Medical University, Debrecen, Hungary

(Received April 2, 1974)

Rabbit skeletal muscle phosphorylase *b* was investigated by the dielectric dispersion method in different media. Comparison of calculated and measured relaxation times revealed the effective molecular diameters to be higher than published earlier. Using an estimated value of 4 Å for the thickness of the hydration layer of the protein, a good agreement was obtained between the calculated and measured relaxation times. On the basis of these calculations and measurements the molecular dimensions of hydrated phosphorylase *b* were taken for $118 \times 74 \times 63$ Å. Dispersion measurements suggested that the volume of a subunit was smaller than the half volume of the dimeric form.

Introduction

Rabbit skeletal muscle phosphorylase is generally active in a dimeric form having a molecular weight of 185,000 (DeVincenzi, Hedrick, 1970, Seery et al., 1967). The dimeric phosphorylase *b* consists of two nearly identical subunits (Chignell et al., 1968; Valentine, Chignell, 1968). Molecular diameters of the dimeric form, $l \times w \times h = 110 \times 55 \times 65$ Å were determined by electron microscopy. The subunits of phosphorylase *b* can be approximated by a prolate ellipsoid of revolution. Low-angle X-ray scattering data confirmed these values (Puchwein et al., 1970). DeVincenzi and Hedrick obtained average Stokes' radii of 49.3 Å for the dimeric and 36 Å for the monomeric forms (DeVincenzi, Hedrick, 1967, 1970).

In our earlier work the dielectric dispersion behaviour of phosphorylase *b* was investigated in various media. We found that application of the Stokes–Perrin equation, using molecular diameters obtained by Valentine and Chignell, led to a disagreement between the calculated and measured relaxation times (Fitori, 1971a, b).

Theoretical considerations

The relaxation time (τ) of hydrated protein molecules can be calculated from the Debye–Perrin equation if we take these molecules for ellipsoids with half axes a, b, c and

$$\tau = \frac{4 \pi a b c}{kT} \eta f_i \qquad (1)$$

where k, T, η denote Boltzmann constant, temperature and solvent viscosity, respectively, and f_i is the Perrin factor depending on the molecular shape (Perrin, 1934).

Higasi observed the relaxation time to depend on solvent viscosity in an exponential way:

$$\tau = A\eta^x \tag{2}$$

where A and x are constants (Higasi, 1961).

The Cole–Cole equation gives the general description of the dielectric relaxation properties of proteins:

$$\varepsilon^* = \varepsilon_\infty + \frac{\varepsilon_0 - \varepsilon_\infty}{1 + (i\omega\tau)^{1-\alpha}} \tag{3}$$

where ε^* is the complex dielectric constant, which has a real (ε') and an imaginary ($i\varepsilon''$) part, ε_0 and ε_∞ are the low and high frequency limits of the dielectric constant, ω means the angular frequency, and α is the Cole–Cole parameter depending on the distribution of relaxation time around τ (Cole, Cole, 1941).

Materials and methods

Crystalline rabbit skeletal muscle phosphorylase *b* was prepared according to Fischer and Krebs and the enzyme was recrystallized three times (Fischer, Krebs, 1958). Further purification has been described earlier (Fitori, 1971a, b).

Homogeneity of phosphorylase *b* was investigated by SDS (sodium dodecylsulphate) polyacrylamide gel electrophoresis, sedimentation velocity and enzyme activity measurements.

SDS gel electrophoresis was carried out in 5% acrylamide gel using 0.1 M disodium hydrogen phosphate, 0.1% SDS (pH 7.2) electrode buffer solution at room temperature. The gels were stained with 0.2% Coomassie Brilliant Blue R 250 solution.

Sedimentation velocity measurements were performed with a MOM G 120 type ultracentrifuge in double sector cells at 46,000 rpm at 25.0 ± 0.1 °C.

Activity measurements were carried out in 0.05 M Tris-HCl (pH 6.8) buffer solution at 30°C using 16 mM glucose-1-phosphate and 10^{-7} M phosphorylase concentration and determining the amount of inorganic P liberated.

Ion exchange resins (Amberlite IR 120 and IRA 410) were purchased from Serva Co., glycerol was obtained from Merck GmbH and *p*-chloromercuribenzoic acid (PCMB) was obtained from L. Light & Co.

The dielectric measurements were performed between 20 kHz and 1 MHz in the experimental apparatus used earlier (Fitori, 1971a).

The viscosity of the solvents was determined in an Ubbelohde viscometer at 25°C.

Results and discussion

Sedimentation velocity measurements showed that phosphorylase *b* existed in dimeric form both at low ionic strength ($\mu < 10^{-4}$) and under medium conditions ($\mu = 0.05$). This was confirmed by the sedimentation coefficient, resulting

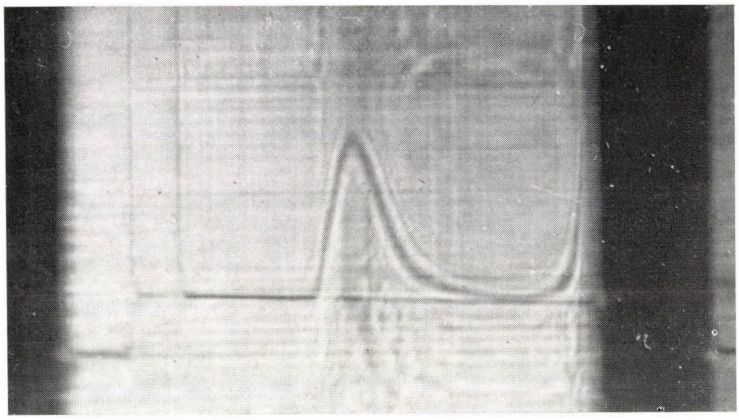

Fig. 1. Sedimentation of phosphorylase *b* at 46 000 rpm after treatment with mixed bed ion exchange resin. Temperature was 25°C, protein concentration 8 mg/ml (4.3×10^{-5} M). $s_{20,w} = 8.52 \pm 0.12$ S. Philphot angle was 30°

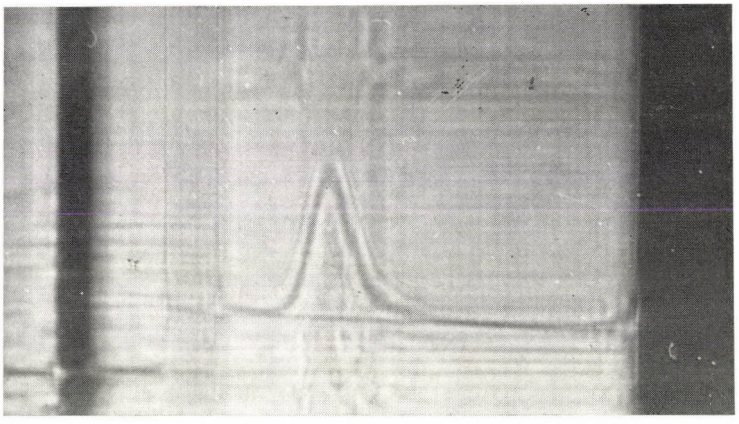

Fig. 2. Sedimentation of deionized phosphorylase *b* after reconstitution of ionic strength by 0.05 M maleate buffer solution. Experimental conditions as in Fig. 1

in a value of $s_{20,w} = 8.52 \pm 0.12$ S after extrapolation to zero concentration (Figs 1, 2).

Investigations with SDS gel electrophoresis revealed contamination under 1%; activity measurements led to the same result.

The effect of electrode polarization, which will be increased below 200 kHz, was corrected by the comparison of the apparent dielectric increment of protein solution to that of dilute (5×10^{-5} M) KCl solution having nearly equal conductivity. Plotting the difference of $\Delta\varepsilon_p - \Delta\varepsilon_{KCl}$ against frequency$^{-3/2}$ (Fig. 3) shows the correction of a typical polarization effect.

Here, $\Delta\varepsilon_p$ and $\Delta\varepsilon_{KCl}$ are the dielectric increments of protein and potassium chloride solutions at the same frequency (Ferry, Oncley, 1941).

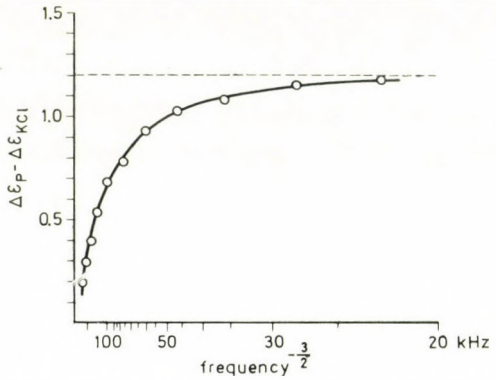

Fig. 3. Correction of electrode polarization effect by comparison of apparent dielectric increments of protein and potassium chloride solutions having nearly equal conductivity ($\kappa = 8 \times 10^{-6}$ mho/cm)

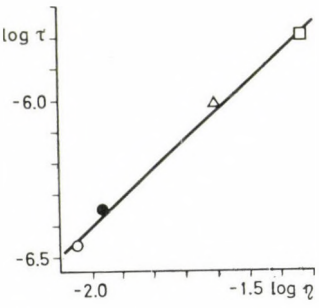

Fig. 4. Log relaxation time—log viscosity diagram of phosphorylase *b* in several solvents at 25°C; ○, water; ●, 99.8% heavy water; △, 33% (v/v) glycerol; □, 50% (v/v) glycerol

Dispersion measurements show that the dimeric form of phosphorylase *b* follows the Higasi equation when the logarithm of relaxation time is plotted against the logarithm of solvent viscosity (Fig. 4). The value of exponent of the Higasi formula is 0.92. Water, 99.8% heavy water, 33% (v/v) and 50% (v/v) glycerol were used as solvents. All measurements were carried out at 25°C. The pH values were 6.8 – 7.0 or pD = 7.2, and protein concentration was 7.8 – 8 mg/ml (4.32×10^{-5} M).

Using the data of solvent viscosity for calculating the relaxation time of the dimeric molecule, we obtained lower values than the measured ones. These values are shown in Table 1.

Table 1

Measured and calculated relaxation times of phosphorylase b in different solvents, using molecular dimensions of 110 × 55 × 65 Å for calculation

Solvent	Solvent viscocity (cP)	$\tau \times 10^7$ (sec) measured	$\tau \times 10^7$ (sec) calculated
water	0.895	3.43 ± 0.14	1.97
heavy water	1.08	4.43 ± 0.14	2.41
33% glycerol	2.47 ± 0.01	9.41 ± 0.13	5.44
50% glycerol	4.68 ± 0.01	15.92 ± 0.32	8.85

$t = 25°C$, pH = 6.8, pD = 7.2

Calculated relaxation times were obtained from Eq. (1) on the basis of the molecular dimensions of phosphorylase *b* determined by Valentine and Chignell (1968), using $\frac{b}{a} = 0.543$ value of axial ratio for calculation of the Perrin-factor. The result of the latter was 1.47.

These results suggest that the molecular dimensions of dimeric phosphorylase *b* molecule are higher than the above mentioned ones, since the average Stokes' radius of this molecule, as calculated from the measured relaxation time, is in a good agreement with the results determined by DeVincenzi and Hedrick and also appears to be 49 ± 1 Å (DeVincenzi, Hedrick, 1967).

Microwave dispersion measurements show that, in aqueous media, protein molecules do not generally have more structural water than do bimolecular layers (Harvey, Hoekstra, 1972).

This observation gives us the possibility for estimating the thickness of the hydration layer of a protein molecule, assuming uniform coverage. We assumed, that the thickness of the bimolecular layers was 4 Å. So we estimated the effective molecular dimensions of phosphorylase *b* as being $l \times w \times h = 118 \times 63 \times 73$ Å. Fig. 5 shows the molecular model for dimeric phosphorylase *b* according to Valentine and Chignell, after modification by covering the molecule with a bimolecular hydration envelope.

It is assumed that the "intermediate" volume between the subunits during rotational diffusion can behave as an organic part of the molecule. This volume augments the effective molecular volume by about 17% without increasing the size of the molecule. The total volume of hydrated molecule with "intermediate" volume is 350 400 Å^3. Table 2 shows the measured and the recalculated values of the relaxation times. The Perrin factor changed from 1.47 to 1.33.

Table 2

Measured and recalculated relaxation times of phosphorylates b at 25°C, assuming a 4 Å thick hydration layer for calculations. Experimental conditions as Table 1

Solvent	$\tau_{measd} \times 10^7$ (sec)	$\tau_{calcd} \times 10^7$ (sec)
Water	3.43±0.14	3.04
Heavy water	4.43±0.14	3.67
33% glycerol	9.41±0.13	8.38
50% glycerol	15.92±0.32	15.89

The comparison of the values of measured and calculated relaxation times shows a good agreement which supports our assumption.

The monomer molecule can be approximated by a prolate ellipsoid of revolution and, assuming a 4 Å thick hydrate coat, its half axes are $a = 36.5$ Å,

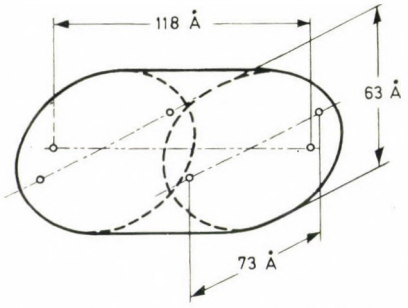

Fig. 5. Molecular dimensions of dimeric phosphorylase *b* after Valentine and Chignell, modified by the addition of a hydration layer 4 Å in thickness

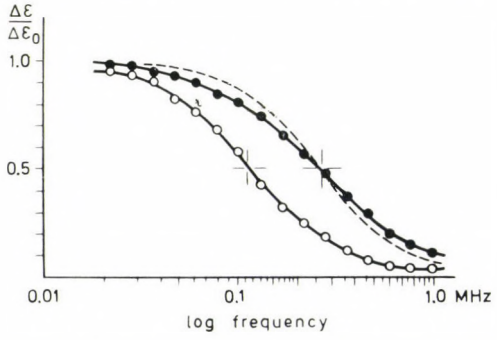

Fig. 6. Dispersion curves of phosphorylase *b* in 50% (v/v) glycerol at 25°C (pH 7.2). ○—○ dimer (treated only with mixed bed resin), ●—● monomer in the presence of PCMB (the dotted line is the calculated dispersion curve of the monomer assuming a single relaxation process). Protein concentrations were 8 mg/ml (4.3×10^{-5} M)

$b = 31.5$ Å. The value of molecular volume calculated for hydrated molecule is 151,700 Å^3.

As it is well known the phosphorylase *b* dissociates into subunits in the presence of SH reagents, such as PCMB (Madsen, Cori, 1955, 1956). We investigated the dielectric dispersion of phosphorylase *b* in the presence of PCMB, using 50% (v/v) glycerol as solvent.

The concentration of PCMB was slightly under 11 mg/ml (0.03 M). The sedimentation pattern showed that, in the presence of PCMB, only one fraction could be observed ($s_{20,w} = 5.3$ S). Dispersion curves of dimeric and of monomeric form are shown in Fig. 6.

The measured relaxation time of the monomer was 5.68×10^{-7} sec and the calculated time was 5.40×10^{-7} sec (the calculated Perrin factor was 1.04). This confirms our earlier suggestion since the relaxation time of the monomer is smaller than that of the half of the dimer. The latter proved to be 15.92×10^{-7} sec. Using a calculation for average Stokes' radius of the monomer, a good agreement can be seen between the 36.5 Å obtained by us and the 36 Å obtained for apophosphorylase *b* by DeVincenzi and Hedrick (1970).

Since the object of our investigations is an allosteric enzyme, which shows quaternary structure, the fact that an "intermediate" volume can exist seems to be of special interest during allosteric transitions. Further investigations may give more information on this question.

The authors are greatly indebted to Dr. P. Závodszky and to Mr. I. Francia for the sedimentation investigations.

References

Appleman, M. M., Yunis, A. A., Krebs, E. G., Fischer, E. H. (1963) J. Biol. Chem. *238* 1358
Chignell, D. A., Gratzer, W. B., Valentine, R. C. (1968) Biochemistry *4* 1082
Cole, K. S., Cole, R. H. (1941) J. Chem. Phys. *9* 341
DeVincenzi, D. L., Hedrick, J. L. (1967) Biochemistry *6* 3489
DeVincenzi, D. L., Hedrick, J. L. (1970) Biochemistry *9* 2048
Ferry, J. D., Oncley, J. L. (1941) J. Am. Chem. Soc. *63* 272
Fischer, E. H., Krebs, E. G. (1958) J. Biol. Chem. *231* 65
Fitori, J. (1971a) Acta Biochim. Biophys. Acad. Sci. Hung. *6* 427
Fitori, J. (1971b) Proc. 1st Eur. Biophys. Congress I. 177
Harvey, S. C., Hoekstra, P. (1972) J. Phys. Chem. *76* 2987
Higasi, K. (1961) Dielectric Relaxation and Molecular Structure (Research Institute of Applied Electricity, Hokkaido University, Sapporo, Japan)
Madsen, N. B., Cori, C. F. (1955) Biochim. Biophys. Acta *18* 156
Madsen, N. B., Cori, C. F. (1956) J. Biol. Chem. *223* 1055
Perrin, F. J. (1934) Phys. Radium Paris *5* 497
Puchwein, G., Krattky, O., Gölker, F., Helmreich, E. (1970) Biochemistry *9* 4691
Seery, V. L., Fischer, E. H., Teller, D. C. (1967) Biochemistry *6* 3315
Valentine, R. C., Chignell, D. A. (1968) Nature *218* 950

Book Reviews

M. Wollemann: *Biochemistry of Brain Tumours*. Akadémiai Kiadó, Budapest, 1972

Very often a book is regarded as highly valuable because it summarizes, systematizes and evaluates all that is known or believed to be known on a subject and attempts to determine what more should be done and investigated in order to further improve our knowledge.

If there exist complicated tasks in modern medical research, the question of the induction, development and therapy of tumours is surely one of the most difficult problems; and within this subject, the elucidation of the biochemical reactions taking place in tumours and during tumour transformation represents an even more special problem.

Ever since Warburg's time one of the main aims of biochemistry has been to characterize the biochemical reactions underlying the transformation of normal cells into neoblasts and to specify the difference between tumorous and normal tissues at the biochemical level.

Biochemical experimentation has been concentrated mainly on the latter subject and the same is discussed by Mária Wollemann, too. Her work is of a special significance because human brain tumours were chosen as an object, and it is this field of which our knowledge is the least deep and extensive.

The publication summarizes all that is presently known of the biochemistry of brain tumours, including the author's own experimental results which are by no means insignificant. The view predominating throughout the whole book is the one considered as most progressive in modern tumour research: for a full understanding of tumour processes a joint knowledge of biochemistry, pathomorphology and even several further interdisciplinary fields (genetics, embryology, evolution, etc.) is necessary.

The book consists of three chapters. In the introduction the histological classification of brain tumours is briefly discussed. Experimental brain tumours and possibilities of tissue culturing are also mentioned. This is followed by a general survey of the metabolism of the normal brain.

The second part of some 20 pages deals with the chemical alterations which have been hitherto observed in brain tumours or which seem to be more or less characteristic of the different brain tumours.

In the last and longest chapter (112 pages) enzymes and metabolism of tumours are discussed and a full account of the most important metabolic pathways under normal and pathological conditions is given. It must be added that this is the most interesting part of the book; it is perceptibly this field where the author is really at ease and the subject on which most of her own research work was done. The subject of various isozyme systems is treated fully, partly as markers of gene expression and partly with respect to differences between adult, embryonic and tumour tissues. It is shown that the isozyme pattern of certain enzyme systems found in tumours bears a close resemblance to that of embryonic tissues (lactate dehydrogenase, aldolase), while in other cases (e.g. creatine phosphotrans-

ferase, esterase) the changes in the isozyme pattern found in tumours have no equivalent in either adult or embryonic tissues. The author assumes — and there one can only agree with her — that a further detailed investigation of isozymes is going to be an even more significant field of tumour research than it is today.

When discussing metabolic pathways, the author does not concentrate on Weber's key-enzymes but describes these processes separately which is most useful from a didactic point of view. It is revealed by the numerous — though often contradictory — data presented that, on the whole, in brain tumours approximately the same tendencies are found as in other kinds of tumours as regards metabolic pathways, i.e. the most important biochemical changes are parallel to the growth rate of tumours in the first place. Naturally, an exception to this correlation is the neurotransmitter metabolism characteristic of the brain tissue which is either considerably impaired or absent.

In some cases it seems as if certain distinct biochemical differences could be demonstrated between tumours of different histological structure, e.g. the low glycogen level of oligodendroglyomata as compared to other brain tumours, or different enzyme activities; however, a summary of the relevant data from which the "biochemical map" of the different tumour species could be drawn is lacking.

Within the present state of knowledge, the diagnostic value of metabolic alterations in the differentiation of individual types, specially emphasized by the author in the summary of her book, is rather dubious; at present it still seems that light and electron microscopy will continue to play a leading role in tumour diagnostics.

The book as a whole is the kind of standard work that will prove to be extremely useful not only for those who experiment on brain tumours but also for those who work in other fields of tumour research. Owing to its excellent didactic structure, it will at the same time render service to anybody working in fields other than biochemistry.

The book was published in a well-designed get-up and neat typography by Akadémiai Kiadó Budapest.

L. HOLCZINGER

J. M. Romanovsky, N. V. Stepanova, D. S. Chernavsky: *Kinetische Modelle in der Biophysik*. VEB Gustav Fischer Verlag, Jena 1974

The book, consisting of 164 pages, 53 figures and 52 references is a translation of the Russian edition appeared in 1971 and entitled "What is mathematical biophysics? Kinetic models in biophysics."

A great deal of information has been added during the last years to our knowledge on the structure and function of living systems, and the interest in the investigation on regulation, and dynamics of these systems has become fairly considerable.

An increasingly closer contact has been established between biology and the so-called "exact sciences". This process has resulted in construction of interdisciplines such as biophysical chemistry, mathematical biophysics, etc. and in providing new possibilities for the investigation of biological substances. The application of mathematical methods will probably help to clarify the mechanism of processes in living organisms.

After a short introduction the first chapter gives a short review of chemical and enzyme-kinetics at an elementary level. In the second chapter this is followed by a treatment of the theoretical basis, necessary for analyzing dynamic systems. The reader is supposed to be acquainted with only the elements of mathematical analysis. However it is not an absolute requirement except for, understanding the paragraph about the method of slowly changing amplitudes.

The third chapter deals with the mathematical models useful for kinetic description of microorganisms' growth. The authors elaborate the concept of chemostasis, an appropriate model for its description and give a treatment of both the dynamic equilibrium in chemostasis and the non-stationary behaviour of chemostasis. These problems have been treated in detail perhaps because of their being involved in the practice of the nowadays fast developing microbiological industry.

It is highly probable, the authors say, that living organisms need something like a "biological clock" with the help of which the processes in them can be synchronized

and the organisms can prepare themselves to periodic alterations in environmental conditions. Such biological clocks could be realized by oscillating reactions.

The authors treat the most simple one of this type of reactions, proposed originally by Lotka, as well as a model for chemical autocatalytic reactions. The oscillating reactions analyzed next are the ones being stable or instable under disturbing influences. As examples they give a thorough analysis of the photosynthesis and the glycolysis. Finally they deal with the problem of triggering chemical oscillating reactions.

The book is very valuable for both students of biological sciences and specialists. Many parts of it are written in popular-scientific style but sometimes the problems are discussed in a manner also satisfying high requirements.

L. TRÓN

Dietmar Börnert: *Leitfaden der Biotelemetrie.* VEB Gustav Fischer Verlag, Jena 1974. 211 pages

Promoted by space travel biotelemetry has developed very rapidly during the last two decades and nowadays it represents a self-consistent, complete topic in science with several special branches and a wide range of applications. Because of the complexity of the subject it seems to be important to provide a systematic survey. This statement of the author in the preface of the book will be verified after reading the six chapters carefully built up to give a full picture of biotelemetry of our days. The aim of the book is a presentation of the principles, problems and procedures of biotelemetry to the interested readers, potential users such as physicians, veterinaries, ethologists, students and technicians. Accordingly, the way of presentation is chosen to meet the expectations of readers with different backgrounds. The technical details are omitted, technical problems are treated in general and examples of applications are discussed in abundance from different fields. The special interest is referred to the 283 citations from the literature with the title of the original papers.

The main chapters of the book are as follows. Indication — general principles of the selection of adequate methods (about 10 pages). Wireless and wirebound methods of telemetry (80 pages). Obtaining the resulting value of measurement (40 pages). Recording, storage and processing of information (20 pages). Complex systems for telemetric processing of biological primary data (10 pages).

The book is warmly recommended to those interested in biotelemetry.

L. SZALAY

Hoppe-Seyler's Zeitschrift für Physiologische Chemie

Editors in Chief

A. BUTENANDT · F. LYNEN · G. WEITZEL

Subscription Rate

For one volume (12 parts) DM 480,—

Vol. 355 No. 9 September 1974

CONTENTS

INDEXED IN CURRENT CONTENTS

AUTHOR INDEX

Walter de Gruyter · Berlin · New York

Hoppe-Seyler's Zeitschrift für Physiologische Chemie

Editors in Chief

A. Butenandt · F. Lynen · G. Weitzel

Subscription Rate

For one volume (12 parts) DM 480,—

Vol. 355 NO. 10 Oktober 1974

CONTENTS

AUTHOR INDEX

Walter de Gruyter · Berlin · New York

Hoppe-Seyler's Zeitschrift für Physiologische Chemie

Editors in Chief

A. BUTENANDT · F. LYNEN · G. WEITZEL

Subscription Rate

For one volume (12 parts) DM 480,—

Vol 355 No. 11 November 1974

CONTENTS

INDEXED IN CURRENT CONTENTS

W DE G

Walter de Gruyter · Berlin · New York

Hoppe-Seyler's Zeitschrift für Physiologische Chemie

Editors in Chief

A. BUTENANDT · F. LYNEN · G. WEITZEL

Subscription Rate

For one volume (12 pats) DM 480,–

Vol. 355 No. 12 Dezember 1974

CONTENTS

AUTHOR INDEX

W DE G

Walter de Gruyter · Berlin · New York

Hoppe-Seyler's Zeitschrift für Physiologische Chemie

Editors in Chief

A. BUTENANDT · F. LYNEN · G. WEITZEL

Snbscription Rate

For one volu .e (12 parts) DM 480,—

Vol. 356. No. 1 CONTENTS Januar 1975

AUTHOR INDEX

W DE G

Walter de Gruyter · Berlin · New York

Hoppe-Seyler's Zeitschrift für Physiologische Chemie

Editors in Chief

A. BUTENANDT · F. LYNEN · G. WEITZEL

Subscription Rate

For one volume (12 parts) DM 480,—

Vol. 356. Nr. 2 CONTENTS Februar 1975

AUTHOR INDEX

W DE G

Walter de Gruyter · Berlin · New York

Hoppe-Seyler's Zeitschrift für Physiologische Chemie

Editors in Chief

A. BUTENANDT · F. LYNEN · G. WEITZEL

Subscription Rate

For one volume (12 parts) DM 480,—

Vol. 356 No. 3 CONTENTS März 1975

INDEXED IN CURRENT CONTENTS

W DE G

Walter de Gruyter · Berlin · New York

Hoppe-Seyler's Zeitschrift für Physiologische Chemie

Editors in Chief

A. BUTENANDT · F. LYNEN · G. WEITZEL

Subscription Rate

For one volume (12 parts) DM 480,—

Vol. 356 No. 4 April 1975

CONTENTS

AUTHOR INDEX

Walter de Gruyter · Berlin · New York

Hoppe-Seyler's Zeitschrift für Physiologische Chemie

Editors in Chief
A. Butenandt · F. Lynen · G. Weitzel

Subscription Rate
For one volume (12 parts) DM 480,—

Vol. 356 No. 5 Mai 1975

CONTENTS

Indexed in Current Contents

AUTHOR INDEX

W DE G

Walter de Gruyter · Berlin · New York

Hoppe-Seyler's Zeitschrift für Physiologische Chemie

Editors in Chief

A. BUTENANDT · F. LYNEN · G. WEITZEL

Subscription Rate

For one volume (12 parts) DM 480,–

Vol. 356 No. 6 Juni 1975

CONTENTS

AUTHOR INDEX

Hoppe-Seyler's Zeitschrift für Physiologische Chemie

Editors in Chief

A. BUTENANDT · F. LYNEN · G. WEITZEL

Subscription Rate

For one volume (12 parts) DM 480,—

Vol. 356 No 7 CONTENTS Juli 1975

AUTHOR INDEX

W DE G

Walter de Gruyter · Berlin · New York

Hope-Seyler's Zeitschrift für Physiologische Chemie

Editors in Chief
A. BUTENANDT · F. LYNEN · G. WEITZEL

Subscription Rate
For one volume (12 parts) DM 480,–

Vol. 356 No. 8 August 1975

CONTENTS

Vol. 356 No. 8 CONTENTS August 1975

INDEXED IN CURRENT CONTENTS

AUTHOR INDEX

Walter de Gruyter · Berlin · New York

CALL FOR PAPERS

1976 ANNUAL CONFERENCE OF THE SOCIETY FOR BIOMATERIALS

in conjunction with the

EIGHTH INTERNATIONAL BIOMATERIALS SYMPOSIUM

To be held in Philadelphia, Pa. April 10–13, 1976. Papers are invited in all aspects of implant materials including tissue-materials interfaces, tissue properties and mechanics, restorative materials, and related basic sciences. Abstracts of approximately 400 words typed within space 19. 5 cm in width and 13. 5 cm in height including title and authors should be sent to Dr. S. R. Pollack, Program Chairman, L. R. S. M. Bldg., University of Pennsylvania, Philadelphia, Pennsylvania 19174, U.S.A. by October 1, 1975.

ANNOUNCEMENT OF IAEA SYMPOSIUM

Title:	Medical Radionuclide Imaging
Date:	25–29 October 1976
Location:	Los Angeles, California, USA
Organizers:	International Atomic Energy Agency P.O. Box 590, A-1011 Vienna, Austria
Scientific Secretaries:	L. J. Johansson and T. Munkner Medical Applications Section

This Symposium, the fifth to be organized by the International Atomic Energy Agency in the subject field, will cover all aspects of radionuclide imaging techniques and their applications in clinical medicine and research.

The Symposium will place emphasis on recent advances in methods and techniques, particularly as regards the development and refinement of instrumentation, the use of computers for data processing and analysis, and the introduction of new radiopharmaceuticals. It will also consider the results of radionuclide imaging in relation to those of other imaging techniques.

Further information and forms to accompany abstracts of papers intended for presentation at the Symposium may be obtained from national authorities for atomic energy matters. Abstracts must be submitted through these authorities so as to reach the International Atomic Energy Agency before 21 May 1976.

Ninth FEBS *Meeting* 31-37

Federation of European Biochemical Societies Ninth Meeting, Budapest, 1974

IN SEVEN VOLUMES

Edited by Gy. Gárdos

The material of the Meeting will be published in the following seven volumes:

31. PROTEINS OF CONTRACTILE SYSTEMS. ISBN 963 05 0599 1
32. MECHANISM OF ACTION AND REGULATION ENZYMES. ISBN 963 05 0600 9
33. BIOCHEMISTRY OF THE CELL NUCLEUS. Mechanism and regulation of the Gene Expression. ISBN 963 05 0601 7
34. POST-SYNTHETIC MODIFICATION OF MACROMOLECULES. ISBN 963 05 0602 5
35. BIOMEMBRANES. Structure and Function. ISBN 963 05 0603 3
36. ANTIBODY STRUCTURE AND MOLECULAR IMMUNOLOGY. ISBN 963 05 0604 1
37. PROPERTIES OF PURIFIED CHOLINERGIC AND ADRENERGIC RECEPTORS. ISBN 963 05 0605 X

In English · The seven volumes together approx. 2000 pages · Cloth

AKADÉMIAI KIADÓ
Budapest

NORTH HOLLAND PUBLISHING CO.
Amsterdam

A co-edition — distributed in the socialist countries by KULTURA, Budapest, ISBN 963 05 0598 3, in all other countries by NORTH HOLLAND PUBLISHING CO., Amsterdam

Printed in Hungary

A kiadásért felel az Akadémiai Kiadó igazgatója Műszaki szerkesztő: Zacsik Annamária

A kézirat nyomdába érkezett: 1975. VI. 24. — Terjedelem: 11,9 (A/5) 40 ábra 1 melléklet

75.1967 Akadémiai Kiadó, Budapest — Felelős vezető: Bernát György igazgató

Reviews of the Hungarian Academy of Sciences are obtainable at the following addresses:

AUSTRALIA

C. B. D. Library and Subscription Service
Box 4886, G. P. O.
Sydney N. S. W. 2001

Cosmos Bookshop
145 Acland St.
St. Kilda 3182

AUSTRIA

Globus
Höchstädtplatz 3
A—1200 Wien XX

BELGIUM

Office International de Librairie
30 Avenue Marnix
1050-Bruxelles

Du Monde Entier
162 Rue du Midi
1000—Bruxelles

BULGARIA

Hemus
Bulvar Ruszki 6
Sofia

CANADA

Pannonia Books
P. O. Box 1017
Postal Station "B"
Toronto, Ont. M5T 2T8

CHINA

C N P I C O R
Periodical Department
P. O. Box 50
Peking

CZECHOSLOVAKIA

Mad'arská Kultura
Národní třida 22
115 66 Praha

PNS Dovoz tisku
Vinohradská 46
Praha 2

PNS Dovoz tlače
Bratislava 2

DENMARK

Ejnar Munksgaard
Nörregade 6
DK—1165 Copenhagen K

FINLAND

Akateeminen Kirjakauppa
P. O. Box 128
SF—00101 Helsinki 10

FRANCE

Office International de Doumentation et Librairie
48,cRue Gay Lussac
Paris 5

Librairie Lavoisier
11 Rue Lavoisier
Paris 8

Europeriodiques S. A.
31 Avenue de Versailles
78170 La Celle St. Cloud

GERMAN DEMOCRATIC REPUBLIC

Haus der Ungarischen Kultur
Karl-Liebknecht-Strasse 9
DDR—102 Berlin

Deutsche Post
Zeitungsvertriebsamt
Strasse der Pariser Kommüne 3—4
DDR—104 Berlin

GERMAN FEDERAL REPUBLIC

Kunst und Wissen
Erich Bieber
Postfach 46
7 Stuttgart S

GREAT BRITAIN

Blackwell's Periodicals
P. O. Box 40
Hythe Bridge Street
Oxford OX1 2EU

Collet's Holdings Ltd.
Denington Estate
London Road
Wellingborough Northants NN8 2QT

Bumpus Haldane and Maxwell Ltd.
5 Fitzroy Square
London W1P 5AH

Dawson and Sons Ltd.
Cannon House
Park Farm Road
Folkestone, Kent

HOLLAND

Swets and Zeitlinger
Heereweg 347b
Lisse

Martinus Nijhoff
Lange Voorhout 9
The Hague

INDIA

Hind Book House
66 Babar Road
New Delhi 1

India Book House
Subscription Agency
249 Dr. D. N. Road
Bombay 1

ITALY

Santo Vanasia
Via M. Macchi 71
20124 Milano

Libreria Commissionaria Sansoni
Via Lamarmora 45
50121 Firenze

JAPAN

Kinokuniya Book-Store Co. Ltd.
826 Tsunohazu 1-chome
Shinjuku-ku
Tokyo 160—91

Maruzen and Co. Ltd.
P. O. Box 5050
Tokyo International 100—31

Nauka Ltd—Export Department
2—2 Kanda
Jinbocho
Chiyoda-ku
Tokyo 101

KOREA

Chulpanmul
Phenjan

NORWAY

Tanum-Cammermeyer
Karl Johansgatan 41—43
Oslo 1

POLAND

Węgierski Instytut Kultury
Marszalkowska 80
Warszawa

BKWZ Ruch
ul. Wronia 23
00—840 Warszawa

ROUMANIA

D. E. P.
Bucureşti

Romlibri
Str. Biserica Amzei 7
Bucureşti

SOVIET UNION

Sojuzpechatj — Import
Moscow
and the post offices in each town
Mezhdunarodnaya Kniga
Moscow G—200

SWEDEN

Almqvist and Wiksell
Gamla Brogatan 26
S—101 20 Stockholm

A. B. Nordiska Bokhandeln
Kunstgatan 4
101 10 Stockholm 1 Fack

SWITZERLAND

Karger Libri AG.
Arnold-Böcklin-Str. 25
4000 Basel 11

USA

F. W. Faxon Co. Inc.
15 Southwest Park
Westwood, Mass. 02090

Stechert-Hafner Inc.
Serials Fulfillment
P. O. Box 900
Riverside N. J. 08075

Fam Book Service
69 Fifth Avenue
New York N. Y. 10003

Maxwell Scientific International Inc.
Fairview Park
Elmsford N. Y. 10523

Read More Publications Inc.
140 Cedar Street
New York N. Y. 10006

VIETNAM

Xunhasaba
32, Hai Ba Trung
Hanoi

YUGOSLAVIA

Jugoslovenska Knjiga
Terazije 27
Beograd

Forum
Vojvode Mišića 1
21000 Novi Sad

Contents

28. XI. 1975 Index : 26.030

VOLUME 10
NUMBER 4
1975

Acta biochimica et biophysica

ACADEMIAE SCIENTIARUM HUNGARICAE

AKADÉMIAI KIADÓ, BUDAPEST

ABBPAP 10 (4) 263–306 (1975)

Acta Biochimica et Biophysica

Academiae Scientiarum Hungaricae

Szerkeszti:

STRAUB F. BRUNÓ és ERNST JENŐ

Technikai szerkesztők:

SAJGÓ MIHÁLY és NIEDETZKY ANTAL

Szerkesztőség postai címe: 1502 Budapest, Pf. 7 (biokémia)
7643 Pécs, Pf. 99 (biofizika)

Az *Acta Biochimica et Biophysica* a Magyar Tudományos Akadémia idegen nyelvű folyóirata, amely angol nyelven (esetleg német, francia vagy orosz nyelven is) eredeti tanulmányokat közöl a biokémia és a biofizika — fehérjék (struktúra és szintézis), enzimek, nukleinsavak, szabályozó és transzport-folyamatok, bioenergetika, izom-összehúzódás, radiobiológia, biokibernetika, funkcionális és ultrastruktúra stb. — tárgyköréből.

A folyóirat negyedévenként jelenik meg, a négy füzet évente egy kb. 400 oldalas kötetet alkot. Kiadja az Akadémiai Kiadó.

Megrendelhető az Akadémiai Kiadónál (1363 Bp. Pf. 24.), a külföld részére pedig a Kultúra Könyv és Hírlap Külkereskedelmi Vállalatnál (1389 Budapest 62, P.O.B. 149).

The *Acta Biochimica et Biophysica*, a periodical of the Hungarian Academy of Sciences, publishes original papers, in English, on biochemistry and biophysics. Its main topics are: proteins (structure and synthesis), enzymes, nucleic acids, regulatory and transport processes, bioenergetics, excitation, muscular contraction, radiobiology, biocybernetics, functional structure and ultrastructure.

The Acta Biochimica et Biophysica is a quarterly, the four issues make up a volume of some 400 pages per annum. Manuscripts and correspondence with the editors and publishers should be sent to

Akadémiai Kiadó, Budapest 24, P.O.B. 502.

The subscription rate is $32.00 per volume. Orders may be placed with *Kultúra* Trading Co. for Books and Newspapers (1389 Budapest 62, P.O.B. 149) or with its representatives abroad, listed on p. 3 of the cover.

Acta Biochimica et Biophysica — журнал Академии Наук Венгрии, публикующий на английском языке (возможно и на немецком, французском и русском языках) оригинальные статьи по проблемам биохимии и биофизики — белков (структура и синтез), энзимов, нуклеиновых кислот, процессов регуляции и транспорта, биоэнергетики, мышечного сокращения, радиобиологии, биокибернетики, функциональной структуры и ультраструктуры и т. д.

Журнал выходит ежеквартально, выпуски каждого года составляют том объемом около 400 сшпаниц. Журнал выпускает Издательство Академии Наук Венгрии.

Рукописи и корреспонденцию просим направлять по следующему адресу:

Akadémiai Kiadó, Budapest 24, P.O.B. 502.

Подписная цена — $ 32.00 за том. Заказы принимает:

Предприятие по внешней торговле книгами и газетами «Kultúra» (1389 Budapest 62, P.O.B. 149) или его заграничные агентства.

Acta Biochim. et Biophys. Acad. Sci. Hung. Vol. 10 (4), pp. 263–266 (1975)

Purification of Nuclear Ribonucleoprotein Complexes Containing Poly(Adenylic Acid)

J. MOLNÁR, OLGA P. SAMARINA*

Institute of Biology, University Medical School, Pécs, Hungary and
*Institute of Molecular Biology, Academy of Sciences of the U.S.S.R., Moscow, U.S.S.R.

(Received June 13, 1975)

Nuclear 14 *S* ribonucleoprotein particles containing poly(adenylic acid) were isolated from Ehrlich ascites carcinoma cells and purified by a two step method. The nuclear extract obtained at an ionic strength of 0.1 was treated by pancreatic and T_1 ribonucleases and sedimented in a 15–30% sucrose gradient. The 14 *S* peak containing 50–60% poly(adenylic acid) was chromatographed on a poly(dT)-Sepharose column. The particles thus obtained were of high purity: they had an adenosine content of 90% and a protein moiety characteristic of the 14 *S* nuclear particles, i.e. polypeptides with molecular weights of 51 000, 61 000 and 69 000 daltons.

The pre-mRNA in cell nuclei is combined with specific protein particles, informofers, and can be isolated as polysome-like structures (Samarina et al., 1968). The poly(A) blocks at the 3' end of nuclear pre-mRNA also exist as specific ribonucleoprotein particles (Samarina et al., 1973, 1973a). When the extraction buffer contains no inhibitor of ribonuclease, polyparticles, as a result of nuclease effect, are disintegrated into 30 *S* RNP particles containing a part of pre-mRNA and an informofer, and to 14 *S* RNP particles containing poly(A). The latter has a buoyant density in CsCl of 1.36 gcm^{-3} and differs from 30 *S* particles also in protein moiety (Samarina et al., 1973a; Molnár, Samarina, 1975).

In order to characterize the protein composition of 14 *S* particles it was necessary to work out some effective methods of purification. In the present report a very simple method is shown for the preparation of nuclear 14 *S* RNP particles containing poly(A) by the use of affinity chromatography on a poly(dT)-Sepharose column.

Materials and methods

Nuclei from *Ehrlich ascites* carcinoma cells labelled *in vitro* with arreir free ^{32}P-orthophosphate for 90 min were isolated as described earlier (Samarina, 1961). The RNP particles were extracted from nuclei in the usual way (Samarina et al., 1968) without the application of ribonuclease inhibitor. The nuclear extract was ultracentrifuged through a 15–30% sucrose gradient directly or treated with a mixture of RNases (8 $\mu g\ ml^{-1}$ RNase A + 10 U ml^{-1} RNase T_1) at 0°C before centrifugation.

Affinity chromatography on poly(dT)-Sepharose column. The fractions of sucrose gradients were adjusted to contain 300 mM NaCl and 4 mM EDTA, digested by a mixture of ribonucleases (5 μg ml^{-1} RNase A + 10 U ml^{-1} RNase T_1) for 20 min at room temperature and passed through a column of poly(dT)-Sepharose (7 × 35 mm). After 20 min the column was washed with a large volume of the equilibrating buffer (300 mM NaCl, 4 mM EDTA, 10 mM tris-HCl, pH 7.8). The percentage of the material retained on the column was calculated from the difference between the total radioactivity of the starting material and that of the material in the effluent. The radioactivity was measured by the Cherenkov method using an Intertechnique SL-30 scintillation counter.

Proteins from the column were eluted by a solution containing 5 M urea, 0.5% SDS and 0.1 M NaCl. The material still retained on the column was eluted at 65°C by 90% formamide containing 0.5% SDS.

Base composition analysis was performed by paper electrophoresis (Samarina et al., 1973a).

The electrophoresis of proteins in SDS polyacrylamide gels was carried out essentially according to Weber and Osborn (1969) with a few modifications (Molnár, Samarina, 1975). Gels were stained by Coomassie brillant blue and destained gels scanned in a Joyce-Loebl Chromoscan using a 620 nm filter (Molnár, Samarina, 1975).

Results and discussion

Fig. 1A illustrates the sucrose gradient centrifugation of the nuclear extract. There are two peaks, the 30 *S* and the 3–5 *S* peaks. As shown earlier (Samarina et al., 1973; 1973a), the poly(A) containing RNP particles have been found between these two peaks, in the 13–15 *S* zone of the sucrose gradient.

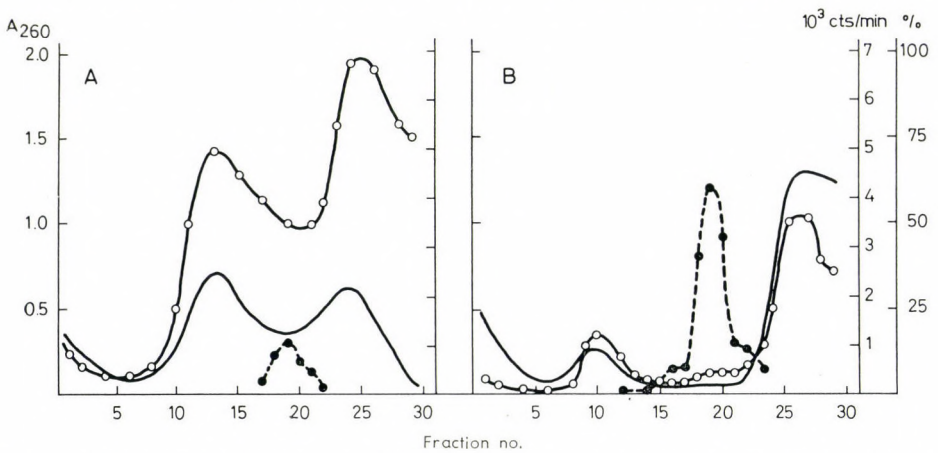

Fig. 1. Ultracentrifugation of nuclear extract (A) and nuclear extract treated by ribonucleases (B) in a 15–30% sucrose gradient. Sedimentation was carried out in a Beckman L-2 65 B ultracentrifuge, in the SW 27 rotor, for 16 hrs at 26 000 rpm and 4°C; ——— absorbance at 260 nm; ○ ○ radioactivity of 10 μl aliquots; – – • – per cent radioactivity of the fractions retained on the poly(dT)-Sepharose column

Ribonuclease treatment of the 30 *S* particles is known from earlier data to result in the solubilization of a part of the particles and a significant aggregation of the surviving, damaged ones (Molnár, Komáromy, 1974). Fig. 1B shows that after ribonuclease treatment, the 30 *S* particles sediment slightly faster. There is a sharp decrease of absorbancy at 260 nm and in the radioactivity "background" in the sucrose gradient and a 14 *S* peak can be observed.

Retention of each fraction of the sucrose gradient on poly(dT)-Sepharose column was then tested. Only the material from the 14 *S* zone was retained to a considerable extent. The maximum radioactivity retained on the column reached 60% in the experiment shown in Fig. 1B, while in the control (nuclear extract not treated with RNase) the proportion of poly(A) containing material remained at a lower level (Fig. 1A).

The adenosine content of particles sedimenting in the 14 *S* region of the sucrose gradients was close to that of the material retained on the poly(dT)-Sepharose column (Table 1).

Table 1

Base composition of poly(A)-containing fractions at different steps of purification

Fractions	C	A	G	U
14 *S* zone of sucrose gradient (see Fig. 1A)	20	38	16	26
14 *S* zone of sucrose gradient (nuclear extract treated by RNase prior to centrifugation)	15	61	12	12
Material eluted by formamide from a poly(dT)-Sepharose column	6	88	4	2

Though the adenosine content of material sedimenting in the 14 *S* zone of the sucrose gradient reached 60% (Fig. 1B), the protein moiety revealed significant heterogeneity (Fig. 2A). No less than half of these polypeptides had electrophoretic mobilities characteristic of the informofer (Fig. 2D). The poly(dT)-Sepharose column retained the particles containing three main protein components with molecular weights of 51 000, 61 000 and 69 000 (Fig. 2B, C), respectively. Two of these (Mwt of 61 000 and 69 000) were tightly bound to the poly(A) because the majority of them could be eluted by formamide only together with poly(A) (Fig. 2C).

Such a protein moiety has been found by other methods of purification, i.e. by resedimentation of 14 *S* particles in sucrose and in Cs_2SO_4 density gradients (Molnár, Samarina, 1975). However, affinity chromatography of the material obtained after the first sucrose gradient centrifugation seems to be a more simple and effective method.

We wish to thank Prof. G. P. Georgiev for continued interest in this work, Dr A. P. Ryskov for the preparation of poly(dT)-Sepharose and Miss N. I. Lupkina for excellent technical assistance.

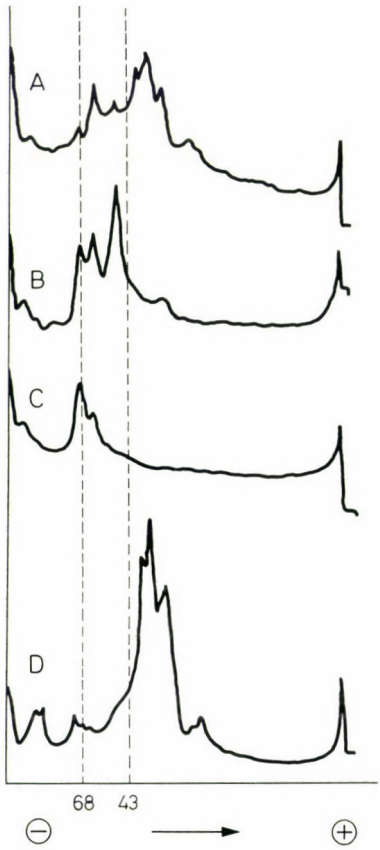

Fig. 2. Electrophoresis of nuclear particles in polyacrylamide gels containing SDS. The proteins of the material sedimenting in the 14 *S* zone of sucrose gradients as shown in Fig. 1B (A); the proteins of the material eluted from the poly(dT)-Sepharose column by a solution of 5 M urea, 0.5% SDS and 0.1 M NaCl (B), or by 90% formamide in 0.5% SDS at 65°C (C); informofer proteins (D). Electrophoresis was performed in glass tubes. The gels were stained by Coomassie brillant blue and scanned in a Joyce–Loebl Chromoscan using a 620 nm filter. Direction of electrophoresis from left to right. The numbers (in thousands) on the abscissa: the position of the markers (bovine serum albumin and egg albumin, Serva)

References

Molnár, J., Komáromy, L. (1974) Acta Biochim. Biophys. Acad. Sci. Hung. *9* 73
Molnár, J., Samarina, O. P. (1975) Mol. Biol. Reports *2* 1
Samarina, O. P. (1961) Biokhimiya (U.S.S.R.) *26* 61
Samarina, O. P., Lukanidin, E. M., Molnár, J., Georgiev, G. P. (1968) J. Mol. Biol. *33* 251
Samarina, O. P., Lukanidin, E. M., Georgiev, G. P. (1973) Acta Endocrinol. (Copenhagen), Suppl. *80* 130
Samarina, O. P., Aitkhozhina, N. A., Besson, J. (1973a) Mol. Biol. Reports *1* 193
Weber, K., Osborn, M. (1969) J. Biol. Chem. *244* 4406

Acta Biochim. et Biophys. Acad. Sci. Hung. Vol. 10 (4), pp. 267—275 (1975)

Microscopic Observations on the Interaction of Heavy Meromyosin-S-1 and Actin in Myofibrils

N. GARAMVÖLGYI, K. VÁCZY, E. N. A. BIRÓ

Research Unit, Hungarian University College of Physical Education and Department of Biochemistry, Eötvös Loránd University, Budapest, Hungary

(Received May 12, 1975)

The binding of the proteolytic myosin fragment, HMM-S-1, to the non-overlapping part of actin filaments in intact myofibrils can be demonstrated under the phase contrast microscope as a contrast reversal of striation. The same effect can be seen on ghost myofibrils (after myosin extraction) where the whole length of the I-filaments is bare.

HMM-S-1-loaded ghost myofibrils contracted upon addition of ATP in agreement with the recent report of Oplatka et al. (1974a, b) but under the same conditions ghost myofibrils not treated with HMM-S-1) also contracted. If the ghosts were prepared under conditions more favourable to myosin extraction, contraction became nil or negligible even when we loaded then ghosts with S-1.* Thus we attribute the effect described by Oplatka's group to a small number of residual myosin filaments in the ghosts.

Introduction

One of the most acute questions of muscle research is the fine mechanism of cross-bridge movement. It is now generally accepted that force development in the consequence of an active movement of parts of the myosin molecule, i.e. of the HMM subunit forming the cross-bridges (see: Huxley, 1969; Huxley, Simmons, 1971). Recently Oplatka and his co-workers (1974a, b) claimed that myofibrils deprived of their myosin content and subsequently washed with S-1 ware able to shorten upon the addition of ATP, whereas untreated ghost myofibrils did not exhibit any shortening. According to these very remarkable findings also supported by other experiments (Oplatka et al., 1974c; Gadasi et al., 1974), it is the head portion of the myosin molecule alone that would lead to the mechanical response and the "shaft" of the myosin molecule would play an inferior role, if any, in this process. Due to its importance we decided to examine this question more closely by designing similar but more rigorous experiments. Oplatka and his group did not provide photomicrographs of sufficient resolution. This was done obviously in order to be able to observe a large field containing as many myofibrils as possible. We carried out all the observations in each experiment on the same myofibril with the highest possible resolution aiming to detect a maximum of detail of the process.

* *Abbreviations:* S-1, sub-fragment-1; HMM, heavy meromyosin

Materials and methods

Myofibrils were isolated from the psoas fixed to glass rods in a substantially extended state and kept for two-three days at 4°C in 50% glycerol containing all ingredients of the "standard salt solution" (see below). After homogenization in "standard salt solution" (see below) the suspension was washed five times in the same solution by low speed centrifugation (2 000 g, 5 min). The final pellet was suspended in standard salt solution.

All subsequent operations were done under coverslip with continuous microscopic observation as described by Hanson (1952). A small drop of the corresponding solution was deposited on one edge of the coverslip and soaked through the specimen by a filter paper strip applied to the opposite edge. The preparation was first washed with the "standard salt solution" (see below) in order to remove myofibrils swimming freely and disturbing the optical conditions. The following solutions were used:

1. Standard salt solution: 0.1 M KCl, 2 mM EDTA, 2 mM mercaptoethanol, 60 mM phosphate buffer, pH 7.0;

2. Low-Mg^{2+} Hasselbach–Schneider's solution (Hanson, Huxley, 1955) 0.47 m KCl, 0.1 M phosphate buffer, pH 6.4, 10 mM $Na_4P_2O_7$, 1 mM $MgCl_2$;

3. High-Mg^{2+} Hasselbach–Schneider's solution: as 2. but with 5 mM $MgCl_2$ (freshly prepared each day);

4. For contraction experiments the following solution was used: 0.1 M KCl, 5 mM tris-acetate, pH 7.0, 1 mM Mg ATP.

HMM-S-1* was prepared by papain digestion as described by Bálint et al. (1975) and kept in 90 mM KCl, 30 mM tris-HCl, pH 7.7, 2 mM EDTA and 1 mM monoiodacetate. Monoiodacetate was included to prevent further digestion by residual papain contamination. The standard S-1 preparations (5–7 mg/ml) were applied to the slide without dilution.

A phase contrast microscope (Carl-Zeiss-Jena) was used for observations. Micrographs were taken with a 90× oil immersion objective. When the first sign of change was observed after ATP addition, we took successive photographs as frequently as possible.

Results

The effect of ATP was checked daily on unextracted myofibrils. These myofibrils shortened till they became little balls, without any recognizable structure. As a further control we washed intact myofibrils with the S-1-containing solution, in order to eliminate the possibility that the increase of optical density may be due to shrinkage or other side effects. In intact myofibrils S-1 was in fact selectively bound by the actin filaments (Fig. 1). This is clearly shown by

* The preparations were kindly provided by Miss Katalin Pintér (Department of Biochemistry).

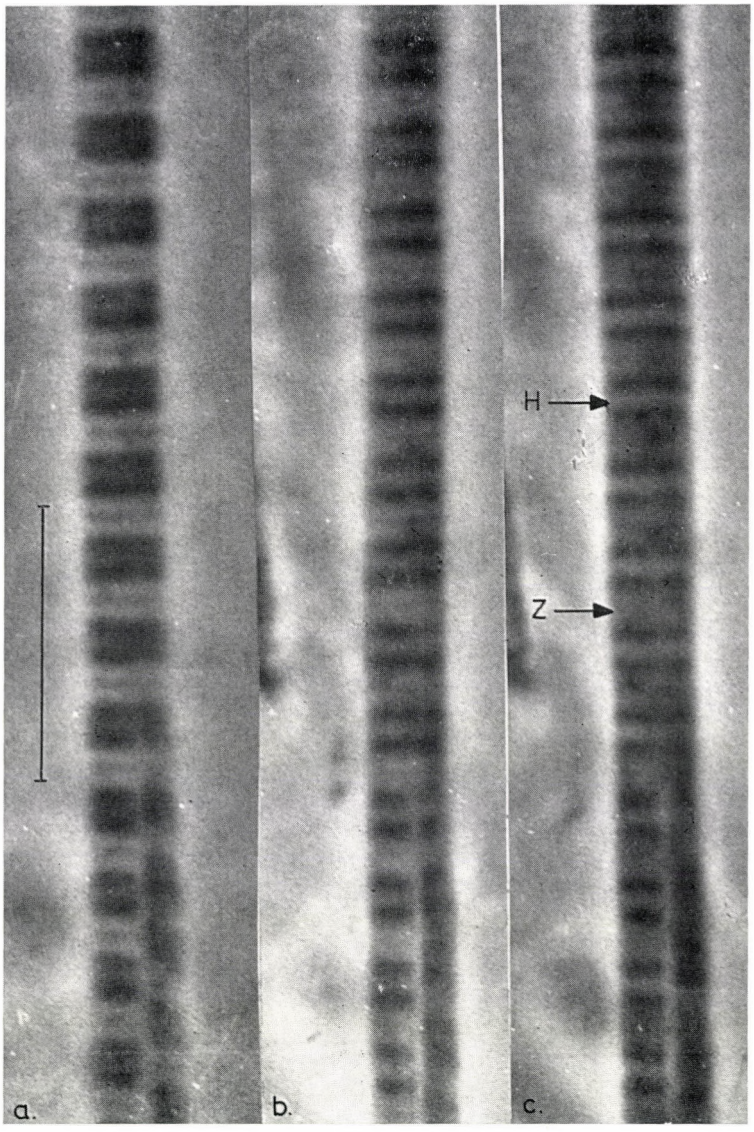

Fig. 1. "Staining" of intact myofibrils with S-1. Intact myofibril treated with S-1; a: before, b: during, c: after treatment. For the orientation the site of a Z-line and of an H-zone is marked in Fig. 1c. The scale valid for all figures represents 10 μm

the strange contrast reversal, as a result of which the density of the I-bands strongly increased and the H-zones became the relatively less dense elements, although myosin filaments were still present.

In Fig. 2 the myofibril was extracted with a "low-Mg^{2+} Hasselbach–Schneider's solution" (see: Methods) to remove its myosin content. Subsequently it was treated with S-1-containing solution. As a result, the areas corresponding to the site of actin filaments became optically much more dense. The addition of ATP caused shortening. Since the myofibrils were adhering to the slide, their entire length did not change, but the striation became irregular due to the coalescing of some adjacent I-segments. The force generated was in most cases insufficient to liberate the myofibrils from the slide, in contrast to what (as this) happened in case of intact myofibrils.

Fig. 3 shows a similar experiment more clearly. After myosin extraction and S-1 binding ATP was added. The areas corresponding to the sets of actin filaments became less dense, more or less simultaneously with the onset of shortening, most probably owing to the dissociation of the S-1-actin complex caused by ATP. The shortening of the fibril was relatively slow and it could be followed during the whole process. As indicated in Fig. 3, shortening is uneven within the myofibril, the individual I-segments can be identified and a more or less pairwise coalescing is indicated by arrows. Since the whole length of the myofibril could not change, the shortening of one portion is necessarily accompanied by lengthening the gap that corresponds to the H-zone and separating it from the neighbouring I-segment.

We performed experiments on myofibrillar ghosts omitting their washing with the S-1-containing solution. Fig. 4 shows an experiment of this type. It is visible that contraction took place in these controls too, contrary to the experiments of Oplatka and his co-workers (1974a, b). It is to be mentioned that in this experiment the final state of shortening was "stained" by subsequent washing with S-1. It is seen that practically the same effect can be obtained without any previous treatment with S-1 as with S-1-pretreated myofibrils.

These experiments suggest that extraction with "low-Mg^{2+} Hasselbach–Schneider's solution" does not remove all myosin in such a short time. This may be due to the fact that most of the pyrophosphate present in this solution is not complexed with Mg^{2+}. Gränicher and Portzehl (1964) reported that dissociation of actomyosin is effected by $MgP_2O_7^{2-}$ but not by free pyrophosphate.

Washing of the intact myofibrils with Hasselbach–Schneider's solution with increased Mg^{2+}-content (see Methods) removed the A-band much more readily than the "low-Mg^{2+} Hasselbach–Schneider's solution". When ATP was added to myofibrils thus treated after washing with S-1-containing solution, there was merely a slight displacement of a few I-segments, but no considerable shortening occurred (Fig. 5).

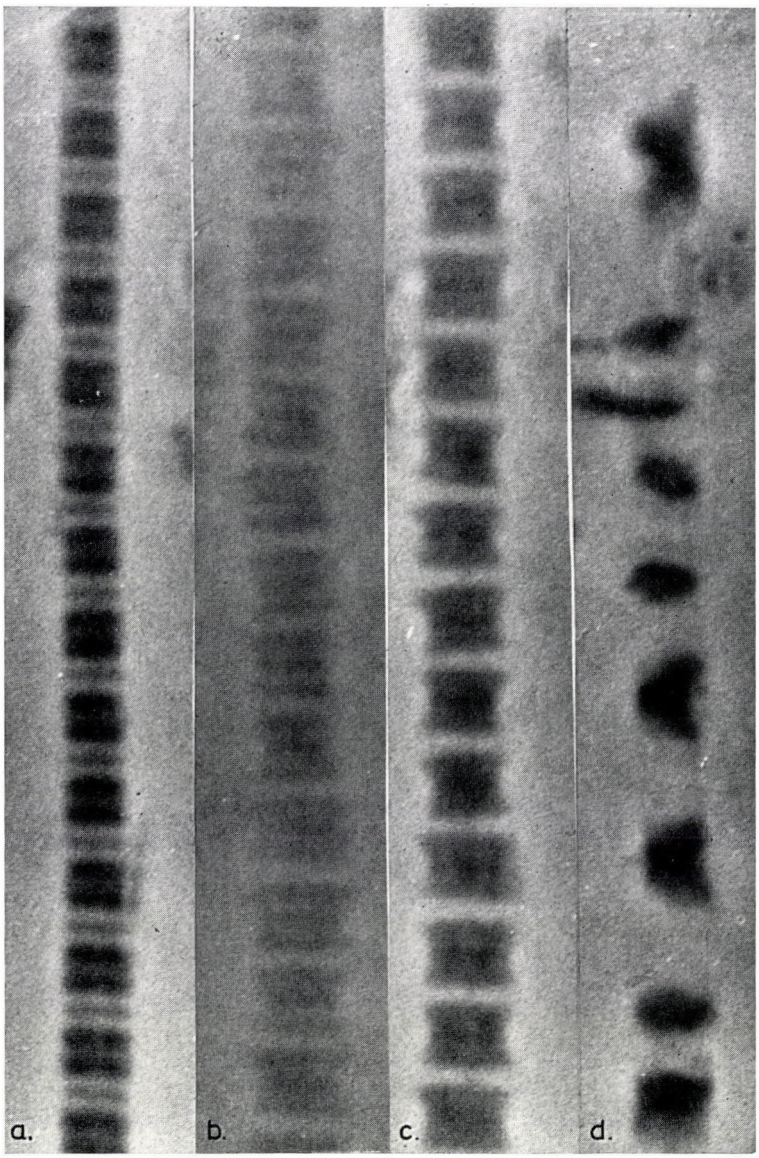

Fig. 2. Contraction of S-1-treated ghost myofibrils; a: before, treatment, b: after myosin extraction, c: treated with HMM-S-1, d: after addition of ATP

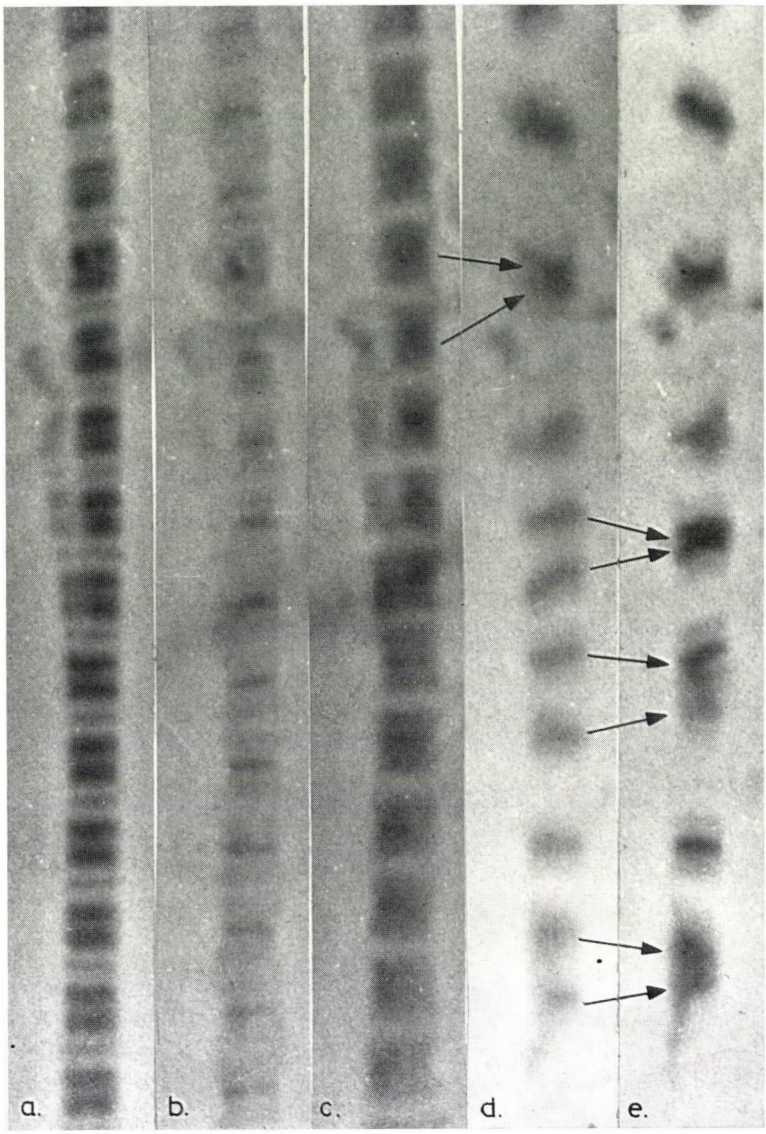

Fig. 3. Contraction of S-1-treated ghost myofibrils; a: before treatment, b: after myosin extraction, c: treated with HMM-S-1, d: after addition of ATP, during shortening, e: after shortening. The arrows indicate identical I-segments. Note that the addition of ATP results in the splitting of the S-1-actin link; this is shown by the lower density of the areas corresponding to the actin filaments

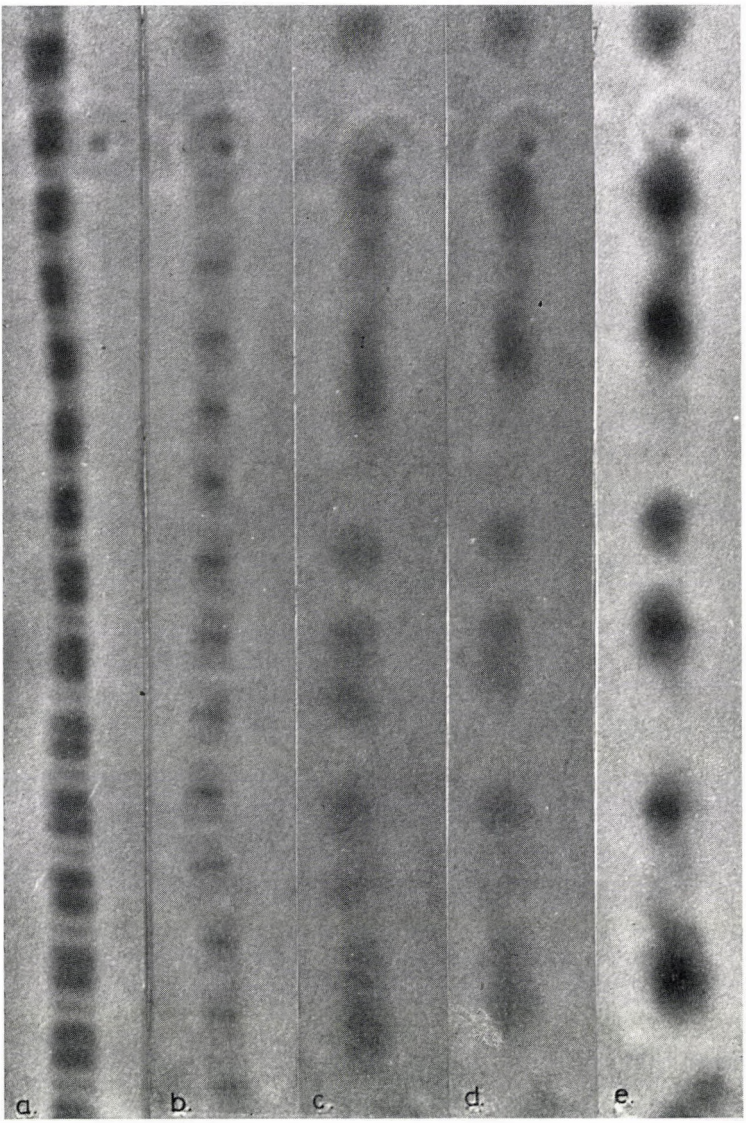

Fig. 4. Shortening of a myofibrillar ghost without pretreatment with S-1; a: before treatment, b: after myosin extraction, c: after addition of ATP, d: during shortening, e: after shortening. In the last state S-1 was added, in order to "stain" the myofibril

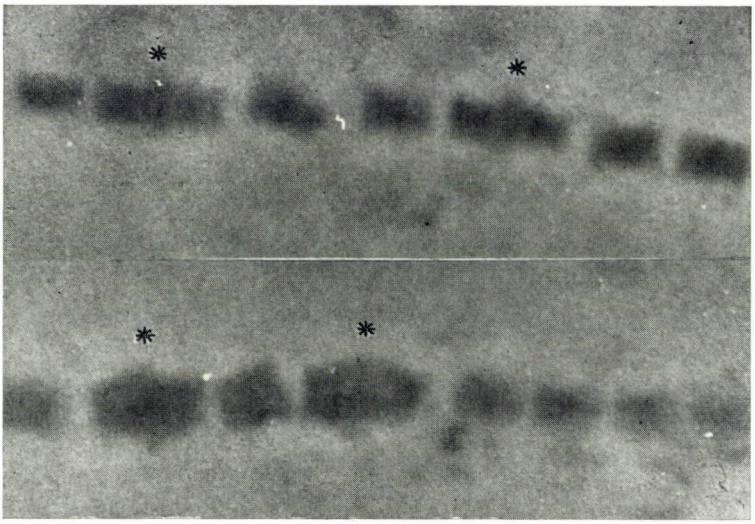

Fig. 5. Effect of extraction with "high-Mg^{2+} Hasselbach—Schneider's solution" on contractility. The final states of experiments (similar to those shown in Figs 2 and 3) in which the extraction was performed with "high-Mg^{2+} Hasselbach—Schneider's solution". (See methods.) Contrary to former figures two *different* myofibrils are seen. There is merely a shift of a few I-segments (marked with asterisks) in spite of treatment with S-1

Discussion

The photomicrographs presented in this paper demonstrate by optical microscopy the binding of S-1 to I-filaments in the non-overlaping region or to the filaments exposed by extraction of myosin.

Where some of our observations could be expected on the ground of the known properties of S-1 and is well in line with the facts described in the "addendum" of Hanson and Huxley's (1955) and in Hanson's (1956) paper our other results are partly at variance with the findings of Hanson and Huxley (1955) and with the recent papers of Oplatka's group (Oplatka et al., 1974a, b). All these authors report that control ghost myofibrils (i.e. those extracted and not treated with myosin or its fragments) do not contract on addition of ATP. In our experiments these controls exhibited essentially the same irregular contraction as shown by the reconstituted ghosts. We suggest that the contraction of control and reconstituted ghosts in all these cases is due to residual myosin filaments. Hanson and Huxley (1955) complemented Hasselbach—Schneider's solution with 1 mM $MgCl_2$ because they observed that without Mg^{2+} ions there was no visible extraction by this solution in the short-term experiments necessitated by the microscopic observation of the process. Later Gränicher and Portzehl (1964) have demonstrated that the dissociating effect of pyrophosphate is caused by the $MgP_2O_7^{2-}$ ionic species whercas $P_2O_7^{4-}$ is ineffective. In agreement with

this fact we found that if 5 mM $MgCl_2$ was added to Hasselbach–Schneider's solution, i.e. virtually all pyrophosphate (10 mM) was in the form of the effective complex (in contrast to all former experiments with practically 1 mM $MgP_2O_7^{2-}$) extraction was instantaneous and the ghosts practically did not contract at all, even when saturated with S-1 (Fig. 5).

Besides the incompleteness of extraction by the "low-Mg Hasselbach–Schneider's solution" there is another difference in our experiments as compared to all former similar studies, which might have rendered the low force generated in unreconstituted ghosts visible, namely that we used substantially stretched myofibrils. The sarcomere length of the fibrils used in Hanson and Huxley's (1955) experiments is not stated. The photomicrographs presented in the papers of Oplatka et al. (1974a, b) show clearly that the myofibrillar preparation used was in a rather contracted state. It is well possible that with unstretched fibrils the force generated by residual myosin filaments (surviving extraction) remains unobservable.

To sum up we believe that the contraction of reconstituted ghosts is due to residual myosin filaments. This view is supported by our observation demonstrated in Fig. 3 (compare d and e) that shortening of S-1 saturated ghosts is continuing even after the contrast of I-segments diminished, i.e. after the release of the bulk of S-1 taken up.

It must be emphasized that Oplatka's claim about the possibility of force generation by "non-aggregating myosin derivatives" has been supported by several lines of evidence (Oplatka et al., 1974a, b, c; Gadasi et al., 1974). The experiment reported in the present paper is only one of them.

References

Bálint, M. Streter, F. Gergely, J. (1975) Arch. Biochem. Biophys. *168* 557
Gadasi, H., Oplatka, A., Lamed, B., Mühlrad, A. (1974) Biophys. Res. Com. *58* 913
Gränicher, D., Portzehl, H. (1964) Biochim. Biophys. Acta *86* 567
Hanson, J. (1952) Nature *169* 530
Hanson, J. (1956) J. Biophys. Biochem. Cytol. *2* 691
Hanson, J., Huxley, H. E. (1955) Symp. Soc. Exp. Biol. *9* 228
Huxley, H. E. (1969) Science *164* 1356
Huxley, A. F., Simmons, R. M. (1971) Nature *233* 533
Oplatka, A., Gadasi, H., Borejdo, J. (1974a) Biochem. Biophys. Res. Com. *58* 905
Oplatka, A., Borejdo, J., Gadasi, H. (1974b) FEBS Letters *45* 55
Oplatka, A., Gadasi, H., Tirosh, R., Lamed, B., Mühlrad, A., Liron, N. (1974c) J. Mechanochem. Cell Motility *2* 295

Acta Biochim. et Biophys. Acad. Sci. Hung. Vol. 10 (4), pp. 277—286 (1975)

Specific Colour Reaction for the Determination of Lysine and/or Ornithine

M. PATTHY, A. PATTHY

Research Institute for Pharmaceutical Chemistry, Budapest, Hungary

(Received October 16, 1974)

A simple procedure was worked out for the direct spectrophotometric determination of lysine and/or ornithine in hydrolysates of proteins and protein-containing materials. The method is based on the estimation of the coloured compound formed in the reaction of lysine and ornithine with furfurol. Since the reaction is specific for lysine and ornithine and separation of amino acids is not necessary for their determination the method is suitable for large scale screening of protein samples.

The lower limit of detection is 0.5 μg for lysine and 2 μg for ornithine and the accuracy of the method is $\pm 0.5\%$ and $\pm 2\%$, respectively.

In hydrolysates lysine is usually determined by nonspecific colour reaction (such as ninhydrin) following a separation step (ion-exchange chromatography, electrophoresis).

Our method offers a possibility to determine lysine and/or ornithine accurately and rapidly without any separation procedure, directly from the hydrolysate of the sample, by means of a specific color reaction.

Storherr (1959) was the first to indicate that in amino acid mixtures, only lysine, hydroxylysine, and ornithine reacted with furfurol (furan-2-aldehyde) in acetic acid medium, to give a characteristic, reddish-purple color.

Although this reaction was valuable for qualitative purposes it was not useful for quantitative analysis because, on the one hand, the auto-oxidation of furfurol could not be efficiently prevented under the experimental conditions given by Storherr and on the other hand, the determination was influenced to a great degree by large excess of other amino acids even though the individual amino acids did not interfere with the assay (Patthy, 1967).

Utilizing Storherr's observations, we elaborated a new procedure which is useful for the rapid determination of lysine and/or ornithine, independently of the degree of excess of other amino acids.

Materials and methods

Spectrophotometric assays were carried out by a visible-range spectrophotometer Spectromom 360 (MOM, Budapest) and spectra were taken on a Unicam SP 500. The results obtained for lysine and/or ornithine content of the samples were also determined by a JEOL JLC-5AH type automatic amino acid analyzer.

All *chemicals* used were of analytical grade. 2,4-Diaminobutyric acid, ornithine, lysine, arginine, citrulline, proline, tryptophan were purchased from AJINOMOTO Co. INC., homolysine was synthesized according to Takagi and Hayashi (1959). Putrescine, cadaverine, α-ε-diaminopimelic acid as well as one of the foodstuff samples (22090) originated from FLUKA AG and cowmilk α-casein from Merck. Soya meal and an other nutriment sample (721214) were received from the United Chemical and Pharmaceutical Works EGYT (Budapest). Insulin (25 IU/mg), porcine ACTH and the Lys-Pro-Gly tripeptide were kindly supplied by Drs Gy. Cseh and S. Bajusz (Research Institute for Pharmaceutical Chemistry, Budapest). Lucerne grists originated from the Protein Program Bureau of OMFB (Budapest). Bis-dinitrophenyl-L-lysine and δ-hydroxylysine were purchased from CALBIOCHEM. N-α-acetyl-L-lysine was the product of SIGMA, lysine-methylester that of REANAL (Budapest), while milk powder was prepared in the Industrial Company for Milk Products of County Hajdú, Hungary. N-ε-methyllysine, N-ε-dimethyllysine, N-ε-trimethyllysine and N-ε-formyllysine were kindly provided by Dr E. Tyihák (Research Institute for Medical Plants, Budapest).

Composition of the reagent (R) used for the color reaction was the following:

0.15% solution of $K_2S_2O_5$ in glacial acetic acid	160 ml
abs. ethanol	60 ml
furfurol distilled freshly in vacuo below 100°C (it must be colorless)	20 ml

The reagent should be protected from light and heat in a refrigerator. When the reagent is stored under these conditions it may be used for one week.

On completion of the color reaction (see below) the reaction mixture is diluted with one of the following solutions:

water–glycerol = 4 : 1 (G)

water-glycerol-NH_4OH of 25% = 3 : 1 : 1.5 (A)

The measurements were carried out on air-dried samples and the results provided by the present procedure were compared with those obtained by automatic amino acid analysis. In both cases the measurements were accomplished on aliquots of the same solution of the hydrolysed sample, on the same day and fresh standard solutions were prepared from time to time.

Hydrolysis: 20 to 200 mg of the powdered air-dried sample was suspended in 4 to 8 ml of 6N hydrochloric acid, the test tube was sealed under vacuum and the sample was hydrolysed at 115°C for 24 hours. After hydrolysis the sample was diluted with water and evaporated to dryness under vacuum. Dilution with water and evaporation were twice repeated. The residue was suspended in a few milliliters of 0.1N hydrochloric acid, the suspension was filtered through a small paper filter and the precipitate washed with 0.1N hydrochloric acid. The filtrate (S) was made up with water to give an anticipated lysine or ornithine concentration of 200 to 2000 μg/ml.

Method 1. Determination of lysine

An aliquot of the solution S containing 5 to 50 μg of lysine was dropped on filter paper by a micropipette, the wet spot was demarcated by pencil and then dried by air flow. The completely dry spot was cut out by scissors, cut up to pieces and the paper pieces were placed in a glass-stoppered test tube. 1.20 ml of reagent R was pipetted on the paper pieces and the tube was placed in a metal block test tube thermostat adjusted to 95°C. After 30 minutes the test tube was cooled by cold water. The mixture was then diluted with 2.0 ml of solution G, shaken thoroughly and light absorption was read at 535 nm against an adequate blank solution. Preparation of the blank solution as well as that of the standard lysine solution was carried out as described above, except that the same volume of 0.1N hydrochloric acid or standard solution, containing 5 to 50 μg of lysine was applied on the filter paper instead of an aliquot part of the solution S.

Lysine content of the sample was calculated by comparing the 535 nm absorption value of standard solution to that of the sample investigated.

Method 2. Determination of lysine and/or ornithine

An aliquot of solution S containing 10 to 100 μg of lysine and/or ornithine was dropped on filter paper by a micropipette and processed further as in the case of method 1 until completion of thermostating.

The cooled reaction mixture was diluted with 2.0 ml of solution A, shaken thoroughly and light absorption was read at two wave-lengths, i.e. at 485 and 600 nm against an adequate blank solution. Preparation of the blank as well as of standard lysine and ornithine solutions was carried out as above, except that the same volume of 0.1N hydrochloric acid or standard solution, containing 10 to 100 μg of lysine or ornithine was applied on the filter paper.

Lysine content of the sample was calculated by comparing the 600 nm absorption value of lysine standard solution to that of the sample.

For calculation of the ornithine content of the sample, the following abbreviations and equation were introduced:

Light absorption at 485 nm of the lysine standard = L(485)
Light absorption at 600 nm of the lysine standard = L(600)
Light absorption at 485 nm of the sample investigated = M(485)
Light absorption at 600 nm of the sample investigated = M(600)
Light absorption at 485 nm owing to ornithine in an aliquot part of the sample = A(or)

$$A(or) = M(485) - \frac{L(485) \times M(600)}{L(600)}$$

Ornithine content of the sample was calculated by comparing the A (or) value to light absorption at 485 nm of the standard ornithine solution used for color comparison. When the value of A (or) is zero or negative, then the sample contains no ornithine.

For determination of the lysine and/or ornithine content of a sample, a total of 6 measurements were carried out from the solution S. Two aliquot parts of different volumes and 3 parallels of each were used. The standard solutions were prepared in the same way, with 2×3 parallels.

Result and discussion

In order to study the nature of the color reaction between furfurol and various amino acids, several aliphatic diamines, amino acids and amino acid derivatives were investigated. The results obtained supported Storherr's observations and it was found that furfurol reacted with an overwhelming majority of amino acids in glacial acetic acid medium and all the reaction products showed light absorption in the spectrum region between 360 and 380 nm. When the color reaction was carried out according to Storherr or method 1 of this paper, in the case of α-δ, α-ε-diaminomonocarboxylic acids and some of their derivatives, auother light absorption maximum appeared between 515 and 535 nm (Figs 1 and 2). This maximum is valuable for both qualitative and quantitative

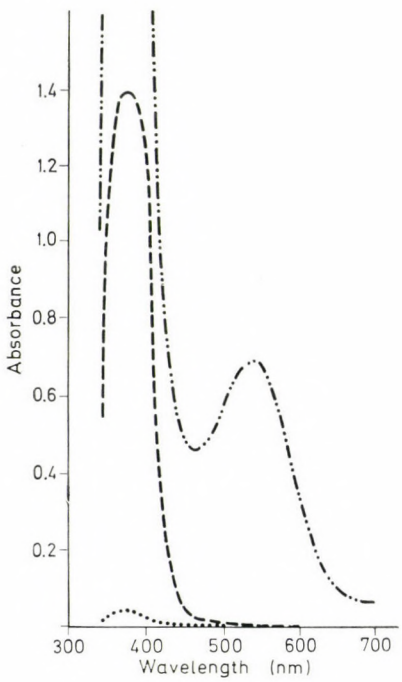

Fig. 1. Absorption spectrum of 3.0×10^{-7} mole of arginine (. . . . . .), 2.2×10^{-7} mole of proline (---------) and that of soya hydrolysate containing 1.9×10^{-7} mole of lysine (-..-..-..-), under the conditions of the color reaction according to method 1

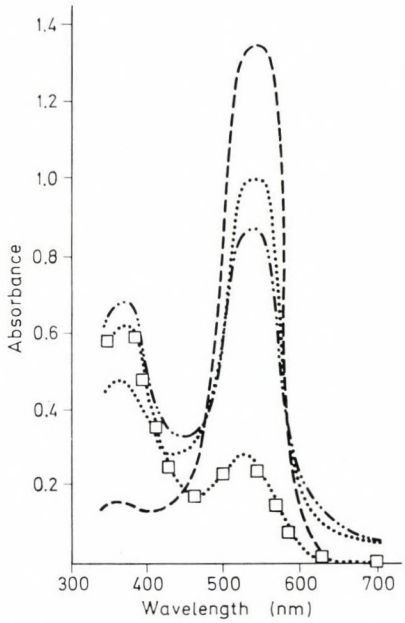

Fig. 2. Absorption spectrum of 2.5×10^{-7} mole of lysine (-..-..-..-), 3.0×10^{-7} mole of ornithine (□ . . . . □), 3.0×10^{-7} mole of δ-hydroxylysine (. . . . . .) and 1.5×10^{-7} mole of lysine methylester (---------) under the conditions of the color reaction according to method 1

purposes, because only compounds satisfying *all* the conditions listed below give a maximum here under the given conditions:

a) The molecule contains two primary amino groups.

b) The two primary amino groups in the molecule are separated by at least 4 but not more than 5 carbon atoms.

c) The molecule contains one undissociated or esterified carboxyl group. (The reaction does not proceed if the carboxyl or amino groups are in peptide bond or in aqueous solution where the carboxyl groups are dissociated.)

d) The molecule contains only one carboxyl group. (The weakly positive reaction of α-ε-diaminopimelic acid arises probably from a lysine contamination.)

It is likely that of the compounds satisfying the above conditions only lysine is present in acidic hydrolysate of protein-containing materials as ornithine and hydroxylysine are rarely found in proteins, thus the determination as carried out according to the method 1 is specific for lysine.

The maximum between 360 and 380 nm is not useful for differentiation of the natural amino acids, because it appears in every case – although the intensity varies e.g. in the case of arginine and proline (Fig. 1) – when the molecule contains at least one amino group beside the undissociated carboxyl group(s), irrespective of the fact that the amino group is primary or secondary.

This maximum does not appear when the carboxyl group is absent, and strangely enough, in case when it is present in an esterified form.

Distinction of lysine from ornithine

In order to isolate and study the substance formed in the color reaction according to method 1, the reaction was carried out in case of lysine and ornithine on a larger scale (5.0×10^{-1} mole).

The dye product formed can be extracted into dichloromethane, dichloroethane, amyl alcohol or chloroform, from a medium containing 75% of water. After evaporating the solvent a black, lustrous, amorphous powder was obtained. The materials obtained from lysine as well as ornithine showed an indicator character. Three or four drops of their 0.05% abs. ethanolic solution gave a remanent color in 100 ml of an aqueous solution. Both materials showed a red color in acidic area (pH below 3.0), and a yellow one in the neutral (pH above 5.5) or alkaline region. Area of the color transition was between pH 3.7 and 5.5 in the case of the material prepared from lysine while between pH 3.0 and 4.5 in the case of that from ornithine. Therefore it seemed plausible to presume that these amino acids should behave in a different manner when pH of the reaction mixture is adjusted to pH 4.5–4.6 together with aqueous dilution, after completion of the color reaction. Our supposition was verified, therefore we obtained the possibility to distinguish spectrophotometrically these two compounds of similar character and even to determine them in the presence of each other.

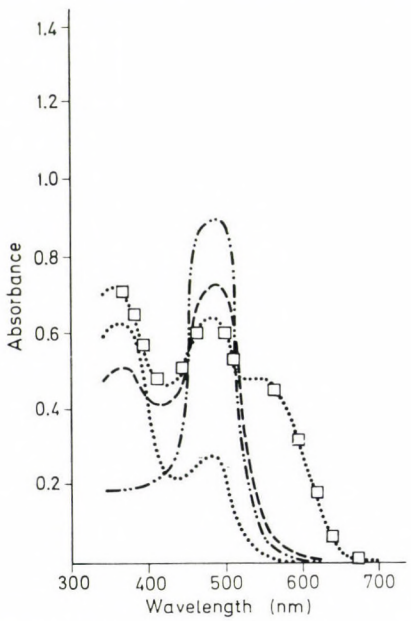

Fig. 3. Absorption spectrum of 2.5×10^{-7} mole of lysine (□ . . . . □), 3.0×10^{-7} mole of ornithine (. . . . . .), 3.0×10^{-7} mole of δ-hydroxy lysine (---------) and 1.5×10^{-7} mole of lysine methylester (-..-..-..-) under the conditions of the color reaction according to method 2

Thus when the color reaction was carried out according to method 2, i.e. the dilution was performed by the ammoniacal A solution instead of the nearly neutral G solution, a very significant hypsochromic shift (40–50 nm) was observed in the spectra of the compounds. The novel maximum appeared in every case at 485 nm at the expense of the maximum between 515 and 535 nm (Figs 3 and 4). observed in method 1. The maxima between 360 and 380 nm were unaffected. Beside the novel maximum appearing at 485 nm only lysine was able to retain under the conditions of method 2 the maximum between 515 and 535 nm characteristic of method 1, although the intensity of the latter maximum was somewhat decreased.

When the spectra of pure lysine and ornithine shown in Fig. 3 are compared to their spectra found in Fig. 2, the change is obvious. While the spectra of the two substances showed quite a similar pattern in Fig. 2, lysine in Fig. 3 showed a strong absorption in the band between 515 and 600 nm beside the maximum at 485 nm. The novel absorption region of ornithine was localized unambiguously at around 485 nm and no absorption was observed at 600 nm. So the absorption measured at this point originated only from lysine.

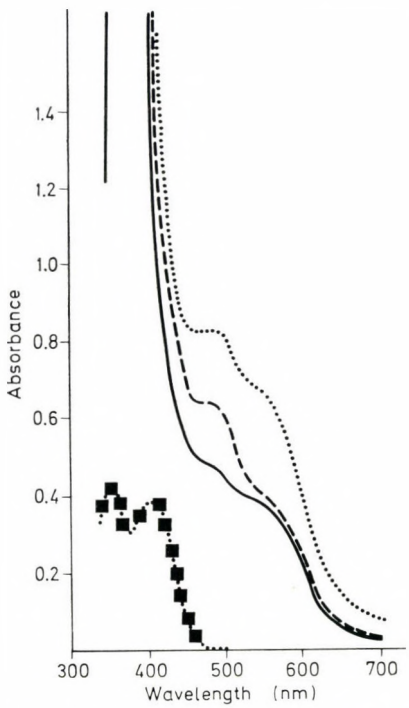

Fig. 4. Absorption spectrum of 1.9×10^{-7} mole of tryptophan (■ . . . . ■), of soya hydrolysate containing 1.9×10^{-7} mole of lysine (————), of soya hydrolysate containing 1.9×10^{-7} mole of lysine + 1.5×10^{-7} mole of ornithine (added) (---------) and of soya hydrolysate containing 1.9×10^{-7} mole of lysine + 1.25×10^{-7} mole of lysine (added) (. . . . . .) under the conditions of the color reaction according to method 2

Beside the spectra taken with the pure substances, this difference between lysine and ornithine was also clearly observed when lysine or ornithine was dropped on soya hydrolysate containing lysine (from the beginning) and the spectra were taken following the color reaction according to method 2 (Fig. 4).

These striking divergences in their spectra furnished a basis for the determination of lysine and ornithine in the presence of each other. When a sample containing both lysine and ornithine was analyzed according to method 2, the lysine content of the sample was measured at 600 nm individually. The total absorbance originating from lysine and ornithine was measured at 485 nm and the ornithine content of the sample was calculated from the A (or) value obtained by the equation given in method 2.

Relationship between light absorption and concentration is linear for both lysine and ornithine as shown in Fig. 5.

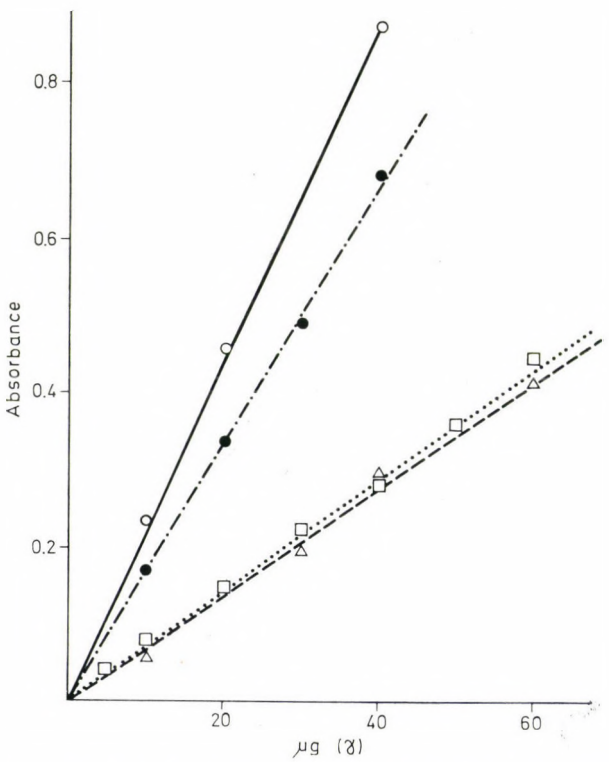

Fig. 5. Relationship between light absorption of lysine and ornithine respectively and their concentration in the reaction mixture (3.2 ml). Calibration curve for lysine according to method 1 (535 nm) (————), calibration curve for lysine according to method 2 (485 nm) (- . - . -), for lysine according to method 2 (600 nm) (. . □ . . □ .), for ornithine according to method 2 (485 nm) (. △ . △ .)

The lysine content of samples from proteins and protein-containing materials are shown in Table 1. It is evident from the data that the results of the methods reported here are in good agreement with those obtained by the JLC-5AH type amino acid analyzer.

Storherr's valuable observations could not be utilized for the direct determination of lysine because of the particularly unstable character of furfurol. The freshly distilled, pale-yellow liquid becomes dark yellow at room temperature within a few hours even in a nitrogen atmosphere, at a higher temperature, it gets brown within some minutes and furfurol becomes oxidized or polymerized. Lead acetate suggested by Storherr for the prevention of the autooxidation proved not to be completely effective. One of our most important objectives was therefore to find compounds that are capable of preventing the spontaneous oxidation of furfurol even at a temperature of about 100°C at least for one hour.

Table 1

Lysine content of some air-dried proteins and protein-containing materials

Comparison of the results provided by the methods presented here with those obtained on a JLC-5AH type amino acid analyzer

Name of the sample investigated	Lysine content(%) according to		
	Method 1	Method 2	Amino acid analyzer
α-Casein (cow)	8.48	8.46	8.53
Food-product (EGYT) (721214)	7.64	7.60	7.70
Food-product (FLUKA) (22090)	8.06	8.19	7.96
Soya meal	3.83	3.78	3.83
Milk powder	2.26	2.29	2.19
Lucerne grist H-LPC-1	3.52	3.47	3.47
Lucerne grist H-LPC-2	3.28	3.30	3.32
Lucerne grist H-LPC-7	3.72	3.68	3.77
Insulin (bovine) 25 I. U. (mg)	2.28	2.24	2.35
ACTH (porcine)	10.56	10.61	10.48

Following Storherr, we tried the salts of several metals and we investigated a series of various antioxidants. Finally, of the reducing type sulphur compounds, $K_2S_2O_5$ proved to be suitable.

Using $K_2S_2O_5$ the blank solution shows practically no absorption in the visible region at the end of the reaction time. However, when $K_2S_2O_5$ is used at a final concentration higher than 0.1%, it inhibits not only the oxidation of furfurol but also weakens the color reaction.

Although the color developed remains stable for several hours even after dilution with water, the color reaction itself requires an anhydrous medium because the colour reaction is significantly weakened and even prevented beyond a certain water content by the dissociation of the carboxyl group of lysine (or ornithine). When the water content of the mixture exceeds 15% during the reaction period, the reddish-purple color characteristic of lysine does not appear. Therefore, the water content of the samples was removed by air flow after application on the filter paper. The dropping technique is useful also because in this way samples of small volumes can be "weighed in" in a precise manner.

An important prerequisite of the color reaction is that furfurol should be used in at least 3-fold excess over the amino acids present in the reaction mixture, furthermore, the reaction temperature should be held over 60°C for at least 30 minutes. During thermostating the stoppers of the test tubes should be mildly loaded to avoid extrusion.

The method described here is simple, requires only inexpensive devices and is most suitable for screening the large number of samples associated with fodder-yeast production and fodderplant-breeding programs. (In 8 hours one person is able to examine 20 to 30 samples when the materials to be tested had been previously hydrolyzed and the reagent R had been prepared for use.)

Standard deviation of the method is $\pm 0.5\%$ for lysine and $\pm 2\%$ for ornithine. These values were determined by dropping a known amount of lysine and/or ornithine on an aliquot part of soya hydrolysate on the filter paper and measuring the deviation of recovery.

Method 2 is suggested for use only if the molar ratio of any of these amino acids is not higher than 3 : 1.

This work has been supported by the Research Institute for Pharmaceutical Chemistry, Budapest. The authors are sincerely indebted to Mrs T. Sebestyén and Mrs K. Szentirmai for their skillful and valuable technical assistance.

References

Patthy, M. (1967) Magy. Kém. Lapja *22* 163
Storherr, R. W. (1959) Anal. Chem. *31* 268
Takagi, S., Hayashi, K. (1959) Chemical and Pharmaceutical Bulletin *7* 183

Acta Biochim. et Biophys. Acad. Sci. Hung. Vol. 10 (4), pp. 287–295 (1975)

Nerve Excitation Generated by the Action Potential of Muscle

G. BIRÓ

Biophysical Institute, Medical University, Pécs, Hungary

(Received January 21, 1975)

The effect of the electrical activity of muscle on the nerve in contact with it was investigated. The results obtained on isolated nerve-muscle preparations and on whole leg preparations of frog revealed that, under certain conditions, the action potential of the muscle is capable of producing excitation of the nerve adjacent to the muscle. These results suggest the hypothesis that the muscle activity could have an additional function in the excitatory processes by means of the electrical effect exerted on the nerve.

Introduction

The problem of electrical interaction between excitable tissues was investigated from several points of view. Matteucci (1842) proved that the action potential of a muscle could stimulate a nerve being in contact with it, and Hering (1882) demonstrated that under special condition the excitation of a nerve fibre could represent an effective stimulus for another fibre in the same trunk. Jasper and Monnier (1938) as well as Arvanitaki (1942) brought about transmission of excitation between juxtaposed non-myelinated nerves. However, according to Rosenblueth (1941) such a transmission in the case of myelinated nerves only takes place when the excitability of the nerve is increased. It was demonstrated that the excitability of the nerve fibre changed during the passage of an impulse in an adjacent fibre (Blair, Erlanger, 1940), and this interaction between the nerve fibres could figure in synchronizing the nerve activity (Katz, Schmitt, 1940). Other experiments showed that the electrical activity of the muscle could stimulate the nerve fibres at the neuro-muscular junction (Masland, Wigton, 1940; Lloyd, 1942; Eccles et al., 1942; Epstein, Jackson, 1970) and in the muscle spindles (Granit et al., 1959), too.

The aim of the present paper is to show some experimental circumstances in which the muscle could excite the nerve in its neighbourhood.

Methods

The experiments were performed on isolated sciatic-gastrocnemius preparations and on whole leg preparations of frogs (Rana esculenta) in all the four seasons at room temperature (20–23°C).

The responses of preparations were elicited by square-wave impulses 2 V amplitude and 0.1 ms in duration. In the case of the nerve-muscle preparations the stimulus was applied to the sciatic nerve and in the case of the leg preparations, to the sciatic plexus using platinum wire 0.5 mm in diameter for the stimulation. The electrodes for recording action potentials were platinum wire 1.0 and 0.1 mm in diameter or platinum plate 5 mm in width. In the one part of the experiments the nerve-muscle preparations were connected to each other, similarly to the Matteucci's experiment, the nerve of a preparation having been laid on the surface of the muscle of another preparation. In other cases two platinum plates connected the muscle in the first preparation to the nerve in the second one.

To ensure that the electrical pulse stimulating the first preparation have no direct effect on the second one, experiments were performed with the nerve-muscle preparations taken from frogs previously curarized. When the curarized preparation was used as the first one and the stimulus was given to this nerve, no response could be recorded from the second preparation taken from a normal frog. Action potential of the nerve in the curarized preparation was also recorded and it showed normal activity.

The connections between the electrodes and the preparations are demonstrated on the figures in detail. The action potentials were recorded by oscillographical method. Because the stimulus artefact appeared only at high amplifications, in order to see clearly the time of the stimulus, the stimulus was recorded directly on the lower beam as a point above the time markers.

To avoid dessication of the preparations they were kept under wet condition by moistening them with Ringer's solution in some cases or the preparations were closed in a moist-chamber in others.

Results

In order to investigate the stimulating effect of the electrical activity of muscle on the nerve several nerve-muscle preparations were connected to each other (Fig. 1) similarly to Matteucci's experiments. The stimulus was applied to the nerve of the first preparation and the responses of the muscle of the different preparations were recorded after each other. According to these oscillograms the responses of the different muscles appear after a delay of about 4 ms. This delay includes the time which is necessary for the conduction of excitation from the portion of the nerve laid on the muscle to the muscle fibres and the time of the first part of the muscle action potential.

This kind of experiments were performed with more than four preparations, too. In some cases the excitation of the first preparation that was stimulated with one square-impulse could be transmitted to the sixth preparation. Because the tetanic excitation has a well-known effect of potentiation, tetanic stimulation was also used to make the transmission of excitation easier between the

preparations. The Fig. 2 shows the action potentials recorded from the muscles of six different preparations connected to each other in the previous way. In this case first nerve was stimulated with a series of square-impulses.

For investigating the electrical effect of the muscle activity on a nerve, platinum plates were used as electrodes for recording the muscle action potential

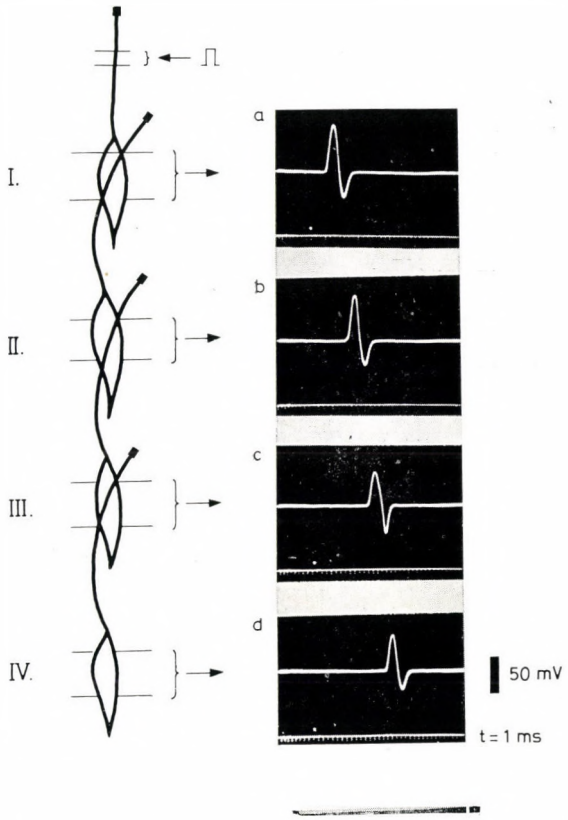

Fig. 1. Successive action potentials recorded from isolated nerve-muscle preparations connected to each other by means of the nerve laying on the previous muscle. Action potentials of muscles I—IV are shown in oscillograms a—d, respectively

and for conducting this electrical activity of the first preparation to the nerve of the second one. In this way it was possible to record that action potential of the muscle which was able to generate excitation in the second preparation (Fig. 3).

Using two additional pairs of electrodes for recording the nerve activity directly, we obtained the oscillograms shown in the Fig. 4, which demonstrate

the right correspondence in time between the action potential of the first muscle and the action potential of the nerve of the second preparation.

In the case of whole leg preparations the sciatic plexus was stimulated and the action potential was recorded from the m. gastrocnemius (Fig. 5a). The sciatic nerve was cut in the upper third of the thigh and its distal portion placed

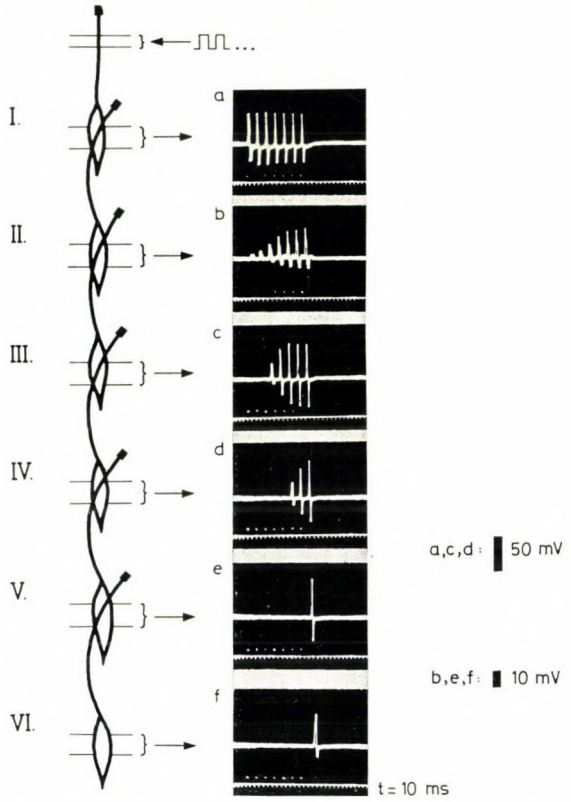

Fig. 2. Series of action potentials successively recorded from isolated nerve-muscle preparations connected to each other by means of the nerve laying on the previous muscle. Action potentials of muscle I—VI are shown in oscillograms a—f, respectively

on the surface of femoral muscles. Under such conditions, the stimulation of the sciatic plexus resulted in action potentials of the m. gastrocnemius (Fig. 5b). The oscillograms demonstrate a difference of about 5 ms in the latency of the muscle action potentials as measured before and after cutting the nerve. This result indicates that the activity of the thigh muscles innervated by nerves branching from the plexus above cutting could produce an action potential in the m.

gastrocnemius by means of a stimulatory effect exerted by the muscles on the nerve being in contact with them.

Similar results were obtained when the sciatic nerve was not cut but ligated, i.e. when the nerve remained under in situ conditions. After the stimulation of the plexus, action potentials were recorded from the thigh and gastrocnemius muscles simultaneously. Comparison of the records taken before and after

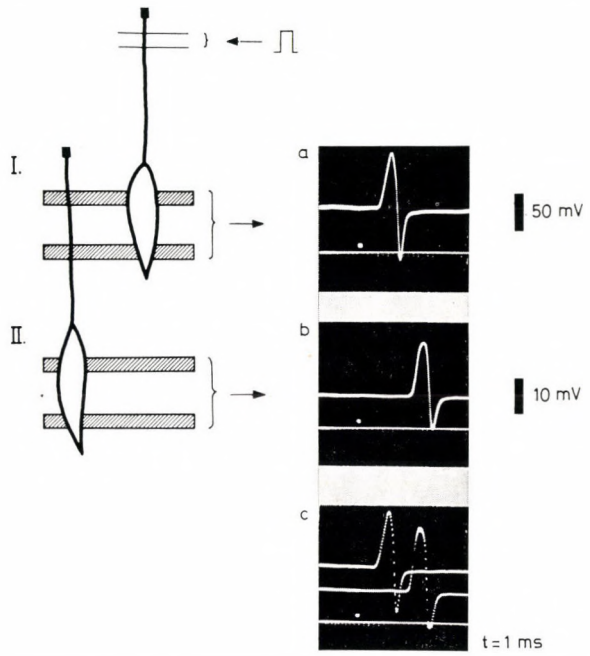

Fig. 3. Action potentials recorded from isolated nerve-muscle preparations connected to each other by means of platinum plates; a: action potential of muscle I, b: action potential of muscle II, (a and b were recorded after each other) c: action potentials of muscles I and II (simultaneous record)

ligature reveals that the action potentials of the m. gastrocnemius appears about 4 ms later in the ligated case (Fig. 6). This result also demonstrated that the thigh muscles can generate excitation in the resting portion of the nerve surrounded by muscles below the ligature. The effectiveness of interruption of nerve conduction by ligature is demonstrated in the oscillograms of Fig. 7, which show that the distal one of the two action potentials recorded from an isolated sciatic nerve disappeared after the nerve had been ligated below the proximal pair of the recording electrodes.

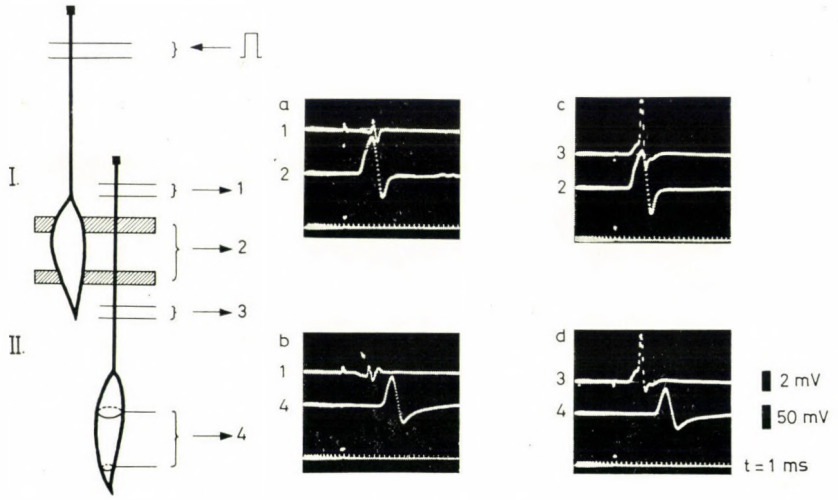

Fig. 4. Action potentials simultaneously recorded from isolated nerve-muscle preparations connected to each other by means of platinum plates. a: proximal action potential of nerve II (1) and action potential of muscle I (2); b: proximal action potential of nerve II (1) and the action potential of muscle II (4); c: distal action potential of nerve II (3) and action potential of muscle I (2); d: distal action potential of nerve II (3) and action potential of muscle II (4)

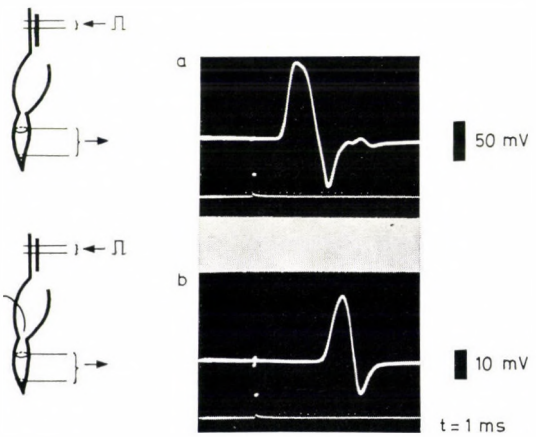

Fig. 5. Action potentials of the m. gastrocnemius in whole leg preparation. a: intact preparation; b: the sciatic nerve is cut and laid on the surface of the thigh muscles

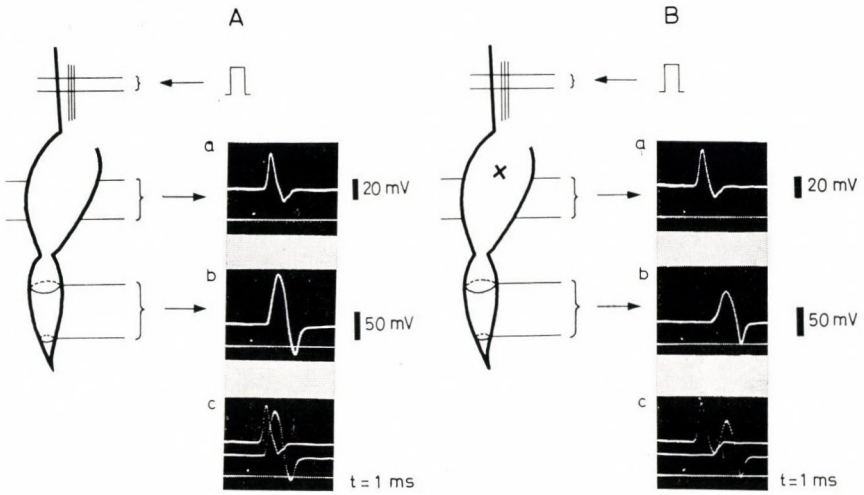

Fig. 6. Action potentials recorded from whole leg preparations. a: action potential recorded from the thigh; b: action potential recorded from the m. gastrocnemius; c: simultaneous records of a and b; A: intact preparation; B: the sciatic nerve is ligated at "x"

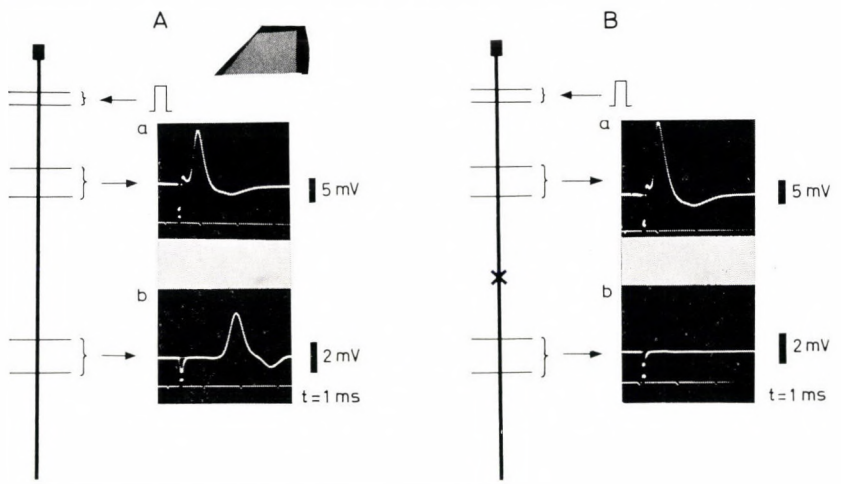

Fig. 7. Successive action potentials recorded from isolated sciatic nerve. a: proximal record; b: distal record; A: intact nerve; B: the nerve is ligated at "x"

In connection with all the above results it should be emphasized that the transmission of excitation from muscle to the nerve does not take place in every position of the muscles or nerves, however, it was possible to find a favourable position for the transmission of excitation in most preparations.

Discussion

The results obtained by means of developing the Matteucci's experiment have not only corroborated Matteucci's experiment, but directed attention to the possibility of a not-negligible effect of the electrical activity of muscles on the nerve trunks or fibres among or inside the muscles.

The Matteucci's experiment is carried out with two nerve-muscle preparations connected to each other on the same way as the first two preparations on Fig. 1. In the Matteucci's experiment the nerve of the first preparation is stimulated with a supramaximal pulse and the other preparation reveals the so-called secondary contraction which results in the excitation generated in the second nerve by the compound action potential of all the motor units in the first muscle. This is not a physiological case at all because, in physiological circumstances, the motor units of a muscle are not in action simultaneously. However, the results shown in Figs 1 and 2 approach to the physiological situation inasmuch as the responses of the preparations beyond the second one appear as a consequence of nerve excitation generated by the muscle action potential that includes the activity produced by only a part of the motor units, this action potential being a submaximal stimulus for a nerve. Since the general form of the excitation in the organisms has tetanic characteristics, the result, according to which the tetanic stimulation renders the transmission of excitation from the muscle to the nerve easier, also increases the physiological significance of this kind of electrical interaction between muscle and nerve tissues.

Our results are in accordance with previous results published by several authors. Eccles et al. (1942) showed the retrograde propagation of an impulse from muscle to nerve. This effect results in the "secondary centripetal discharge" of the ventral root. Similar results were obtained by Leksell (1945) as well as Brown and Mattews (1960) who called the similar activity of the ventral root as the "back response". Burst activity of the ventral root was also observed during muscle contraction of fascicular type elicited by the effect of prostigmine at the distal end of the motor nerve (Masland, Wigton, 1940). Lloyd (1942) also pointed out that the action potential of a muscle could stimulate the nerve at its terminal portion.

The sensory nerves could also be stimulated by the electrical activity of the muscle. This result was demonstrated in the form of the "early response" of the muscle spindle (Granit et al., 1959). Werner (1961) showed that antidromic activity in the motor nerves could be also generated by the overlooping motor units. Similar results were obtained by Epstein and Jackson (1970) who demonstrated in human experiments that repetitive muscle firing arised from the re-excitation of the nerve inside the muscle.

In connection with our experiments it is a very important point of view that not in all circumstance will muscle activity excite the nerve. The experiments revealed the importance of which part of the muscle surface is connected to the nerve and of how long a portion of the nerve is subject by the effect of the muscle electrical activity. Our next experiments will aim at elucidating the role of these circumstances.

Our results seem to be in contradiction with the conception concerning the principle of isolated conduction generally accepted in the physiology. However, our results and the experiments published by the authors mentioned above agree that muscles can stimulate a nerve with their electrical activity and produce excitation in nerves being in contact with them.

If the muscle stimulates the nerve in its neighbourhood under some special conditions, nerve excitation can be generated in both the sensory and motor fibres and this excitation can be conducted in both peripheral and the central direction. Consequently, there would be an additional way by which the muscle activity can influence the mechanism of the regulation taking place in the excitatory processes. However, this hypothesis has to be supported by further experiments.

The advices of Professor J. Tigyi are gratefully acknowledged.

References

Arvanitaki, A. (1942) J. Neurophysiol. *5* 89
Blair, E. A., Erlanger, J. (1940) Amer. J. Physiol. *131* 483
Brown, M. C., Matthews, P. B. C. (1960) J. Physiol. *150* 332
Eccles, J. C., Katz, B., Kuffler, S. W. (1942) J. Neurophysiol. *5* 211
Epstein, R. A., Jackson, S. H. (1970) J. Appl. Physiol. *28* 407
Granit, R., Pompeiano, O., Waltman, B. (1959) J. Physiol. *147* 399
Hering, E. (1882) Sitzungsberichte der mathematisch-naturwissenschaftlichen Classe der kaiserlichen Akademie der Wissenschaften *85* 237
Jasper, H. H., Monnier, A. M. (1938) J. Cell Comp. Physiol. *11* 259
Katz, B., Schmitt, O. (1940) J. Physiol. *97* 471
Leksell, L. (1945) Acta Physiol. Scand. *10* Suppl. XXXI.
Lloyd, D. P. C. (1942) J. Neurophysiol. *5* 153
Masland, R. L., Wigton, R. S. (1940) J. Neurophysiol. *3* 269
Matteucci, C. (1842) cited in: Handbook of Physiology. Ed.: J. Field, Section 1: Neurophysiology, American Physiological Society, Washington, D. C. 1959. Vol. 1. p. 20
Rosenblueth, A. (1941) Amer. J. Physiol. *132* 119
Werner, G. (1961) J. Neurophysiol. *24* 401

Acta Biochim. et Biophys. Acad. Sci. Hung. Vol. 10(4), pp. 297—306 (1975)

Examination with X-ray Diffraction of Cartilaginous Tissues of Rats of Different Ages with and without Vitamin D Treatment

I. FÖLDES, G. RISCHÁK, M. PETKÓ

Institute of Anatomy, Histology and Embriology, Medical University, Debrecen, Hungary

(Received March 8, 1975)

X-ray diffraction examinations were performed on different cartilages (epiphysis, joint, rib, nose-cartilage and discus intervertebralis) of 10 young and 10 old rats. Half of the animals served as untreated control, the other half was treated daily with 40,000 U of vitamin D_3 through a gastric tube for 14 days. The examinations were performed partly with a Philips diffractometer and partly in a Guinier chamber, in order to determine the quantitative and qualitative crystallite size. The results obtained are as follows: 1. Cartilage crystallites, except those of the epiphysis, are more rough-grained in the old than in the young animals. 2. A difference was found between cartilages of the same age but of different types. In epiphysial cartilage thin crystals of medium length are formed while thick ones can be seen in discus intervertebralis, joint and rib cartilage. 3. According to the data obtained with the method of X-ray diffraction the crystals in epiphysial cartilage and discus intervertebralis will be lengthened upon the effect of vitamin D, while those in the rib and nose-cartilage shortened and bulkier. It can be imagined that cartilage and bone cells as well as basal substance have an influence on the morphological picture of calcium phosphate. Thus different forms of crystal are formed in cartilages of different functional activity.

Introduction

In our previous comparative histological examinations and studies on calcification different cartilage tissues (epiphysis, joint, rib, — and nose cartilages as well as discus intervertebralis) showed different affinities to calcium salts in normal circumstances. According to our electron microscopic examinations a difference appeared even in the morphology of calcification of epiphysis and other cartilages: *calcium salt had long-shaped crystal-like sediment in epiphysial cartilage* while, in the other cartilages, the sediment manifested itself in dense round or oval structures (unpublished data). The latter structure may correspond to the so-called amorphous, or non-crystal, mineral phase, first demonstrated by electron microscopic studies (Robinson, Watson, 1955; Fitton-Jackson, Randall, 1956). Starting from these data we thought of supporting our observations also with the method of X-ray diffraction. X-ray diffraction examination is widely applied for studying the crystal structure of mineral substances of the bone (Posner, Eanes, 1963; Posner et al., 1965; Harper and Posner, 1966; Ter-

mine, Posner, 1966; 1967; Lénárt et al., 1968). X-ray and electron-diffraction examinations were only performed in epiphysial cartilage (Lénárt et al., 1971a and b). Muller et al. (1966) demonstrated that under pathologic conditions, notably in the case of vitamin D deficiency, the development of crystals was slower and the degree of crystallization lower than under normal conditions. On the basis of what was said above different cartilages were examined with the method of X-ray diffraction in order to answer the question of whether X-ray diffraction would reveal any crystallographic difference between: 1. cartilages o young and old animals; 2. cartilages of untreated control animals, and of animals treated with vitamin D; 3. different cartilaginous tissues.

Material and method

Twenty albino rats were used in the radiocrystallographic examinations. Ten of them were young (4 weeks old, with an initial body weight of 100 g). Five of the animals had not been given any treatment, the other five received 40, 000 U of vitamin D_3 a day through a gastric tube for 14 days. The other 10 animals were older (10 weeks, with an average body weight of 250 g). Half of them served as control, the others received the same treatment as the young rats. The animals were killed simultaneously by cutting through the heart under superficial ether anaesthesia. The epiphyses of the tibia and femur as well as the rib joint and nose cartilages, the thoracic and lumbal disci intervertebrales were taken out as quickly as possible and carefully cleaned from the soft tissue. The pieces of cartilage removed in this way were soaked in abs. alcohol for 24 hours and kept in a cabinet drier at 90°C for 2 hours. Thereafter the cartilage substance was put into the agate vessel of 30 ml of the Agate Stonecutters vibration mill. An equal volume of purified rough steel grindings was added, followed by shaking for 30 minutes after providing it with the prescribed 3 agate balls. Then the content of the vibromill was poured into aqueous alcohol of 1 : 1 dilution and even the traces of iron dust were removed with the aid of a strong permanent magnet. After taking the grinding balls out we decanted the unnecessary fluid and extracted the cartilage flour by evaporating the fluid. This substance was used in the X-ray diffraction examinations.

In the examinations we used the Mueller Mikro 111 generator, Phillips PW 1050 goniometer and PW 1051 measuring panel. The Guinier-chamber examinations were performed with an AEG Jagodzinsky-chamber and with an AEG Johannson monocromator. Guinier photographs were taken on Agfa-Gevaert D-10 film. The curve of blackening of the cartilage apatite (002) reflexion was drawn by a Zeiss Lirepho-2 registering photometer. The time of exposition was chosen so as to enable the straight section of the blackening curve to be used; in this way transformation of blackening intensity became very simple. Every X-ray diffraction examination was performed with Cu K_α radiation. The velocity of goniometer was 1/2 20°/min, the velocity of registering was 2.67 cm/min. The following gap-system was used in the goniometer: $1/2° - 0.1° - 1°$. In the

diffractometer a rotating preparate spinner was used for a more reliable measuring of intensity. In Guinier-chamber examinations the so-called cellite cellophane method was used (Flörke et al., 1968).

The determinations of crystallite size were performed with the so-called Warren–Averbach method. The photograph of the dust of quartz crystal and its (10-1) reflection, respectively, were used for correcting the widening of the line caused by the instrument. The Warren formula is $\beta^2 = B^2 - b^2$

β = the real width of the line measured at half height
B = the width of the line measured at half height
b = the correction of the instrument related to the reflection of bone-apatite (002)

$b = 0.23$ 20° in the diffractometric photograph; $b = 0.21$ 20° in the Guinier-chamber photograph. It should be noted that the theoretical correction calculated for the latter one is: 0.1987 20°. The average crystallite length of bone apatite was calculated on the basis of the Scherrel formula.

$$L = \frac{K}{\beta \cos \Theta}$$

L: the average crystallite size
K: 1 with regard to the (002) reflection
Θ*:* the angle of reflection belonging to the main point of the curve.

Besides, the complex integrated intensities I (002) and I (hk0) were determined and the quotient I (002)/I (hk0) complex was formed from them. In the case of a crystal having two parameters this quotient gives information on the change of one size of the crystallite if we know the other. It was not possible to reliably determine the clear (hK0) reflection profile from the diffractograms of cartilages even with the Fourier analysis, as the complex reflection at 20 $\cong$ 32° is as wide as the three lines to be theoretically expected melt together completely. The results of our measurements and the parameters calculated from them are shown in Table 1.

Discussion of the results

Discussion of the data of measurements

Joint cartilage (Fig. 1):

The length of crystallites is 160 Å in the case of young animals, which does not change upon the effect of vitamin D treatment. We can only estimate the change of thickness and the direction of the change on the basis of the quotient of intensity, but we do not obtain any information on the absolute thickness of crystallites. A comparison with data of the other cartilages leads to the conclusion that the crystallites of cartilage apatites of young animals are very tiny and

Table 1

		$B^{\circ}_{(002)}$ *	$B^{\circ}_{(hk0)}$ *	$\beta^{\circ}_{(022)}$ *	$L_{(002)}$ Å *	$100.\frac{I_{(002)}}{I_{(hk0)}}$ complex
Joint	KA	0.87	2.12	0.64	160 ± 10	10.1
Joint	A	0.87	2.04	0.64	160 ± 10	10.2
Joint	KB	0.65	2.12	0.42	340 ± 15	9.1
Joint	B	0.55	2.10	0.32	450 ± 15	10.1
Epiphysis	KA	0.64	2.27	0.41	150 ± 10	7.2
Epiphysis	A	0.75	2.27	0.52	220 ± 10	5.1
Epiphysis	KB	0.91	2.38	0.68	130 ± 10	10.4
Epiphysis	B	0.80	2.24	0.57	200 ± 10	9.4
Nose	KA		2.23	not		
Nose	A		2.20	appre-		
Nose	KB		1.84	ciable		
Nose	B	0.59	1.93	0.36	400 ± 15	11.6
Rib	KA	0.86	2.37	0.63	180 ± 10	11.3
Rib	A	1.05	2.37	0.82	100 ± 10	15.0
Rib	KB	0.60	2.16	0.37	380 ± 15	17.5
Rib	B	0.86	2.14	0.63	180 ± 10	12.1
Discus intervertebralis	KA	1.00	2.10	0.77	110 ± 10	13.1
Discus intervertebralis	A	0.76	2.07	0.53	210 ± 10	6.1
Discus intervertebralis	KB	0.86	2.09	0.63	180 ± 10	10.2
Discus intervertebralis	B	0.85	2.19	0.62	190 ± 10	7.25

* Measured from Guinier-chamber

their width can be considered average. The crystals in old animals are a priori longer and somewhat thinner than the average; upon the effect of vitamin D they extend further in every direction.

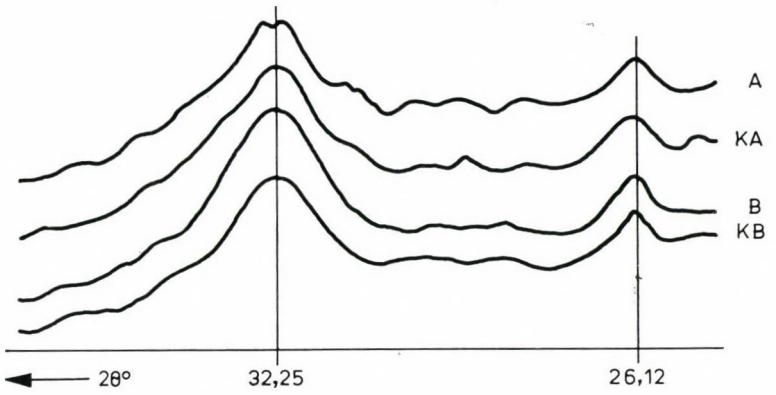

Fig. 1. Part of a diffractogram of joint cartilage apatite. The base and prism reflections of apatite are shown in the figure. The Bragg-angle of reflection is shown in the horizontal axis, and the intensity of reflection in arbitrary units in the vertical axis. *A* = young animal treated with vitamin D; *KA* = untreated young animal; *B* = old animal treated with vitamin D; *KB* = untreated old animal

Epiphysis cartilage (Fig. 2):

In young animals very small crystals, thinner than the average, can be found. Upon the effect of vitamin D the crystals lengthen and become fine needles. In old animals shorter and more bulky small crystals are formed; upon the effect of vitamin D longer and thinner crystals are formed. Vitamin D treatment is less effective in old than in young animals.

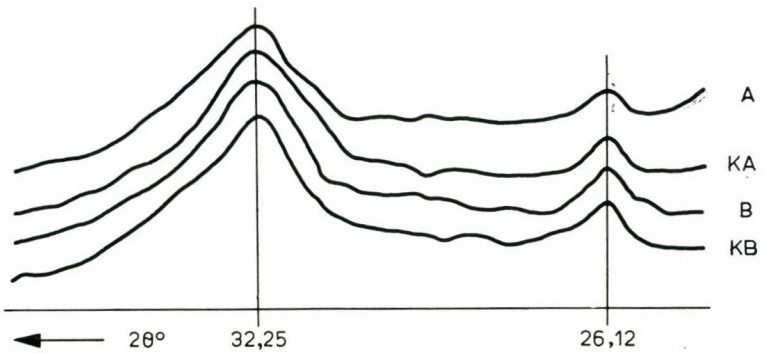

Fig. 2. Part of a diffractogram of epiphysial cartilage apatite

Nose cartilage:

Substance enough for an appropriate examination could only be obtained from old animals treated with vitamin D. According to this, here we obtained the longest crystals which were a little thicker.

Rib cartilage (Fig. 3):

In the rib cartilage of young animals larger apatite crystals were found than in other young cartilages. As an effect of vitamin D treatment the length of crystals diminished and their thickness increased. In old animals the bulkiest apatite crystals with the largest grains were found in the rib cartilage. Vitamin D treatment had a similar effect as in young animals, and the crystals diminished almost to the same size as in young animals.

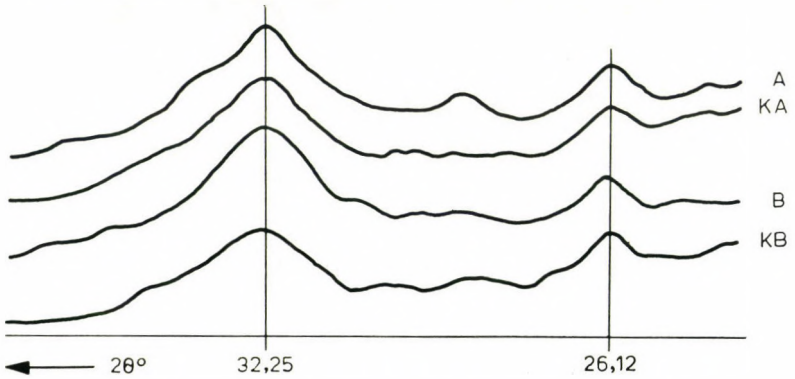

Fig. 3. Part of a diffractogram of costal cartilage apatite

Discus intervertebralis (Fig. 4):

Very tiny crystals, thicker than the average, were found in young animals. Upon the effect of vitamin D the length of crystallites was almost doubled, while the thickness seemed to remain unaltered. Longer and smaller, slimmer crystal-

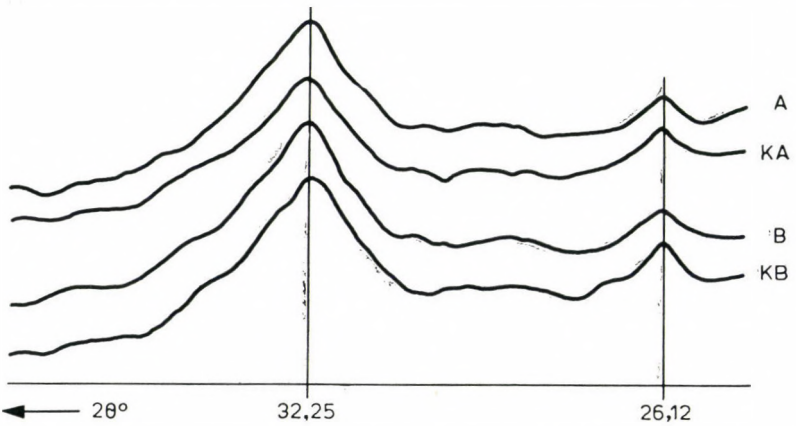

Fig. 4. Part of a diffractogram of intervertebral cartilage apatite. Symbols in Figs 2, 3 and 4 correspond to those in Fig. 1

lites were observed in old animals than in young ones. The length of crystallites was not increased but their thickness diminished upon the effect of vitamin D.

We wish to make some remarks in connection with the results reported:

1. According to our results there is a difference between the size and forms of crystals in the cartilages of young and old animals; the greatest difference can be found in rib and joint cartilages, a smaller one in discus intervertebralis and the slightest one in epiphysial cartilage.

At more advanced age the crystals usually become longer; in joint cartilage and discus intervertebralis they become slimmer, in epiphysial and chiefly in costal cartilages bulkier. Eanes et al. (1965) published some data on rats; in the young, growing rat (from 8 to 38 days) the Ca/P molar ratio is 1.41 – 1.59, non-crystalline calcium phosphate is 36 to 39 per cent of the whole inorganic substance (in apatite the Ca/P molar ratio is 1.67). Accordingly, in the case of cartilaginous tissues a tendency similar to that in bones can be discovered.

2. The data obtained with the method of X-ray diffraction show that vitamin D influenced the crystals of various cartilages. This effect partly appears in the younger group (epiphysis, rib cartilages, discus intervertebralis), partly in the older one (joint cartilage) and partly in both groups (epiphysial and costal cartilages). Vitamin D application usually leads to the formation of longer and slimmer crystals (in the epiphysial cartilage in both groups and in the discus in young animals). In rib cartilage shorter and bulkier crystals can be observed in young animals and shorter and slimmer ones in old animals after vitamin D treatment. The effect of vitamin D on joint cartilage could only be observed in older animals; the effect manifested itself in elongation of the crystals. In the case of nasal cartilage only the results obtained after vitamin D treatment in older animals could be evaluated. The longest crystals appeared in this group. This seems to be in connection with the data in the literature and our histological data, according to which the nose-cartilage is not calcified in normal circumstances. Histologically evaluable calcification could only be obtained with a high dose of vitamin D also in the present experiments.

3. Our results revealed that the crystal forms of different cartilaginous tissues are not the same, either at young or old age. In young animals the crystals of joint and epiphysis cartilage are of about the same length, but in the latter one they are definitely slimmer. The crystals are longer in the rib cartilage and shorter in the discus, but they are considerably bulkier in both cartilages. In older animals there are considerably longer crystals in the joint and mainly in the rib cartilage, and there are extremely bulky crystals in the latter. The shortest crystals occur in the epiphysial cartilage.

Chatterji et al. (1972) published the X-ray diffraction diagram of the femoral bone from the age of 6 to 76 years. Apatite crystals are rarely orientated at the time of birth. The degree of orientation increases with increasing age. The question arises of whether the biological origin and exact localization of these morphologically different mineral particles are different in the calcified

matrix (Table 2). Another very important point of view is that the inorganic components of the bone are settled in an environment that is different from the one used in the synthetic system. It can be imagined that the bone cells and matrix change the morphology of calcium phosphate, though Doty and Matthews (1971) examining a small quantity of ACP observed that the ultrastructure of bone fixed in abs. alcohol was very similar to that seen in vitro. In the opinion of Termine et al. (1973) 1/5 of the apatite is constituted by very small crystals and, accord-

Table 2

Component	Mark	Formula	Ca/P Ratio	External form
Amorphous calcium phosphate	ACP		1.45—1.55	globule
Octa calcium phosphate	OCP	$Ca_8H_2(PO_4)_6 \cdot 5\ H_2O$	1.33	thin sheets
Hydrated dicalcium phosphate	TCPH	$Ca_9H(PO_4)_6OH$	1.50	
Monolite		$Ca_2HPO_4 \cdot 2\ H_2O$	1.0	laminiform
Monetite		$CaHPO_4$	1.0	isometric
Calcium pyrophosphate		$Ca_2P_2O_7$		
Whitelockit		$Ca_3(PO_4)_2$ or $Ca_9MgP_7(O \cdot OH)_8$	1.5	isometric
Hydroxyapatite	HA	$Ca_{10}(PO_4)_6(OH)_2$	1.67	bacilliform
Fluoroapatite	FA	$Ca_5(PO_4)_3F$	1.67	bacilliform
Carbonat hydroxy-apatite		$Ca_9O_3H_5(PO_4)_3(CO_3)_4$		

ing to their hypothesis, these constitute the amorphous part of bone minerals. Urist and Dowell (1967) demonstrated that the chemical composition of the earliest sediments of crystalline minerals differs from the new diaphysis bone in the provisory calcification zone. The molar ratio of Ca/P is low in the cartilage, the tetracycline uptake is high.

On the basis of all the above considerations we think that a difference exists between the crystallographic relations of different cartilaginous tissues. We cannot yet express and evaluate these differences reliably because of the complexity of tissue samples, the limits of the method and a lot of unknown factors. We have no completely correct knowledge of every step of the in vitro crystallization process and know even less of the in vivo mechanism.

It seems natural that the environment can play an important role in determining the form of the crystal, just as the crystal influences its environment. Eanes et al. (1970) described that minerals have an influence on the characteristics of the collagen. It follows from this that, in the epiphysial cartilage mainly crystals of medium length and thinness occur which are connected with, or impacted into, the mucopolysaccharides, while in the joint and rib cartilages as well as in discus intervertebralis, where collagen bundles dominate, thicker crystals are inserted with their "c" axis between polypeptid chains.

Some problems should yet be mentioned in connection with the method used:

A. This method is of static nature. Since, because of the reorganization of the bone, the sample to be analyzed contains a mixture of crystals under formation, crystals developed completely and crystals in the state of destruction it is extraordinarily difficult, almost unimaginable, to examine homogeneous samples.

B. The organic fraction, especially the protein, greatly disturbs the measurements of physical and chemical characteristics of the inorganic constituents of hard tissues (Scott, 1960; Swedlow et al., 1972).

C. The intensity of X-ray diffraction is affected by the damage to the crystals (e.g. defects of the lattice, microcrystal structure as well as non-crystal substance and crystal orientation; Alexander, 1969). Though our results should be evaluated cautiously, they still indicate some differences in the crystals of various kinds of cartilages.

References

Alexander, L. E. (1969) X-ray Diffraction Methods in Polymer Science. John Wiley and Sons, Interscience, 137

Chatterji, S., Wall, J. C., Jeffery, J. W. (1972) Experientia *28* 156

Doty, S. B., Mathews, R. S. (1971) Clin. Orthop. *80* 191

Eanes, E. D., Gilessen, I. H., Posner, A. S. (1965) Nature (Lond.) *208* 365

Eanes, E. D., Lundy, D. R., Martin, G. N. (1970) Calc. Tiss. Res. *6* 239

Fitton-Jackson, S., Randall, J. T. (1956) Fibrogenezis and the Formation of Matrix in Developing Bone. 47—64. In: Bone Structure and Metabolism. Eds. Wohlstonholme G. E. W. O'Connor, C. M., Little Brown Comp. Boston

Flörke, G. W., Sealfield (1968) M. M. P. I. für Silikatforschung, Würtzburg Herstellung dünner, ebener, Pulverpreparate für Röntgen-Feinstrukturuntersuchungen unter Verwendung von Zellulose-Kunststoffen.

Harper, R. A., Posner, A. S. (1966) Proc. Soc. Exp. Biol. Med. *122* 137

Lénárt, G., Bidló, G., Pintér, J. (1968) Acta Biochim. Biophys. Acad. Sci. Hung. *3* 305

Lénárt, G., Bidló, G., Kéry, L. (1971a) Acta Biochim. Biophys. Acad. Sci. Hung. *6* 307

Lénárt, G., Veres, I., Bidló, G., Pintér, J. (1971b) Acta Biol. Acad. Sci. Hung. *22* 431

Muller, S. A., Posner, A. S., Firschein, H. E. (1966) Proc. Soc. Exp. Biol. Med. *121* 844

Posner, A. S., Eanes, E. D. (1963) Norelco Rep. *10* 71

Posner, A. S., Eanes, E. D., Harper, R. A., Zipkin, I. (1965) Arch. Oral Biol. *8* 549

Robinson, R. A., Watson, M. L. (1955) Ann. N. Acad. Sci. *60* 596
Scott, D. B. (1960) The Crystalline Component of Dental Enamel. In: Proc. fourth international congress of electron microscopy vol. 2. Springer, Berlin—Heidelberg—New York, 348
Swedlow, D. B., Harper, R. A., Katz, J. L. (1972) Evaluation of a new preparative technique for bone examination in the SEM Research Institute 335, In: Scanning electron microscopy. Part III. Proceedings, workshop on biological scanning electron microscopy.
Termine, J. D., Posner, A. S. (1966) Science *153* 1523
Termine, J. D., Posner, A. S. (1967) Calc. Tiss. Res. *1* 8
Termine, J. D., Eanes, E. D., Greenfield, D. J., Nylen, M. U. (1973) Calc. Tiss. Res. *12* 73
Urist, M. R., Dowell, T. A. (1967) Clin. Orthop. *50* 291

Hoppe-Seyler's Zeitschrift für Physiologische Chemie

Editors in Chief

A. BUTENANDT · F. LYNEN · G. WEITZEL

Subscription Rate

For one volume (12 parts) DM 480,—

Vol. 356 No. 9 September 1975

CONTENTS

AUTORENVERZEICHNIS

Walter de Gruyter · Berlin · New York

Hoppe-Seyler's Zeitschrift für Physiologische Chemie

Editors in Chief

A. Butenandt · F. Lynen · G. Weitzel

Subscription Rate

For one volume (12 parts) DM 480,—

Vol. 356 No. 10 October 1975

CONTENTS

Walter de Gruyter · Berlin · New York

Printed in Hungary

A kiadásért felel az Akadémiai Kiadó igazgatója — Műszaki szerkesztő: Zacsik Annamária

A kézirat nyomdába érkezett: 1975. X. 9. — Terjedelem: 4,2 (A/5) 23 ábra

76.2361 Akadémiai Kiadó, Budapest — Felelős vezető: Bernát György igazgató

Reviews of the Hungarian Academy of Sciences are obtainable at the following addresses:

AUSTRALIA

C. B. D. Library and Subscription Service
Box 4886, G. P. O.
Sydney N. S. W. 2001

Cosmos Bookshop
145 Acland St.
St. Kilda 3182

AUSTRIA

Globus
Höchstädtplatz 3
A—1200 Wien XX

BELGIUM

Office International de Librairie
30 Avenue Marnix
1050-Bruxelles

Du Monde Entier
162 Rue du Midi
1000—Bruxelles

BULGARIA

Hemus
Bulvar Ruszki 6
Sofia

CANADA

Pannonia Books
P. O. Box 1017
Postal Station "B"
Toronto, Ont. M5T 2T8

CHINA

C N P I C O R
Periodical Department
P. O. Box 50
Peking

CZECHOSLOVAKIA

Mad'arská Kultura
Národní trida 22
115 66 Praha

PNS Dovoz tisku
Vinohradská 46
Praha 2

PNS Dovoz tlače
Bratislava 2

DENMARK

Ejnar Munksgaard
Nörregade 6
DK—1165 Copenhagen K

FINLAND

Akateeminen Kirjakauppa
P. O. Box 128
SF—00101 Helsinki 10

FRANCE

Office International de Doumentation et Librairie
48, Rue Gay-Lussac
Paris 5

Librairie Lavoisier
11 Rue Lavoisier
Paris 8

Europeriodiques S. A.
31 Avenue de Versailles
78170 La Celle St.-Cloud

GERMAN DEMOCRATIC REPUBLIC

Haus der Ungarischen Kultur
Karl-Liebknecht-Strasse 9
DDR—102 Berlin

Deutsche Post
Zeitungsvertriebsamt
Strasse der Pariser Kommüne 3—4
DDR—104 Berlin

GERMAN FEDERAL REPUBLIC

Kunst und Wissen
Erich Bieber
Postfach 46
7 Stuttgart S

GREAT BRITAIN

Blackwell's Periodicals
P. O. Box 40
Hythe Bridge Street
Oxford OX1 2EU

Collet's Holdings Ltd.
Denington Estate
London Road
Wellingborough Northants NN8 2QT

Bumpus Haldane and Maxwell Ltd.
5 Fitzroy Square
London W1P 5AH

Dawson and Sons Ltd.
Cannon House
Park Farm Road
Folkestone, Kent

HOLLAND

Swets and Zeitlinger
Heereweg 347b
Lisse

Martinus Nijhoff
Lange Voorhout 9
The Hague

INDIA

Hind Book House
66 Babar Road
New Delhi 1

India Book House
Subscription Agency
249 Dr. D. N. Road
Bombay 1

ITALY

Santo Vanasia
Via M. Macchi 71
20124 Milano

Libreria Commissionaria Sansoni
Via Lamarmora 45
50121 Firenze

JAPAN

Kinokuniya Book-Store Co. Ltd.
826 Tsunohazu 1-chome
Shinjuku-ku
Tokyo 160—91

Maruzen and Co. Ltd.
P. O. Box 5050
Tokyo International 100—31

Nauka Ltd—Export Department
2—2 Kanda
Jinbocho
Chiyoda-ku
Tokyo 101

KOREA

Chulpanmul
Phenjan

NORWAY

Tanum-Cammermeyer
Karl Johansgatan 41—43
Oslo 1

POLAND

Węgierski Instytut Kultury
Marszalkowska 80
Warszawa

BKWZ Ruch
ul. Wronia 23
00—840 Warszawa

ROUMANIA

D. E. P.
Bucureşti

Romlibri
Str. Biserica Amzei 7
Bucureşti

SOVIET UNION

Sojuzpechatj — Import
Moscow
and the post offices in each town
Mezhdunarodnaya Kniga
Moscow G—200

SWEDEN

Almqvist and Wiksell
Gamla Brogatan 26
S—101 20 Stockholm

A. B. Nordiska Bokhandeln
Kunstgatan 4
101 10 Stockholm 1 Fack

SWITZERLAND

Karger Libri AG.
Arnold-Böcklin-Str. 25
4000 Basel 11

USA

F. W. Faxon Co. Inc.
15 Southwest Park
Westwood, Mass. 02090

Stechert-Hafner Inc.
Serials Fulfillment
P. O. Box 900
Riverside N. J. 08075

Fam Book Service
69 Fifth Avenue
New York N. Y. 10003

Maxwell Scientific International Inc.
Fairview Park
Elmsford N. Y. 10523

Read More Publications Inc.
140 Cedar Street
New York N. Y. 10006

VIETNAM

Xunhasaba
32, Hai Ba Trung
Hanoi

YUGOSLAVIA

Jugoslovenska Knjiga
Terazije 27
Beograd

Forum
Vojvode Mišića 1
21000 Novi Sad

Contents

12. III. 1976 Index: 26.030